Power System Integration of Flexible Demand in the Low Voltage Network

Thavlov, Anders

Publication date:
2014

Document Version
Publisher's PDF, also known as Version of record

Power System Integration of Flexible Demand in the Low Voltage Network

Anders Thavlov

PhD Thesis

Kongens Lyngby 2014

Technical University of Denmark
Department of Electrical Engineering
Ørsteds Plads
Building 348, DK-2800 Kongens Lyngby, Denmark
Phone +45 45253800
elektro@elektro.dtu.dk
www.elektro.dtu.dk

"Essentially, all models are wrong, but some are useful."

– George E. P. Box

Summary (English)

Flexible demand for electric power is expected to play an increasing role in the future power system where an increased share of the power generation will come from renewable energy sources. In Denmark, households accounts for approximately one third of the total electricity consumption; thus, it is natural to consider electricity consumption from households as an integrated part of a potential flexible demand side in the future power system. However, as an individual unit a single household is not able to generate a large impact in the power system. Therefore, a mechanism is needed which can coordinate the response from numerous of small entities: in other words, we need a tool for aggregation of a large number of small units and coordinate the electricity consumption among them. This thesis investigates the possibilities of utilising flexible demand from small household entities connected in the low voltage grid. A special emphasis is placed on control of electric space heating as a flexible resource due to the fact that power consumption for heating and cooling applications constitute a significant share of the total electricity consumption in Denmark. In a Nordic perspective the potential is even greater as almost 50% of the electricity consumption in households is utilised for space heating and cooling and for heating of domestic hot water. Consequently, there exists a significant potential in the integration of power consumption for heating purposes in households for demand response in the Nordic power system.

This thesis describes how power consumption in an intelligent building can be controlled and coordinated with other entities by aggregating the unit into a so-called *virtual power plant*. This approach is demonstrated by telecontrol of the electric space heating in the intelligent building by use of the infrastructure of a commercially running virtual power plant, which has been developed by the Danish energy company DONG Energy. The virtual power plant continuously optimises the power consumption of a portfolio of flexible distributed energy resources with respect to the cost of electricity on the Nordic energy exchange, Nord Pool, or alternatively the flexibility can be sold as an ancillary service to the transmission system operator. In this way, the electricity consumption in households are indirectly integrated into the power market, through the virtual power plant, and a coupling between consumption and the cost of electricity is made.

Field experiments with control of space heating show that electricity consumption for heating can be partially lowered or entirely postponed during peak load hours and thus contribute to a reduced need for transmission capacity in the distribution grid. Moreover, simulations show that at least 20% of the daily electricity consumption for heating in an aggregated unit of households can be shifted from midday to midnight, where there is typically a surplus of renewable generation.

Finally, it is concluded that aggregated electricity consumption for space heating can provide fast, reliable and accurate demand response, and thus provide a high flexibility in the power system. Consequently, electric space heating offers a good technical candidate for demand response in the future power system, especially when taking into account the expected increased utilisation of electricity for space heating towards year 2035, where all forms of centralised heating based on fossil fuels in the Danish energy system are to be phased out and replaced by renewable alternatives.

Summary (Danish)

Fleksibelt elforbrug forventes at spille en stadig større rolle i fremtidens elsystem, hvor en stigende andel af den samlede elproduktion vil komme fra vedvarende energikilder. Idet husholdninger står for næsten en tredjedel af elforbruget i Danmark er det nærliggende at overveje elforbrug fra private husstande som en integreret del af en potentiel fleksibel forbrugsside i fremtidens elsystem. I sig selv er husstande dog for små til at gøre en forskel i det samlede elsystem. Derfor er der brug mekanismer der kan koordinere responset fra talrige enheder; med andre ord, har vi brug for værktøjer der kan aggregere en række små enheder under sig og koordinere disse enheders elforbrug. I denne afhandling undersøges muligheden for at gøre elforbruget fleksibelt i små forbrugsenheder som er forbundet i lavspændingsnettet. Specielt fokuseres der på styring af elvarme som en fleksibel forbrugsenhed, idet elforbruget til opvarmning af husstande i Danmark udgør en betydelig andel af det samlede private elforbrug. I et nordisk perspektiv er potentialet endnu større da næsten 50% af elforbruget i husholdninger går til opvarmning og nedkøling af husstande samt til opvarmning af forbrugsvand. Der eksisterer således et betydeligt potentiale i at integrere elforbruget til opvarmning af husstande som en aktiv spiller det nordiske elsystem.

Denne afhandling beskriver hvordan elforbruget i en intelligent bygning kan reguleres og koordineres med andre enheder ved at aggregere denne som en del af et såkaldt *virtuelt kraftværk*. Dette demonstreres ved at fjernstyre elvarmen i den intelligente bygning fra et kommercielt virtuelt kraftværk, som er udviklet af det danske energiselskab DONG

Energy. Det virtuelle kraftværk optimerer elforbruget i forhold til systemprisen på elektricitet på den nordiske elbørs, Nord Pool; alternativt kan fleksibiliteten sælges som en systemydelse til den ansvarlige for det danske elsystem, Energinet.dk. Dermed integreres elforbruget i husstande indirekte i elmarkedet, igennem det virtuelle kraftværk, og der opstår således en kobling mellem elforbrug og prisen på elektricitet.

Eksperimenter med regulering af elforbruget til elvarme i den intelligente bygning viser, at elforbruget til opvarmning kan delvist sænkes eller helt udskydes i perioder med spidsbelastninger og dermed være med til at sænke behovet for transmissionskapacitet i lavspændingsnettet. Ydermere viser simuleringer, at omkring 20% af gennemsnitsforbruget til elvarme i en aggregeret enhed kan flyttes fra middag til midnat hvor der typisk er en overproduktion af vedvarende energi.

Det konkluderes at aggregeret elforbrug til opvarmning af bygninger kan reguleres hurtigt, driftssikkert og præcist, og dermed tilbyde en høj fleksibilitet i elnettet. Således er elvarme en god teknisk kandidat for fleksibelt elforbrug i fremtidens elsystem, især hvis man tager højde for den forventede stigende anvendelse af elektricitet til opvarmning af bygninger frem mod 2035, hvor varmeforsyningen fra fossile brændstoffer udfases i den danske energisystem og erstattes af vedvarende alternativer.

Acknowledgements

I wish to thank several persons who have aided me during this project by providing both technical or moral support.

First of all, I would like to express my gratitude to my principal supervisor Henrik Bindner, for many inspiring discussions, motivation and for guiding me in the right direction when things – from time to time – looked futile.

I would also like to thank my supervisors in DONG Energy, Klaus Baggesen Hilger and Lars Henrik Hansen; Klaus for providing a part of the funding for this project and for giving me the opportunity for pursuing my Ph.D. degree and Lars Henrik for his supervision and for being a source of inspiration during the project. Additionally, I would like to acknowledge Andreas Bjerre, also from DONG Energy, for his invaluable technical support and many good discussions.

Also, I would like to acknowledge DAWE, Danish Academy of Wind Energy, for providing a part of the funding for this project.

From DTU Compute, I would like to thank Professor Henrik Madsen and Peder Bacher, for the many discussions regarding heat dynamic modelling and for their support for using CTSM and R. Likewise, from DTU Wind Energy I would like to acknowledge the meteorology group for providing weather forecasts as well as historical weather data.

Moreover, I would like to thank Professor David E. Culler for inviting me to University of California, Berkeley, where I did my external stay. Studying at Berkeley University was a memorable experience both professionally and personally, which gave me the opportunity to explore one of the most pristine and beautiful regions of the world.

From Center for Electric Power and Energy (DTU Electrical Engineering), I would like to thank Oliver Gehrke and Professor Pierre Pinson for their invaluable input to methods for aggregation. Also, I would like to express my gratitude to Per Munch Jakobsen for his technical support and Eva Bülow Nielsen for her administrative support during the project.

Finally, I would like to acknowledge the co-founders of the Danish Smart Grid Research Network, who have been a source for inspiration and input to this project.

Last but not least, I would like to acknowledge my family and friends, especially my girlfriend Anette and daughters Karla and Matilde, for their patience and invaluable support. Likewise, I would like to thank Søren Dahl Petersen, for his involvement in the process of reviewing this thesis and for his invaluable suggestions and comments.

Contents

List of Publications

In the following, references using numbers will refer to material that is found outside the work presented in this thesis; these references can be found in the bibliography at the back of the thesis. References using letters – A to G – are referring to publications that have been accepted for peer-reviewed publications during this thesis. These publication can be found in their full length in the end of this thesis.
Paper A to D are considered core publications of this thesis, whereas Paper E, F and G have received minor contributions from this author. Following publications have been written during the project.

[A] Anders Thavlov and Henrik W. Bindner, "A Heat Dynamic Model for Intelligent Heating of Buildings", presented at the *International Conference on Applied Energy*, Suzhou, China, 2012. A revised version has been accepted for publication in *International Journal of Green Energy, Volume 12, issue 3, 2015, Special Issue: Innovative Research for Sustainable Energy Systems*

[B] Anders Thavlov and Henrik Madsen, "A Stochastic Model for an Office Building with Air Infiltration", This paper has been accepted for publication in the *International Journal of Sustainable Energy Planning and Management.*

[C] Anders Thavlov and Henrik W. Bindner, "An Aggregation Model for Households Connected in the Low-voltage Grid using a VPP Interface", presented at the *IEEE Innovative Smart Grid Technologies Conference*, Copenhagen, Denmark, 2013.

[D] Anders Thavlov and Henrik W. Bindner, "Utilization of Flexible Demand in a Virtual Power Plant Set-Up", This paper has been accepted for publication in *IEEE Transactions on Smart Grid*, Volume 6, issue 2, 2015.

[E] Yi Zong, Daniel Kullmann, Anders Thavlov, Oliver Gehrke, and Henrik W. Bindner, "Application of Model Predictive Control for Active Load Management in a Distributed Power System With High Wind Penetration", Published in *IEEE Transactions on Smart Grid*, Vol. 3, No. 2, June 2012.

[F] Yi Zong, Daniel Kullmann, Anders Thavlov, Oliver Gehrke, Henrik W. Bindner, "Active load management in an intelligent building using model predictive control strategy", presented at the *IEEE PES PowerTech*, Trondheim, Norway, 2011.

[G] Yi Zong, Lucian Mihet-Popa, Daniel Kullmann, Anders Thavlov, Oliver Gehrke, Henrik W. Bindner, "Model Predictive Controller for Active Demand Side Management with PV self-consumption in an intelligent building", presented at the *IEEE Innovative Smart Grid Technologies Conference*, Berlin, Germany, 2012.

Abbreviations

A/C	Air Conditioning
BMS	Building Management System
BRP	Balance Responsible Party
CBRP	Consumption Balance Responsible Party
CHP	Combined Heating and Power
COP	Coefficient of Performance
CTSM	Continuous Time Stochastic Modelling
CVPP	Commercial Virtual Power Plant
DER	Distributed Energy Resource
DR	Demand Response
DSM	Demand Side Management
DSO	Distribution System Operators
EV	Electric Vehicle
FCD	Frequency Controlled Disturbance reserve
FCNO	Frequency Controlled Normal Operation reserve
GLPK	GNU Linear Programming Kit
ICT	Information and Communications Technology
I/O	Input and Output
LU	Local Unit
MIP	Mixed Integer Programming

MPC	Model Predictive Control
NOIS	Nordic Operational Information System
PBRP	Production Balance Responsible Party
QP	Quadratic Programming
RES	Renewable Energy Source
RMSD	Root-Mean-Square Deviation
RTU	Remoter Terminal Unit
SCADA	Supervisory Control And Data Acquisition
SGAM	Smart Grid Reference Architecture
TSO	Transmission System Operator
TVPP	Technical Virtual Power Plant
UML	Unified Modelling Language
VPN	Virtual Private Network
VPP	Virtual Power Plant

Nomenclature

η	Coefficient of Performance (COP)
τ	Time step length
Φ_h	Heat input
Φ_s	Solar irradiance
A_w	Effective area of window
C	Heat capacity
C_i	Capacity level at time step i
D	Duty cycle
i	Time step
P_i	Power at time i
P_{min}	Minimum power
P_{max}	Maximum power
P_{up}	Power for up regulation
P_{down}	Power for down regulation
$\dot{Q}$	Rate of heat transfer
R	Thermal resistance
S	Aggregator setpoint
t	Time
T	Temperature
$\boldsymbol{T}$	Temperature state vector

T_{min}	Minimum temperature
T_{max}	Maximum temperature
T_s	Length of time step
u	Heat transfer coefficient (U-value), [$^{W}/_{m^2\,°C}$, $^{W}/_{m^2\,K}$]
U	Thermal conductance, [$^{W}/_{°C}$, $^{W}/_{K}$]
$\boldsymbol{U}$	Input vector to state space model
W_{spd}	Wind speed, [$^{m}/_{s^2}$]

Chapter 1

Introduction

1.1 Background

During the past three decades, the Danish power system has gone through a tremendous transformation: from being a power system that was almost entirely based on centralised power generation, more than half of the domestic electricity supply now comes from a broad range of diverse distributed energy sources (DERs). Originally, the main driver for the transformation of the power system was to increase the security of energy supply. However, within the last two decades the driver has changed towards reducing CO_2 emissions in the Danish energy system and to be a pioneering country for development of green technologies. After the first oil crisis in 1973, where the price of oil grew fourfold, the western world realised their strong dependency on the import of foreign oil, primarily from the Middle East. Many western countries sought to reduce this dependency by investing in nuclear power. In Denmark, however, there was a strong public opinion against nuclear power, which manifested itself in a political will to instead pursue a green energy alternative. Through the 1980s and especially the 1990s, wind power generation was extensively developed on land. During this period, the role of wind power changed from being a negligible source of electricity to be a considerable contributor to the Danish power supply, and at the turn of the millennium wind

power covered more than 10% of the domestic demand. From the turn of the millennium until today, the development of wind power has continued especially offshore, such that the wind power capacity has more than doubled. In 2013, wind power accounted for more than 35% of the total installed generation capacity and in 2014 nearly 40% of the domestic electricity supply was covered by wind power alone [1]. Table 1.1 presents the development of the Danish power system from year 2000 to 2013.

	2000	2005	2010	2011	2012	2013
Installed wind power capacity [MW]	2,390	3,128	3,802	3,952	4,163	4,810
Installed large-scale power plant capacity [MW]	8,160	7,710	7,175	7,175	7,175	5,693
Total installed capacity [MW]	12,598	13,088	13,450	13,603	14,212	13,550
Wind power capacity penetration [%]	18.97	23.90	28.27	29.05	29.29	35.50
Large-scale power plant penetration [%]	64.77	58.91	53.35	52.75	50.59	42.01
Wind energy production [GWh]	4,241	6,614	7,809	9,774	10,270	11,123
Renewable energy production [GWh]	5,572	9,813	12,430	14,181	14,834	15,989
Gross domestic supply [GWh]	35,109	35,778	35,739	34,868	34,439	34,224
Wind energy share of supply [%]	12.08	18.49	21.85	28.03	29.82	32.50
Renewable energy share of supply [%]	15.87	27.43	34.78	40.67	43.07	46.72

Table 1.1: Electricity generation and consumption in the Danish power system from 2000 to 2013. Source: Danish Energy Agency [2], [3] and [4].

From the table is seen that since year 2000 the wind power share of the domestic electricity supply has increased from 12% to more than 30%. Likewise, renewable generation has increased with more than 150%, now covering more than 40% of the domestic supply. The rapid development of wind power is expected to continue in the coming decades, in particular with the ambitious climate and energy plan for a complete phase-out of fossil-fuels in the Danish energy supply, which was presented by the Danish government in 2011 [5]. The plan consists of four milestones to be achieved in 2020, 2030, 2035 and 2050, respectively. In 2020, half of the domestic electricity consumption should be covered by wind power. By 2030, coal in power generation should be completely phased-out, and by 2035 all heat and electricity generation should come entirely from renewable energy sources (RESs). Finally, in 2050 the gross domestic energy consumption, i.e. for electricity generation, heating, transport and industry, should be covered entirely by RESs.

In parallel to the development of wind power, a large number of small-scale combined heating and power (CHP) plants were constructed in Denmark. Typically, these CHP plants were founded as cooperatives for providing local district heating only, but were producing electricity as a by-product. Today there are more than 500 small-scale CHP plants generating more than 10% of the electricity in Denmark. The development of CHP generation, together with generation from centralised power plants, wind and autoproducers, is depicted in Figure 1.1, where both the actual and share of the total electricity generation by source are plotted. The two plots show that from being a negligible source of power generation in 1980, decentralised power generation is now a major contributor to the power generation and that it today accounts for approximately 50% of the total electricity production. On the contrary, during the period from 1994, when the capacity of centralised large-scale power plants peaked, to 2013 the installed capacity of centralised power plants has diminished by almost 40%. This tendency is expected to continue as fossil based power generation is being replaced by renewable energy sources.

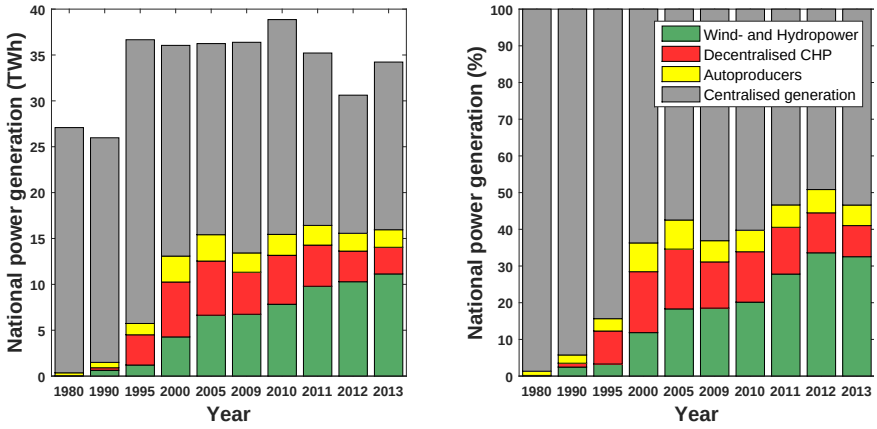

Figure 1.1: Actual electricity production by source (left) and share of electricity generation (right) in Denmark from 1980 to 2013. Source: Danish Energy Agency [4].

The shift from an entirely centralised power production to a more decentralised power generation puts a high pressure on the conventional large-scale units still in operation. These units have traditionally provided power system services, like provision of regulating power, reserve capacity and voltage control. Hence, as the number of large-scale units is being reduced and their overall capacity is diminishing, the need to find other solutions for providing the same essential services is critical. DERs in general, and especially RESs, does not offer the same level of control as traditional large-scale fossil based power plants and they will have a difficult task in delivering the power system services that are currently being provided by large-scale power generating units. There are, however, some ongoing projects investigating how aggregation of DERs into virtual power plants (VPP) can be utilised for providing power system services [6].

The penetration from wind power is expected to increase the coming years, consequently making the output of the generation side of the power system even more intermittent and less predictable than today. Merely balancing the 30% of wind power generation that is present today is stressing the power system from time to time. This is reflected

in the prices on electricity, which are highly dependent on wind power generation in the Danish power system. This is illustrated by the plots in Figure 1.2 where the duration curves for the yearly spot price of electricity in the western part of Denmark (DK1) are plotted for 2011 to 2014.

From Figure 1.2 (a) is seen that the average power price was significantly higher in 2011 compared to 2012, 2013 and 2014 (47.96 €/MWh, 36.33 €/MWh, 38.98 €/MWh and 30.67 €/MWh, respectively). This was primarily caused by a large generation from wind and hydro power in the Nordic power market from 2012 to 2014. Likewise, in Figure 1.2 (b), which shows the highest 5‰ of the duration curve, is seen that negative prices were occurring increasingly more frequent from 2011 to 2014 (17, 38, 45 and 53 hours with negative spot prices, respectively). Similarly, prices over 100 €/MWh are being observed more frequently after 2011 (2, 46, 7 and 4 hours, respectively). On June 7th 2013,

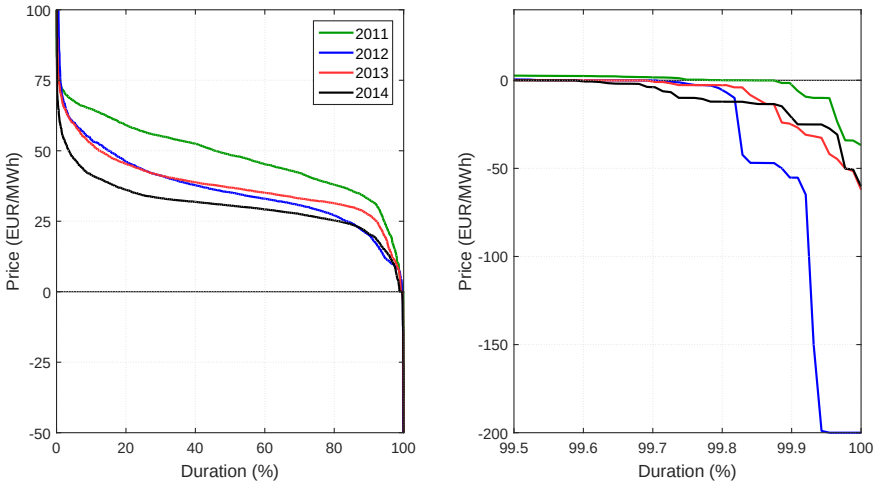

(a) (b)

Figure 1.2: Yearly price duration curves for hourly spot prices for the western part of Denmark (DK1). Source: Nord Pool Spot [7].

the power price peaked in the power market for the western part of Denmark (DK1), with a price of 2000 €/MWh, compared to the average price of less than 40 €/MWh. This extreme power price was caused by the absence of wind power generation and two large-scale power plants and an interconnector were down for maintenance. If balancing the 30% of wind power generation is causing such large fluctuations in the power system, how will it influence the power system when 50% – or even more – of the electricity generation comes from RESs?

A solution to the increased variation and intermittency in the Danish power supply is to reinforce the electrical interconnections to the neighbouring countries. This would allow a larger amount of renewable electricity to be transmitted over longer distances when there is excess generation, and likewise imported when there is a generation shortage from RESs. As an example, Denmark has relied on long term power balancing using pumped hydro power in Norway. However, as the neighbouring countries to Denmark are also increasing their renewable energy generation capacity, better interconnections might not be the right – or whole – solution, and we might just end up in replacing one dependency with another. Instead, we should rethink how we generate, consume and distribute electricity, and the paradigm of "demand-driven supply" should be replaced by "supply-driven demand", or more likely somewhere in-between. It is therefore essential that we rethink the role of the demand side in the power system and integrate it as an active player for balancing power. An increased usage of information and communications technologies (ICT) in the power system should be used to implement a flexible demand side for controlling the balance between power generation and consumption, thus achieving a reliable and stable power system which is independent of foreign resources.

1.2 Demand Response

Demand response (DR) is expected to play a key role for balancing power in the future power system, where a major part of the electricity generation will come from intermittent renewable energy source. The idea of DR originates from the late 1970s and was first introduced as a concept in 1980 by Schweppe et al. in the paper "*Homeostatic Utility Control*" [8]. In the paper, the present – and now current – power system philosophy of "supply follows demand" is criticised for being inefficient for several reasons: for instance, the need for a large reserve capacity due to a large ratio between peak and average demand. Instead, Schweppe et al. suggests that another approach is taken where "load follows supply". This is to be implemented by broadcasting a time-varying spot price for electricity to customers from a virtual marketplace, where the price is settled based on supply and demand. The measured power usage of the customer is sent back to the marketplace, where the consumption is multiplied by the price and integrated, thus providing an automatic billing service. In Figure 1.3 is depicted how Schweppe et al. envision a 24 hours scenario of DR from a residential household. Even though this scenario was conceived more than 30 years ago it is not far from how scientists today envision how DR could be implemented in a future scenario. Despite DR programs have already been implemented in some power systems, dynamic DR from small units, as envisioned by Schweppe et al., have never had a major breakthrough.

When considering DR from households, electricity consuming appliances can be separated into three categories. These categories are presented in Table 1.2 together with some typical examples. First, there are thermal applications, which are typically associated with a thermal energy storing medium. This medium can serve as unidirectional energy storage and in this way be utilised for shifting electricity consumption away from hours of peak demand. Typically, these media have long time constants which makes them indifferent when consumption is applied as long as a given amount of energy is provided within a given time period. Second, there are residential appliances running processes for the end-user, which are typically unconcerned

A future residential energy-control scenario

7 a.m.
- Computer displays its energy use plan for next 24 hours, based on predicted weather and spot price patterns and on customers average use, which the computer has learned.
- Owner modifies plan because guests are expected for dinner and to spend the night.

10 a.m.
- Computer receives revised weather forecast and then changes its air-conditioning strategy for the rest of the day.

3 p.m.
- Major storm knocks out many power plants and transmission lines.
- Utility's market coordinator seeks to shed loads. Owner's computer responds by turning off air-conditioning.

3:05 p.m.
- The cost of electricity increases sharply because of equipment knocked out of service by the storm.
- Computer reacts to high prices by turning off everything except the refrigerator, freezer, and itself.
- Owner instructs computer to air-condition the living room starting at 6 p.m., in spite of the very high prices.

8 p.m.
- Power system restoration proceeds rapidly.
- Electricity price starts to fall and is predicted to be at a minimum at 3 a.m.
- Owner instructs computer to have guest room and master bedroom air-conditioned by midnight.

12 midnight
- Owner and overnight guests retire.

3 a.m.
- Computer starts to run dishwasher and laundry machines.
- Latest price and weather forecasts cause computer to start cooling parts of the house, so the house can stay cool during the next afternoon.

4 a.m.
- Second storm causes major power system disturbances that result in system frequency swings.
- Computer cycles electrical use in phase with frequency (use drops when frequency drops).

Figure 1.3: Future residential demand response scenario as envisioned by Schweppe et al. in 1982, [9].

Thermal applications	Batch applications	Non-flexible applications
Refrigerator, freezer, space heating and water heating	Dishwasher, washing machine and tumble dryer	TV, cooking appliances, lighting, computer

Table 1.2: Categorisation of demand response applications in residential households.

when the process is run, just that it has finished before a given point in time. These processes are named batch applications in Table 1.2. Third, there are appliances whose consumption can not be shifted at all due to the high time dependency of the application.

The characteristics of the thermal- and batch applications, presented in the two first columns are fundamentally different in the way they consume electricity. Thermal applications are continuously running processes that require a fixed amount of energy over a given amount of time, which is defined by the temperature constraints and time constants of the thermal system. Batch processes are also running continuously, however, once a batch process has been started it can not be stopped until the process has terminated. When a batch process has finished, it has to be manually reset by the user before it can be restarted. In Section 3.2, a more comprehensive analysis of DR applications in residential households is given.

1.2.1 Implementation of demand response

The motivation for enrolling end-users in DR programs varies with power system infrastructure. In most cases, a reduction in peak demand is wanted: first of all to reduce the peak load in the distribution grid, thus reducing the investments needed to provide a high distribution capacity which is only utilised a few hours – if not minutes – during the day, but also to reduce the need for expensive reserve

generation capacity. In France, a two tariff system is used to smooth electricity consumption during the day, thus allowing nuclear power plants, which are supplying more than 70% of the electricity, to be run with a nearly constant output. Here, the customers that are enrolled in the DR program are given a discount on electricity consumed in the time interval from 10.00 p.m. to 6.00 a.m. Likewise, in the United Kingdom (UK), a two tariff system has been implemented, where a 20% discount is given on electricity consumption during seven hours of night time[1]. The night tariff is mostly offered in a fixed time interval; however, in some areas of the UK the starting time for the seven hours period is partly dynamic. Here, the period is initiated using British Broadcasting Corporation's (BBCs) radio broadcasting network to send a starting signal to teleswitchers to switch to the night tariff. Moreover, a new ten hours DR program[2] has been introduced to end-users, where the ten hours is split over three off-peak periods during the day, e.g. from 4.30 a.m. to 7.30 a.m., from 1.30 p.m. to 4.30 p.m. and from 8.30 p.m. to 12.30 a.m. Finally, one of UKs largest utility companies is offering free electricity on Saturdays to their customers in the United States (US), to shift demand from weekdays to weekends. Currently, the company is considering implementing this price scheme in the UK as well.

It can be discussed whether the examples above is "*dynamic*" DR as envisioned by Schweppe et al., since they all rely on a more or less static tariff system, i.e. night time versus daytime. Some more dynamic examples have been implemented in the US where a direct control approach is taken. For example, customers in the Kandiyohi Power Cooperative in Minnesota are offered a discount on their energy bill if they allow their water heater to be controlled by the utility company. Likewise, in California, the largest electric utility company is enrolling customers in demand response programs, where they offer a discount on electricity if they allow the utility company to cycle or even switch off their central air conditioning unit for up to six hours during the day. Finally, in some countries, e.g. Italy and France, a

[1] Economy 7 tariff system
[2] Economy 10 tariff system

contractual peak demand is imposed on private customers to enforce a cap on power consumption in the distribution grid. This has led to several aggregation projects, where cooperatives of households are aggregated to fulfil an aggregate contractual peak demand, by relieving each other when a high demand is needed [10].

1.2.2 Demand response from heating and cooling applications

The majority of DR programs offered to private end-users are addressing heating and cooling applications. In these applications, the combination of a high heat capacity and resistance against heat loss stabilises temperature fluctuations from a given reference, even when left without power for a short period. Such systems are said to have a high thermal inertia, meaning that it can sustain its own temperature for shorter periods of time. This, together with the estimates of space heating and cooling of buildings account for approximately half of global energy consumption in building [11], makes heating and cooling applications an ideal source for demand response.

Energy consumption for heating – both space and water – is by far the largest contributor to energy consumption in Danish households. In 2011, more than 80% of the annual energy consumption in Danish households were utilised for space and water heating [2]. District heating is by far the largest contributor to space heating, with 62% of all Danish households being heated by district heating [2]. The second largest contributor is central heating based on fossil fuels, with 15% being heated by natural gas and 12% by oil. Currently, only 7% of all occupied households use electricity for space heating, either by use of resistance heaters or heat pumps [12]. The number of households using electricity for space heating might seem small, but with an average annual energy consumption of approximately 15,000 kWh for a detached household used for space heating alone [13], the annual consumption from space heating is almost 3 TWh, or equivalent to an average heat load close to 500 MW during the eight months of heating season in Denmark. Assuming an average coefficient of

performance (COP) of around 1.5, the electricity consumption from electrical heating is approximately 300 MW. In addition to that, in [14] it is estimated that additionally 200.000 households, equivalent to almost 10% of the Danish residential building stock, will convert from fossil based central heating to heat pumps by 2025. This development is expected to continue towards year 2035, where fossil fuels are to be completely phased out of the heat supply, and potentially 700,000 households will have to convert from oil or gas to either a renewable alternative or district heating. Since most households currently heated with central heating are located in rural areas, and the installation costs of district heating or gas infrastructure, therefore, is substantially high, most of these households are expected to convert to heat pumps. To create an incentive for the conversion from oil and gas burners to electric heating, a 42% tax reduction on electricity for heating was enacted by the Danish parliament in 2012 [15]. Contrary, taxation on district heating is being increased, making this solution less attractive relative to the electric solutions based on heat pumps.

In a Nordic perspective, electric space heating is much more widespread. Figure 1.4 shows how electricity was utilised in the residential sector in the Nordic countries in 2010. The figure shows that in total 404 PJ of electricity was used in the residential sector of which 120 PJ was used for space heating (30%), 47 PJ for water heating (12%), 19 PJ for cooking appliances (5%), 17 PJ for space cooling (4%), 47 PJ for lighting (12%) and 155 PJ for appliances (38%). Consequently, close to 50% of the electricity used in the residential sector was used for thermal applications, i.e. space heating, water heating or space cooling. This implies that there is an immense potential for utilising thermal applications for DR in the Nordic power system. For buildings in general, the total share of electricity used for thermal applications is closer to 40%, but still the potential is large. Furthermore, an increased integration of heat pumps in the Danish power system is going to increase the share of electricity used for space heating.

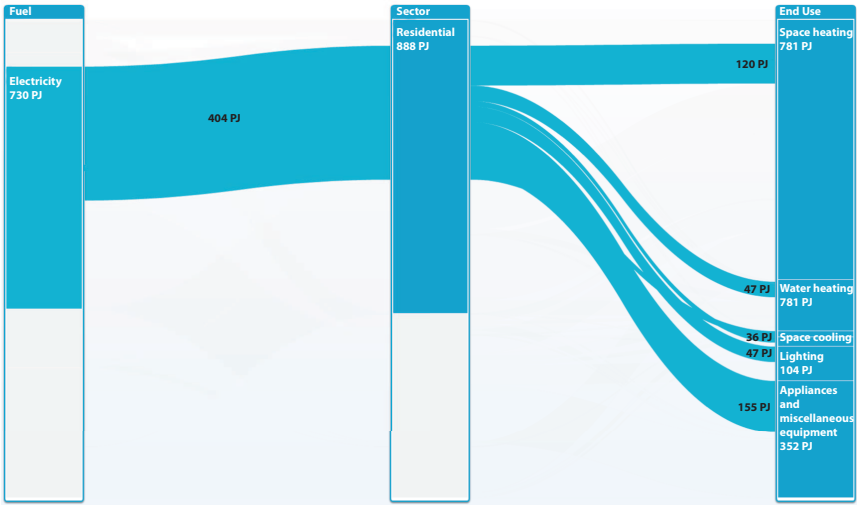

Figure 1.4: Utilisation of electricity in the residential sector in the Nordic countries 2010. Source: IEA data visualisation [16].

The benefits of using space heating for demand response purposes are many: firstly, the electricity consumption for space heating correlates well with wind power generation, which is nearly twice as high during the windy winter months compared to summer. This is illustrated in Figure 1.5 where the annual average distribution of wind power generation and consumption are plotted. Furthermore, the figure shows that nearly one third of the wind power is indeed generated during winter, i.e. in December, January and February. Secondly, the heat capacity of building structures is relatively high compared to other applications. Typically, the total heat capacity of a single-family detached house, build from bricks or concrete, is approximately 10–15 kWh/℃. Consequently, the thermal inertia of buildings is generally quite high, which means that heating can be postponed for up to a few hours without having a significant impact on the indoor temperature.

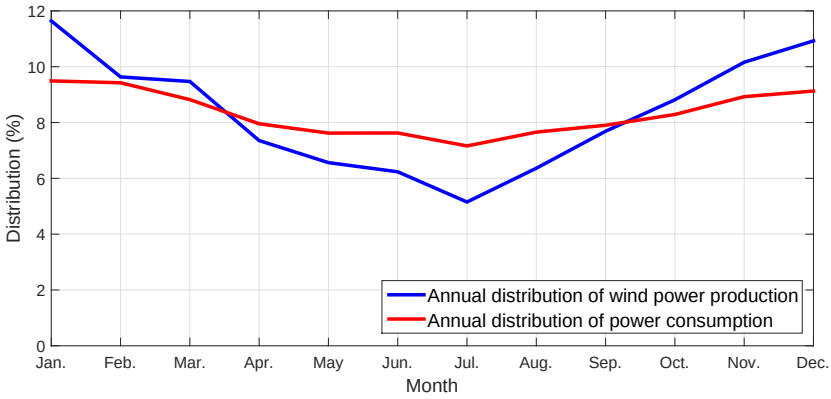

Figure 1.5: Annual average yearly distribution of wind power generation and power consumption in Denmark (2005–2014). Source: Energinet.dk [17].

1.3 State of the Art

As previously outlined, currently DR is being utilised in many power systems. However, often DR programs are implemented using fixed time of use tariffs and thus the response is rather static with respect time. Such an approach would most likely not be able to control consumption with respect to the intermittency of renewable electricity generation, and hence will not be considered as state of the art for the work presented in this project.

As outlined in Section 1.2, the idea of DR is not new, but the concept of dynamic demand response has never had a real breakthrough as a service provided by residential households. However, with an increasing interest in smart grids and a declining cost of communication and microcontrollers, the interest in dynamic demand response has been revived.

Within the last decade, the potential for demand response has been investigated in several projects. For instance, in the Olympic Peninsula project [18], which was a large-scale field demonstration carried out in the state of Washington (US), where many diverse loads, including

112 households, were being controlled to deliver power system services in the low voltage grid. Likewise, in the European project EcoGrid EU [19], 2000 households on the Danish island Bornholm are being controlled to balance power in an isolated power system with up to 50% wind penetration. A common characteristic of these projects is the utilisation of a broadcast price signal to incentivise changes in electricity consumption.

An alternative approach to price based control is to aggregate units into a VPP, where the units internally are controlled directly by use of setpoints as a control reference for power generation or consumption. Such an approach is used in the European Fenix project [20], where several DERs in the distribution grid are being controlled by sending a real time control setpoint. In this project, it has been demonstrated that ancillary services, like voltage control and provision of tertiary reserve, can be delivered in the distributions grid. Likewise, in the Danish Cell Controller Pilot Project [6], DERs were aggregated and controlled as a VPP, using setpoints for both active and reactive power generation. In both of these projects, emphasis has been placed on aggregation of larger generation units, e.g. wind turbines and CHPs, while control of small consumption units has been neglected.

In England the company Open Energi [21], is providing autonomous primary control to the TSO using an aggregate portfolio of DERs, e.g. water treatment plants and supermarket refrigeration system. Here, the units are equipped with a frequency meter and local control hardware, which enable the DERs to be utilised for primary frequency reserve. Also in research projects, DR is provided using autonomous control based on local measurements of the frequency. For example, in [22], a thermostatic controller for refrigerators and space heating has been designed to deliver DR based on local frequency measurement.

So far the interest in using a direct control approach, i.e. by use of a power setpoint, for controlling small-scale consumption entities connected in the low voltage grid, e.g. households, has been limited. This is most likely caused by the relatively high cost of establishing

two way communication and implementation of a local controller compared the simplicity of broadcasting a price signal. Furthermore, the price based approach creates a clear separation of responsibility, consequently reducing the liability of the controlling entity. However, the cost of both communication and embedded systems has decreased significantly within the last decade, why a direct control might become profitable in time. Especially, if the direct control approach reaches the critical mass needed to start mass producing building management systems (BMS) software and flexible appliances targeting DR in the low voltage grid. An analogy to this, is the development of the GPS chip, which was an exclusive product just a decade ago, whereas today it is integrated with very low costs into a wide range of common products, e.g. smart phones, bicycle computers, watches and even clothes.

1.4 Thesis Objectives

In this project, a method for aggregation of households, which are connected in the low voltage grid, into a VPP is investigated. The electricity consumption of a building is integrated into a commercial VPP and DR from space heating is provided based on a given power setpoint for requested consumption. Feedback on the indoor temperature is sent back to the VPP to provide an abstract measure for available flexibility of the household. To this author's knowledge, electric space heating in residential buildings has not been utilised for DR using a VPP setup in other projects.
Preceding this project, the following objectives were defined:

1. To develop a method for integrating entities connected in the low voltage network as parts of a VPP to provide services to the power system. The entities will include households with active control of the consumption and households with both active control of the consumption as well as power production from for example micro CHP. Physical limitations, user constraints and participation will be taken into account such as comfort level and willingness to provide flexibility.

2. To develop a simulation model of a VPP in an appropriate time scale that includes models of the households, user decisions and aggregation and deaggregation.

3. Implement an interface between DONG Energy's VPP infrastructure and SYSLAB and make example implementation of integration of household.

The first and third objective are addressed in Paper D, while Paper A and B presents two heat dynamic models – a linear and non-linear – for prediction of the heat load of a building. Finally, Paper C addresses the second objective, where control of the aggregated heat loads of 100 households in a distribution system is simulated. The aggregator optimises the aggregate consumption of the households with respect to a received setpoint from an operator or a higher level aggregator. Furthermore, the aggregator respects local constraints on the indoor temperature in each individual household, which are specified be the residents of the building. The heat dynamic models presented in Paper B have formed a foundation for simulation of each individual building.

1.5 Thesis Contributions

The overall scientific contribution of this thesis is an implementation and demonstration of a method for utilisation of flexible demand from detached households connected in the low voltage grid. The implemented method covers a wide range of scientific topics which are reflected in the diverse contributions comprising system identification of DERs, optimal dispatch in a portfolio of aggregated entities and software implementation. In general the scientific contributions from this project can be separated into following categories:

System identification of DERs

Formulation of a series, both linear and non-linear, heat dynamic models of electric heat loads in detached households using a stochastic modelling approach. Such an approach is also called grey-box modelling which combines prior physical knowledge about the system with statistics on collected data. The models will be used for both forecast and control of heat loads.

Formulation of portfolio dispatch problem

Formulation of a mathematical problem for optimisation of a portfolio of electric entities. The dispatch problem is utilised for allocation of power among a number of DERs and can be utilised on both residential level (BMS) and aggregator level (VPP).

Development of a simulation framework of a VPP

A simulation framework for estimation of the flexibility in detached households has been implemented in MATLAB. The framework implements the aforementioned DER models and dispatch problem which, together with actual building data, can be used to estimate the aggregate flexibility of a portfolio of detached households that are heated by either resistive- or heat pump based heating.

Conduction of demand response experiments

During this project, a series of DR experiment were conducted using an intelligent office building on the DTU Risø premise and DONG Energy's VPP called Power Hub. The motivation for using Power Hub was the availability of communication hardware developed by DONG Energy as well as access to their VPP framework and technical support.

Furthermore, a large share of the work carried out during this project has been placed on implementing an experimental platform that can be used to facilitate DR experiments. Hence, a non-academic contribution is:

Implementation of an experimental platform for demand response experiments

A platform for demand response experiments has been implemented in the BMS of an intelligent office building. The platform handles communication with Power Hub and provides optimal dispatch of the electric heat loads in the building with respect to the temperature distribution inside the building and temperature constraints specified by the users of the building.

1.6 Thesis Scope

As the title of this thesis implies, the scope of this thesis is confined to entities connected in the low voltage grid, which is assumed to comprise the distribution grid below 10 kV. Naturally, this excludes most industrials entities from the scope of this thesis, since most of these are connected at higher voltage levels. To further limit the scope, a deliberate decision between commercial or private entities had to be made in the initial phase of this project. Considering the physical limitations and possibilities that available research facilities offer for implementation and demonstration, commercial entities was excluded from the scope. Furthermore, DR from commercial applications is a research topic that has received increasing attention during the last decade, whereas DR from private applications is still a more open research area. Consequently, the focus of this thesis will be limited to private detached households connected in the low voltage grid.

A special emphasis will be placed on heating applications, due to the high amount of electricity utilised for space and water heating in the Nordic countries, cf. Figure 1.4. Despite electricity consumption for space cooling and air conditioning (A/C) has significantly increased during the last decade, these will be neglected in the following, since the concepts are more or less the same as with heating. Furthermore, the methodology for utilisation of DR from heating, as presented here, can straightforwardly be extended to include space cooling applications as well.

Even though electric vehicles (EV) might be considered a part of the domain of private entities, EV will not be considered in the following. Although such units can greatly increase the flexibility of a household, the capabilities of EVs deviate significantly from the electricity consumption in households, especially if including vehicle-to-grid (V2G) operation, where power can be transferred back into the grid. Moreover, the consumption – and potential generation – from EVs is location specific whereas households have a fixed location in the distribution grid. Readers who are interested in integration and intelligent controls of EVs are instead referred to [23].

Finally, in this thesis the focus is entirely placed on DR of real power consumption. However, it is known from literature [24] that appliances with electric motors, which are often found in washing machines and heat pumps, have a high consumption of reactive power during start-up. The effects of reactive power consumption from residential appliances are neglected in the following. Readers that are interested in reactive power and voltage control in distributed power systems are instead referred to [25].

1.7 Thesis Outline

This thesis is organised as follows: Introductory, Chapter 2 gives an overview of the Danish power system and the Nordic power market. Following, in Chapter 3, a description of the future smart grid is given together with a comprehensive analysis of DR and flexible appliances that are typically found in residential households. Next, Chapter 4 gives a description of the VPP and the intelligent office building, namely Power Hub and PowerFlexHouse that were used for demonstration of DR. This chapter also presents how the integration of PowerFlexHouse into Power Hub was implemented. In Chapter 5, theory behind heat dynamic modelling of buildings is introduced and a technique for estimation of model parameters is presented. Furthermore, this chapter presents the heat dynamic model that has been identified of PowerFlexHouse and the related model parameter estimates. Next, Chapter 6 presents the simulation framework that was developed during this project for estimation of the aggregated flexibility of households connected in the low voltage grid as well as some simulation results. Finally, in Chapter 7 the results of this thesis are summarised and discussed, and a conclusion is given in Chapter 8.

Chapter 2

The Danish Power System and Nordic Power Market

In this chapter, the Danish power system and the Nordic power market are described. Knowledge about the concepts and infrastructure of these two systems is essential for the understanding of the role of the commercial virtual power plant Power Hub, which is described in the following chapter. This chapter has been included for completeness of the thesis; readers with a detailed knowledge about these two systems can skip this chapter or skim through it for a brush up.

2.1 The Danish Power System

The power system in Denmark comprises two separate synchronous power systems: the western part of Denmark belongs to the Continental European synchronous power system and the eastern part of Denmark belongs to the Nordic synchronous power system. Traditionally, these two power systems have been named DK1 and DK2, for the eastern and western power system respectively. This terminology is adopted in the following. Figure 2.1 shows the infrastructure of the Danish transmission system together with a line separating the two synchronous areas. Moreover, typical values of electricity demand and generation in the two power systems are presented in Table 2.1.

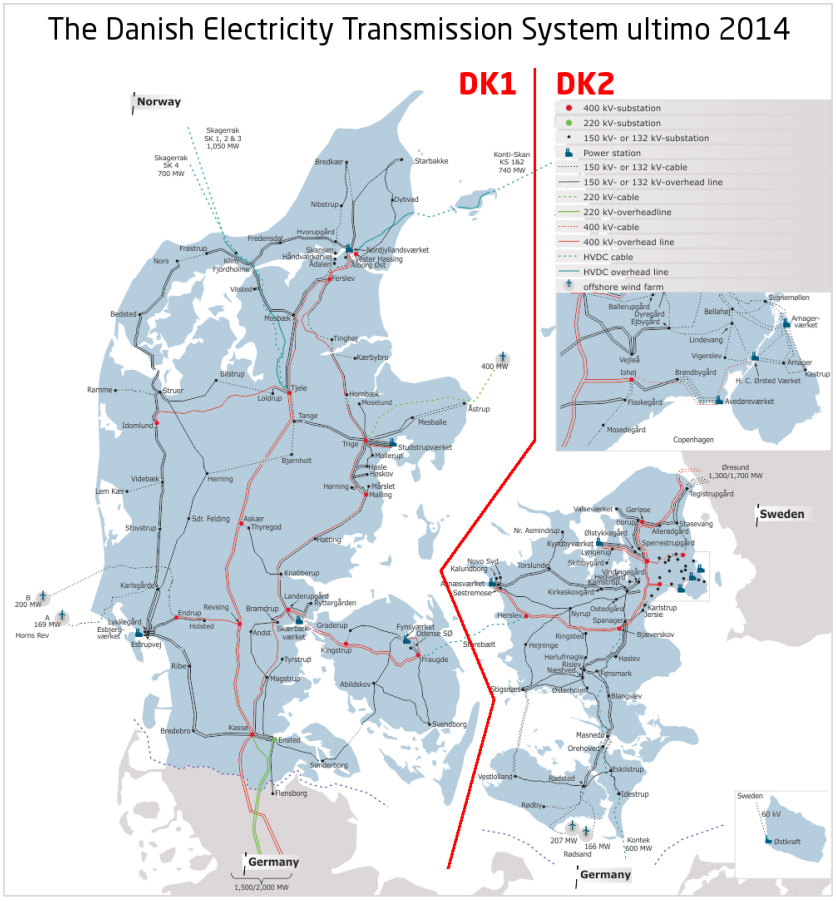

Figure 2.1: Danish power system infrastructure. Source: Energinet.dk [17].

	DK1	DK2
Average power consumption (MW)	2,300	1,520
Annual power consumption (TWh)	20.2	13.3
Annual wind power generation (TWh)	10.3	2.7
Peak demand (MW)	3,550	2,500
Wind power share of annual power generation (%)	51.3	20.5

Table 2.1: Danish power system data (2014). Source: Nord Pool Spot [7].

As seen from the figure, DK1 and DK2 are only directly coupled by one interconnector across the Great Belt, which separates the two power systems. This interconnector has a rated transfer capacity of 600 MW. Moreover, DK1 has interconnections with the power system in Norway (1750 MW HVDC), Germany (1200 MW AC) and Sweden (740 MW HVDC). DK2 is connected to Sweden (1700 MW AC) and to Germany (600 MW HVDC). These interconnectors have been vital for reaching the high penetration levels from wind power that is presents in the Danish power system today, because they allow wind generated electricity, which can not be utilised regionally, to be transferred to neighbouring power systems.

As outlined in the previous chapter, the Danish power system has gone through a comprehensive transformation during the past three decades. Especially, the wind power capacity in DK1 has been increased substantially, due to an abundance of natural resources for wind power generation. This has created a skewed distribution of wind power generation between DK1 and DK2. Population wise, DK1 is approximately 25% larger than DK2, which is also reflected by the annual power consumption and peak demand presented in the table in Figure 2.1. However, the share of wind power is nearly four times higher in DK1 relative to DK2. A consequence of such a high wind power capacity is that wind power generation in DK1 often exceeds consumption. This is illustrated in Figure 2.2, where the wind power generation and consumption are plotted for December 2014.

From the figure is seen that the wind power generation exceeds consumption several times during the month. The surplus of wind power generation is seen to be particular high during the night between the 14th and 15th, where the difference between generation and consumption was almost 1300 MW. Consequently, the interconnectors from DK1 to DK2, Sweden and Norway were almost fully utilised, causing the electricity price to go negative in DK1. Likewise, on December 9th, the wind power generation changed from a 2900 MW deficit to a 900 MW surplus within 12 hours. With an increased expansion of wind power generation in the Danish power system, such situations are expected to occur more frequently, which is also apparent in trend

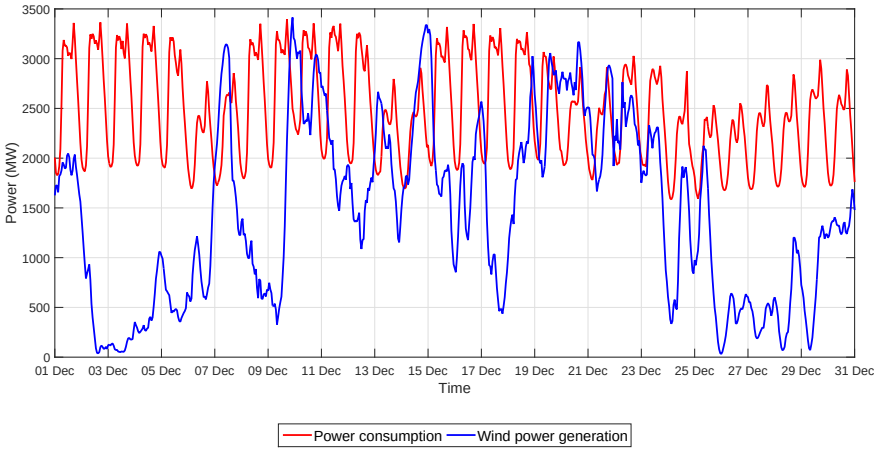

Figure 2.2: Wind power generation and consumption in the western part of Denmark (DK1) in December 2014. Source: Energinet.dk [17].

in the power market for DK1, cf. Figure 1.2. This example illustrates the significance of strong interconnectors to the neighbouring power systems or alternatively the potential of being able to manage the consumption side in the power system.

The Danish transmission system operator (TSO) Energinet.dk is responsible for the operation of the Danish power system. As TSO, Energinet.dk is responsible for the procurement of the services needed to ensure a stable and reliable operation of the Danish power system. Such services are called ancillary services and are bought by Energinet.dk from balance responsible parties (BRPs), responsible for either consumption (CBRP) or production (PBRP) [26]. Ancillary services comprise provision of primary, secondary and tertiary reserves, together with other services like voltage control. In case of a major contingency, which causes a large imbalance between consumption and generation, e.g. an outage of a power plant or a broken interconnector, primary reserves are activated to stabilise the frequency and prevent it from declining further. Primary reserve is typically provided by fast responding generation or consumption units, reacting automat-

ically to changes in the frequency in the power system. Within 15 minutes secondary reserves are activated upon a signal from the TSO to relieve the primary reserve and bring the frequency back to the reference. Following secondary reserve generation, manual (tertiary) reserves are activated to relieve secondary reserves. Figure 2.3 depicts the activation and reliving of the three types of reserves.

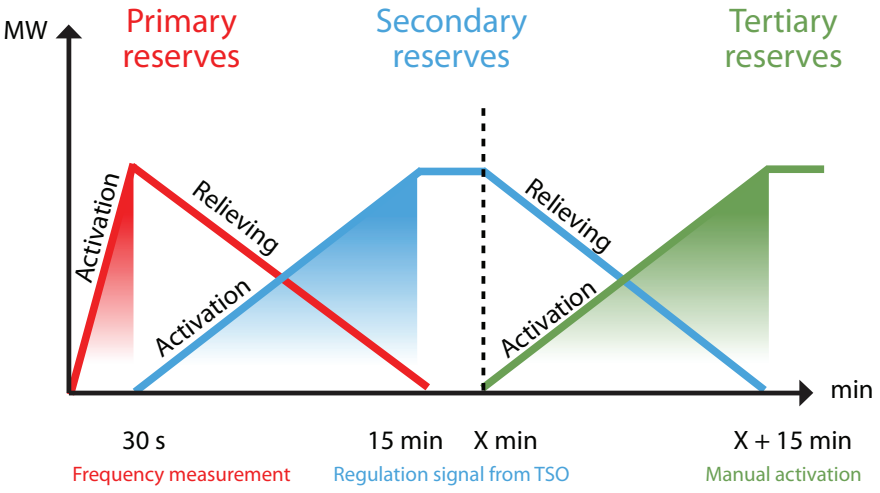

Figure 2.3: Danish power system operating reserves.

Due to the affiliation to two different synchronous power systems, the ancillary services requested in DK1 and DK2 are different. In DK2 there are two types of primary reserves: Frequency controlled normal operation reserve (FCNO) and Frequency controlled disturbance reserve (FCD). The two services are active in different frequency ranges: FCNO provides regulation close to the reference frequency, whereas FCD provides up-regulation when the frequency falls below 49.9 Hz. The latter is mainly intended to be active in events of major system disturbances in the power system, e.g. an outage of a large scale power plant. As FCD only addresses drops in frequency only up-regulation is provided. Secondary reserves are only utilised in DK1 and is activated by a regulation signal send from the TSO. Likewise, manual reserves are activated upon request from the TSO in both DK1 and

DK1. Additionally, there are ancillary services for short-circuit power, reactive reserves and voltage control. These services are exclusively provided by large-scale power plants connected directly to the transmission grid. Table 2.2 and Table 2.3 provide an overview of the ancillary services requested by Energinet.dk and their characteristics, respectively.

Service	DK1	DK2
Primary reserve capacity (Frequency containment)	Primary reserve	Frequency controlled normal operation reserve
		Frequency controlled disturbance reserve
Secondary reserve capacity (Frequency restoration)	Load Frequency Control (LFC)	
Manual (tertiary) reserve capacity (Frequency restoration)	Manual reserve	Manual reserve
Short-circuit power, reactive reserves and voltage control	Large-scale power plants connected in the high voltage grid (>132 kV)	Large-scale power plants connected in the high voltage grid (>132 kV)

Table 2.2: Ancillary services to be delivered to the Danish TSO, Energinet.dk. Source: [27] and [28].

The reserve services presented in Table 2.3 can be provided by both GBRPs and CBRPs, though the latter is rare. As will be outlined in the following chapter, DR from residential households can fulfil the requirements to be utilised as reserve services. However, due to their limited size, they are not allowed to act in the ancillary market by themselves; thus, we need aggregators that can aggregate several small-scale consumption units to reach the minimum capacity that is needed to bid in the market for ancillary services.

Service	Activation range	Size	Response time	Duration	Bid size
Primary reserve	50 Hz ± [20−200] mHz	± 27 MW	50% within 15 s 100% within 30 s	15 min.	> 0.3 MW
Load Frequency Control	Regulation signal from TSO	± 90 MW	Full activation within 15 min.	Continuously	
Frequency controlled normal operation reserve	50 Hz ± 100 mHz	± 23 MW	Full activation within 150 s	Continuously	> 0.3 MW
Frequency controlled distur-bance reserve	50 Hz - [100 − 500] mHz	+25–55 MW	50% within 5 s 100% within 30 s		> 0.3 MW
Manual (tertiary) reserve capacity	Upon request from TSO	+300 MW (DK1) +600 MW (DK2)	Full activation within 15 min.	Continuously	10–50 MW

Table 2.3: Ancillary services characteristics. Source: [27] and [28].

2.2 The Nordic Power Market

Nord Pool Spot manages the exchange for power trading in the Nordic countries. It was established by the Norwegian TSO Statnett in 1993, and with the deregulation and liberalisation of the Nordic power markets through the 1990s, more Nordic countries joined Nord Pool. Today, Nord Pool Spot operates in all the Nordic and Baltic countries and has recently expanded into the German, Polish, British, Dutch and Belgian market too.

The Nordic power market is divided into 15 bidding areas, two in Denmark, five in Norway, four in Sweden and one in Finland, Estonia, Latvia and Lithuania. In each of the bidding areas, the electricity price is calculated on an hourly basis; this is found from the intersection between the supply and demand curves that are generated by the aggregated bids from power producers and consumer respectively. Also, available transmission capacities between adjacent bidding areas are considered when the spot prices are calculated. The two bidding areas in Denmark, correspond to the two areas encompassed by DK1 and DK2, and are called likewise in the Nordic power market.

From the incoming bids of generation a supply curve is generated by sorting the bids in increasing order, such that bids with the lower generation cost appear first, i.e. merit order. In general, bids from the power producers are close to the marginal cost of producing electricity on the generation facility they own. Consequently, when the bids are ranked by merit order, the generation facilities with the lowest marginal cost are typically activated before the others. In Figure 2.4 a typical supply and demand curve are depicted, from which is seen that renewable sources, i.e. wind and hydro power, are the generation forms which are activated first and then comes traditional power generation from nuclear, coal, gas and finally oil. The demand curve in the figure is plotted with a steep slope to indicate that the demand for electricity in the Nordic power market is rather non-flexible, implying that the actors on the demand side are more willing to pay a higher price for electricity than to change their electricity consumption. In general, the Nordic power market lacks active participation

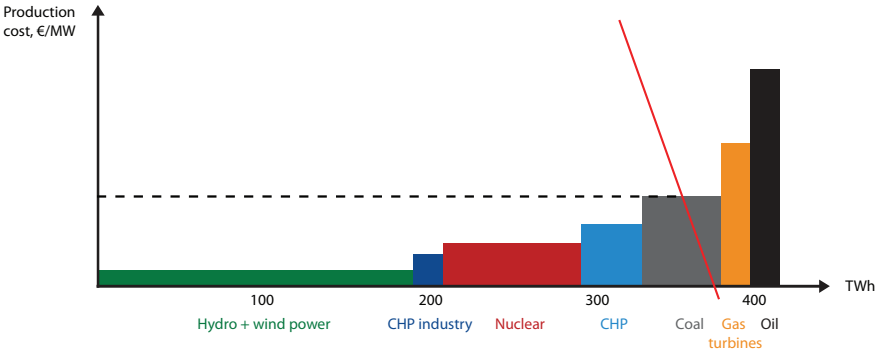

Figure 2.4: Typical merit order in the Nordic power system.

of the demand side, which means that it is mainly the supply side that influences the price of electricity.

The Nordic power market is dominated by a high electricity production from RESs; favourable terrain conditions in Sweden and Norway, permits a large amount of electricity to be produced from hydropower and in Denmark a large share of the electricity generation comes from wind energy sources. Table 2.4 presents the annual share of electricity consumption being covered by renewable energy sources in each of the Nordic countries. Moreover, the last row presents the weighted average of renewable generation by population. The table shows that in 2012 more than half of the Nordic electricity generation came from renewable sources, which is a 17% increase from 2004. Due to the high level of generation from RESs, the price of electricity in the Nordic market is highly dependent on the weather conditions, i.e. annual average rainfall in Norway and Sweden and wind speed and direction in Denmark. On an annual scale the electricity price varies with the inflow of water into the hydro reservoirs in Norway and Sweden, while the intermittency of wind power generation influences the price on the daily time-scale.

	2004	2005	2006	2007	2008	2009	2010	2011	2012
Denmark	23.8	24.7	24.0	25.0	25.9	28.3	32.7	35.9	38.7
Sweden	51.2	50.9	51.8	53.2	53.6	58.3	56.0	59.9	60.0
Norway	97.3	96.8	100.2	98.5	99.6	104.7	97.9	105.5	104.3
Finland	26.7	26.9	26.4	25.5	27.3	27.3	27.6	29.4	29.5
Weighted	49.2	49.2	50.0	50.2	51.1	54.4	53.2	57.3	57.7

Table 2.4: Percent renewable generation in the Nordic countries. Source: Eurostat [29].

In the Danish bidding areas, the electricity price can fluctuate substantially within a short time period due to the high penetration of wind power generation. From Figure 2.4, it can be seen that a large increase in generation from wind power might eliminate coal, nuclear and gas from being activated, consequently leading to a large drop in the market price. Likewise, during late-night hours, when the demand for electricity is typically low, the demand curve shifts left causing a similar drop in market price. Moreover, if the day-ahead prediction of wind power generation in a specific timeslot is incorrect, the balance between consumption and generation as traded in the day-ahead market is off. This then has to be settled in the intraday market by the BRPs themselves or it will be handled by the TSO at the expense of the BRP that caused the imbalance. The high fluctuation of the electricity price in the Danish bidding areas, due to the high penetration of renewable electricity generation, can even cause the price of electricity to be negative from time to time, cf. the example in Figure 2.2. An example of large variations in power price was observed on June 7th 2013, when the electricity price grew from below 40 €/MWh to 2000 €/MWh ($\approx$ 2300 $/MWh) within four hours.

Nord Pool operates two platforms for trading power: Elspot and ELBAS, addressing the day-ahead and intraday market respectively. For regulating and balancing power in the shorter time-scale, the TSO maintains a list of providers of regulating power in the Nordic power market, called the NOIS-list[1]. Additionally, there are ancillary ser-

[1] Nordic Operational Information System

vices, which are provided by BRPs and managed by the TSO in each country. These services include voltage control and provision of reactive reserves. The two markets operated by Nord Pool, together with the market for ancillary services, are presented in detail in the following.

2.2.1 Nord Pool Elspot

Nord Pool Elspot is the day-ahead market for electrical power bought and sold in the Nordic and Baltic countries. In 2012, Elspot had a market share of almost 80% of the total consumption of power in the Nordic countries. Moreover, it is the largest power market in northern Europe [30].

The process for trading in the Elspot market is that buyers and sellers of power announce their bids for the following day to the Elspot trading system before gate closure at 12:00 CET. The minimum bid volume that is accepted by Elspot is 1 MW. After gate closure, hourly power prices are calculated for the following day of operation. The hourly prices are calculated by the trading system and found from the intersection between the supply and demand curves, cf. Figure 2.4, taking the physical constraints of the transmission system into consideration, e.g. transmission capacity. No later than 13:00 CET, the calculated prices are announced to sellers and buyers and published on the Nord Pool Elspot webpage [7].

2.2.2 Nord Pool Elbas

Nord Pool Elbas is the intraday market for buying and selling power during the day of operation. This market is much smaller than Elspot (approximately 1% of the volume sold on Elspot) and is mainly used to trade power for neutralisation of the imbalances from the day-ahead market. For example, imbalances from the day-ahead market can occur if the forecast of power consumption or generation deviates from what was predicted the day before, e.g. if predicted wind power pro-

duction is absent. The minimum volume that can be bid on Elbas is 1 MW and has to be announced no later than one hour before the hour of operation. Similarly to Elspot, the prices of electricity on Elbas are found from supply, demand and available transmission capacity between bidding areas.

2.2.3 Regulating power market

Energinet.dk is responsible for the stability of the Danish power system, including keeping the balance between generation and consumption at any time. To ensure balance between generation and consumption, the TSOs in the Nordic power system buy regulating power from BRPs. The market for regulating power is managed by the Nordic TSOs themselves, and consists of a list of provides called the NOIS-list [31]. Bids into the NOIS market are announced directly to the TSO no later than 45 minutes before the hour of operation; the TSO then forwards the bid to the common Nordic NOIS-list, where the bids are sorted with increasing prices for up-regulation and decreasing prices for down-regulation. If regulating power is needed the lowest bids are activated first, given that the necessary transmission capacity is available. Upon activation the BRP, whose bid has been activated, must deliver the power within 15 minutes from notification.

2.2.4 Ancillary services

As outlined in Section 2.1, Energinet.dk buys ancillary services from BRPs to ensure the stability of the power system in Denmark. The provision of all types of reserve capacity can be supplied from both GBRPs and CBRPs. Bidding into reserve capacity market is based on daily auctions held by Energinet.dk, except for the provision LFC, which is held on a monthly basis. CBRPs in control of flexible consumption units – or DERs – can utilise these units for provision of reserve capacity. As presented in Table 2.3, the smallest bid from BRPs that is accepted by Energinet.dk is 0.3 MW for primary reserve, FCNO and FCD, while manual reserve requires at least 10 MW

capacity [27]. Typically, consumption units in the low-voltage grid will not be able to provide 0.3 MW reserve capacity by themselves. Therefore, if CBRPs want to bid flexibility from small consuming units, these units will have to be aggregated such that a large combined response can be provided.

The ancillary services for short-circuit power, reactive reserves and voltage control in both DK1 and DK2 are found on a weekly or monthly basis. Since these services can only be supplied by large power stations, DERs in the low-voltage grid can not be utilised to supply such services.

Chapter 3

Smart Grid and Demand Response

In this chapter the concepts of smart grids, aggregators and demand response are introduced. Emphasis is placed on demand response from appliances and services, which are typically found in residential households.

3.1 Smart Grid

The present power system was designed in an age where electricity was generated by natural monopolies at large-scale power stations and distributed to end-users through the transmission and distribution network. In Figure 3.1 (a) is illustrated how electricity was generated and distributed only a few decades ago. As outlined in the introduction, electricity generation was centralised at large power stations in close proximity to major cities and large-scale production to minimise transmission and distribution losses. The power system of today – and the future – is illustrated in Figure 3.1 (b). Today, cf. Chapter 1, electricity generation is more distributed and a large share comes from numerous small entities. These are ranging from local CHP plants with several mega-watts electricity generation capacity down to a few kilo-watts photovoltaics (PV) installations. The decentral-

isation of the power system is expected to continue in the coming years where a large number of units are expected to be connected in the low-voltage network. These units will comprise private installation of micro CHP plants and PV with a generation capacity in the order of a few kilo-watts, supplying electricity and potentially heat to small detached buildings. Moreover, many of these units will be RESs whose electricity generation is inherently intermittent, less predictable and not dispatchable to the same extent large-scale power plants. In the Danish power system, the installed capacity of PV alone has increased substantially within the last two years; from well below 50 MW in the beginning of 2012 to more than 500 MW by the end of 2013 [17]. Even though private installed microgeneration systems are dimensioned to cover a share of the annual electricity consumption, the owners will unavoidably have excess electricity generation from time to time. Therefore, when end-users install their own renewable electricity source, they will have to rely on the power system to balance their daily power consumption, by exporting the surplus of electricity generation to the power system when generation exceeds consumption and vice versa when generation lacks consumption. Such end-users have been named *prosumers*, due to their varying role between producers and consumers of electricity. Currently, and in the near future, there are no economical viable solutions for energy storage; therefore prosumers will also prospectively have to rely on the power system as an infinite battery available to their disposal. A consequence of a growing number of prosumers in the power system is that the DSOs lose control of the flow of electricity in the distribution grid. Likewise, the TSO loses control of an increasing share of the power generating capacity. An increased generation from prosumers can cause electricity to flow in the opposite direction of what the distribution system was originally designed for, i.e. upwards towards the transmission system. With this increased complexity in mind, the current power system needs to be enhanced with an intelligence that can coordinate the electricity generation and consumption from a multitude of units to ensure a reliable supply. Such an intelligent power system is called a *smart grid*.

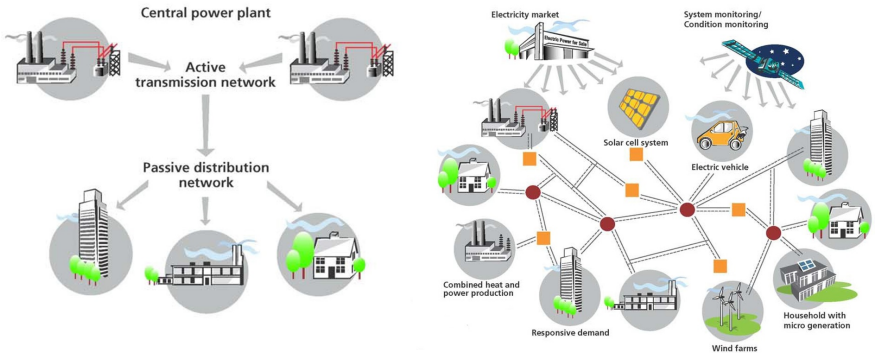

(a) (b)

Figure 3.1: Power system of the past (left), where electricity was distributed vertically, and next-generation power system (right) with a more interconnected power system. Source: DTU Center for Electric Power and Energy, `http://www.cee.elektro.dtu.dk/about`.

Despite the fact that research efforts within smart grids - or intelligent power systems - have increased substantially within the last decade, there does not exist a predominant definition of what a smart grid is and what requirements such a grid should fulfil. Instead, the definitions vary with application of interest; from self-detecting and self-healing power grids to balancing power in a power system by coordination of innumerable DERs.

A widely used description of the smart grid, which is also used by IEEE, is that it is a power system with an increased usage of information and communications technology (ICT) in the generation, delivery and consumption of electrical energy. This broad definition covers a large range of application, from even the simplest application of telemetry of electricity consumption and automated billing systems. In 2009, U.S. Department of Energy (DOE) published a report describing their vision of the future smart grid. In the report seven characteristics of the smart grid were identified [32]:

The Smart grid [...],

- enables active participation by consumers.
- allows accommodation of all types of generation and storage units.
- enables new types of products, services and markets.
- increases power quality.
- provides better utilisation of power system assets and efficient operation.
- provides self-healing capabilities.
- provides better resilience against attacks and natural disasters.

In the report, the involvement of the consumption side in the power system was emphasised to play a decisive role for shifting consumption away from peak load hours, thus reducing the need for distribution capacity in the low voltage network. Another advantage of a reduced peak demand is that there is less need for expensive peaking power plants, consequently increasing the load factor of the generation side, as envisioned by Schweppe et al. in [8]. Moreover, active participation of the consumption side can be used to support the balance between consumption and generation during short-term contingencies, e.g. by turning off appliances that can be left without power for a short moment of time without it is influencing the long term operation of the appliance. For example, to support TV pickups, where power consumption can increase abruptly during commercial breaks in popular TV programs. A well-known example of such an event was immediately after the wedding service of the royal wedding in United Kingdom in 2011, where power consumption increased with 2.5 GW within a few minutes from an average of 40 GW. Due to the short time duration of the power surge from TV pickups, electric heating and refrigerators could have been switched off, thus helping to keep the power consumption more stable.

In a Danish perspective, the smart grid is seen as a prerequisite for coping with the high penetration levels from RESs, which is necessary to reach the 2050 goals of a completely fossil free energy supply. In 2010, the Danish transmission system operator Energinet.dk, together with the Danish Energy Association[1], presented a report assessing the benefits of implementation of a smart grid in Denmark. In the report the following definition was used,

[A smart grid is an] *"electricity network that can intelligently integrate the behaviour and actions of all users connected to it - generators, consumers and those that do both - in order to efficiently deliver sustainable, economic and secure electricity supplies"*

– Smart Grid in Denmark [33]

The definition originates from the Smart Grids European Technology Platform, which is a European platform for cross-country collaboration on Smart Grid projects, supported by the European Commission. This definition, addressing an increased integration of renewable energy resources, is much in line with the objective of this project and is therefore adopted in the following.

Two main problems will arise in the power system when fossil fuels are completely phased out; firstly, traditional fossil fuelled power generation has to be replaced by renewable alternatives, primarily wind and solar power. The electricity generated by these types of energy sources are inherently highly intermittent and to a large extend non-dispatchable. This means power system services, especially the provision of regulating power, have to be provided by other units in the power system. Secondly, fossil based energy carriers that are used for non-electrical purposes, e.g. petrol and natural gas, have to be replaced by renewable alternatives. It is most likely that electrical power will be one of the main successors of these energy carriers. For example, electricity, together with biofuels, is expected to be the main successor of oil in Denmark. In 2011, oil was by far the largest energy carrier in Denmark, providing energy for almost 40% of the

[1] The organisation representing energy companies in Denmark.

gross energy consumption in Denmark [3]. The large share that oil constitutes of the total consumption is mainly due to the heavy utilisation of petrol and diesel for transportation. If the same amount of energy was to be delivered by the power system in 2050, it would mean that the power system will have to deliver three times more energy than today. Fortunately, electric vehicles (EVs) are 2-3 times more efficient than petrol cars and therefore the electric energy needed for transport in 2050 will not be as high as when oil is used. However, with the potential for EVs and electric space heating in mind, the need for electrical power in 2050 is expected to be significant higher relative to today. To meet this high demand for electricity in the future, large investments in grid infrastructure is needed. In 2010, the first large smart grid assessment for the Danish power system was carried out by the Danish TSO and the Danish Energy Association [33]. Here, the traditional approach of grid reinforcement to meet rising demand is compared to an implementation of a smart grid that can handle demand response. The report concludes that the estimated investment cost to meet the demand for electricity in 2025 using grid reinforcements alone amounts to 7.7 bn Danish kroner (DKK) (1.2 bn \$), whereas less grid reinforcements and implementation of a smart grid would require investments of 9.8 bn DKK (1.5 bn \$). However, the socio-economic benefits of having a smart grid are estimated to be 8.2 bn (1.3 bn \$). Consequently, the overall cost of implementing a smart grid is 1.6 bn DKK (0.2 bn \$) or 7.1 bn DKK (1.1 bn \$) less than using the traditional approach. The socio-economic benefits primarily come from lower cost of electricity generation and savings in regulation power and reserves.

Figure 3.2 depicts how the Danish TSO envisions how a smart grid could be implemented in Denmark. Here, the smart grid builds on the existing transmission and distribution infrastructure and utilisation of ICT to tie all the players in the power system together and coordinate the actions of one another.

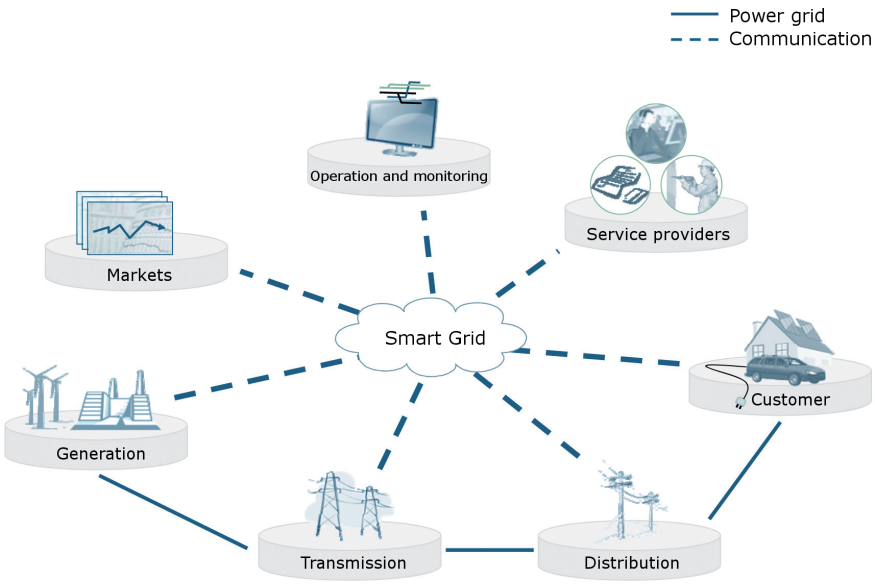

Figure 3.2: Energinet.dk's envision of a future smart grid. Here, the existing power grid infrastructure is extended with ICT solutions which ties all the power system players together and create new services. Source: Energinet.dk [33].

By integration of demand as an active player in the power system, it is estimated that 3.6 bn DKK (0.6 bn $) can be saved in reinforcement of the existing distribution grid. The reduced cost in the smart grid scenario comes from the ability to uncorrelate loads on the demand side, such that they are not active at the same point in time, thereby reducing the annual peak demand, and thus the dimensioning of the distribution grid infrastructure can be reduced.

As outlined previously, a smart grid in Denmark is considered a prerequisite for managing the high penetration levels from RESs that is needed to reach the 2050 energy targets. Therefore, the establishment of a smart grid, together with strong interconnectors to neighbouring power systems, is an integral part of the energy plan presented by

the Danish government [5]. Following the energy plan, a strategy for the establishment of a smart grid in Denmark was presented in May 2013 [34]. Here, a full roll-out of remotely read hourly meters to all consumers by no later than 2020 is planed. These are to be used in connection with varying tariffs of electricity to provide an incentive for end-users to shift their consumption to off-peak hours.

Given the substantial savings that can be achieved by implementing a smart grid, together with diminishing costs of embedded systems and communication, makes the smart grid a viable solution to handling the complexity of the future power system. Therefore, in Denmark, research in smart grid has been increased substantially within the last years, why Denmark currently is the country in Europe spending most money per capita on research and development within smart grid [35].

3.2 Demand Side Management

Demand Side Management (DSM), also called load management, defines how electricity consumption of DERs can be managed. This is primarily defined by the characteristics of a given unit. Generally, DSM can be grouped into four categories: load shifting, peak clipping, valley filling and fuel shifting. The concept of each of these categories is depicted in Figure 3.3.

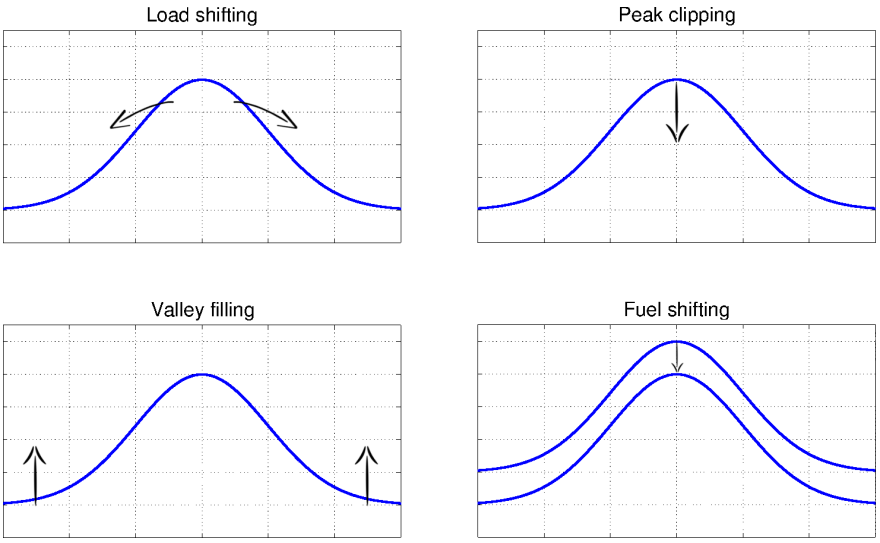

Figure 3.3: Types of load management.

Load shifting is when electric energy consumption of a DER is shifted from one point in time to another; for instance, when heating is deferred or accelerated. Typically, power consumption would be shifted away from peak load hours to hours with less demand, but could potentially also be shifted the other way if there is a high generation from RESs coinciding with peak load hours and there is no risk for congestions in the distribution grid. Peak clipping is when power consumption from less-important units is reduced during peak load hours,

e.g. pool pumps, garden and Christmas lighting or air conditioning. Likewise, valley filling is when power consumption from less important units is increased during peak load hours, e.g. utilise tumble dryer instead of clothesline. Fuel shifting is when one energy source is replace by another, for instance, when electric heating is replaced by heating from a wood fired stove.

Load shifting is the most common type of DSM and can be considered as a combination of peak clipping and valley filling. Whereas, load shifting typically is related to processes that requires a fixed amount of energy to be delivered over a given time interval, peak clipping and valley filling are typically related to what can be considered as non-essential or "luxury" consumption. Fuel shifting involves more than one source of energy of which one of them most likely will not be controllable from a smart grid point of view; therefore, this type of load management is considered out of scope of this thesis and will not be discussed in the following.

In the following, the traditional power system terminology for up- and down regulation is adopted. This means that up- and down regulation is with respect to the generation side. Thus, up regulation with respect to the consumption side, is when a DER *decreases* its electricity consumption and vice versa with down regulation. Unless explicitly stating down or up regulation with respect to the consumption side, the generation side terminology will prevail.

3.3 Control Schemes for Demand Side Management

In [36] four control schemes for implementation of DSM are defined: autonomous, direct, indirect and transactional control. In indirect control a price – or incentive – signals is broadcast to the end-user to incentivise a change in their electricity consumption. This kind of control relies on a one-way communication system and therefore there is no feedback from the DERs to the system that generates the incentive signal. Moreover, there is no formal agreement between the DER

and aggregator (BRP) which obliges the DER to respond to changes in the signal. Thus, the indirect control scheme relies on a stochastic response from many units rather than having full control over DERs. Indirect control is characterised by a relatively low-cost infrastructure for communication and a simple communication protocol. A local controller of the DER will be responsible for the control of the DER; thus, the responsibility for any control errors that might occur in managing the power consumption of a DER is entirely the owner of the DER. Consequently, this setup removes the liability from the BRP or whoever provides the incentive signal. Autonomous control builds on local measurements of power system parameters that represent the state of the power system. Typically, measurements of frequency are used due to its global representation of the balance between power generation and consumption in the power system, i.e. like units providing primary reserve capacity. However, autonomous control based on local measurements of voltage can also be used to control DERs. With autonomous control there is no need for infrastructure for communication of control signals. Transactional control is characterised by an internal negotiation approach, where a number of DERs are negotiating internally for how a given amount of power – or resource – should be split among them. Finally, there is the direct control approach, which builds on two-way communication between the DERs and a higher level controller, possibly an aggregator. The feedback consists of DER state measurements, which provides the aggregator with information on the short- and long time capabilities of the DER. From the feedback, the aggregator is able to optimise the operation of the connected DERs, and can with a high probability predict the response from the DERs, which is not the case in the market bases approaches, i.e. indirect and transactional control. In fact, there can be a bilateral agreement between the BRP and the DER owner about how a DER must comply with requests from the aggregator. Contrary indirect control, the aggregator has a higher degree of liability, due to his direct influence on the control of a DER. To reduce this liability a DER might be allowed to deviate from what has been agreed-upon, or even chose to opt out if the direct control of the DER is influencing its operation negatively.

Typically, like in this dissertation, aggregators using an indirect control approach for controlling DERs are called virtual power plants. This is due to the high degree of knowledge the aggregator has about its connected DERs and how they will respond to control signals. This gives a high reliability on the response from the aggregator, which means that it can be run virtually as a power plant.

In this project, the thermal load of a building is aggregated under a VPP, thus a direct control approach for DSM is exclusively considered in this project.

For further information on control schemes for DSM, readers are referred to [36].

3.4 Flexible Appliances and Services

To utilise demand response from DERs connected in the low-voltage grid, the potential electricity consuming appliances and processes that can be shifted in time have to be identified. In this section, an analysis of the potential sources for flexible demand is presented and their flexibility is estimated. As outlined in Section 1.6, the scope of this thesis is limited to smaller households, therefore the analysis of appliances and processes, which can be utilised for flexible electricity demand (flexible demand in the following) is confined to applications that are naturally found in households only. However, it should be emphasised that there exists many other sources of flexible demand found outside the scope of this thesis, i.e. within industrial and commercial applications. Examples of such applications are waste water treatment and horticultural farming.

In the following, the term *service* will be used to describe heating and cooling services and services provided by electrical appliances as a whole. When referring to one of the two, it will appear clearly from the text. Likewise, the term *comfort* is used to describe how an end-user perceives the level of a service; this includes perceptible services,

like services provided by televisions and cooking appliances, but also with respect to the physical comfort provided by more hidden processes, e.g. the control of the indoor air temperature.

Flexible demand is the part of the electricity consumption that can be shifted from one point in time to another, i.e. accelerated or deferred, without having a significant negative impact on the comfort felt by the end-user. *Impact* on comfort is a rather subjective measure and should thus be specified by the user. The flexibility should be regarded as a trade-off between full flexibility (or potential savings for the end-user) and the loss of comfort felt by the end-user. Generally, end-users have an abstract view on electricity usage and seldom regard electricity as a product by itself, instead they recognise the services that electricity provides; therefore, the end-user should not specify tolerable limits on up- and down regulation of his electricity consumption, instead he should allow his services to be controlled within a specified comfort band which he finds acceptable. This, in general, should be done for each flexible service in a household and aggregated, such that only one common aggregate flexibility is exposed towards the point of control.

Household services can be separated into two categories: flexible and inflexible services. The inflexible services are primarily inflexible because the services they provide to the user are highly time dependent and the loss of comfort if shifted to another point in time is so high that the user is not willing to change his consumption. Consequently, the price elasticity of such services is relatively low, which means that the user will not change his consumption almost regardless of the cost. This applies to services provided by TVs, lighting, cooking appliances, etc. In the following, these inflexible services are disregarded and their total consumption is considered to form a base load of the household, which can not be manipulated. Flexible services are processes which are not absolutely time specific or processes where a relatively constant amount of energy has to be delivered during a given period. The latter is typically related to thermal processes, where a thermal inertia keeps the temperature stable for a short period of time. This applies to most heating and cooling processes found in residential households,

e.g. refrigeration of foods and space heating. Table 3.1 presents some of the most common household services which are considered flexible, together with their typical cycle and average annual power consumption.

	Service	Energy consumption	Average annual power
Thermal services	Resistive heating	14,000 kWh/y	1,600 W
	Heat pump heating	4,000 kWh/y	460 W
	Water-heater	3,000 kWh/y	340 W
	Freezer	300 kWh/y	34 W
	Refrigerator	200 kWh/y	23 W
Batch services	Tumble dryer	2 kWh/cycle 160 cycles/year of 1 hours	37 W
	Dishwasher	1 kWh/cycle 280 cycles/year of 2 hours	32 W
	Washing machine	1 kWh/cycle 220 cycles/year of 2 hours	25 W

Table 3.1: Typical Danish household appliances and their average annual power consumption. Cycles per year are standard cycles as defined by the European Commission [37].

In the table the services are separated into two categories: thermal processes at the top and batch services below. The latter is named batch services due to the way the processes of these services are running, i.e. they have to be executed in one go without any interruptions. The services presented in the table are interesting sources for flexible

consumption due to their relatively high annual power consumption. However, it should be emphasised that the table should not be seen as a complete list of flexible appliances found in households. Other flexible services exist; for example, charging of various battery driven devices, like mobile phones and robotic vacuum cleaners, but due to their negligible consumption these are considered uninteresting for flexible demand in this thesis.

Thermal services are related to heating and cooling processes. From the table is seen that services related to space and water heating have significant higher annual power consumption relative to all the other services. Typically, these services control a temperature within a temperature band around a temperature reference, which is specified by the user, i.e. hysteresis controlled. Two time series of such processes are depicted in Figure 3.4, where the electric power consumed by a resistive heating system (top) and a heat pump system (bottom) are plotted. The resistive heated building has an area of approximately 120 m^2 and is heated by ten electric space heaters with a nominal heating capacity of 9,750 W. The heat pump heated building has an area of approximately 215 m^2 and is centrally heated from a geothermal heat pump with a nominal power consumption of 3,200 W. The heat pump also provides heating for water. Both time series are from March 2nd 2013, and collected under similar weather conditions. The average outdoor temperature for the given day was around 2 °C, which is 6 °C below the annual average outdoor temperature, why the heat loads are expected to be slightly above the annual average. From the figure is seen that the average power needed for resistive heating is significant higher than by use of a heat pump. Not including water heating, the power consumption is almost four times as high per area for the resistive heated house relative to the house heated by a heat pump. Another thing to note from the plots is that the power consumption from resistive heating is very intermittent and experiences large discrete jumps, whereas the consumed power from the heat pump system is much more periodic with jumps between two states. In general resistive heating comes from a number of electric heaters distributed within the household, and thus can be seen as an

aggregate heat load that can be controlled in discrete steps, which is also seen in the figure. On the contrary, typical commercial heat pump systems consist of only one major load, which is the compressor. This can only be switched either on or off, which means that the power consumed by a heat pump can not be controlled with the same degree of precision as a resistive heating system. Finally, from the lower plot, it is noted that there is a base load of the heat pump system of approximately 60 W, which comes from a circulator pump.

The two examples in Figure 3.4 illustrate that heat pump systems are much more efficient than direct heating because they do not create the thermal energy; they move it from one location to another. How efficient a heat pump is, is specified by the coefficient of performance (COP), which is the ratio between the output of thermal energy and the electric power consumed. The variation of heat pump systems is high and ranges from air-sourced, i.e. air-to-air or air-to-liquid based, to ground-sourced heat pumps, i.e. liquid-to-air of liquid-to-liquid. Naturally, the characteristics of such systems vary, but in the following a general assumption of a central based solution with one compressor and a COP in the range of 2–4, is adopted. These assumptions hold for most centrally based heat pumps solutions, where a single compressor is driving the heating process of a whole building. Naturally, space cooling by use of heat pumps has the same characteristics as the heating equivalent. In these processes the heat pumps are simply running in reverse, but still the pattern for power consumption, as observed in Figure 3.4, applies. Likewise, does the on and off control of the compressor and the COP.

One of the great advantages of using electricity for heating in Denmark, with respect to demand response, is that it correlates very well with the electricity generation from wind turbines, which nearly generates twice as much electricity during the cold winter months compared to July where wind power generation reaches a minimum, cf. Figure 1.5.

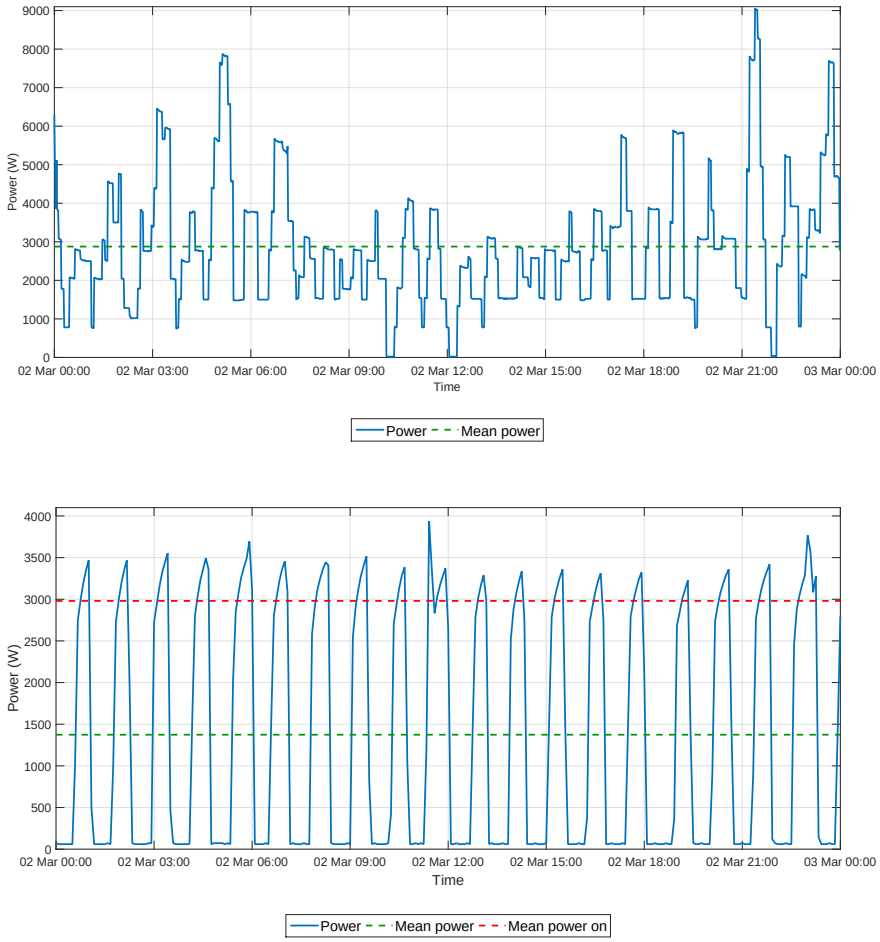

Figure 3.4: Power consumption for a direct heating system (top) and a heat pump based heating system (Vølund Fighter 1245) (bottom). Source: SYSLAB (top) and www.styrdinvarmepumpe.dk (bottom).

Cooling processes in refrigerators and freezers are very similar to heat pump systems for space heating and can likewise be utilised for flexible demand. These appliances do not have the same potential individually as space heating due to the relative low thermal mass and power consumption; however, they are much more frequent in households than electric space heating. In Denmark, nearly all households have a refrigerator and most likely also a freezer, and together they form a sizeable load in the Danish power system ($\approx 2\%$). Another advantage of refrigerators and freezers over space heating is that these appliances are available for flexible demand all year round. In Figure 3.5, a typical time series of the power consumption from a refrigerator (top) and freezer (bottom) are plotted. The plots show that the two processes are very similar to each other and to the heat pump process in Figure 3.4 (bottom). Fundamentally, these three processes are also the same, where a compressor is driving the process of moving thermal energy. The period of the freezer is seen to be approximate half as long as for the refrigerator, which is typical due to the relative higher temperature difference to the ambient environment. Moreover, the average power consumed by the refrigerator is around 22 W, which is comparable to the value presented in Table 3.1, while the average power consumption for the freezer is close to 50 W, which is significant higher than what would be expected from a modern freezer. Two main characteristics separate the three processes: firstly, the ratio between being on and off, i.e. the duty cycle, vary among the three processes. Secondly, the power consumed when the compressor is running is different. Moreover, similar to the heat pump system, the freezer is seen to have a background power consumption of approximately 5 W, which is most likely from the hardware controlling the compressor. In the following section, these two parameters will be used to estimate the potential for up- and down regulation of the electricity consumption.

Unfortunately, no time series for a typical water heater has been found and likewise for the batch processes. However, according to DONG Energy, the largest energy company in Denmark, the annual energy consumption used for hot water is 850 kWh per capita or equivalent to an average load of almost 100 W per capita, thus making it a sub-

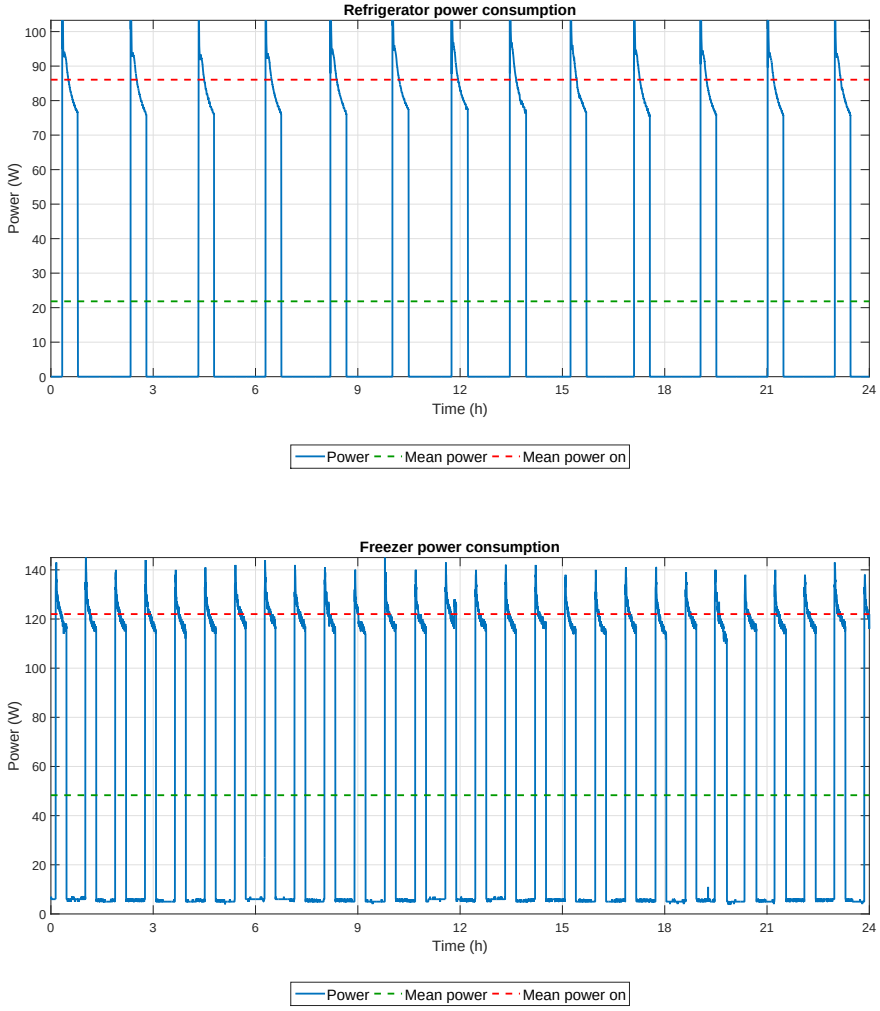

Figure 3.5: Power consumption from an A+ type of refrigerator (top) and freezer (bottom). Source: SYSLAB (top) and INCAP project [38] (bottom).

stantial load in households where electricity is used for water heating. Electricity consumption for hot water correlates with water usage due to the reason that the heating element starts to heat the water when the water level in the hot water tank declines. Hot water is primarily utilised in the morning and the early evening, why there is no particular reason for heating the water directly after usage because the user will most likely have left for work or gone to bed. This means that the heating of water can be postponed for several hours, without the user felling any loss of comfort. This makes water heaters an ideal source for flexible demand, why they have been heavily utilised for DR in some power systems. Only a small fraction of Danish residential households use electricity for heating of water, why the overall potential from water heaters is quite limited. However, in summer houses electricity is the most typical source for hot water generation. Considering, that more than 10% of the building stock in Denmark consists of summer houses, there is a large potential for DR which can be used during the summer period, when summer houses are typically occupies. A potential barrier for integrations of these water heaters is the lack of communication in the area where summer houses are typically located, as well as a low economic incentive for end-users to replace their old water heater with a new one, due to its low utilisation.

Like refrigerators and freezers, the batch processes presented in Table 3.1 have a relative low annual power consumption. Hence, the potential for flexible demand from batch processes does not lie in their electricity consumption, but in their prevalence in Danish households: 80% of all households have a washing machine, while 67% and 52% have a dish washer and tumble dryer, respectively [12]. From the standard cycles, as defined by the European Commission ([37]), the weighted electricity consumption of the batch processes presented in Table 3.1 is approximately 60 W per household, which is considerable less than both space and water heating. Even though electricity demand from washing appliances can be coordinated to provide a substantial flexible demand, the potential is quite low. Especially considering that end-users typically tend to wash clothes during weekends, where the power consumption is already low. Moreover, recent

experiences from the EcoGrid EU project, where appliances in 2000 residential households are being controlled using a price signal, have shown that end-users are reluctant to shift their electricity consumption from washing machines and tumble dryers because they find the cleaned clothes smelly and wrinkled after lying in the machine for up to hours.

In this section, electric space cooling has not been addressed due to its low utilisation in the Nordic countries. Here, the potential for flexible demand from such services is simply too small relative to space heating. However, for most applications involving space heating in cold regions, there exists an equivalent application in warm regions, where space cooling can be used for DR. An example of this is central cooling units, which are frequently used for DR in warm environments; for example, in the southern part of the US.

3.5 Estimation of Up- and Down Regulation

In this section the four examples presented in Figure 3.4 and 3.5 are used as basis for estimating the potential for up- and down regulation of the electricity consumption used for space heating and for cooling foodstuffs in refrigerators and freezers. The expressions derived should be regarded as an annual average for refrigerators and freezers, and an average for the heating season for space heating. However, the expressions can also be used to estimate the short term potential by using instantaneous values instead.

The two space heating examples in Figure 3.4 are good representatives for a typical day of space heating in Denmark; both time series were collected during a day with an average outdoor temperature of around 1 °C which is typical for a day in the official heating season in Denmark (October to April), where the average outdoor temperature is 3 °C [39]. Therefore, these two examples are used to estimate the average potential for up- and down regulation during the heating season. In this period almost 90% of the energy for heating in Denmark is consumed. Likewise, the time series presented in Figure 3.5

was generated in an ambient environment with a temperature around 21 ℃, which is typical for refrigerators and freezers.

For a resistive heating system, the up- and down regulation can be directly estimated from the average power consumption. Here, up regulation (with respect to generation) is simply given by the average power consumption. Likewise, down regulation is the difference between the average power consumption and nominal peak power consumption of the heating system. For a resistive heating system, the up- and down regulation can typically be provided in discrete steps, because the heat load is composed of several smaller loads.

For processes involving heat pumps, including both space heating and refrigeration, the power consumption can be approximated with an aperiodic square wave function with minimum P_{min} and maximum P_{max}. From this, the estimated up- and down regulation can be found from the probability of the compressor running. Extending the notion of a duty cycle to include aperiodic signals, as the fraction of time a given process is active, then the duty cycle over a given period T is given by,

$$D = \frac{\tau}{T} \tag{3.1}$$

where τ is total amount of time the process is active during the period T. By assuming unchanged temperature bands on the hysteresis process controlled by the compressor, the duty cycle can be used to estimate the up regulation as the conditional expectation of the height of the square waves,

$$\hat{P}_{up} = E\left[\Delta P \mid \text{ process is on }\right] = D\left(P_{max} - P_{min}\right) \tag{3.2}$$

where P_{max} is the nominal maximum power of the heat pump and P_{min} is the base- or standby consumption, which typically comes from a circulation pump or an embedded control system. Likewise, the estimated down regulation can be found

$$\hat{P}_{down} = E\left[\Delta P \mid \text{ process is off }\right] = (1 - D)\left(P_{max} - P_{min}\right) \tag{3.3}$$

	Resistive heating system	Heat pump system
Peak power consumption	9.8 kW	3.0 kW
Average consumption	2.9 kW	1.4 kW
Duty Cycle	-	0.45
Up regulation	2.9 kW	1.3 kW
Down regulation	6.9 kW	1.6 kW

Table 3.2: Estimated up and down regulation capabilities of the two space heating systems presented in Figure 3.4.

From these two equations the figures in Table 3.2 have been found for the two heating systems presented in Figure 3.4. From the table is seen that on average the magnitude of down regulation is higher than up regulation. This is due to the fact that most heating systems are oversized so that they are able to supply enough heat during the coldest periods of the year. Naturally, the average power consumption of space heating systems, and thus the duty cycle, varies with weather conditions of the ambient environment. This means that the potential for regulation has both a diurnal and annual variation.

Similar to heating systems, estimates for up- and down regulation of refrigeration systems can be found from Equation (3.2) and (3.3). In Table 3.3 the estimated values for up- and down regulation of the two refrigeration systems, as presented in Figure 3.5, are shown. Like heating systems, the magnitude of down regulation is higher than up regulation, for the same reason. For refrigerating systems, the duty cycle of the power consumption varies with how often the door is opened and new goods are added. This makes the duty cycle a stochastic process on a shorter time scale. However, on a longer time scale the duty cycle is more or less constant due to its independence of the amount of the goods inside refrigeration in stable state, which only influences the length of the period. This makes refrigerating system a very stable source for load shifting.

	Refrigerator	Freezer
Duty Cycle	0.25	0.37
Mean consumption	22 W	48 W
Power on	86 W	122 W
Power off	0 W	5.5 W
Up regulation	22 W	43 W
Down regulation	64 W	74 W

Table 3.3: Estimated up and down regulation capabilities of the two refrigeration systems presented in Figure 3.5.

The potential for up- and down regulation of batch services can not be directly derived from the information presented in Table 3.1. This is primarily due to the fact that the electricity consumption from these services does not show the same regularity as heat pumps and refrigeration appliances, but is subject to the habits and practices of the end-user. Therefore, the probability distribution of the utilisation of batch services is much more stochastic and varies among households, e.g. with the number of residents and whether they are staying at home during weekdays or not. However, assuming that the standard cycles in Table 3.1 hold and that the usage is uniformly distributed over that year, then the down regulation is equal to the weighted average consumption, which is 60 W per household, cf. previous section. A similar weighted average power consumption was found in a Norwegian study where 57 W per household (507 kWh yearly) were utilised for the three types of batch services [40]. Since batch processes can not be stopped once started only down regulation can be provided by such processes.

The potential for flexible demand is two-dimensional; the first dimension being the magnitude of the load that can be reduced or increased as already discussed. The second dimension of demand response is the duration an up- or down regulation can be sustained. Assuming that the power delivered to a compressor based heating – or cooling – system over a short period of time can be approximated by the average

power, then the total energy delivered is given by,

$$E = \int_0^t P(t)\, dt \approx P_{avg} \cdot t \tag{3.4}$$

This equation shows that time and power are inversely proportional. Therefore, in general if up regulation is larger than down regulation, it can be maintained for a shorter duration of time, and vice versa. Like the magnitude of regulation, the maximum duration can be estimated from the duty cycle and the period of the duty cycle. Consider the ideal duty cycle depicted in Figure 3.6 where the duration of the "on" domain is given by $D \cdot T$ and the "off" domain given by $(1 - D)\, T$.

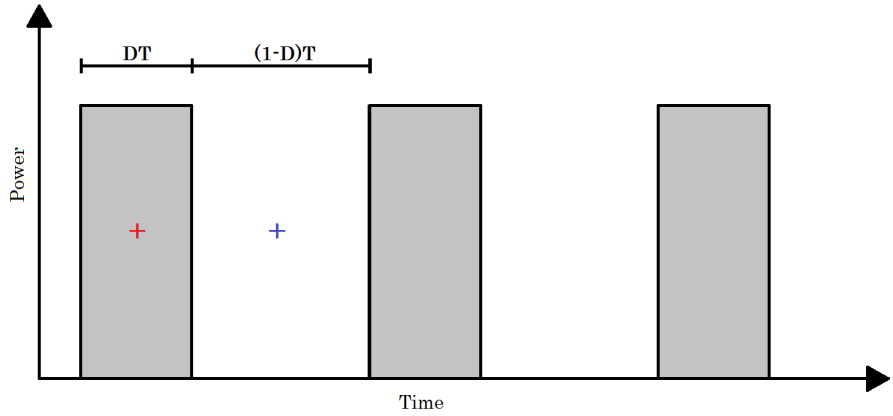

Figure 3.6: Ideal duty cycle.

On average the state of a heat pump being on will be in the middle of the "on" domain, marked by the red cross. Likewise, for the heat pump being off the average state will be in the middle of the "off" domain, marked by the blue cross. Thus, on average the duration of maximum up- and down regulation are given by,

$$\begin{aligned} \hat{t}_{up} &= 0.5\, D \cdot T \\ \hat{t}_{down} &= 0.5\, (1 - D)\, T \end{aligned} \tag{3.5}$$

For the services presented in Table 3.1, the maximum duration ranges from 10–15 minutes for the freezer presented in Figure 3.5, which has a very short period, up to hours for batch processes. The main reason for these short durations is that the temperature band, in which the temperature is controlled, is typically quite narrow. Flexibility in the time-scale can thus be extended by increasing the temperature band of the control process.

The examples provided in this section serve as basis for estimation of up- and down regulation. Naturally, the average power consumption of the thermal services presented in Table 1.2 varies over the year and with it the duty cycle. For space heating the average power consumption varies with the outdoor temperature and solar irradiance. For water heating, refrigerator and freezer the consumption varies with usage, e.g. volume of hot water used and how often the door to the refrigerator or freezer is opened.

3.6 Aggregation

Aggregators are expected to fulfil multiple roles in the future power system or smart grid. Firstly, they can be used to combine the response from many small entities, thus be able to deliver ancillary services in the power system. As outlined in Section 2.2.4, at least 0.3 MW capacity of up- or down regulation is needed if a BRP want to provide primary or secondary reserve to the TSO, and 10 MW for manual reserve. Likewise, the volume of the bids on Elspot and Elbas has to be at least 1 MW. Only few consumption units can by themselves offer such a large capacity for up- or down regulation, that it can be used for ancillary services. Therefore, a large number of units have to be aggregated to be able to deliver the requested response. Consequently, the aggregator concept opens up for new business models that utilise the flexibility of many small units and sells the aggregate flexibility as ancillary services or in the power market. Since only BRPs are allowed to act in the power market and the market for ancillary services, these services can be developed by BRPs themselves, or by third party actors in collaboration with BRSs. In Denmark two busi-

ness models are currently being developed by third party actors where the flexibility of heat pumps and EVs, respectively, are being utilised as flexible DERs. A common characteristic of the two business models is that they do not sell electricity to the end-user, they sell a service instead: space heating from heat pumps and driving distance for EVs. The investment costs for both heat pumps and EVs are substantially high for the end-user. Therefore, the aggregating company will do the initial investment on behalf of the customers, which then pays the company back over a given period. In the case of heat pumps, the aggregating company pays the initial investment and installation costs of the heat pump for the customers and in return the end-user will subscribe to a heating service, which provides space heating to the customer's household. By providing a service rather than electricity, the risk of unexpected expenses for maintenance is completely moved away from the customer. For EVs, the aggregating company owns the battery in the EV, thereby reducing the investment costs of the EV. When connected for charging, the aggregator will optimise the charging of the EVs such that charging is conducted when the price is low or when it is most favourable for the power system. Moreover, EVs can feed electricity back to the low voltage network to support local demand during peak load hours. Like heat pumps, a service from the batteries is provided to the end-users and the risk of wear and tear on the battery due to continuously cycling is shifted away from the end-user to the aggregating company.

Secondly, aggregators can be used to reduce the level of abstraction. This is done by aggregating DERs into VPPs, which allows many DERs to be controlled as one conventional power plant. By aggregation of DERs into VPP structures, the control problem is broken down into sub-problems, thus reducing the complexity of control relative to controlling all the units individually. An example of this is the Cell Controller Pilot project in Denmark, where a large amount of CHP plants, wind turbines and different loads were aggregated and operated as one single large power plant [6].

Lastly, aggregators are expected to play a role in the distribution grids of future smart grid, by supplying services directly to the DSOs; for example, by providing services for congestion management and voltage control in the distribution grid [41].

In Paper C, simulations of an aggregator delivering DR from 100 heating systems were presented. In the paper it was shown that heat loads can be coordinated to deliver an aggregate demand response. Moreover, it was shown that a large share of the aggregated loads can be shifted in time to deliver up- and down regulation as an ancillary service, cf. Section 2.2.4. In the simulations, like in the analysis in the previous section, it was observed that due to oversized heating systems, the down regulation of heating systems is generally larger than up regulation. Moreover, it was observed that after a period with a reduction of the aggregated load, the need for heating required higher electricity consumption than before providing up regulation. This is evident from the plot of down regulation of the aggregated load in Fig. 5 (left) Paper C, where a large increase in power consumption is observed immediately after the up regulation period. Likewise, after a period with down regulation, the aggregated system becomes saturated with energy and thus can not maintain the increased power consumption. This is apparent from the plot in Fig. 5 (right) Paper C, where the aggregated consumption declines to zero following a period with down regulation. The two simulations show the importance for the aggregator to have a long term strategy for how to reconnect the heat loads without coinciding with other large loads, e.g. during peak load hours. In connection with a few smart grid related projects, this effect has been named the *kickback effect* and will be named so in the following. A more detailed description of the kickback effect is given in the following section.

3.7 Kickback Effect

A common characteristic of the thermal applications presented in Table 3.1 is a nearly constant need for energy over a short time interval. Therefore, there are consequences for shifting power consumption: reduced heating has to be caught up later in time by increased heating later and likewise when accelerating heating, power consumption has to be reduced later in time.

Due to the similar dynamics of heating systems, heat loads tend to become correlated when shifting the aggregated loads in time. An example of this is provided in Figure 3.7, where the states of 200 heat pumps are plotted before a 50% up regulation of the aggregate heat load. The abscissa represents the duty cycle, where the grey area marks the "on" domain of the duty cycle. Likewise, the ordinate represents the temperature of an indoor temperature being heated by a heat pump. Each triangle marks the state of a heat pump, where red represents a heat pump being on and blue represents a heat pump being off. Likewise, the direction of the triangle illustrates the direction of the temperature development. The states were generated from a continuous uniform distribution, which is also reflected by the histogram – or estimated probability distribution – plotted below.
In Figure 3.8, the same 200 heat pumps are plotted immediately after a 50% up regulation has been provided by the aggregator. This has been done by switching off half of the heat pumps, turning off those with the highest temperature (marked with green triangles). These heat pumps now reside in the "off" domain of the duty cycle and the temperature of these will now start to decline. In the histogram below, a hump in the first half part of the "off" domain of the duty cycle is now observed. This hump will continue to grow, as heat pumps only are allowed to reside half the time in the "on" domain of the heat pump, why they are moved faster to the "off" domain than before the up regulation. After approximately a quarter of a duty cycle, these heat pump systems will have to be started again to provide heating. Consequently, after some time, the aggregate consumption will start to increase, and the consumption will be significantly higher when the period of up regulation has ended. This illustrates that up regulation

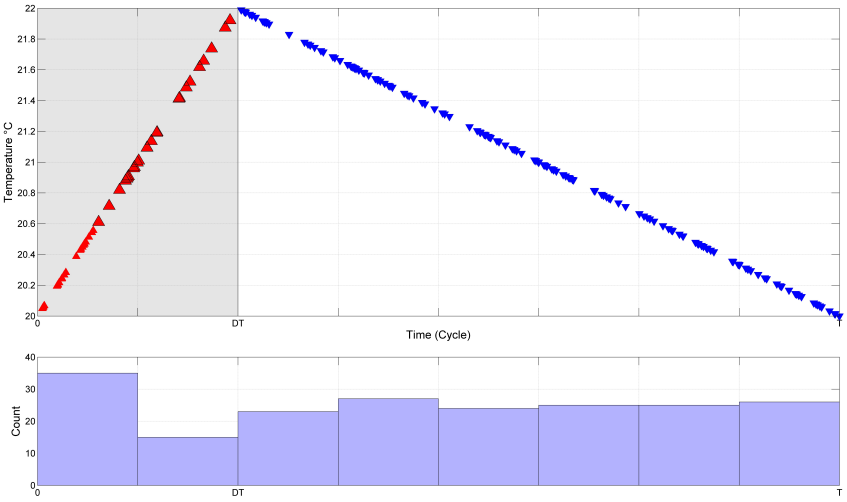

Figure 3.7: Heat pump state distribution before up regulation.

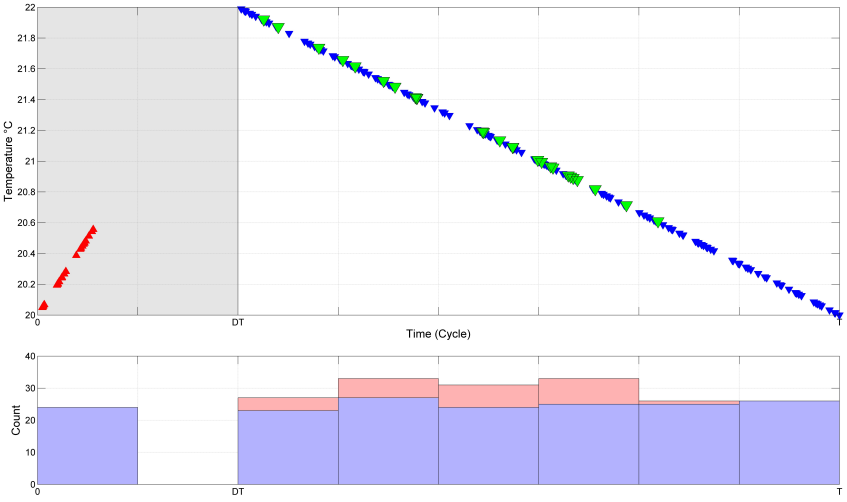

Figure 3.8: Heat pump state distribution after up regulation.

comes at a price, which has to be compensated for within a time period of the average duty cycle. Moreover, aggregators should be designed with this phenomenon in mind, such that correlation of the heat loads is avoided and especially the load of other aggregators in the power system.

3.8 Summary

In this chapter a general analysis of flexible residential appliances has been presented. The analysis has shown that the largest potential for flexibility, with respect to regulation of power consumption, comes from electric space heating, either using resistive heaters or heat pumps.

Based on the examples given in this chapter, estimates of the overall Danish potential for regulation of electricity consumption is presented in Table 3.4 as well as estimates of the maximum duration of time a regulation can be sustained. The values in the table should not be regarded as exact values, but as rough estimates of the overall flexibility and should merely serve to illustrate the potential of flexibility among different services. The last column estimates the potential in a future scenario where 700,000 households are heated with heat pumps.

The greatest potential is seen to lie within space- and water heating applications, especially when considering the potential of 700,000 fossil based central heating systems being converted to heat pumps by 2035. Despite these two processes are both seasonal dependant, they generally complement each other well by being utilised in different periods of the year. This is primarily due to the fact that electric water heaters are mainly utilised in summer houses, which are typically only occupied during summer, whereas space heating, naturally, are utilised in the winter time. Next comes refrigeration services, which are available all year round and are more symmetric in their potential for providing up- and down regulation. This is due to the reason that the duty cycle of these services is close to 50%. Finally, there are batch processes, which are also available all year round, but are limited to provide down regulation only.

Unit	Water heaters	Batch services	Refrigerators	Freezers	Heat pumps (2013)	Heat pumps (Potential in 2035)
Number	250,000	2,500,000	2,500,000	1,500,000	200,000	700,000
Maximum $\hat{P}_{up}$	35 MW	0	55 MW	50 MW	260 MW	910 MW
Maximum duration, t_{up}^{max}	12 h	0	45 min.	15 min.	20 min.	20 min.
Maximum $\hat{P}_{down}$	860 MW	150 MW	160 MW	90 MW	320 MW	1,120 MW
Maximum duration, t_{down}^{max}	30 min.	1-2 hours	15 min.	10 min.	10 min.	10 min.
Availability	Summer	All year	All year	All year	Heating season	Heating season

Table 3.4: Total potential for regulation of consumption in the Danish power system.

Chapter 4

SYSLAB and Power Hub

One of the main objectives of this Ph.D. project has been integration of households into a VPP framework with the purpose of delivering up- and down regulation of active power consumption as a power system service. As a demonstration and for estimation of the potential flexibility, the intelligent office building PowerFlexHouse has been integrated into the commercial virtual power plant Power Hub [43]. In this chapter, the facilities that were used during this project are described; this includes the research facility SYSLAB and PowerFlexHouse I along with the VPP Power Hub.

4.1 SYSLAB and PowerFlexHouse

SYSLAB is an experimental research facility for research in distributed power systems with a high penetration from renewable energy sources. More specifically, since much of the research conducted in SYSLAB lies within the field of smart grids as defined by the Danish TSO, cf. Section 3.1, SYSLAB is utilised as a research facility for trialling of smart grids concepts.

SYSLAB is located on the DTU Risø Campus near Roskilde, Denmark. The facility comprises a number of electricity generating and

consuming units (DERs) connected in a 400 V microgrid. The DERs are distributed over the large area of the campus site and at present time the main DER installations include,

- Diesel generator [48 kW generation].
- Gaia wind turbine [11 kW generation].
- Aircon wind turbine [10 kW generation].
- Photovoltaics [25 kW generation].
- Dump load [75 kW consumption].
- PowerFlexHouse I, an intelligent office building [20 kW consumption].
- PowerFlexHouse II, an intelligent residential building [10 kW consumption].
- PowerFlexHouse III, an intelligent residential building [10 kW consumption].
- Vanadium battery [15 kW/120 kWh storage/generation/consumption].
- Toyota Prius, Plug-in Hybrid [9 kWh storage/consumption].
- Peugeot iOn, EV [16 kWh storage/consumption].
- Renault Kangoo Z.E., EV [22 kWh storage/consumption].
- Back-to-back converter [45 kVA power converter].

where the values for electric power in the brackets are peak values. The DERs are connected at three substations within the campus perimeter and a fourth substation outside in connection with the two newly integrated residential houses, PowerFlexHouse II and III. At each substation there are two busbars which can be connected to one of three centrally located busbars, i.e. a crossbar. This creates a very flexible setup, thereby allowing DERs in SYSLAB to be connected in virtually any configuration on the crossbar, which makes SYSLAB

and ideal laboratory for research in intelligent distributed power systems and smart grids. Additionally, at each location of the substations there is a connection to the local distribution grid, which allows the DERs to take part in the Danish power system. Alternative, the connection can be closed, thereby allowing the DERs to be run in isolated operation. A layout of the infrastructure of SYSLAB is depicted in Figure 4.1.

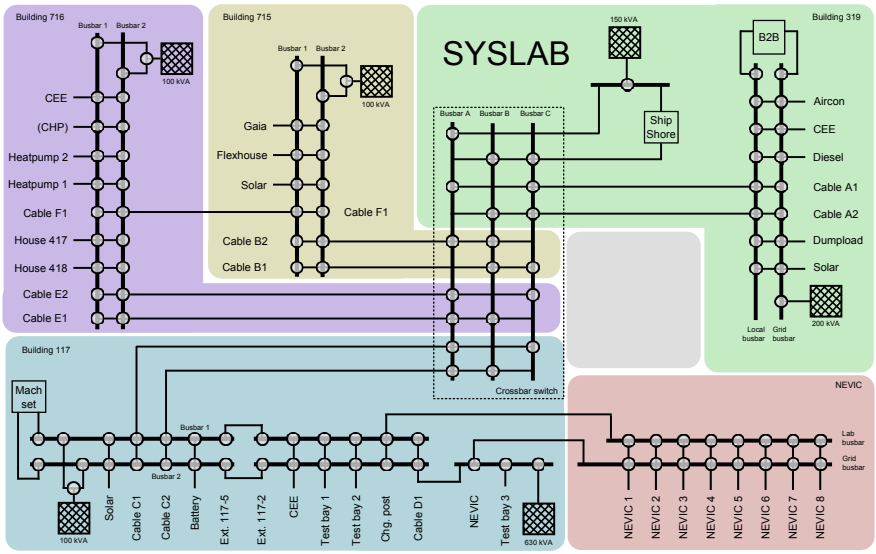

Figure 4.1: Electrical layout of the SYSLAB infrastructure.

In the figure, the colours violet, yellow, green and blue, each represents a location of a substation on the Risø campus site, whereas the colour red, in the lower right corner, represents the NEVIC test center[1], which is a test center for trialling of EV charging technologies and compatibility between charging components.

[1] Nordic Electric Vehicle Interoperability Center, `http://www.cee.elektro.dtu.dk/research/NEVIC`

Each DER in SYSLAB is equipped with a dedicated computer, which in the following is denoted a node computer. The node computers are responsible for running low level control of the attached DER and collecting and storing local measurements with a high temporal resolution. Like in a SCADA[2] system, the node computers also provides an interface for control to the communication network, which is built around the SYSLAB microgrid, similar to the smart grid envisioned by the Danish TSO, cf. Section 3.1. The control interface provides methods for remote data acquisition and high level control of the attached DER.

4.2 PowerFlexHouse I

PowerFlexHouse I is a fully automated office building, which has been designed to act as a flexible load in the SYSLAB network. A building management system (BMS) has been specifically developed for control of the appliances in PowerFlexHouse. The BMS has been designed such that controllers can be easily implemented, swapped and run in parallel with other controllers, thereby creating a flexible controller setup, which allows the building to be operated and tested with respect to various control strategies. The building has a special relevance and interest to this project due to its capabilities for providing demand response within the SYSLAB network.

PowerFlexHouse I is a free-standing building with an area of approximately 120 m^2, consisting of seven office rooms centred around a main hall, which serves as a meeting room. Next to the main hall there is a small toilet and a kitchenette equipped with a water boiler (2 kW), a coffee machine (1 kW) and a refrigerator (100 W). The main part of the peak load of PowerFlexHouse I comes from ten electric resistance heaters (0.75–1.25 kW, 9.75 kW in total) and five air-to-air heat pumps (1 kW each), which can also provide cooling during warm periods. Finally, there is a water heater (3.7 kW) in the toilet which provides hot water for the building. A picture of PowerFlexHouse and

[2] Supervisory Control and Data Acquisition

its layout are depicted in Figure 4.2. Moreover, a large number of actuators on doors and windows have been installed, which allow these to be opened and closed from the building controller implemented in the BMS. These actuators enable emulation of presence and stochastic behaviour of building residents.

Figure 4.2: Layout and orientation of PowerFlexHouse I.

The custom build BMS, which has been developed internally for automation of PowerFlexHouse I, is running on a dedicated computer within the building and is responsible for the control of the electric appliances and heating. Moreover, a node computer, which is connected to the control computer, is providing an interface to the SYSLAB network, thus allowing data acquisition and remote control from other nodes in SYSLAB. The BMS collects input from a wide range of wireless sensors, comprising temperature, motion, door and window sensors that are mounted inside the building and are communicating with the BMS using radio signals. The temperature, window and door sensors are all driven by a small photovoltaic cell and a backup battery, making them completely energy independent of external energy supply and free from wiring; consequently, the sensors can easily be installed virtually anywhere inside the building. Likewise, energy for electrical switches is provided by a piezo generator, which generates sufficient energy to send a wireless message to the BMS whenever a switch is pushed. Communication with the sensors and actuators are only unidirectional, which means that sensors and actuators can not be polled for their present state; they can only send periodic updates or when events trigger them, e.g. when a door is opened. A radio

transceiver is mounted centrally inside the building and connected to the BMS computer. The transceiver is collecting radio telegrams from the sensors and forwards the messages from the BMS to the actuators. The actuators, which are controlling the electric appliances and resistance heaters inside the building, works as a relay for the unit, hence control of appliances is limited to on/off control. Heat pumps are controlled using infrared signals, which have been mapped from the enclosed remote control of the heat pump. Finally, the BMS collects weather data, comprising temperature, solar irradiance, wind speed and direction from a weather mast raised next to the building.

The first version of the PowerFlexHouse BMS was developed in 2007 and was designed around the wireless EnOcean communication standard. Continuously, with the emerging on new communication standards, the BMS has been extended to handle new communication standards as well; this includes the ZigBee and Digital Addressable Lighting Interface (DALI) communication standards. With more standards supported by the BMS, new types of smart appliances are easily integrated into the control of the building. The BMS has primarily been developed in Java, while C has been used for low-level communication with the transceiver. The BMS is divided into several modules that are running independently of each other; these include a database module for storing the state of the building, a SYSLAB interface module, which handles communication with the node computer, a hardware module, which handles communication with hardware, e.g. the transceiver, and finally a controlling module, which handles the overall control of the building.

The heating of PowerFlexHouse I is based entirely on electrical sources and comes from five heat pumps and ten resistive convection heaters. The heat pumps are mounted in the south facing rooms, whereas the convection heaters are equally distributed inside the building. Various controllers have been implemented in the BMS, seeking to optimise the heating of the building with respect to different criteria. These controllers include a simple hysteresis controller of the heating in the individual rooms and a model predictive controller (MPC) optimising

heating with respect the day-ahead price of electricity provided by Nord Pool Elspot, cf. Section 2.2.1. Moreover, there is another hysteresis controller which increases space heating when local generation from the Gaia wind turbine is high. This is achieved by manipulating the temperature setpoint in correlation with a moving average of the wind power generation. Exogenous data for the wind power generation is provided by the node computer controlling the Gaia wind turbine.

4.3 Power Hub

Power Hub is an implementation of a virtual power plant, whose development was initiated by the Danish Energy company DONG Energy and was further developed as a part of the TWENTIES[3] project [44]. The TWENTIES project was a large-scale European demonstration project co-funded by the European Commission under the 7th Framework Programme, which was completed in the summer of 2013. The main objective of the project was to investigate how a large penetration from wind power can be integrated into the European power system. The project is regarded as a key project in the goal of achieving the European Union's 2020 targets for climate and energy: 20% of the consumed energy should come from renewable sources, the energy efficiency should be increased by 20% and there should be a minimum 20% reduction in greenhouse emissions [45].

Power Hub was developed to demonstrate the potential of VPPs and how ICT can be utilised to maintain the balance between electricity generation and consumption in a power system based on a high share of intermittent renewable electricity generation. By coordination of its aggregated DERs, Power Hub has demonstrated being able to provide ancillary services to the TSO, like for example provision of reserve capacity, cf. Section 2.1. In November 2012, Power Hub was used in a large-scale demonstration on the Faroe Islands, where it

[3]TWENTIES - Transmission system operation with a large penetration of Wind and other renewable Electricity sources in electricity Networks using innovative Tools and Integrated Energy Solutions

provided load shedding from several DERs to counteract a simulated blackout of one of the islands diesel power stations, equivalent to 10% of the national power supply. During the simulated incident, Power Hub delivered primary reserve by decoupling the load of three large industrial companies, with a total consumption of more than 4 MW. This reserve was provided until another diesel generator was started to relieve the units providing the load shedding. Since the large-scale demonstration in 2012, Power Hub has continued its operations in the power system on the Faroe Islands. Before the initialisation of Power Hub, blackouts were a frequent recurring problem with around 30 outages each year of which a few have ended up as total blackouts. Since the introduction of Power Hub, major loads have been decoupled 16 times by Power Hub during grid instabilities, which – according to the main energy provider, SEV – has most likely prevented several outages in the islands power system and increased the stability of the whole power system.

As part of trialling Power Hub, a variety of DERs located in Denmark were integrated into Power Hub and had their power consumption optimised and remotely controlled by Power Hub. The units comprised up to 47 DERs running diverse industrial processes which are considered flexible; mainly because they have a fixed need for energy during a given period rather than a need for continuous power like the thermal processes described in previous chapter. Alternatively, because the DER has a generation capability that is not fully utilised, e.g. backup generators. Examples of processes that were integrated include:

- Lighting at a horticultural farm.
- Pumping of water at a pumping station.
- Pumping of water at a waste water treatment plant.
- Control of a HVAC system in an office building.
- Control of a gas turbine.
- Control of an emergency diesel genset.

By integration of these units, Power Hub has demonstrated that the DERs power consumption or generation could be controlled remotely, without having a significant negative impact on the processes run by the DERs; and more importantly, it was demonstrated that Power Hub could generate value for its customers – either economical value or by promoting the green agenda of a company – and that there is a potential business case for aggregated control of DERs connected in the low voltage grid.

Already before the finalisation of the TWENTIES project, Power Hub started operating on fully commercial terms in the Nordic power market, in which it has been operating since. Figure 4.3 presents the current role of Power Hub as a facilitator for market integration of DERs or possibly other aggregators. Here, Power Hub is depicted as a coordinator between flexible DERs on one side and the market for electric power and ancillary services on the other. In this way, DERs or other aggregating companies are granted an indirect access to operate in the power market and schedule their activities optimally with respect to the cost of electricity. The access to the power market is only indirect due to the fact that it is Power Hub that facilitates the market interactions through an optimisation process with respect to the current electricity price, and as such the DERs do not have any direct involvement in selling and buying power in the power market, except through a production or consumption plan, which is to be submitted to Power Hub on a day-ahead basis, cf. Section 4.5.

Currently, Power Hub is continuing its operation on the Faroe Islands and expanding into the English and German markets as well. Even though the market setup here are quite different from the Nordic market, the flexible front-end of Power Hub allows it to be easily integrated into other markets. For further information on Power Hub readers are referred to the Power Hub website [43].

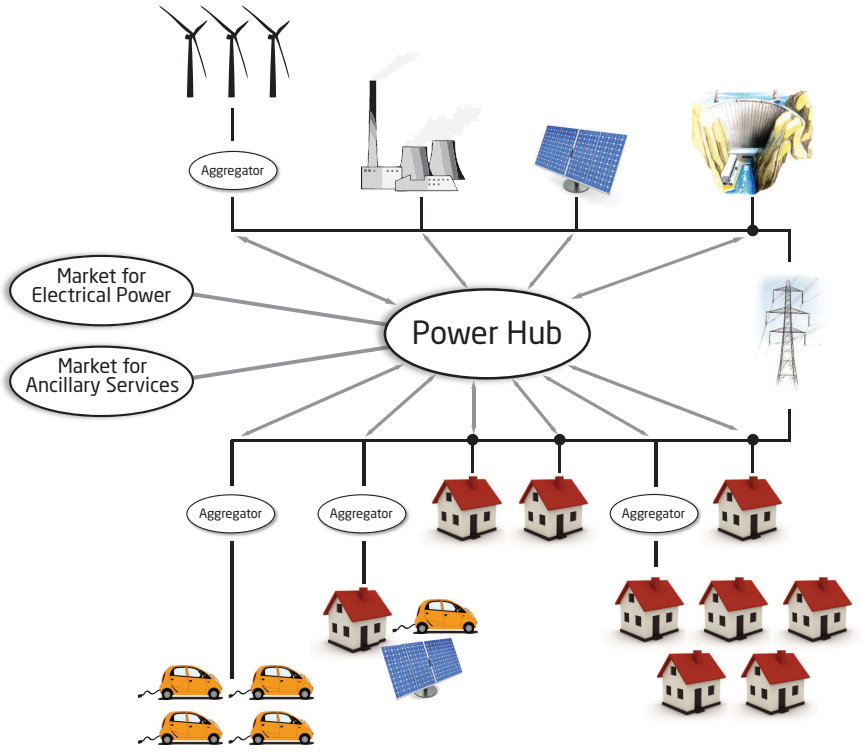

Figure 4.3: Role of Power Hub as a market integrator of DERs and aggregators.

4.4 Power Hub Control

When a DER is providing flexibility in the power system through Power Hub, priority of the process run by the DER will always precede the utilisation of flexibility. To guarantee that only the available flexibility is utilised a feedback control signal of the present capacity – or available flexibility – is communicated from the DER to Power Hub. It is the DER owner, likely together with Power Hub consultants, which must analyse the process run by the DER and determine where in the process the flexibility lies. When the source of flexibility

has been identified, a physical parameter in the process is selected to represent the defined flexibility. In the following, this parameter representing the flexibility that is available from a DER at a given time will be denoted the present *capacity* of the DER. Examples of capacity parameters for various flexible processes are given in Section 4.7. Finally, the DER owner specifies bounds of an acceptable interval of the capacity that he is willing to provide to Power Hub.

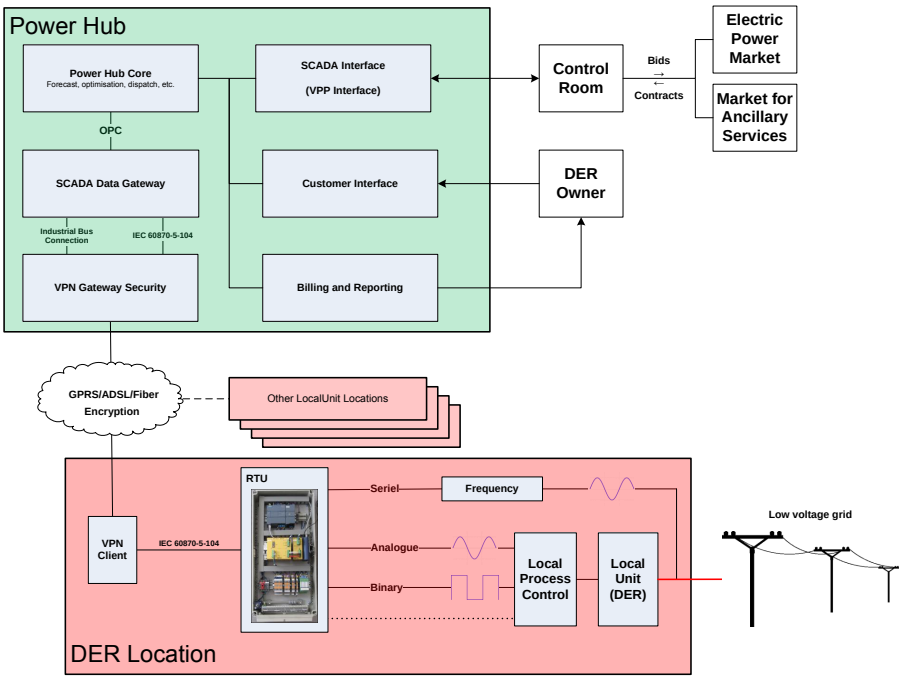

Figure 4.4: Simplified schematics drawing of the Power Hub architecture.

Figure 4.4 shows a simplified schematic drawing of the most essential parts of Power Hub and the actors involved. In the green box the basic parts of Power Hub are depicted: in the top right corner the SCADA interface to the control room, which handles the interactions with the power market, is depicted. Below is an external interface to

Power Hub where DER owners can enter static data for their DER, e.g. capacity constraints, and submit a schedule of operation for the following day. Further below is an automatic billing and reporting system, which provides an overview of the power consumed or generated by a DER. In the top left corner the core of Power Hub is depicted, here is the optimisation, forecast of the available capacity of DERs and dispatch carried out. The communication with the DERs goes via a SCADA data gateway and a virtual private network (VPN) gateway providing encryption of the communication between Power Hub and DERs. An Ethernet – possible Internet – connection is used for communication, for instance using a standard internet connection or the mobile network. The underlying protocol used for communication is the IEC 60870-5 transmission protocol, which is a well-established protocol for telecontrol of DERs. The lower red box marks the location of a DER; here, a VPN client is running, which is decryption the data coming from Power Hub and likewise encrypting the data going back. Finally, a remote terminal unit (RTU) is providing the control signals to the local controller which is controlling the process of the DER.

To facilitate the communication between Power Hub and DERs a standardised interface for communication has been developed. The interface is represented by a number of input and output (I/O) of the RTU, as depicted in Figure 4.4. Table 4.1 presents the control- and feedback signals being communicated between Power Hub and a DER.

Name	Type	I/O
Present power consumption or generation	Analogue	Input
Power setpoint for generation or consumption	Analogue	Output
Present capacity	Analogue	Input
Power Hub enabled	Digital	Input
DER running	Digital	Input
DER error	Digital	Input
DER start	Digital	Output
DER stop	Digital	Output
Pulse measurement	Digital	Input
Frequency measurement (optional)	Analogue	Input

Table 4.1: Interface for communication between Power Hub and a DER. Input and output are relative to the RTU, i.e. Power Hub.

The *present power consumption or generation* is a local measurement of the power exchanged between the DER and the grid, which is send to Power Hub. The *power setpoint* is a power reference, which is send from Power Hub to the DER, for the requested power consumption or generation, which under ideal conditions should match the power exchanged with the grid at any given time. The *present capacity* is an abstract measure of flexibility that is available in the local process run by the DER. Typically, the capacity is a local measurement of a physical process parameter, e.g. volume of water to be pumped, temperature or lighting to be provided. *Power Hub enabled* is input to the Power Hub which informs Power Hub whether telecontrol of the DER is allowed. This provides an option for the DER owner to opt out of telecontrol from Power Hub. *DER running* and *error* informs Power Hub whether the DER is running – or is online – and whether there has occurred an error on the DER, respectively. In case of an error, telecontrol from Power Hub is automatically disabled. *DER start* and

DER stop are start and stop commands send from Power Hub to the DER, which starts and stops the local process. The *Pulse measurement* is a forwarding of the pulse signal coming from an electricity meter installed on the site of the DER. Using the pulse measurement, Power Hub is able to verify the power consumption signal returned by the process controller. Finally, there is an optional frequency input for provision of a local frequency measurement to Power Hub. Local frequency measurements are required by the Danish TSO if the flexibility of the DER is to be provided as primarily or secondary regulating power as an ancillary service. By introduction of a standardised interface the roles and responsibilities are clearly defined, i.e. DONG Energy is responsible for the processes lying behind the RTU, relative to the DER, whereas the DER owner is responsible for the local process control and the maintenance of the DER.

To be able to bid the flexibility of its connected DERs into the day-ahead market, Power Hub has to receive an operation schedule on a daily basis for the following day of operation, i.e. a plan of the expected consumption or generation. Furthermore, to be able to reach the gate closure at noon in the Nord Pool Elspot market, the operation schedule has to be received by Power Hub no later than 10 a.m. The operation schedules submitted by the DERs are aggregated and bids on supply and demand, respectively, are placed in the Nord Pool Elspot trading system. If Power Hub receives contracts of either generation or consumption, or both, Power Hub will deliver on an hourly basis on the following day accordingly to settled contracts. Alternatively, if Power Hub does not receive any contracts in the day-ahead market, the flexibility of the DERs can instead be bid into the intraday market – Elbas – or into the market for ancillary services. The operation schedules are generated individually by the DER owners and uploaded to Power Hub through the customer web interface, which is shown in Figure 4.4. The operation schedule is entered as pairs of time interval and expected generation or consumption during the given interval.

4.5 Integration of PowerFlexHouse I into Power Hub

With the initiation of this project, a control panel with an integrated RTU, mobile broadband modem and an uninterruptible power supply (UPS) were installed in PowerFlexHouse I. The interface to Power Hub is accessible on a screw terminal board which is mounted inside the control panel. Here, the I/O is represented by electric signals, where digital I/O of the RTU is represented by an isolated voltage, where zero voltage equals 0 and 24 V equals 1. Likewise, analogue I/O is represented by a 4–20 mA current loop, where the I/O value from Power Hub is given by a linear mapping of the current. The electric I/O from the RTU can not be directly read by the BMS; therefore the screw terminal was wired to a bus coupler, which is converting the electric signal to Modbus over Ethernet (TCP/IP). The whole hardware setup is shown in Figure 4.5, where the Power Hub control panel is depicted to the left and the bus coupler to the right. In the control panel the following can be seen from the top: the RTU, USP, GPRS modem and the screw terminal board at the bottom. Additionally, the *Power Hub enabled* input is wired to a manual switch (below the bus coupler), which allows a user of the building to override the control from Power Hub. The state of the switch is shown by a small light bulb mounted next to the switch.

To provide demand response from the heat load of PowerFlexHouse I using Power Hub, a comprehensive amount of software has been developed during this project. The heat load controller was implemented as an extension to the controller module in the existing BMS. Figure 4.6 depicts a Unified Modelling Language (UML) class diagram of the software that was developed to control the heat load from the output provided by Power Hub. Here, in the center of the diagram, the ControllerManager class (black) is representing the controller module of the existing BMS, which is implemented as a base class for all the building controllers; hence, offering basic control functionalities, but does not contain any "intelligence" as such. Below the ControllerManager class is the implemented Power Hub controller – PowerHubCon-

Power Hub interface:

- Current consumption
- Current capacity
- Power Hub enabled
- Online
- Error
- Current setpoint
- Use setpoint
- Start/Stop command

Figure 4.5: Control panel (left) with the RTU, UPS, GPRS modem and screw terminal board. Bus coupler, switch and light bulb (right).

troller (green) – that was added to the portfolio of controllers in the BMS. The controller has been implemented as a mediator between the I/O classes from Power Hub (red) and control logic (yellow). Moreover, the controller is responsible for storing the data and requested commands coming from Power Hub in a local database (blue). To the right, marked in red, are the classes that handle communication with

Power Hub. The four implementations of I/O classes include a Modbus polling routine for reading the I/O from the bus converter, a local Power Hub server and a server and client for remote reading of the bus converter. The local server was developed for simulation of I/O from Power Hub, thereby providing a higher level of control of the I/O. To the left are the implementations of the control logic, which are responsible for dispatching power equal to the requested setpoint and also for keeping the temperature inside the comfort band that is specified by the users of the building. These classes contain both an optimisation procedure, which is optimising the aggregated power consumption from the ten space heaters with respect to the given setpoint and indoor comfort, i.e. temperature, as well as a dispatch procedure, which sends an actuating command to each of the heaters in the building. The dispatch problem is formulated as a mixed integer programming (MIP) problem with soft constraints on the temperature bands. This dispatch problem is presented in the following section and in Paper D.

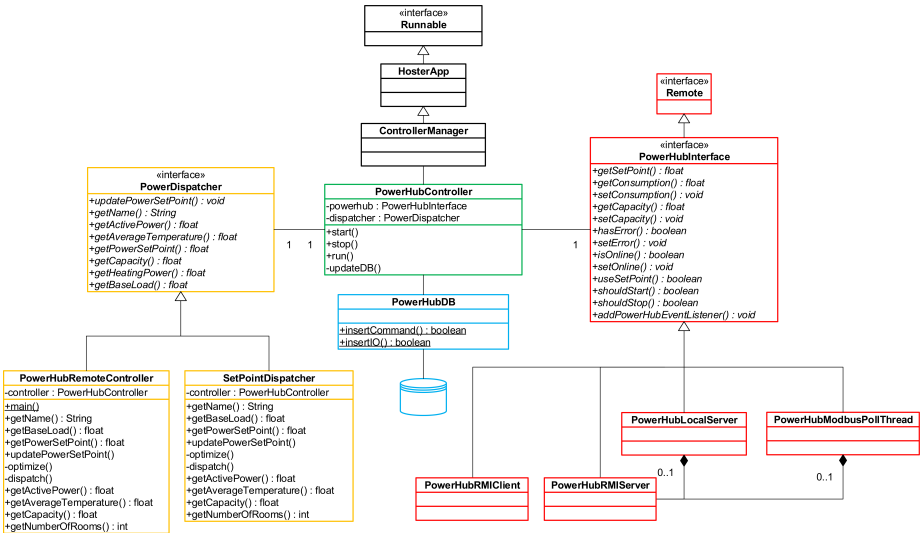

Figure 4.6: UML class diagram of the software developed during the project.

Furthermore, to guarantee the indoor comfort of the office building, a fallback thermostatic (hysteresis) controller has been implemented as part of the PowerHubController class. The fallback controller is activated if Power Hub telecontrol is disabled, either by manually flipping the switch or in case of a lost connection with Power Hub and erroneous I/O. When the thermostatic controller is active all I/O from Power Hub is ignored until Power Hub control is enabled again or the controller has been reset. The fallback controller has been used several times during this project to bring PowerFlexHouse into a well know state before providing up- and down regulation; especially, during the field experiments presented in Paper D.

4.6 Optimal Dispatch of the Heat Load in PowerFlexHouse

The heat load in PowerFlexHouse comes from ten electric space heaters each with a rated power in the interval from 0.95 kW to 1.25 kW. To dispatch an aggregate heat load of the ten heaters as close to the given power setpoint as possible, without violating the temperature constraints given by the residents, an optimisation problem is formulated. Here, the cost function in the power dispatch problem is given by

$$\left| \sum_{j=1}^{n} (x_j P_j) - S \right| + \sum_{j=1}^{n} x_j P_j \, w\left(T_j\right) \tag{4.1}$$

where the decision variable $x_j \in \{0, 1\}$ is the off/on state of heater j, P_j is the rated power of heater j, S is the power setpoint received from Power Hub and $n \equiv 10$ is the number of heaters in the PowerFlexHouse. The weight function, $w\left(\cdot\right)$, of the temperature in the room with heater j, is used to enforce a soft constraint on the discomfort felt by the building residents. Soft constraints were chosen to gradually penalise deviations from the desired temperature reference. The optimisation problem is given by a minimisation of the cost function defined in Equation (4.1), which is non-linear due to the absolute term and hence the solution can not be found straightforwardly; instead the

cost function is split into two sub-problems, which are then solved individually i.e.

For $\sum_{j=1}^{n}(x_j P_j) \geq S$	and for $\sum_{j=1}^{n}(x_j P_j) < S$
$\min \sum_{j=1}^{n}(x_j P_j) - S + \sum_{j=1}^{n} x_j P_j\, w(T_j)$	$\min S - \sum_{j=1}^{n}(x_j P_j) + \sum_{j=1}^{n} x_j P_j\, w(T_j)$
$\min \sum_{j=1}^{n}(w(T_j)+1)\, x_j P_j$	$\min \sum_{j=1}^{n}(w(T_j)-1)\, x_j P_j$
s.t. $\sum_{i=1}^{n} x_j P_j \geq S$	s.t. $\sum_{i=1}^{n} x_j P_j < S$

where each of the two sub-problems is a binary integer programming problem. The two problems are formulated as MIP problems and solved individually using the GNU Linear Programming Kit (GLPK) for Java. The solution having the lowest cost function is the global optimal solution to Equation (4.1). Finally, when the optimal solution has been found the binary commands are sent to the actuators controlling the resistive heaters.

For implementation of the soft constraints in Equation (4.1) the following weight function was used,

$$w(T_j) = \left(\frac{2(T_j - T_{ref})}{\Delta T}\right)^m \tag{4.2}$$

where T_{ref} is the desired indoor temperature reference and ΔT is the width of the temperature band in which the temperature is allowed to vary; both parameters are set by the users of PowerFlexHouse. m defines the steepness of the weight function at the bounds of the temperature band. To make the function in Equation (4.2) odd around T_{ref}, m has to be an odd number. In the implementation of the Power Hub controller $m \equiv 9$ was used.

For a more detailed description of the dispatch problem readers are referred to Paper D.

4.7 Power Hub Energy Model

To ensure a smooth operation of the DERs in the portfolio that is maintained by Power Hub, a generalised model of the state of energy of a DER is used. The model is used to continuously ensure that acceptable operational conditions are kept and for making forecasts of the potential future flexibility of the DERs. The model builds on the assumption that the returned capacity reading is representing the level of energy in a generalised energy reservoir. Table 4.2 presents some examples of flexible DERs, together with proposed capacity parameters and the type of energy reservoir that is being utilised.

DER	**Capacity measurement**	**Physical energy reservoir**
Hydroelectricity plant	Water level in reservoir	Potential energy in the water reservoir
Cold storage/HVAC	Temperature	Thermal energy reservoir
Flywheel	Revolutions per minute	Kinetic energy reservoir
Diesel genset	Volume of available diesel	Chemical energy reservoir

Table 4.2: Examples of DERs, capacity readings and type of energy reservoir.

Since only one measurement is returned by a DER to Power Hub the energy model is restricted to one independent – observable – variable; therefore, the model is formulated as a first-order difference equation, where the state variable is representing the energy level in the reservoir. The level in the reservoir is subject to external disturbances causing a non-controllable inflow and outflow of energy. Likewise, the reservoir is subject to a controllable inflow and outflow of energy through a controllable conversion process that converts electrical power into energy and vice versa. The energy reservoir model is illustrated in Figure 4.7.

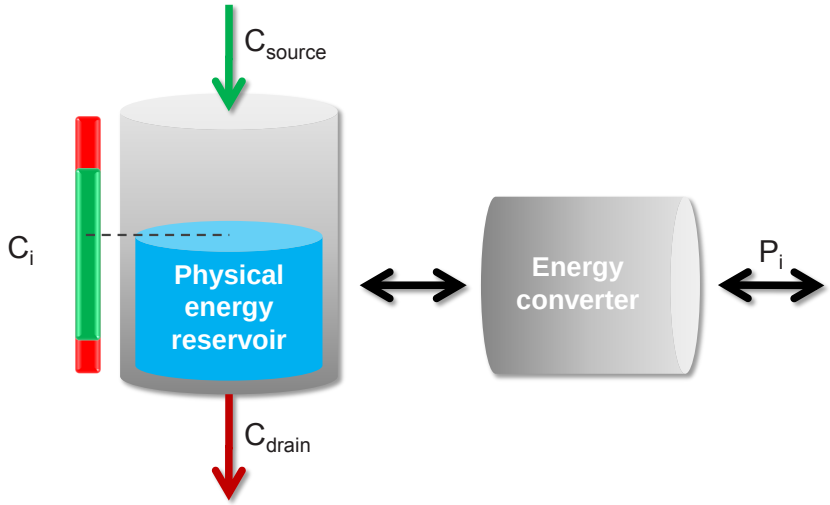

Figure 4.7: Power Hub energy reservoir model of a DER. Source: DONG Energy [46].

On mathematical form the reservoir model is given by,

$$C_{i+1} = C_i + C_{source,i} - C_{drain,i} + \tau\eta P_i \tag{4.3}$$

where τ is the length of the time interval between observations, C_i is the observed capacity at time step i and $C_{source,i}$ and $C_{drain,i}$ are the exogenous disturbances from inflow and outflow, respectively. P_i is the electric power output from or input to the DER at time i and η is a linear conversion factor from power to capacity. In operation of the DER the capacity has to respect the given constraints,

$$C_{min} \leq C_i \leq C_{max} \tag{4.4}$$

where C_{min} and C_{max} are the minimum and maximum constraint on the capacity level, which are specified by the DER owner before his DER unit is commissioned under Power Hub. Likewise, the amount of electrical power that can be generated or consumed by a DER is physically limited by the constraints,

$$P_{min} \leq P_i \leq P_{max} \tag{4.5}$$

where P_{min} and P_{max} are the minimum and maximum power that a DER is physically possible of generating or consuming, respectively. Values for both minimum and maximum electric power and capacity constraints are kept as static data in Power Hub and are specified before a DER is commissioned for Power Hub control. Likewise, the type of DER is specified as generating, consuming or potentially storage, such that the operational signs on the energy conversion process are known to Power Hub. Moreover, Power Hub stores static data for how a DER can be controlled, i.e. whether the power of the unit can be controlled binary or continuously, whether the DER can be started and stopped – decoupled from the grid – and whether the unit can be utilised for primary regulation. Finally, static data can be entered for minimum and maximum runtime for the unit, as well as minimum downtime after being turned off and data for economical parameters, e.g. cost of operation and startup cost. In operation Power Hub will comply with the specified constraints and in return expect the DER to comply with setpoint changes and commands send to it as long as the capacity is kept within the agreed bounds. Capacity constraints can be changed manually through the Power Hub interface and specified as either constant or with a daily variation.

Model input from external disturbances, i.e. C_{drain} and C_{source} can be handled by Power Hub in several ways; they can be measured onsite and provided to Power Hub using an on-line service, they can be estimated by Power Hub or they can be entered as static data by the DER owner or a Power Hub operator. Alternatively, they can simply be ignored if the impact on the reservoir is negligible or as an approximation.

In Paper C, the reservoir model has been used as a basis for an autoregressive model with exogenous inputs (ARX) for aggregated control of electric heating from heat pumps and resistive heating systems.

Chapter 5

Heat Dynamic Modelling

System identification of heat dynamic models for buildings – and especially PowerFlexHouse – constitutes a major part of the scientific contributions of this thesis: firstly, two models, a linear and non-linear, have been identified for PowerFlexHouse, which have been published in Paper A and B, respectively. Both models were used during several field experiments where PowerFlexHouse was utilised as a flexible load under supervisory control of Power Hub. The two models were used for estimation of the heat load for the following day of operation, which was compiled into a daily operation schedule for the heat load and submitted to Power Hub, cf. the description given in Section 4.4. The field experiments are presented in Paper D, where also the outcomes of these experiments are presented. Secondly, in Paper C, two linear models are used for simulations of the heat dynamics of two different types of buildings each utilising a different type of space heating, i.e. resistive heating and heating using a heat pump. The two models were implemented in MATLAB as part of a simulation framework for simulation of aggregated control of heat loads connected in the low-voltage grid. The simulation framework is presented in the following chapter. Thirdly, the linear model presented in Paper A has been used in a model predictive control (MPC) of the heat load in PowerFlexHouse, which is optimising the dispatch of the heat load with respect to a given signal of the day-ahead spot price in the Nord

Pool Spot market, cf. Section 2.2. This work is presented in Paper E, F and G.

In this chapter, the heat dynamic models that were identified for PowerFlexHouse during this project are presented. The models range from a simple generic model of a household utilising resistive heating, which has been used for optimisation of aggregate power consumption in Paper C, to a non-linear stochastic model, which includes the non-linear effects from air-infiltration through the building envelope. Models of adequate accuracy are essential for both control and forecast of the heat load in buildings. Moreover, in relation to Power Hub, predictions of the heat load in buildings up to 38 hours in advance are needed to generate the operation schedule for the following day such that the consumption can be aggregated and bid into the Nord Pool day-ahead market before gate closure at noon, cf. Section 4.4.

In this thesis, the general approach of identifying models for the heat dynamics of PowerFlexHouse has been to use a grey-box modelling approach: first, a set of coupled stochastic differential equations describing the heat dynamics of the building are formulated using prior knowledge about heat dynamics of buildings. Then, when an expected model structure has been established, statistical methods are used to estimate model parameters from a time series of system input and output. Finally, the model is validated in both the time and frequency domain using statistical analysis of the residuals. If validation fails the model structure is updated and parameter estimation and validation are repeated. A presentation of such an approach is given in [48].

Initially, this chapter gives an elementary introduction to the principles of heat dynamics and their relation to RC-circuits: electric circuits composed of resistors and capacitors. Following, a grey box approach is used to formulate a set of coupled differential equations, which are written on state space form in continuous time, describing the heat dynamics of a building. Next, a stochastic process is added to the state space model and the solution to the new stochastic differential system is derived, which is then used to formulate a prediction

model in discrete time. Following this, a method for estimation of the parameters in the stochastic continuous state space model is described. Finally, some of the models that were identified during this project are presented together with the estimates of model parameters.

5.1 Heat Dynamic Theory and RC-circuits

An often used approach for formulating heat dynamic models is to divide the system of interest into a number of objects – *lumps* in the following – in which the temperatures are approximated to be homogeneously distributed. Consequently, the system can be modelled as a number of discrete lumps, which are exchanging thermal energy with each other and typically an ambient environment. In this way the dimension of the heat dynamic model is reduced from – in theory – an infinite to a finite problem.

Using a lumped model approach, the temperature in each lump is modelled by its own state variable. This temperature state varies due to a net inflow or outflow of thermal energy coming from adjacent lumps or other thermal sources, e.g. solar irradiance or electric heating. In the lump, the rate of change in temperature is directly proportional to the net rate of heat flow, where the coefficient of proportionality is given by the heat capacity of the lump. Hence, the heat capacity describes how much energy that can be accumulated inside a lump in a given temperature interval, i.e.

$$\dot{Q} = \frac{dQ}{dt} = C\left(T\right)\frac{dT}{dt} \approx C\frac{dT}{dt} \tag{5.1}$$

where $\dot{Q}$ is the net rate of heat transfer with the lump and $C\left(T\right)$ is the aggregated heat capacity of the lump. The heat capacity is in general temperature dependent, however, due to the low temperature interval in which a building is operated the heat capacity is in the following assumed to be constant.

Exchange of thermal energy occurs by several different physical mechanisms, which comprise conduction, convection, ventilation and radi-

ation. When formulating a lumped model of a heat dynamic system, heat transfer between adjacent lumps due to conduction and convection is typically assumed to be proportional to the temperature difference between the two. Here, the coefficient of proportionality is given by the thermal conductance, U, but due to the resemblance with Ohmic resistors the thermal resistance, $R = 1/U$, is often used instead. Assuming a linear relationship between the heat exchanged between lumps and their temperature difference the rate of heat exchange is given by,

$$\dot{Q} = \frac{dQ}{dt} = U\left(T_1 - T_2\right) = \frac{1}{R}\left(T_1 - T_2\right)$$

where T_1 and T_2 are the temperatures of the first and second lump, respectively. According to the laws of thermodynamics, the heat flow will always be in the direction of the negative temperature gradient, which means that if $T_1 > T_2$ the net flow, $\dot{Q}$, will be from the first lump to the second and vice versa.

Contrary conduction and convection, energy exchanged by radiation is non-linear and thus an approximation of linearity can not be justified. However, due to the low temperature differences between lumps inside a building, the thermal energy exchanged by them due to radiation can be assumed to be negligible relative to the energy exchanged by conduction and convection. Another source of radiation is the sun, which can carry a significant amount of energy and thus can not be neglected in heat dynamic models of buildings. Therefore, solar irradiance is typically measured or estimated and modelled as an exogenous input to the heat dynamic model, similarly to the ambient temperature. Also, the heat exchanged by ventilation of air – natural or forced – to the outside ambient environment is non-linear, but has in general been approximated to be linear with a direct coupling between the inside- and outside environment in most of the models used in this thesis. However, in Paper B the coupling to the outside is modelled with a non-linear function of the wind speed. For a more comprehensive description of heat dynamics readers are referred to [49] or Chapter 2 in [50].

Due to the many similarities between heat transfer and transfer of electric charge, a commonly used method for modelling a heat dynamic system is to use equivalent RC-diagrams, where resistors and capacitor are combined in an electric circuit that is representing the heat flow in the heat dynamic system. Using this method, it is easy to outline the heat dynamics of a system as an RC-diagram from which the differential equations can be derived straightforwardly. Moreover, RC-diagrams serves as a good tool for presenting how thermal energy flows between lumps. Table 5.1 provides an overview of heat dynamic concepts and their electrical equivalents. From the table is seen that temperature difference is equal to electric potential difference – voltage – and flow of energy due to temperature differences, i.e. heat flow, is equivalent to flow of electric charge due to voltage differences. Likewise, the equivalent to thermal resistance is the electrical resistance and the equivalence of heat capacity is electric capacitance.

Heat dynamics		**Electrical equivalent**	
Temperature	°C	Voltage	V
Rate of heat flow	$W = J/s$	Rate of charge flow	$A = C/s$
Thermal resistance	$°C/W$	Electrical resistance	$\Omega = V/A$
Heat capacity	$J/°C = Wh/°C$	Capacitance	$F = As/V$

Table 5.1: Heat dynamic concepts and their electrical equivalents.

Figure 5.1 presents an RC-diagram of a simple heat dynamic system, which could be used as a model for the heat dynamics of an oven. In the RC-diagram, T_i is the temperature of a lump having heat capacitance C_i. The thermal storage of the lump is exchanging thermal energy with an ambient environment with temperature T_a through the thermal resistance R_i. Moreover, it is receiving an inflow of thermal energy from the controllable heat input Φ_h.

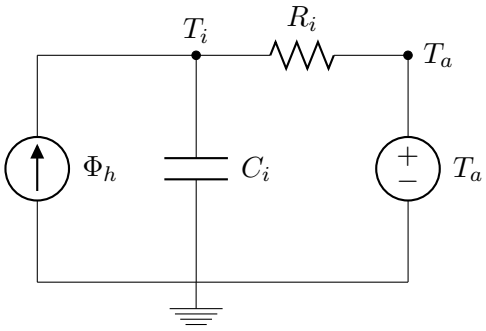

Figure 5.1: Simple RC-diagram of the heat dynamics of an oven.

From the RC-diagram in Figure 5.1 the differential equation describing the temperature state can straightforwardly be derived as,

$$C_i \frac{dT_i}{dt} = \frac{T_a - T_i}{R_i} + \Phi_h \tag{5.2}$$

In general, the heat dynamic models are not as simple as the one described by Equation (5.2) but comprises several coupled first order differential equations. Since the coupled differential equations are assumed linear and their parameters to be time-invariant, the coupled differential equations can be written on compact matrix form using state space representation, i.e.

$$\frac{d\boldsymbol{T}(t)}{dt} = \boldsymbol{A}\boldsymbol{T}(t) + \boldsymbol{B}\boldsymbol{U}(t) \tag{5.3}$$

where $\boldsymbol{T} \in \mathbb{R}^n$ is the state vector, which is containing the temperature states of the n lumps, and $\boldsymbol{U} \in \mathbb{R}^m$ is an input vector containing both control input and exogenous disturbances. $\boldsymbol{A} \in \mathbb{R}^{n \times n}$ and $\boldsymbol{B} \in \mathbb{R}^{n \times m}$ are the system- and input matrix, respectively. Typically, all the states in $\boldsymbol{T}$ are not observable, hence a measurement equation is introduced,

$$\boldsymbol{Y}(t) = \boldsymbol{C}\boldsymbol{T}(t) \tag{5.4}$$

where $Y \in \mathbb{R}^q \subseteq \mathbb{R}^n$ is the measurement vector and $\boldsymbol{C} \in \mathbb{R}^{q \times n}$ is a matrix that is extracting the measured states from $\boldsymbol{T}$.

5.2 Continuous and Discrete Linear State Space Model

In most cases a deterministic state space model, as the one formulated in the previous section, is insufficient to give an adequate description of the heat dynamics of a building. This can be due to several reasons: for example, the model is most likely only an approximation to the real system, there might be unrecognised inputs, e.g. rain and wind, or the measurements of the input, $\boldsymbol{U}$, are associated with measurement errors. Therefore, a stochastic process is added to the deterministic state space model (5.3), which gives the stochastic differential equation,

$$d\boldsymbol{T}(t) = \boldsymbol{A}\boldsymbol{T}(t)\,dt + \boldsymbol{B}\boldsymbol{U}(t)\,dt + d\boldsymbol{\omega}(t) \tag{5.5}$$

where $d\boldsymbol{\omega} \in \mathbb{R}^n$ is a stochastic process. Likewise, to decouple measurement errors from $d\boldsymbol{\omega}$, another random process is added to the measurement equation describing the measurement error associated with observing $\boldsymbol{T}$. Hence,

$$\boldsymbol{Y}(t) = \boldsymbol{C}\boldsymbol{T}(t) + \boldsymbol{e}(t) \tag{5.6}$$

where $\boldsymbol{e} \in \mathbb{R}^q$ is the measurement error. In the following the measurement error and the diffusion term, $d\boldsymbol{\omega}$, are assumed the be mutually independent.

Assuming that both the system and input matrix are time invariant, the solution to Equation (5.5) can be found analytically [51] as,

$$\boldsymbol{T}(t+\tau) = e^{\boldsymbol{A}\tau}\boldsymbol{T}(t) + \int_t^{t+\tau} e^{\boldsymbol{A}(t+\tau-s)}\boldsymbol{B}\boldsymbol{U}(s)\,ds + \int_t^{t+\tau} e^{\boldsymbol{A}(t+\tau-s)}d\boldsymbol{\omega}(s) \tag{5.7}$$

where the matrix exponential is given by the power series

$$e^{\boldsymbol{A}} = \sum_{i=0}^{\infty} \frac{\boldsymbol{A}^i}{i!} \tag{5.8}$$

Further, assuming that the input $\boldsymbol{U}(t)$ is constant in the interval $[t, t+\tau]$, Equation (5.7) can be reformulated as

$$\boldsymbol{T}(t+\tau) = \boldsymbol{\Phi}(\tau)\boldsymbol{T}(t) + \boldsymbol{\Gamma}(\tau)\boldsymbol{U}(t) + \boldsymbol{v}(t,\tau) \tag{5.9}$$

where

$$\begin{aligned}\boldsymbol{\Phi}(\tau) &= e^{\boldsymbol{A}\tau} \\ \boldsymbol{\Gamma}(\tau) &= \int_0^{\tau} e^{\boldsymbol{A}s}\boldsymbol{B}ds \\ \boldsymbol{v}(t,\tau) &= \int_t^{t+\tau} e^{\boldsymbol{A}(t+\tau-s)}d\boldsymbol{\omega}(s)\end{aligned} \tag{5.10}$$

On the assumption that $\boldsymbol{\omega}(t)$ is a Gaussian white noise process with mutually independent and normally distributed increments, i.e. $d\boldsymbol{\omega}$ is a Wiener process, $\boldsymbol{v}(t,\tau)$ becomes normally distributed with zero mean and covariance,

$$\boldsymbol{\sigma}(\tau) = \begin{bmatrix} \sigma_1^2 & 0 & \cdots & 0 \\ 0 & \sigma_2^2 & \cdots & 0 \\ \vdots & \vdots & \ddots & \vdots \\ 0 & 0 & \cdots & \sigma_n^2 \end{bmatrix} \tag{5.11}$$

Finally, τ can be scaled such that it equals the length of one time step, or sampling period, i.e. Equation (5.5) in discrete time becomes,

$$\boldsymbol{T}(t+1) = \boldsymbol{\Phi}\boldsymbol{T}(t) + \boldsymbol{\Gamma}\boldsymbol{U}(t) + \boldsymbol{v}(t) \tag{5.12}$$

Since $\boldsymbol{v}(t)$ is normally distributed with zero mean, the one step prediction is simply given by

$$\hat{\boldsymbol{T}}(t+1) = \mathrm{E}\left[\boldsymbol{T}(t+1) \mid \boldsymbol{T}(t)\right] = \boldsymbol{\Phi}\boldsymbol{T}(t) + \boldsymbol{\Gamma}\boldsymbol{U}(t) \tag{5.13}$$

5.3 Model Parameter Estimation

This section presents a method for estimation of model parameters in the stochastic state space model derived in Equation (5.5). Consider an n-dimensional system of first-order ordinary differential equations given by,

$$d\boldsymbol{x}_t = \boldsymbol{f}(\boldsymbol{x}_t, \boldsymbol{u}_t, t, \boldsymbol{\theta})\, dt \tag{5.14}$$

where $t \in \mathbb{R}$ is the time, $\boldsymbol{x}_t \in \mathbb{R}^n$ is a vector containing the state variables, $\boldsymbol{u}_t \in \mathbb{R}^m$ is a vector containing the exogenous input to the

system and $\boldsymbol{\theta} \in \mathbb{R}^p$ is a vector with the unknown parametrisation of the linear or non-linear function $\boldsymbol{f}(\cdot) \mapsto \mathbb{R}^n$. In the following, $\boldsymbol{\theta}$ is assumed to be time-invariant. Under normal conditions a deterministic model is rarely sufficient to fully describe a physical system, cf. Section 5.2. Therefore, to account for variations not encompassed by a deterministic model, a noise term is added to the deterministic differential equation,

$$d\boldsymbol{x}_t = \boldsymbol{f}(\boldsymbol{x}_t, \boldsymbol{u}_t, t, \boldsymbol{\theta})\, dt + \boldsymbol{\sigma}(\boldsymbol{u}_t, t, \boldsymbol{\theta})\, d\boldsymbol{\omega}_t \tag{5.15}$$

where the noise term - or diffusion term - is driven by the stochastic process $d\boldsymbol{\omega}_t \in \mathbb{R}^n$, which in the following is assumed to be a standard Wiener process. $\boldsymbol{\sigma}(\cdot) \in \mathbb{R}^{n \times n}$ is a diagonal matrix containing the diffusion coefficients of the noise process.

Often only some of the system states are being observed and, furthermore, the observations are being sampled in discrete time and are typically subject to measurement errors. Thus, Equations (5.15) is supplemented with a measurement equation,

$$\boldsymbol{y}_k = \boldsymbol{h}(\boldsymbol{x}_t, \boldsymbol{u}_t, t, \boldsymbol{\theta}) + \boldsymbol{e}_k \tag{5.16}$$

where $\boldsymbol{y}_k \in \mathbb{R}^q$ is a vector with the observed values and $\boldsymbol{e}_k$ is the measurement error, which is assumed to be a q-dimensional Gaussian white noise process. $\boldsymbol{h}(\cdot) \in \mathbb{R}^q$ is a potentially non-linear function linking the system states to the observed output.

Given a time series of the observed output,

$$\mathcal{Y}_N = \left[\boldsymbol{y}_N, \boldsymbol{y}_{N-1}, \boldsymbol{y}_{N-2}, \ldots, \boldsymbol{y}_0\right] \tag{5.17}$$

the parameters in $\boldsymbol{\theta}$ can be estimated using the likelihood function. By finding the optimum of the likelihood function given the time series $\mathcal{Y}_N$, the most likely parameter set, $\hat{\boldsymbol{\theta}}$, is found. Hence,

$$\hat{\boldsymbol{\theta}} = \underset{\boldsymbol{\theta}}{\operatorname{argmax}} \left\{ L(\mathcal{Y}_N; \boldsymbol{\theta}) \right\} \tag{5.18}$$

where $\hat{\boldsymbol{\theta}} \in \mathbb{R}^p$ is the maximum-likelihood estimator. The maximum likelihood function is given by the joint probability density, which is

given by

$$L\left(\mathcal{Y}_N;\boldsymbol{\theta}\right) = p\left(\mathcal{Y}_N|\boldsymbol{\theta}\right) = p\left(\boldsymbol{y}_N|\mathcal{Y}_{N-1},\boldsymbol{\theta}\right) p\left(\mathcal{Y}_{N-1}|\boldsymbol{\theta}\right) \tag{5.19}$$

$$= p\left(\boldsymbol{y}_N|\mathcal{Y}_{N-1},\boldsymbol{\theta}\right) p\left(\boldsymbol{y}_{N-1}|\mathcal{Y}_{N-2},\boldsymbol{\theta}\right) p\left(\boldsymbol{y}_{N-2}|\mathcal{Y}_{N-3},\boldsymbol{\theta}\right) \cdots p\left(\boldsymbol{y}_0|\boldsymbol{\theta}\right)$$

$$= \left(\prod_{i=1}^{N} p\left(\boldsymbol{y}_i|\mathcal{Y}_{i-1},\boldsymbol{\theta}\right)\right) p\left(\boldsymbol{y}_0|\boldsymbol{\theta}\right)$$

where Bayes' rule has been applied N-times in the last equation to form the joint probability density function as a product of conditional densities.

Since both $\boldsymbol{\omega}_t$ in Equation (5.15) and $\boldsymbol{e}_k$ in Equation (5.16) are assumed to be normally distributed so are the conditional densities and thus fully characterised by its mean and variance. Introducing the conditional mean

$$\hat{\boldsymbol{y}}_{i|i-1} = \mathrm{E}\left[\boldsymbol{y}_i \mid \mathcal{Y}_{i-1},\boldsymbol{\theta}\right]$$

associated with the conditional covariance

$$\boldsymbol{\Sigma}_{i|i-1} = \mathrm{Var}\left[\boldsymbol{y}_i \mid \mathcal{Y}_{i-1},\boldsymbol{\theta}\right]$$

and the residual vector

$$\boldsymbol{\epsilon}_i = \boldsymbol{y}_i - \hat{\boldsymbol{y}}_{i|i-1} \tag{5.20}$$

the likelihood function can be written as,

$$L\left(\mathcal{Y}_N;\boldsymbol{\theta}\right) = \left(\prod_{i=1}^{N} \frac{\exp\left(-\frac{1}{2}\boldsymbol{\epsilon}_i^T \boldsymbol{\Sigma}_{i|i-1}^{-1} \boldsymbol{\epsilon}_i\right)}{\sqrt{(2\pi)^q \det\left(\boldsymbol{\Sigma}_{i|i-1}\right)}}\right) p\left(\boldsymbol{y}_0|\boldsymbol{\theta}\right) \tag{5.21}$$

The conditional mean $\hat{\boldsymbol{y}}_{i|i-1}$ and variance $\boldsymbol{\Sigma}_{i|i-1}$ can be estimated using various exact state filtering techniques; for example, a standard Kalman filter if $\boldsymbol{f}\left(\cdot\right)$ and $\boldsymbol{h}\left(\cdot\right)$ are linear and an extended Kalman filter otherwise.

An optimisation routine of the likelihood function given by Equation (5.21) has been implemented in CTSM[1], a tool for estimation of model parameter in stochastic differential equations. The optimisation routing finds the maximum likelihood estimate, $\hat{\boldsymbol{\theta}}$, using a quasi-Newton implementation. Estimates of the parameters in the identified models of the heat dynamics of PowerFlexHouse, found by CTSM, are presented in Section 5.5. CTSM has recently been extended with an interface to R and is freely distributed from its website [52].

5.4 Model Validation

In Section 5.2 it is assumed that $d\boldsymbol{\omega}$ is a Wiener process and thus $\boldsymbol{v}(t)$ in Equation (5.12) is normally distributed with zero mean. Consequently, provided that this assumption holds, the residuals of the one step prediction given by Equation (5.13) should be normally distributed with zero mean, i.e. Gaussian white noise; hence, if the residuals resemble a Gaussian white noise process it can be deduced that the dynamics of the system are adequately described by the mathematical model.

Several statistical methods for test of white noise properties exist, both in the time- and frequency domain. These methods comprise tests in the autocorrelation function, difference sign test, portmanteau test and test in the cumulated periodogram. These tests have been individually applied to the residuals of the identified models of PowerFlexHouse for validation. A general description of the listed tests is given in [53] and [51]. The prediction models are validated using cross validation, where a time series that is independent from the training time series is used for validation.

[1] Continuous Time Stochastic Modelling tool [52]

5.5 Identified Models

Several models of the heat dynamics of PowerFlexHouse have been identified during this project. Paper A presents the first identified linear model, which was developed for control of the electric space heating with respect to a varying price signal. Here, an MPC controller regulates the heat load in PowerFlexHouse such that the cost of heating is minimised. Additionally, several model candidates were presented in Paper B of which two identified models, a linear and non-linear, are presented in the following. In Figure 5.2, the equivalent RC-diagrams of the two models are depicted. From the figure is seen that there exists three temperature states, T_i, T_e and T_h, i.e. in the interior mass of the building, building envelope and heaters. Each of the three states is associated with a thermal heat capacity, C_i, C_e and C_h, respectively. The heaters receive a heat input, Φ_h, from the controllable electric space heaters. Likewise, the interior mass receives a heat input from solar radiation, Φ_s, entering the building through the windows with the effective area A_w. The heaters are giving off heat to the interior mass through the thermal resistance, R_{ih}. Similarly, the interior mass is coupled to the outside environment, with temperature T_a, through the envelope with thermal resistance R_{ie} and directly to the outside through R_{ia}. Finally, the thermal mass of the envelope is coupled to the outside through R_{ea}.

From the figure is seen that the two models are very alike only being different from each other in how the thermal resistance directly from the inside to the outside, R_{ia}, is modelled. In Figure 5.2 (a), R_{ia} is modelled as being linear, whereas in (b) it is modelled using a variable resistance. To model the non-linear effect of air infiltration, which is known to be dependent on the wind pressure on the outside of the building envelope, the following function of the thermal resistance was built into the model,

$$R_{ia}\left(W_{spd}\right) = \frac{1}{k_1 \cdot W_{spd}^{k_2}} \tag{5.22}$$

where W_{spd} is the wind speed outside the building and k_1 and k_2 are unknown parameters.

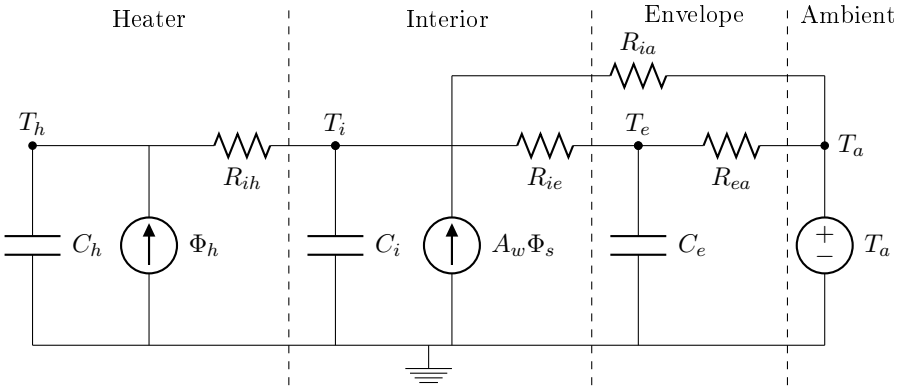

(a)

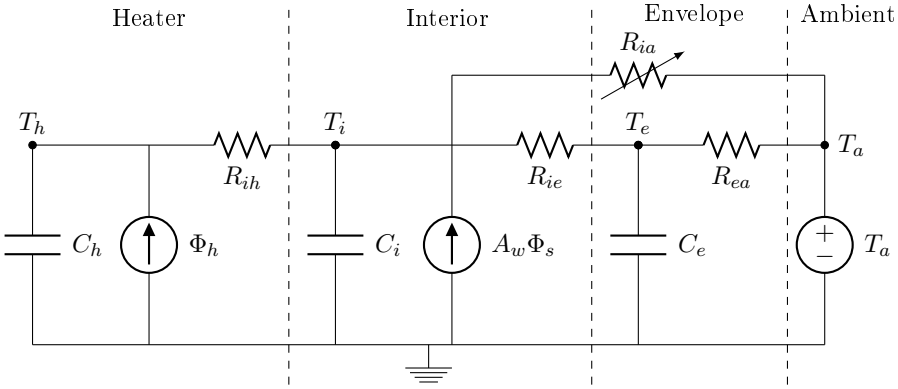

(b)

Figure 5.2: Linear (a) and non-linear (b) RC-diagram of the heat dynamics models of PowerFlexHouse presented in Paper B.

5.6 Heat Load Predictions

After the model parameters in the two heat dynamic models presented in Figure 5.2 have been successfully estimated and the model validated, a discrete model of the heat load can be formulated. The two heat dynamic models presented in Figure 5.2 can be written on discrete state space form, cf. Equation (5.12), i.e.

$$\boldsymbol{T}(t+1) = \boldsymbol{\Phi}\boldsymbol{T}(t) + \boldsymbol{\Gamma_1}\boldsymbol{U}(t) + \boldsymbol{\Gamma_2}\Phi_h(t) + \boldsymbol{v}(t) \tag{5.23}$$

where $\boldsymbol{T} = [T_i, T_e, T_h]^T$ is the state vector with the temperature states, $\boldsymbol{U} = [T_a, \Phi_s]^T$ is a vector containing the external disturbances, and Φ_h is the controllable heat input. $\boldsymbol{\Phi} \in \mathbb{R}^{3\times3}$ is the system matrix and $\boldsymbol{\Gamma}_1 \equiv \boldsymbol{\Gamma}_{(1:3,1:2)} \in \mathbb{R}^{3\times2}$ and $\boldsymbol{\Gamma}_2 \equiv \boldsymbol{\Gamma}_{(1:3,3)} \in \mathbb{R}^{3\times1}$ are the split input matrices such that the horizontal concatenation of $\boldsymbol{\Gamma}_1$ and $\boldsymbol{\Gamma}_2$ is equal to $\boldsymbol{\Gamma}$[2]. From Equation (5.23) the one step prediction of the indoor temperature is given by

$$\hat{T}_i(t+1) = \boldsymbol{\Phi}_{(1,1:3)}\boldsymbol{T}(t) + \boldsymbol{\Gamma_1}_{(1,1:2)}\boldsymbol{U}(t) + \boldsymbol{\Gamma_2}_{(1,1)}\Phi_h(t)$$

Setting $\hat{T}_i(t+1)$ equal to the indoor reference temperature, T_{ref}, gives

$$T_{ref} = \boldsymbol{\Phi}_{(1,1:3)}\boldsymbol{T}(t) + \boldsymbol{\Gamma_1}_{(1,1:2)}\boldsymbol{U}(t) + \boldsymbol{\Gamma_2}_{(1,1)}\Phi_h(t)$$

Hence, the estimated heat load over the one step period with length τ is given by,

$$\Phi_h(t) = \frac{T_{ref} - \boldsymbol{\Phi}_{(1,1:3)}\boldsymbol{T}(t) - \boldsymbol{\Gamma_1}_{(1,1:2)}\boldsymbol{U}(t)}{\boldsymbol{\Gamma_2}_{(1,1)}} \tag{5.24}$$

This equation was used for estimation of the heat load during the field experiments, which are presented in Paper D. During the initial field experiments a step size of one hour was used. However, this approach showed large deviations between the measured and the hourly predicted heat loads, primarily because of the large variations in weather that can occur within an hour, e.g. with respect to solar irradiance

[2] The number in subscript parenthesis uses MATLAB notation to define a subset of elements in the matrix.

during sunrise and sunset. Consequently, the step size was reduced to $\tau = 5$ min., which gave significant better predictions of the heat load within the hours of operation.

As an alternative to the heat load prediction model given by Equation (5.24), an alternative model was formulated. The RC-diagram in Figure 5.3 presents the heat dynamics of the model. Instead of estimating model parameters based on collected data, the model parameters in the alternative heat load model were estimated from a forecast of outdoor temperature and solar irradiance, generated by the local meteorology group at DTU Wind Energy. However, due to the inferior performance of the alternative model in predicting the heat load of PowerFlexHouse relative to the model presented in Equation (5.24). The latter was preferably used for generating the load forecasts – operation schedule – which were submitted to Power Hub.

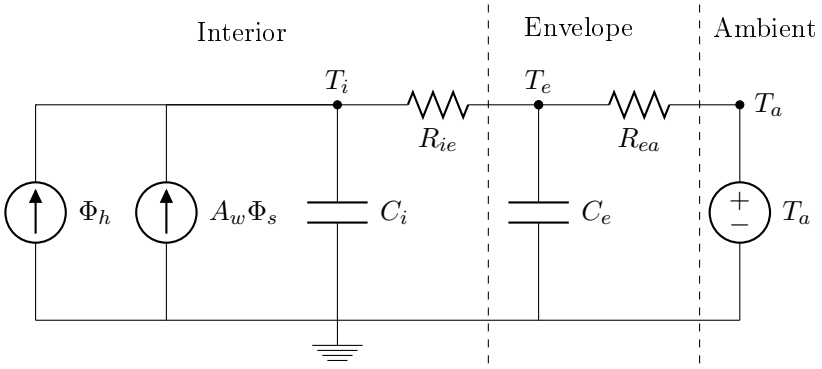

Figure 5.3: RC-diagram of alternative heat load prediction model.

5.7 Results and Model Validation

For the two models presented previously, the model parameters have been estimated using CTSM [52]. Table 5.2 presents the parameter estimates for the linear and non-linear model, respectively. The estimates of the non-linear model give a slightly higher likelihood value relative to the linear, however, at the cost one additional model parameter. In Paper B, a log-likelihood test between the two models shows that the non-linear model is performing slightly better – but statistical significant – than the linear model. The estimates in the table are seen to be quite similar for the two models only deviating significantly in the estimates of C_e. Naturally, also the estimates of R_{ia} are different, being equal to each other for $W_{spd} \approx 3$ m/s, which is close to the measured average wind speed of the collected time series used for parameter estimation. Moreover, from the table is seen that the total heat capacity of PowerFlexHouse is approximately 7 kWh/°C, which means that the heat capacity is slightly less than 60 Wh/(°C m^2). This characterises PowerFlexHouse as being extra thermally light [54], which is expected considering the light materials that the building is constructed from.

The two different models have been validated in Paper B using a statistical approach. The models, and thus implicitly the model parameter estimates presented in Table 5.2, are validated by applying statistical analyses to the residuals, i.e. the one step prediction errors, as defined by Equation (5.20). In the paper, the two models are validated by use of residual analysis, both in the time domain using the auto-correlation function, and in the frequency domain using the cumulated periodogram. However, unlike in a black-box approach, where little or no a priori information is available, an advantage of using the grey box modelling approach as presented above is that the model parameters are directly estimated, i.e. their physical interpretation is preserved. This means that the parameter estimates presented in Table 5.2 can be directly compared to model parameters found using a white box approach, i.e. by use of typical building parameter, which can be found in literature and national building regulations. In the following, the parameter estimates are validated using a white box

approach, where the parameter estimates are compared to expected building parameters.

Parameter		Linear model	Non-linear model
C_e	[kWh/°C]	4.741	4.169
C_h	[kWh/°C]	2.25×10^{-3}	2.27×10^{-3}
C_i	[kWh/°C]	2.555	2.540
R_{ia}	[°C/kW]	37.005	$1/(7.77 \times 10^{-3} W_{spd}^{1.135})$
R_{ea}	[°C/kW]	3.265	3.606
R_{ie}	[°C/kW]	0.817	0.841
R_{ih}	[°C/kW]	140.44	139.22
A_w	[m^2]	14.351	14.524

Table 5.2: Model parameter estimates from the linear and non-linear heat dynamic model for PowerFlexHouse.

Starting with the thermal resistance from the inside to the outside of the building the combined thermal resistance can be found by assuming a steady state in the heat transfer between the inside and outside. Hence, the combined thermal resistance through the building envelope is given by

$$R_{env} = \frac{1}{1/R_{ia} + 1/(R_{ie} + R_{ea})} \tag{5.25}$$

Assuming a wind speed of 5.4 m/s, which is the historical average wind speed measured at the location of PowerFlexHouse, $R_{env} = 3.67$ °C/kW and $R_{env} = 3.60$ °C/kW are found for the linear and non-linear model, respectively. Moreover, approximating PowerFlexHouse with a rectangular box with dimension 15 m × 8 m × 3 m (W×D×H), the total surface of PowerFlexHouse is approximately 378 m^2 and the average U-value of the envelope – including windows and floor – becomes $u = 0.72$ W/(°C m^2) and $u = 0.66$ W/(°C m^2) for the linear and non-linear model. In [55], the Danish requirements for U-values specified for buildings build at the time of construction of PowerFlexHouse is presented. Here, the requirements are $u_{req,wall} = 0.40$ W/(°C m^2)

and $u_{req,window} = 2.90$ W/(°C m^2) for exterior walls and windows, respectively. The window area of PowerFlexHouse is approximately 27 m^2 of the total area of 378 m^2; hence, the weighted U-value of PowerFlexHouse according to [55] is given by,

$$\begin{aligned} u &= \frac{(378-27)\ \text{m}^2 \cdot 0.40\ \text{W/(°C m}^2) + 27\ \text{m}^2 \cdot 2.90\ \text{W/(°C m}^2)}{378\ \text{m}^2} \\ &= 0.58\ \text{W/(°C m}^2) \end{aligned} \tag{5.26}$$

Assuming that PowerFlexHouse is constructed complying with the present regulations, the estimated U-value of the house envelope ($u = 0.72$ W/(°C m^2) and $u = 0.66$ W/(°C m^2)) are quite close to the expected value, as found from Equation (5.26). Using present requirements for U-values [56], the minimum U-values are $u_e = 0.3$, $u_f = 0.4$, $u_r = 0.2$, and $u = 1.8$, for exterior walls, floor, roof, and windows, respectively. Using these values a weighted U-value of $u = 0.41$ W/(°C m^2) is found for a present house with similar dimensions as PowerFlexHouse.

For the heat transfer resistance between the heaters and interior mass, R_{ih}, the estimated values seems quite high relative to the other thermal resistances. However, considering the small area of the heaters relative to the building envelope, the U-value of the heaters are significant higher ($\approx \times 5$) than the U-value of the envelope. In Appendix A, a method for calculating the convective heat transfer coefficient of a vertical plate is presented. Approximating the ten space heaters of PowerFlexHouse with vertical plates, each with dimension 0.4 m×0.6 m and an average activation temperature of the heaters of 40 °C, the convective heat transfer coefficient $R_{ih} = 120$ °C/kW is found. Likewise, this calculated white box estimate is much in line with estimate of R_{ih}, as presented in Table 5.2.

Similarly, the estimated window area, $A_w = 15$ m^2, can be validated by comparing it to the actual physical window area. In this way, it is found that the estimated area equals approximately 60% of the actual. This means that 60% of the outdoor global irradiance, measured on a horizontal surface, enters the building through the windows. This is

close to what is expected for triple glazed windows which are mounted vertically. A similar ratio between estimated and actual window area is achieved in [57].

Using a similar approach, the white box estimate of the heat capacity of the heaters is found. Assuming that the heaters are mainly comprised of iron, which has specific heat capacity $c = 450$ J/(kg°C) $= 0.125 \times 10^{-3}$ kWh/(kg°C). The mass of the space heaters are approximately 2 kg each, which means that the total heat capacity becomes 0.0025 kWh/(kg°C). This is likewise close to the estimated value.

Generally, the parameter estimates found using a white box approach matches the parameter estimates presented in Table 5.2. This further strengthens the conclusion of the residual analysis that is presented Paper B. From the paper it is concluded that the two identified models are providing an adequate description of the real physical system within the hourly time-scale.

Chapter 6

Simulation Framework for Aggregator Control

During this project a simulation framework has been developed for estimation of the potential of aggregated demand response from multiple households connected in a low voltage grid. The framework has been implemented in MATLAB and is based on a similar setup as Power Hub, cf. Chapter 4. Likewise, the Power Hub interface and the Power Hub Energy Model, as presented in Section 4.4 and 4.7, are used to facilitate the simulated communication between the simulated households and the aggregator. Moreover, the energy model is used for estimation of the available capacity of each of the households. In Paper C, the framework was used to estimate the flexibility of 100 households, which are heated by two diverse electric space heating systems: a resistive- and a central heat pump based heating system.

This chapter initially presents the models that were used for simulation of the heat dynamics of the two types of households. Following, the simulation framework is described and finally some simulations are presented and their results discussed.

6.1 Simulation Models for Residential Households

Initially, two models for simulation of the heat dynamics of residential households were implemented in two separate MATLAB classes. The first model is representing a modern type of a residential house in Denmark and hence was implemented as a thermally heavy building heated by underfloor heating from a geothermal heat pump. The other simulation model was implemented as a thermally light building, which is heated by a resistive heating system similar to PowerFlex-House. In Figure 6.1, the two RC-diagrams representing the heat dynamics of the two types of households are presented. The figure depicts the model of the building utilising resistive heating at the top (a) and the underfloor heated building below (b).

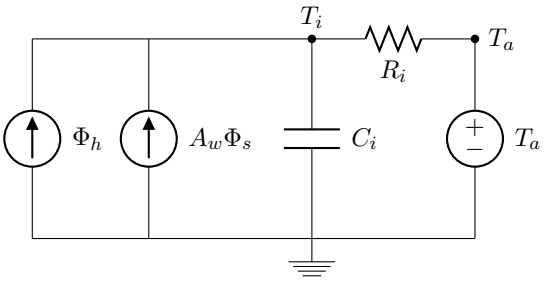

(a)

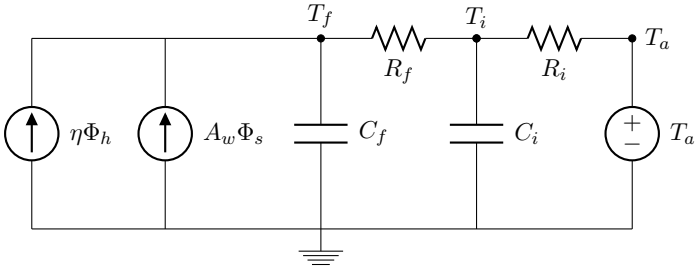

(b)

Figure 6.1: Equivalent RC-diagram for space heated household (a) and heat pump heated household (b).

As seen from Figure 6.1, the heat dynamic model of the thermally heavy building (b) has one additional temperature state, T_f, compared to the model of the thermally light building (a). This extra state represents the temperature in the heated floor, which is assumed to be made of concrete or a similar thermally heavy material. Consequently, the floor acts as an additional heat storage into which it is receiving a heat input from solar irradiance, Φ_s, and from a geothermal heat pump with COP η and power Φ_h. The values of the model parameters used in the simulations are presented in Table 6.1. The presented values are partly inspired by the parameters presented in Table 5.2, which were found from the studies of PowerFlexHouse and from the Danish building regulations, calculation tools from the Danish Technological Institute [58] and ROCKWOOL Energy Design, which is an on-line tool for energy calculations of buildings [59].

		Resistive heated household	Heat pump heated household
C_i	[kWh/°C]	8	3
C_f	[kWh/°C]	–	10
R_i	[°C/kW]	5	8
R_f	[°C/kW]	–	0.3
A_w	$[m^2]$	15	15
η (COP)	[–]	–	3
Φ_h^{max}	[kWh]	15	6
T_{min}	[°C]	20	20
T_{ref}	[°C]	21	21
T_{max}	[°C]	22	22

Table 6.1: Model parameters used for simulations.

Two different buildings with diverse heat dynamics were chosen to represent the variation that is present in the Danish building stock and furthermore to increase the overall dynamics of the aggregator. Another approach could have been pursued by randomly choosing the building specific model parameters, which are presented in Ta-

ble 6.1, centred around a given mean, e.g. by adding a stochastic process to the model parameters presented in the table. Likewise, a fixed temperature band, in which the temperature is allowed to vary, was chosen for all households. Finally, it is assumed in the simulation model that both types of households are able to dispatch a continuous amount of power in the interval $0 \leq \Phi_h \leq P_{max}$ as long as the temperature constraints, $T_{min} \leq T_i \leq T_{max}$, are not violated. Naturally, this is only an approximation to the real world since most commercial heat pumps can not deliver continuous power control. Similarly, the power consumption from a finite number of resistive heaters can only be controlled in discrete steps. However, since the number of aggregated units is high this approximation is assumed to hold because the consumption from each individual unit will even out the aggregate consumption as the number of households increase.

From the model parameters in Table 6.1, a discrete state space model is formulated for the resistive heated house and the heat pump heated house, respectively. First a continuous state space model is formulated as defined by Equation (5.3). Next, the discrete state space model is found from Equation (5.12), where the system- and input matrix are found by Equation (5.10). Integration of the matrix exponential, as defined in Equation (5.8), is numerically found by using the rectangle integration method. Consequently, each of the two households is represented by a system- and input matrix together with a state vector. These three parameters are common for both models and hence were implemented as class variables in an abstract base class, `House`. This class is also providing methods for dispatch of power, i.e. updating the temperature state given input vector $\boldsymbol{U}$ and for retrieving capacity readings. Moreover, the `House` class implements the Power Hub interface, which is the only interface that is exposed to the aggregator. Two subclasses of the `House` base class, `ResistiveHeatedHouse` and `FloorHeatedHouse`, each implements the specific type of household functionalities, e.g. discrete update of the temperature states. An overview of all the MATLAB classes that were developed for this framework is presented in Figure 6.2. In the diagram the `House` base class, together with the `ResistiveHeatedHouse` and `FloorHeatedHouse` are

all depicted in blue. In the lower right corner of the diagram additionally three ancillary functions are depicted. These helper functions implements functionality for obtaining the two discrete state space models and for facilitating matrix integration. Finally, in the top centre, the Power Hub interface is depicted, which is implemented as an abstract class.

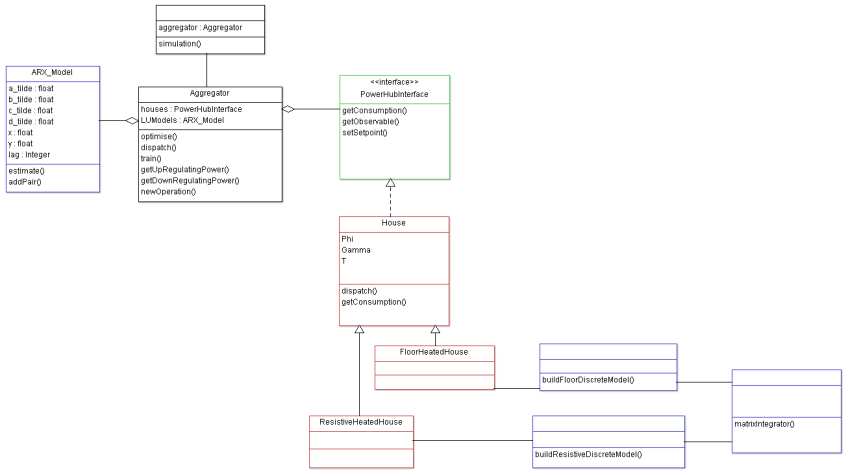

Figure 6.2: Class diagram for MATLAB classes for simulation of aggregate demand response from residential households.

6.2 Simulation Framework

The implementation of the aggregator class, `Aggregator`, in the simulation framework is using the `House` base class indirectly through the Power Hub interface, cf. Section 4.4. A MATLAB object array inside the `Aggregator` class stores the N instances of the `House` class, which represents the aggregated portfolio of households that is being controlled by the aggregator. At each time step of the simulation the future capacity of each of the households in the portfolio is estimated by the aggregator. This is done using an ARX model of the heat dynamics of the household, which is partially inspired by the Power Hub energy model as presented in Section 4.7. The ARX model is given by,

$$C_{i+1} - a \cdot C_i = b \cdot T_{a,i} + c \cdot \Phi_{s,i} + \boldsymbol{d}^T \boldsymbol{\Phi}_{h,i:i-\tau_{lag}} \tag{6.1}$$

where C_i is the capacity returned by the household at time step i, which is simply given by the indoor temperature in the household, T_a is the ambient temperature, Φ_s is the solar irradiance and $\boldsymbol{\Phi}_{h,i:i-\tau_{lag}}$ is a vector with the most recent observed power consumptions, i.e. $\left[\Phi_{h,i}, \Phi_{h,i-1} \cdots \Phi_{h,i-\tau_{lag}}\right]$. The lag parameter of the heat input, $\tau_{lag} \in \mathbb{N}_0$, is used to account for the potential time-lag that exists between when heating is applied and when it is observed in the indoor temperature. a, b, $c \in \mathbb{R}$, and $\boldsymbol{d} \in \mathbb{R}^{\tau_{lag}+1}$ are the unknown parameters of the ARX model. A similar approach is presented in Paper C, where the unknown parameters a, b, c and d ($\tau_{lag} \equiv 0$) in Equation (6.1) were estimated using simple linear regression. However, by using the model presented in Equation (6.1) in combination with the MATLAB arx-function, which similarly can be used for estimation of model parameters in ARX models, calculation time was greatly reduces relative to the self-implementation of linear regression. The ARX model in Equation (6.1) was explicitly implemented in its own class, `ARX_Model`, but is still making use of the existing ARX functionality implemented in MATLAB. In the class diagram in Figure 6.2 the `ARX_Model` class is marked with blue. Upon initialisation of the aggregator each of the ARX models is trained from a 24 hours time series of historical data, hence assuming that the aggregator has

some prior knowledge about its DERs. Alternatively, the aggregator could have been trained using "live" data. However, this would lead to significant variations in the predicted capacity during the initial iterations. Finally, there is a simulation script, which is placed above the aggregator class in Figure 6.2. This script is the driver of the whole simulation by running the iterations and providing the aggregator with updated setpoints for aggregate power consumption and weather data.

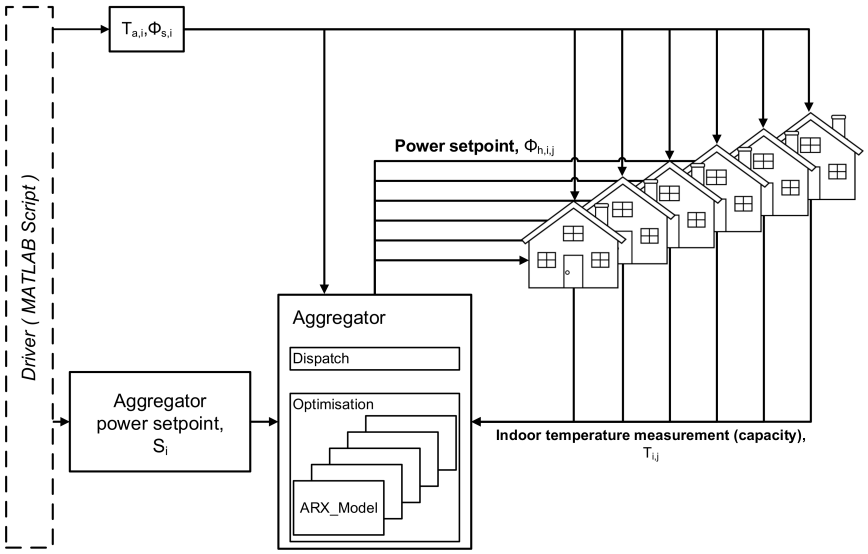

Figure 6.3: Aggregator flow diagram.

Figure 6.3 depicts the flow of data in the simulation framework. To the left is depicted the MATLAB script, which is the driver of the simulations. The script loads weather data and generates the aggregator setpoints, which are passed to the aggregator one iteration at the time. From the weather data and the setpoint the aggregator finds the optimal distribution of power setpoints for the households. The optimum is returned to the script by the `Aggregator` class which then iterates one step forward by transmitting the found power setpoint to each individual household, together with the current solar irradiance, $\Phi_{s,i}$, and outdoor temperature, $T_{a,i}$.

For optimisation of the aggregate power consumption given a power setpoint for the aggregate power consumption at time step i, S_i, the `Aggregator` class formulates a dispatch problem, which is solved for each iteration. The optimum of the dispatch problem determines the optimal distribution of power setpoints over the portfolio of households given constraints on the available capacity – or indoor air temperature. The dispatch problem is given by

$$\min \left| \sum_{j=1}^{N} (\Phi_{h,i,j}) - S_i \right| + \sum_{j=1}^{N} \Phi_{h,i,j} \mathrm{W}\left(C_{i+1,j}\right) \tag{6.2}$$

$$\text{s.t.} \quad P_{min,j} \leq \Phi_{h,i,j} \leq P_{max,j}$$

where $N \in \mathbb{N}^+$ is the number of households in the aggregator portfolio and $\mathrm{W}\left(C_{i+1,j}\right)$ is a weight function of the predicted capacity of the j'th household, $C_{i+1,j}$. The weight function implements a soft constraint on the household capacity and should be constructed such that $\mathrm{W}\left(C_{i+1,j}\right) < -1$ for $C_{i+1,j} < C_{min,j}$, where $C_{min,j}$ is the minimum tolerable indoor temperature of household j, hence ensuring that the last term is dominating when the predicted temperature is below the lower bound. In this way the power setpoint for household j is forced to increase if the indoor temperature is below the tolerable minimum temperature. Similarly, for $\mathrm{W}\left(C_{i+1,j}\right) > 1$ for $C_{i+1,j} > C_{max,j}$, where $C_{max,j}$ is the maximum tolerable indoor temperature, the power setpoint is forced to decrease when the upper bound is reached. In implementation of the optimisation in the `Aggregator` class, following linear weight function has been used

$$\mathrm{W}\left(C_{i+1,j}\right) = \frac{2\left(C_{i+1,j} - C_{min,j}\right)}{C_{max,j} - C_{min,j}} - 1 \tag{6.3}$$

When using a linear weight function, the optimisation problem in Equation (6.2) can be formulated as a quadratic programming (QP) problem. First, the weight function is reformulated using Equation (6.1),

$$\mathrm{W}\left(C_{i+1,j}\right) = \frac{2\left(a_j \cdot C_{i,j} + b_j \cdot T_{a,i} + c_j \cdot \Phi_{s,i} + \boldsymbol{d}_j \cdot \boldsymbol{\Phi}_{h,i,j} - C_{min,j}\right)}{C_{max,j} - C_{min,j}} - 1$$

$$= \alpha_j \cdot \Phi_{h,i,j} + \beta_j \tag{6.4}$$

where

$$\alpha_j = \frac{2d_{1,j}}{C_{max,j} - C_{min,j}} \tag{6.5}$$

and

$$\beta_j = \frac{2\left(a_j \cdot C_{i,j} + b_j \cdot T_{a,i} + c_j \cdot \Phi_{s,i} + \boldsymbol{d}_{2:\tau_{lag},j} \cdot \boldsymbol{\Phi}_{h,(i-1):(i-\tau_{lag}),j} - C_{min,j}\right)}{C_{max,j} - C_{min,j}} - 1 \tag{6.6}$$

Next, Equation (6.4) inserted into Equation (6.2) yields

$$\min \left| \sum_{j=1}^{N} \left(\Phi_{h,i,j}\right) - S_i \right| + \sum_{j=1}^{N} \Phi_{h,i,j} \left(\alpha_j \cdot \Phi_{h,i,j} + \beta_j\right)$$

$$\text{s.t.} \quad P_{min,j} \leq \Phi_{h,i,j} \leq P_{max,j} \tag{6.7}$$

By splitting Equation (6.7) for $\sum_{j=1}^{N}(\Phi_{h,i,j}) \geq S_i$ and $\sum_{j=1}^{N}(\Phi_{h,i,j}) < S_i$ is found

$\sum_{j=1}^{N}\Phi_{h,i,j} \geq S_i$	$\sum_{j=1}^{N}\Phi_{h,i,j} < S_i$
$\min \sum_{j=1}^{N}(\Phi_{h,i,j}) - S_i + \cdots$	$\min -\sum_{j=1}^{N}(\Phi_{h,i,j}) + S_i + \cdots$
$\sum_{j=1}^{N}\Phi_{h,i,j}(\alpha_j\Phi_{h,i,j} + \beta_j) \quad \Leftrightarrow$	$\sum_{j=1}^{N}\Phi_{h,i,j}(\alpha_j\Phi_{h,i,j} + \beta_j) \quad \Leftrightarrow$
$\min \sum_{j=1}^{N}\left(\alpha_j\Phi_{h,i,j}^2 + (\beta_j+1)\Phi_{h,i,j}\right)$	$\min \sum_{j=1}^{N}\left(\alpha_j\Phi_{h,i,j}^2 + (\beta_j-1)\Phi_{h,i,j}\right)$
s.t. $\sum_{j=1}^{N}\Phi_{h,i,j} \geq S_i$	s.t. $\sum_{j=1}^{N}\Phi_{h,i,j} < S_i$
$P_{min,j} \leq \Phi_{h,i,j} \leq P_{max,j}$	$P_{min,j} \leq \Phi_{h,i,j} \leq P_{max,j}$

Both problems can be formulated on standard QP form, i.e.

$$\begin{aligned} \min \quad & \frac{1}{2}\boldsymbol{\Phi}_{h,i}^T\boldsymbol{H}\boldsymbol{\Phi}_{h,i} + \boldsymbol{f}^T\boldsymbol{\Phi}_{h,i} \\ \text{s.t.} \quad & -\mathbf{1}^T\boldsymbol{\Phi}_{h,i} \leq -S_i \qquad \left(\text{or} \quad \mathbf{1}^T\boldsymbol{\Phi}_{h,i} < S_i\right) \\ & P_{min,j} \leq \Phi_{h,i,j} \leq P_{max,j} \end{aligned} \tag{6.8}$$

where $\mathbf{1} \in \mathbb{R}^N$ is a vector with ones, $\boldsymbol{\Phi}_{h,i} \in \mathbb{R}^N$ is a vector with the power setpoints for all the households in the portfolio at time i and $\boldsymbol{H} \in \mathbb{R}^{N\times N}$ is a square diagonal matrix with diagonal $2\boldsymbol{\alpha} \in \mathbb{R}^N$, where $\boldsymbol{\alpha}$ is a vector with the α_j-values for $j \in \{1, 2, \cdots, N\}$ as defined in Equation (6.5). Similarly, $\boldsymbol{f} = \boldsymbol{\beta} + \mathbf{1} \in \mathbb{R}^N$ (or $\boldsymbol{f} = \boldsymbol{\beta} - \mathbf{1} \in \mathbb{R}^N$), where $\boldsymbol{\beta}$ is a vector containing the β_j-values as given by Equation (6.6). The minimisation problem in Equation (6.8) is solved twice by the `Aggregator` class, i.e. for $\sum_{i=1}^{N}\Phi_{h,i} \geq S$ and $\sum_{i=1}^{N}\Phi_{h,i} < S$, and the solution having the lowest cost function is selected as the global solution to the minimisation problem formulated in Equation (6.2).

In the physical world there is a positive correlation between the indoor- and outdoor temperature. Likewise, for solar irradiance and heat input. Hence, the parameter estimates of a, b, c, and $\boldsymbol{d}$ in Equation (6.1) are expected to be positive. Consequently, $\boldsymbol{H}$ is a positive definite matrix and the problem in Equation (6.8) is convex [60] and there exists only one global minimum. In this case the solution can be found using the interior point method implemented in MATLAB, which has a high convergence rate and is guaranteed to converge [61]. In rare occurrences, an estimate of a is negative and the QP-problem becomes non-convex [60]. To find the minimum in this case an active set method is used instead of the interior point method. This method has a higher theoretical convergence rate than the interior point method but does not guarantee that the found minimum is a global minimum [61]. However, during all the simulations that have been carried out during this project, no problems have been observed from using an active set method rather than an interior point method. Finally, it should be emphasised that the dispatch problem does not guarantee that the constraints on C_{min} and C_{max} are respected due to the fact that external disturbances can influence the indoor air temperature in both negative and positive direction; especially solar irradiance can lead to the latter. Moreover, a high "thermal inertia" can be build up in a thermal system with a high thermal mass, e.g. in floor heated systems, which can lead to the maximum indoor temperature constraint being exceeded as the high thermal mass "discharges" into the mass of the interior.

6.3 Simulation Results

Several simulations of aggregate control of power consumption have been conducted during this project of which some the most significant results have been published in Paper C. In the paper, aggregated control of 50 of each of the two types of households was simulated using the framework. In this section the aggregate flexibility of two aggregators with a portfolio consisting of 100 resistive- and 100 heat pump heated households, respectively, are estimated and their performance compared. Likewise, the flexibility of an aggregator contain-

ing 50 households of each type is estimated. The simulations were conducted using real weather data for outdoor temperature and solar irradiance, as presented in Figure 6.4. The weather data was collected by the weather mast located outside PowerFlexHouse during the last ten days of January 2013. The two thermal models, as presented in Figure 6.1, were used for the simulations using the model parameters presented in Table 6.1. All simulations have be conducted with a step-size of 5 minutes and with the diffusion process in the discrete state space model, i.e. $\boldsymbol{v}(t)$ in Equation (5.12), given by a normal distributed process with zero mean and 0.1 and 0.05 standard deviation for the resistive- and heat pump heated household, respectively.

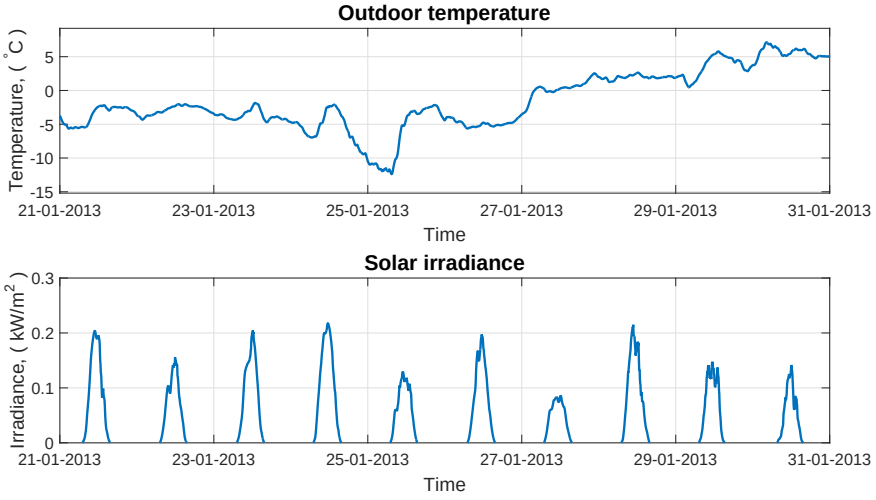

Figure 6.4: Exogenous weather input for simulations, which has been collected by the PowerFlexHouse weather mast in January 2013.

In Figure 6.5, the annual average daily profile of wind power generation and power consumption are plotted. From the figure is seen that in general the wind power production is higher during the afternoon than during the hours of night-time: on average wind power generation is nearly 20% higher at 3 p.m. compared to 6 a.m. This correlates reasonable well with the power consumption which is also high during

daytime. However, during daytime the profile of power consumption is significant higher than the profile of wind power generation. Similarly, power consumption is significant lower during night-time: on average power consumption is almost 60% higher during peak load hours at around 6 p.m. compared to 3 a.m.. Consequently, it is desirable in a power system with at high share of wind power generation to shift power consumption away from the forenoon and early evening to the late evening and hours of night-time.

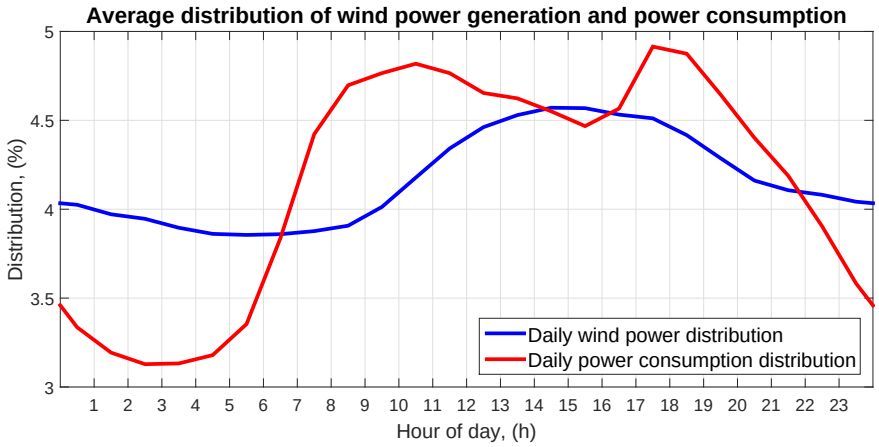

Figure 6.5: Annual average daily distribution of wind power generation and power consumption for 2013. Source: Energinet.dk [17].

To simulate such a shift in power consumption from day to night, a baseline for the requested power consumption is initially generated for the aggregator. The baseline is generated by running a simulation of aggregate consumption without any aggregator control imposed on the households. In this way the simulated households are simply running their own thermostatic controller, thus keeping the simulated indoor temperature close to the given indoor temperature reference. From the baseline, the aggregator setpoint is generated by superimposing a sinusoid onto it. The amplitude of the sinusoid wave is scaled such that a given fraction of the average load is shifted from one period to another. Similarly, the period of the sinusoid is scaled to one day and

the phase chosen such that the maximum occurs at the desired time of the day. From this the aggregator setpoint can be generated from,

$$S_i = \Phi_{base,i} + A\overline{\Phi}_{base} \sin\left(2\pi\left(i/\tau + \varphi\right)\right) \tag{6.9}$$

where S_i is the aggregator setpoint at time step i and $\Phi_{base,i}$ is the aggregate power consumption without aggregator control having average $\overline{\Phi}_{base}$. A is the fraction of the average power consumption to be shifted in time, i.e. the load shift, τ is a time-scaling factor, such that the period of the sinusoid is exactly one day and φ is the phase of the sinusoid used to adjust the point in time where the maximum of the wave occurs. Using this approach, the generated setpoint is energy neutral relative to the baseline – assuming the period is given by a whole number of days. Figure 6.6 (top) depicts an example of a 25% power shift from a baseline that is generated from power consumption from 100 heat pump heated households. The sinusoid is seen to have its maximum at 2 a.m., hence the power consumption is shifted away from midday towards midnight. As the amplitude of the sinusoid increases, the generated setpoint may violate the aggregated nominal power consumption, i.e. the sum of minimum and maximum nominal power of the households. Naturally, the aggregator setpoint is not allowed to be negative, therefore the lower bound of the aggregator setpoint is clamped to zero. This causes the energy balance between the baseline consumption and the clamped setpoint to shift. To restore energy neutrality between the baseline and the clamped setpoint, the setpoint is multiplied with the ratio between the mean of the baseline and the mean of the setpoint. In Figure 6.6 (bottom) the actual power shift from the baseline is plotted. From the plot is seen that especially during periods with high solar irradiance, i.e. around noon, the actual shifted power consumption goes towards zero caused by the less need for power due to the sufficient energy provided by solar irradiance.

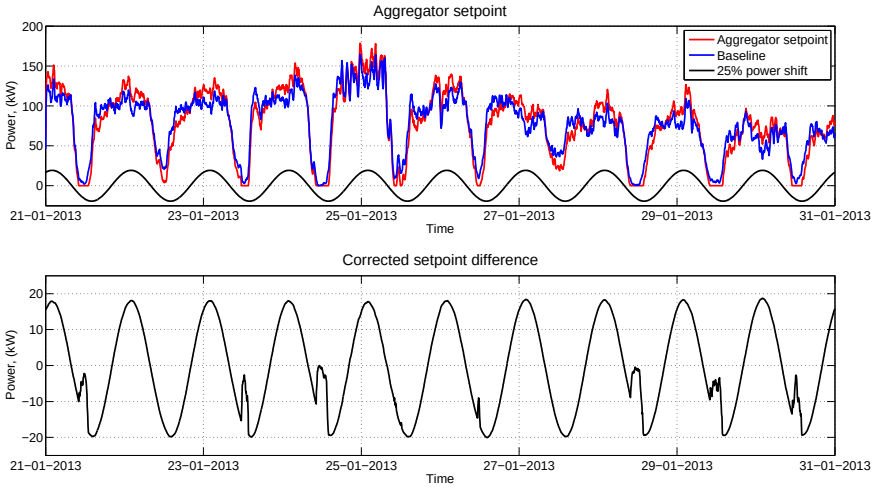

Figure 6.6: Aggregator setpoint as a baseline consumption superimposed with a sinusoid (top). Actual load shift after clamping (bottom).

In Figure 6.7, the simulated control of 100 resistive heated and thermally light households is depicted for 20%, 50% and 80% load shift, i.e. $A = 0.2$, $A = 0.5$ and $A = 0.8$. In each of their respective top plot, the given aggregator setpoint is depicted together with the actual dispatched power. Below is plotted the average capacity of the controlled households, i.e. the indoor temperature, together with the capacity constraints. From the top plot is seen that the setpoint can be tracked very closely by the aggregator, hence a 20% load shift can be achieved by allowing the indoor temperature to vary approximately $\pm 0.6\,^{\circ}\mathrm{C}$ around the temperature reference.

From Figure 6.7 is furthermore seen that when the load shift is increased to 50% the actual dispatched power now starts to deviate from the given setpoint. This situation is seen to occur a few times during the ten days of simulation and is seen to coincide with the minimum and maximum of the superimposed sinusoid, which is expected since the load shift is most significant here. From the capacity plot below is seen that the magnitude of the fluctuations of the average capacity of the households are also becoming larger relative to the 20% load shift. However, the capacity bounds are being respected by the aggregator, which is exactly the reason why the aggregator fails to track the given setpoint. For the 80% load shift, depicted in the two lowermost plots, is seen that the aggregator now completely fails to follow the provided setpoint during longer periods of the simulation. Furthermore, in a few cases the actual dispatched power is more than twice as high than requested and similarly half during other instances. As with the 50% load shift, the large deviations are seen to coincide with the extrema of the sinusoid.

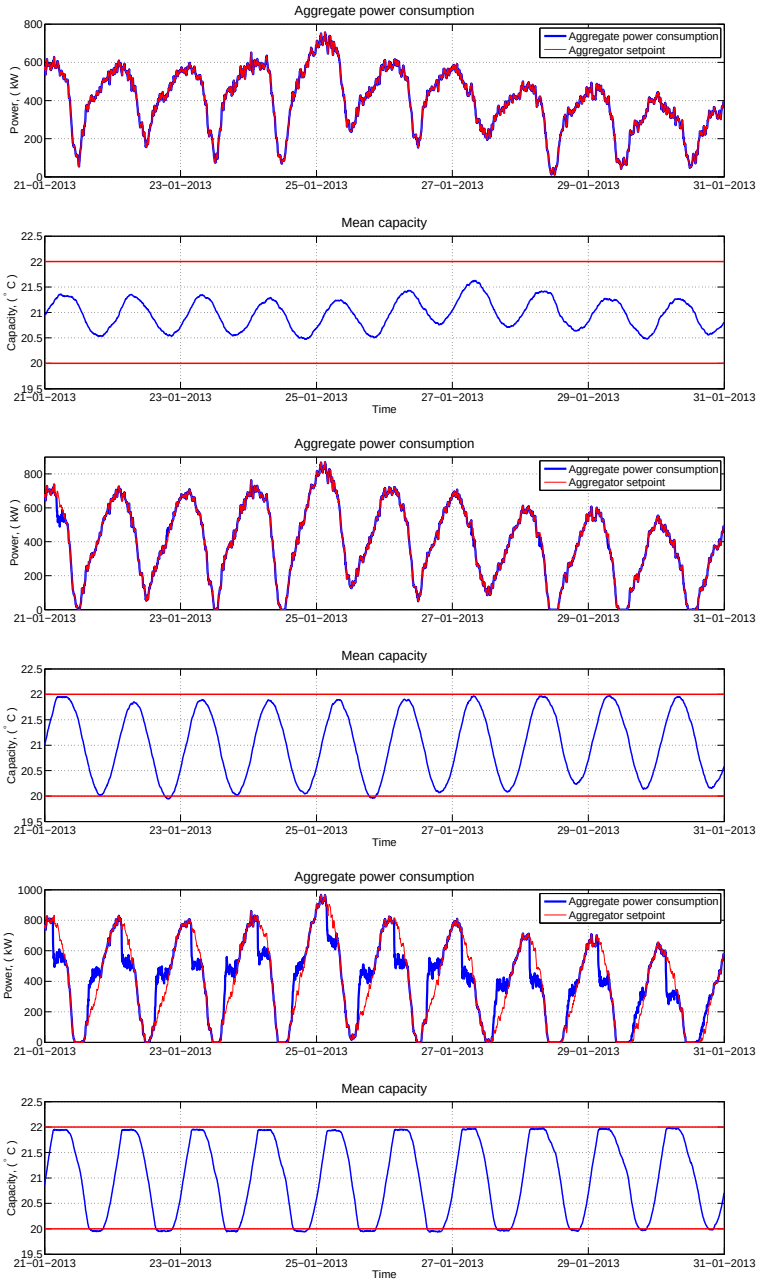

Figure 6.7: Aggregate control of 100 resistive heated households with 20% (top), 50% (centre) and 80% (bottom) load shift.

In Figure 6.8 is presented three simulations of aggregate control of 50 resistive households and 50 floor heated households, i.e. thermally light and heavy households mixed together, for 20%, 50% and 80% load shift. Like the simulations of 100 resistive households the aggregator is able to track the setpoint very closely for 20% load shift utilising a $\pm 0.6\,^{\circ}\mathrm{C}$ band around the temperature reference. Moreover, with the introduction of the thermally heavy households, the mixed aggregator can also provide a 50% load shift using approximately $\pm 0.9\,^{\circ}\mathrm{C}$. Similarly the simulations presented in Figure 6.7, the aggregator fails to track the setpoint for 80% load shift, however, the magnitude of the fluctuations in the average indoor air temperature of the mixed households are somewhat smaller compared to the 80% load shift of the 100 resistive households. Consequently, less time of the simulation is spent near the capacity bounds and hence the aggregator is able to comply with given setpoint more often. A thing to be observed from the lowermost plot, with the capacity of the 80% load shift, is that the aggregator is deviating from the setpoint even though capacity is apparently still available. This effect is discussed in Section 6.5.

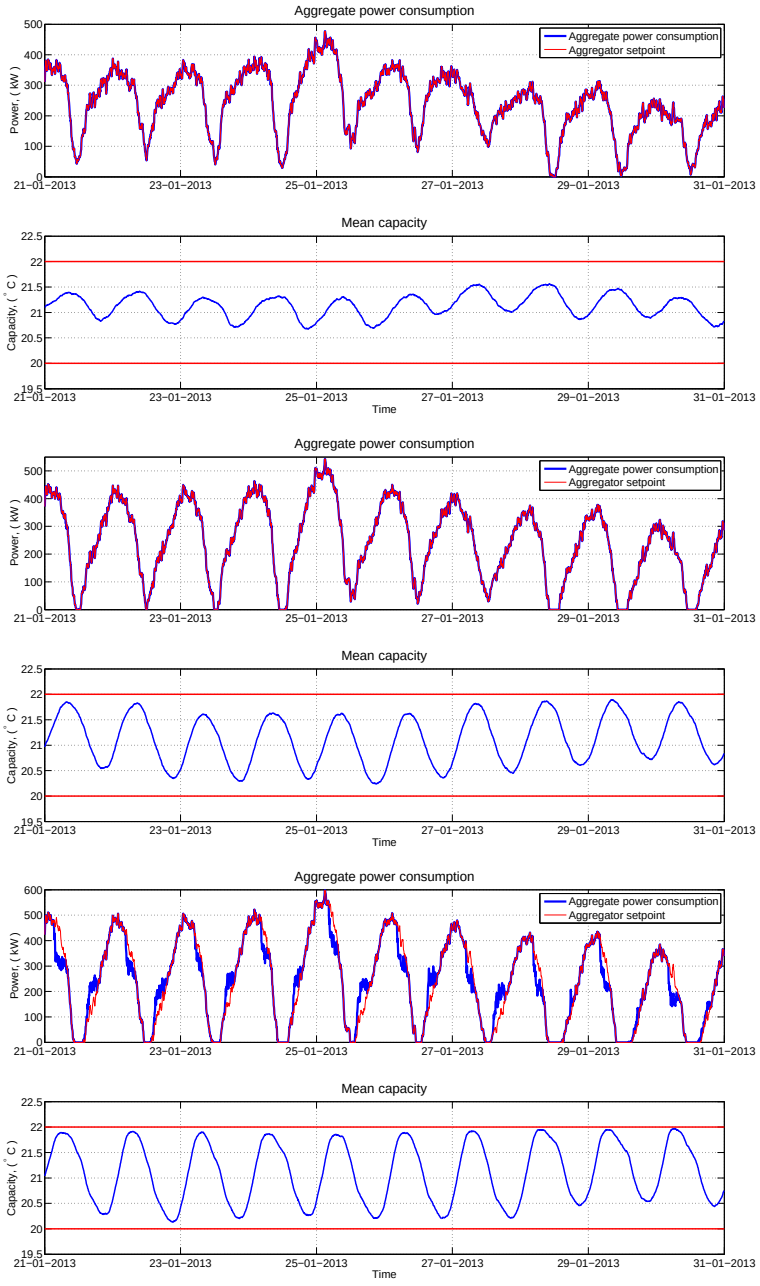

Figure 6.8: Aggregate control of 50 resistive- and 50 heat pump heated households with 20% (top), 50% (centre) and 80% (bottom) load shift.

Finally, Figure 6.9 presents the result of the simulation of aggregate control of 100 floor heated households. Contrary the simulations presented in Figure 6.7 and 6.8, the simulations of the thermally heavy households show that 20%, 50%, and 80% load shift can be achieved if the indoor air temperature is allowed to vary within ±0.3 ℃, ±0.6 ℃ and ±0.9 ℃ around the temperature reference, respectively. With the introduction of additional thermal mass in the portfolio of the aggregator the performance is significantly increased with respect to flexibility. The flexibility in the floor heated households comes from the ability to absorb additional heating during night-time and transfer the energy to the indoor air during daytime when the power for heating is being reduced by the aggregator. However, also the actual amount of load shifted from daytime to night-time is considerably less than with the resistive heated households, due to better insulation of the building envelope and performance of the heating system, i.e. COP of the heat pump.

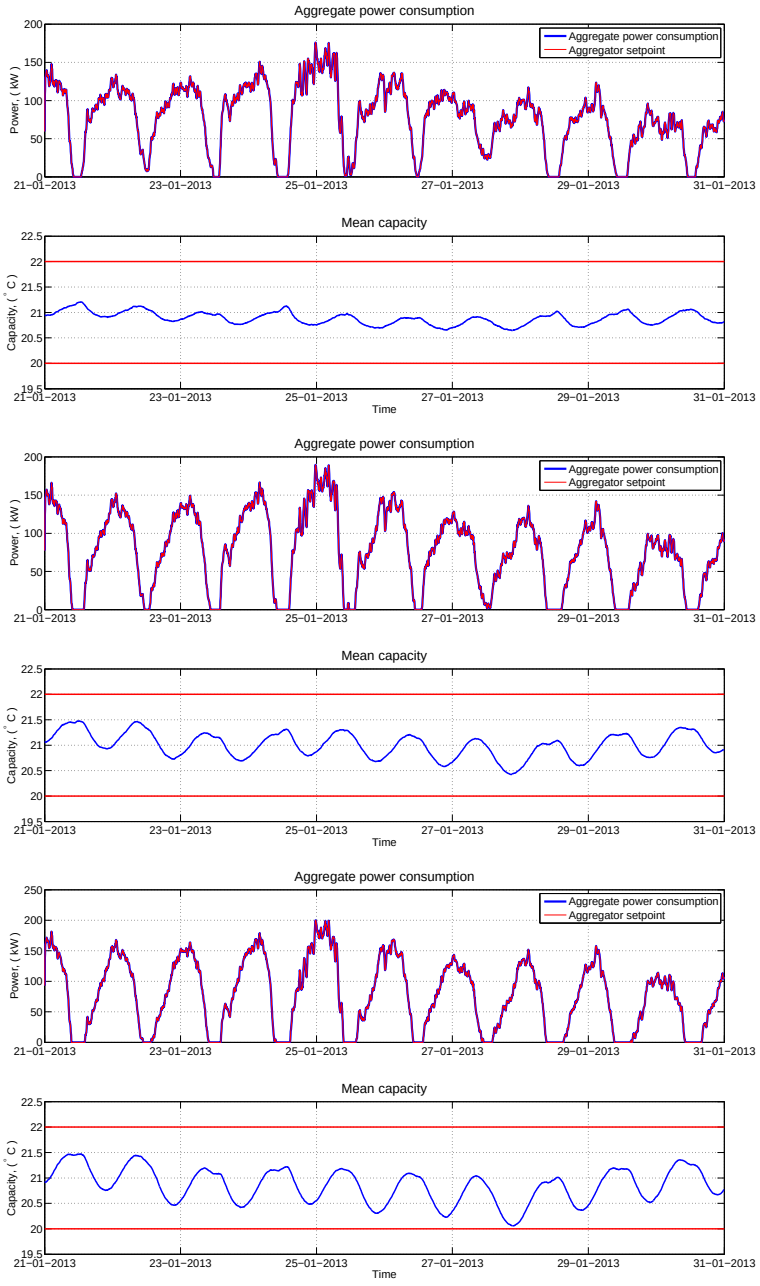

Figure 6.9: Aggregate control of 100 heat pump heated households with 20% (top), 50% (centre) and 80% (bottom) load shift.

6.4 Aggregator Performance

For comparison of the aggregator performance the deviation between the given reference and the actual dispatched power is studied. For this the root-mean-square deviation (RMSD) is used, which is given by,

$$\text{RMSD} = \sqrt{\frac{1}{M}\sum_{i=1}^{M}\left(\sum_{j=1}^{N}\left(\Phi_{h,i,j}\right) - S_i\right)^2} \tag{6.10}$$

where $\Phi_{h,i,j}$ is the power dispatched by household j at time-step i and S_i is the given aggregator setpoint. M and N are the total number of iterations and aggregated households, respectively. In Figure 6.10 (a) the RMSD is plotted for power shift between 0% and 100% for the three different aggregators, which are presented in Figure 6.7 to 6.9. From the RMSD-plot is seen that in general the performance is alike for power shifts below 40%, but above the performance of the aggregator with the 100 thermally heavy households is significantly better than the other two. Moreover, the performance of the aggregator comprising the mixed household lies between the two homogeneous aggregators, which is expected due the increased thermal mass that is found in floor heated households relative to the resistive heated households. This high thermal mass, which is available in the floors, provides a temporally reservoir for energy where thermal energy can be accumulated, thus ensuring a better performance over the more thermally light households. For comparison of the RMSD of the aggregators relative to their nominal size, the RMSD as a fraction of the aggregator maximum nominal power is plotted in Figure 6.10 (b). From the figure is seen that the performance among the three becomes slightly more equal, due to the high nominal power of the light households, but still the performance of the heat pump heated households are significantly better than the other two for power shifts above 40%.

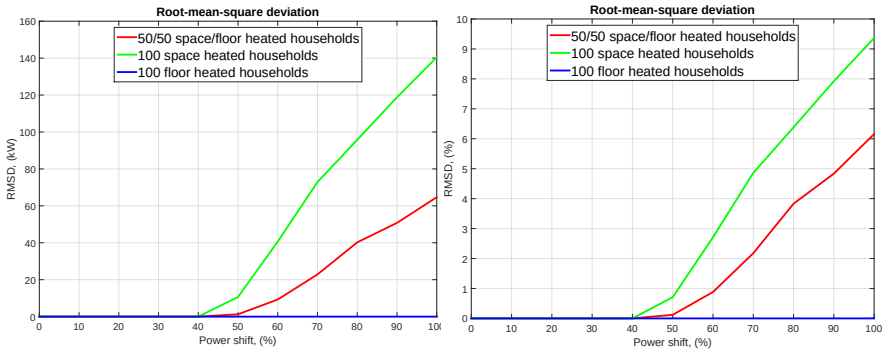

(a) (b)

Figure 6.10: Root-mean-square deviation between aggregator power setpoint and actual power dispatched (a). Percent RMSD of total aggregator maximum nominal power (b).

Another thing that can be observed from Figure 6.10 is that power shifts below 50% can be achieved with a very high reliability for all aggregators, i.e. within less than 10 kW on average or within one percent of the nominal power of the aggregator. For power shift above 50%, aggregators comprising building with a high thermal mass can still deliver a high reliability, whereas aggregators with less thermal mass fails to achieve the same reliability.

6.5 Summary

With the simulations presented above it has been demonstrated that electricity consumption can be shifted from midday to midnight, i.e. within a 12 hours time frame, if a 2 ℃ temperature band is utilised for demand response. This implies that in general the power consumption for electrical heating in thermally heavy buildings can be shifted within the hourly to daily time-scale using a VPP framework similarly to Dong Energy's Power Hub. Despite the simulations in this chapter builds on correlating demand for power with power generation from wind energy resources, power consumption for electric space heating can also be shifted to correlate – or uncorrelate – demand for power

with other sources, e.g. shift demand for space heating away from peak load hours. In such a case, flexible demand can be utilised to lower the overall peak demand for electricity during peak load hours and consequently lower the need for distribution capacity in the distribution grid.

As noted from Figure 6.8 (bottom), the aggregator fails to dispatch the power given by the setpoint even though capacity is apparently available. In Figure 6.11, the same simulation is plotted together with the average temperature in the heat pump and floor heated households, respectively. From the lower plot is seen that despite capacity seems to be available from the aggregated mean capacity (blue), the capacity of the thermally light households has been saturated. This is mostly apparent at the lower boundary of the temperature band, where the indoor temperatures in the space heated households are seen to drop more rapidly than the floor heated households. With the saturation of the thermally light households, a large share of the nominal power of the aggregator is not able to comply with the requested decrease of power consumption. The difference in the temperature response of the two types of households comes primarily from the difference in their heat capacities, which results in different time constants, but also the level of insulation of the building influences the dynamics. In a setup similar to Power Hub, this does not pose a problem since Power Hub is the only aggregator; however, if the flexibility of an aggregator is to be passed upwards in a potential aggregation hierarchy, the average capacity of the households can not be used to represent the capacity that is available in an aggregator. A way to prevent such an issue is to aggregate consumption entities having similar dynamics, i.e. time constants, and let a higher level aggregator coordinate the response among them. Alternatively, aggregator flexibility for up- and down regulation over a predefined period can be used for defining flexibility of an aggregator.

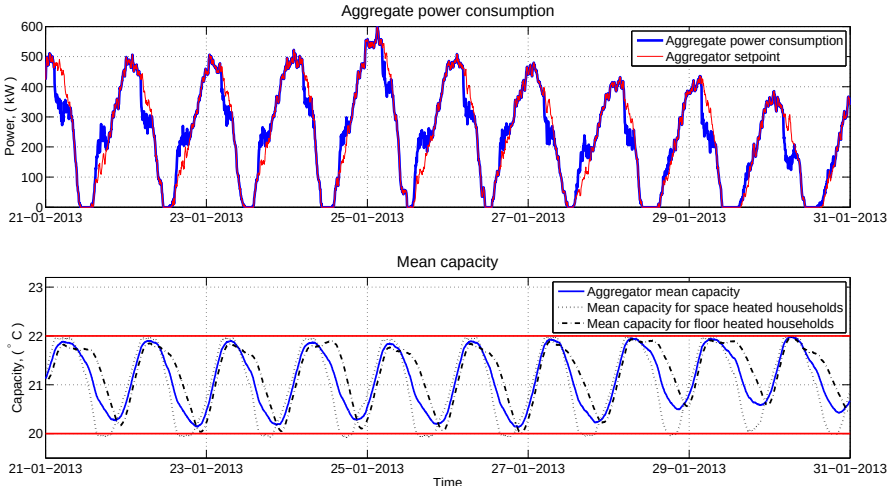

Figure 6.11: Aggregate control of 50 resistive- and 50 heat pump heated households with 80% load shift.

Finally, it should be emphasised that the load shift, A, in Equation (6.9) is not the actual percentage of power shifted from midday to midnight due to the subsequent processing of generated setpoint. Hence, the parameter A is simply a tuning parameter for shifting a given amount of the electricity from one period to another. In Figure 6.12 (left) the correlation between the load shift, A, and the actual shifted power consumption is plotted. Likewise, Figure 6.12 (right) depicts the actual power consumption in percentages of the mean power consumption. From the right figure is seen that the actual power shifted is only approximately half of what is given by A, for both types of aggregators. For the heat pumped households, the actual shifted power consumption is less due to the high level of insulation of the house envelope, which means that the need for power is low during hours with high solar irradiance. Hence, less actual consumption is shifted because the setpoint is clamped to zero.

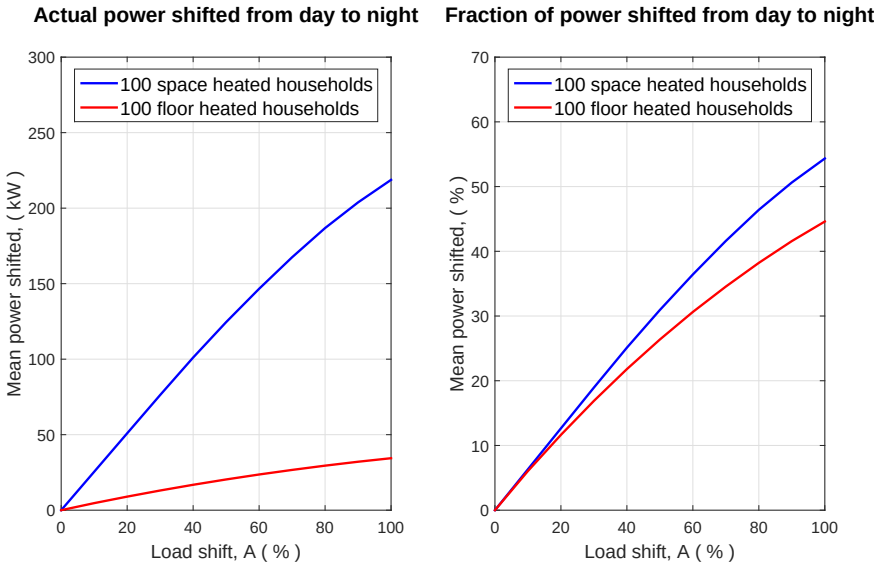

Figure 6.12: Actual power consumption shifted by Equation (6.9) for 100 space heated households and 100 floor heated households, respectively. Actual power consumption shifted (left) and in percentages of mean electricity consumption (right).

Chapter 7

Overview of Results and Discussion

This chapter presents the primary results found during this project and provides an overall discussion of the key findings. For a more detailed presentation of the results and discussions hereof, readers are referred to the seven papers appended to the back of this thesis in which the results are presented in their full form. Finally, this chapter outlines some future work, potential barriers and provides some recommendations.

7.1 Thesis Results

From the scientific contributions, as presented in Section 1.5, the results from this thesis can be separated into following four categories:

1. Heat dynamic models for detached households utilising electric space heating.
2. Development of an experimental platform for demand response experiments.
3. Conduction of demand response experiments.
4. Simulations of control of aggregated heat loads.

The first category came from a realisation for the need of heat dynamic models of heat loads for space heating to guarantee that indoor temperature (or capacity) constraints are being obeyed during operation. Furthermore, with respect to the protocol defined by Power Hub, cf. Section 4.4, a DER model was needed to generate daily operational schedules for the heat load in PowerFlexHouse. Paper A presents the first heat dynamic model that was developed for PowerFlexHouse. As presented in Paper E, F and G, the linear state space model has been successfully implemented in several algorithms for economical MPC of the heat load in PowerFlexHouse, thus minimising the cost of electric heating with respect to hourly prices on electricity in the Nord Pool spot market. Using MPC it has been demonstrated that the heat load of a building can be controlled with respect to the electricity market using a price signal and in this way undertake a more active role in the power system using an indirect control approach. Despite the linear model has been easy to integrate into the traditional linear MPC-framework and has shown good performance within a short time horizon and under normal weather conditions, the model tend to be inadequate within longer time-scales and in weather conditions with high wind speeds. Therefore, a non-linear heat dynamic model was developed which identified a non-linear phenomenon from the free ventilation of the building. This model was presented in Paper B, where the thermal resistance of the building envelope was shown to decline exponentially with increasing wind speeds. This is most likely a consequence of draughty ventilation holes in the building envelope of which several are missing their outside grating. The non-linear model shows significant better results than the linear model, both on the shorter time-scale and the longer time-scale, i.e. both for real-time control and for generating operation schedules for Power Hub. The estimated model parameters in the non-linear model have been shown to be consistent with typical building parameters for that specific type of building, cf. Section 5.7. Another application of the heat load models is to provide estimations of the duration of up- and down-regulation of heat loads. Given predicted weather data and constraints on the indoor temperature, the models can be used to estimate the duration a given regulation can be sustained. An example

of this is provided in Figure 7.1, where the estimation of regulation power for PowerFlexHouse is based on similar weather conditions as during the demand response experiments that were presented in Paper D, and hence should be comparable to what was observed then. Under these weather conditions, the non-linear model estimates the heat load for keeping the indoor temperature at 21 °C – the same as in Paper D – to be approximately 5.1 kW, which is close to the actual power consumption just before decoupling the heat load in the demand response experiment, cf. Fig. 5 in Paper D. Furthermore, given a 2 °C temperature band, the duration of a full decoupling of the heat load, i.e. reducing the load with 5.1 kW, is seen to be slightly less than two hours, which is likewise quite close to what was found during the field experiment. In this way, the heat dynamic model can potentially be utilised by an aggregator – alternatively in a more simple form – to estimate the maximum duration of a given amount of regulating power. Likewise, the aggregate size of regulation from several entities given the duration can be found by adding the plots for up- and down regulation along the ordinate.

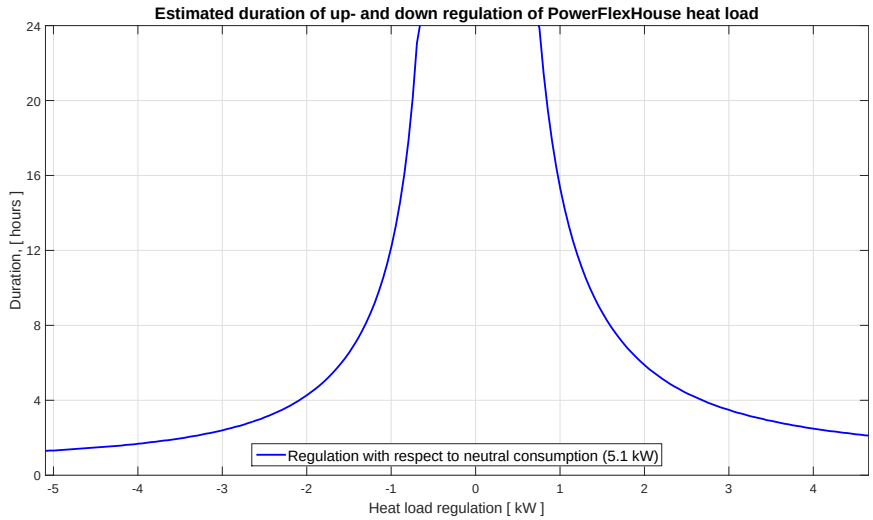

Figure 7.1: Estimated duration of up- and down regulation provided by PowerFlexHouse.

The results from the second category come from the comprehensive software platform that was developed to facilitate the field experiments in PowerFlexHouse. The platform handles communication with Power Hub and provides optimal dispatch of the heat load with respect to a given a power reference and provides an equal distribution of the air temperature inside the building. Except from a few incidents, where the GPRS connection to Power Hub was lost due to the poor mobile reception at the location of PowerFlexHouse, the platform has been demonstrated to be stable, such that demand response can be provided from PowerFlexHouse with a high reliability and accuracy.

The results from the third category come from a series of field experiments that were conducted using PowerFlexHouse as a flexible load under Power Hub control. With the experiments, which were presented in Paper D, it was demonstrated that heat loads from residential-sized buildings connected at distribution level can indeed be utilised for DR applications. Three experiments were conducted to demonstrate:

- Diurnal load shifting – shifting load from day to night.
- Load postponement.
- Performance of heat load model.

One of the results from these experiments was that using a temperature band of 2 °C around the indoor temperature reference, the entire heat load of PowerFlexHouse (5 kW) could be completely decoupled for up to two hours under typical Danish winter weather conditions. This implies that using a 1 °C temperature band, 5 kW can be postponed approximately an hour implying that the building can be utilised as a unidirectional storage for electric energy with a capacity of approximately 5 kWh, which is remarkably close to the estimated heat capacity of the building, cf. Paper B. The results presented in this thesis should be seen in the light of the relatively low thermal mass of PowerFlexHouse compared to Danish standards and hence the available capacity from average Danish buildings are expected to be significant higher (10–15 kWh).

Finally, Paper C presents the results from the fourth category. In the paper a simulation model of a VPP is presented, including models of households connected in the low voltage network. The result from a simulation of 100 households – 50 thermally light and 50 heavy – suggests that more than 20% of an aggregated heat load can be shifted away from peak load hours to hours of night time, where the demand for electricity is smaller. Moreover, simulations show that power consumption for heating can be completely decoupled for up to three hours, with minor impact on the indoor air temperature. Consequently, the results from Paper C support the results from the field experiments: that the electric heat load of small buildings provides a good technical candidate for demand response in the distribution grid.

7.2 Discussion of Results

In this thesis it has been demonstrated that electric space heating can indeed be utilised for demand response with only minor – or no – loss in indoor temperature comfort when compared to standard hysteresis controlled heating. However, an aspect which remains to be studied is whether it is economical profitable to do so. Naturally, instead of starting with small entities like small households, it would often be more economical feasible to start integrating DR from large scale industrial entities running flexible processes, where there is a much larger capacity available to utilise. With a larger capacity available, the investments per controlled capacity [kWh] that is needed in dedicated control software, hardware and communication are much smaller than when integrating smaller units. As presented in Section 4.3, these industrial processes comprises horticultural farming, wastewater treatment and other pumping processes, but also processes for smelting of bitumen in asphalt production and spray drying processes, which are known to require a large amount of energy. Consequently, such industrial processes have traditionally been regarded as the "low hanging fruits" of commercial integration of demand response, since they provide more value for money, and thus less attention has been placed on the integration of electrical space heating

for DR purposes. However, this does not mean that small entities should be completely neglected: decreasing costs of hardware and broadband communication can be a driver for making DR from small scale entities economical feasible in the near future. For instance, in this project a GPRS connection was used to facilitate communication between Power Hub and PowerFlexHouse, which proved to be a quite expensive approach because the cost of communication alone was in the same order of magnitude as the total cost of electricity used in PowerFlexHouse during the same period. This means that using a broadband – or flat rate – connection instead would reduce the operational costs substantially and furthermore provide a more stable connection. As previously outlined, another driver is the reduced costs of control hardware. Before this driver can be fully utilised, the demand for DR hardware has to reach a critical mass such that it can be mass produced. Therefore, standardised communication between actuators, sensors and control systems, i.e. building management system or home automation system, has to be developed. This would mean that controllers and actuators can be built into newly manufactured appliances, e.g. heat pumps and refrigerators, at a low cost hence making retrofitting of external hardware to appliances unnecessary. Furthermore, with standardised communication, end-users will not be confined to one supplier of hardware, but can choose among a range of suppliers. This also means that existing building management systems can easily be extended with new sensors and actuators when new flexible appliances emerges without having to rely on proprietary manufacturer implementations. Finally, integral control of appliances would be preferred since it ensures an ideal integration of the controlled process and the overall performance of the entity. This especially applies to processes that are having specific operation criteria, e.g. compressors in heat pumps and refrigeration systems, which will ensure the lifetime of the appliance. Similarly, a standardised interface between building management systems and aggregator – or a system operator – has to be developed. This will create a dynamic setup, where providers of DR can choose among different energy management companies – or aggregators – possible targeting different flexible processes in the power system, e.g. space heating or EVs. In

this way processes with similar characteristics can be aggregated into one entity, hence creating a homogeneous portfolio and thus reducing the complexity of forecasts and aggregation.

Finally, it should be mentioned that utilisation of space heating for DR applications comes at a cost: heating can postponed or accelerated within a given time frame, but shifted consumption will have to be deliver eventually and at that time the heat loads might be synchronised. This means that the overall power consumption after a period with provision of up regulation can be significant higher than during normal operation, cf. Section 3.7.

7.3 Future Work

Within the field of demand response there exists many obvious open research topics, e.g. if and how other types of household appliances can be utilised for demand response. In this section, three essential topics for future work are listed, which are consider to be a prerequisite for a comprehensive and seamless utilisation of the flexibility that can be provided by small entities on the consumption side.

7.3.1 Development of aggregation infrastructures

In this project, emphasis has primarily been placed on the lower parts of the demand response hierarchy, i.e. on DERs and partly aggregators. However, the results presented here rely on a comprehensive framework being available to utilise the potential from distributed entities. Assuming a direct control approach, Figure 7.2 envisions how this framework could be implemented using the concepts for zones as defined in the Smart Grid Reference Architecture (SGAM) [62]. From the top are plotted two different markets for ancillary services addressing respectively the DSO and TSO, together with the electricity market as we know it today, e.g. Elspot and Elbas. Below are the enterprise roles depicted, namely the TSO and DSOs as buyers of

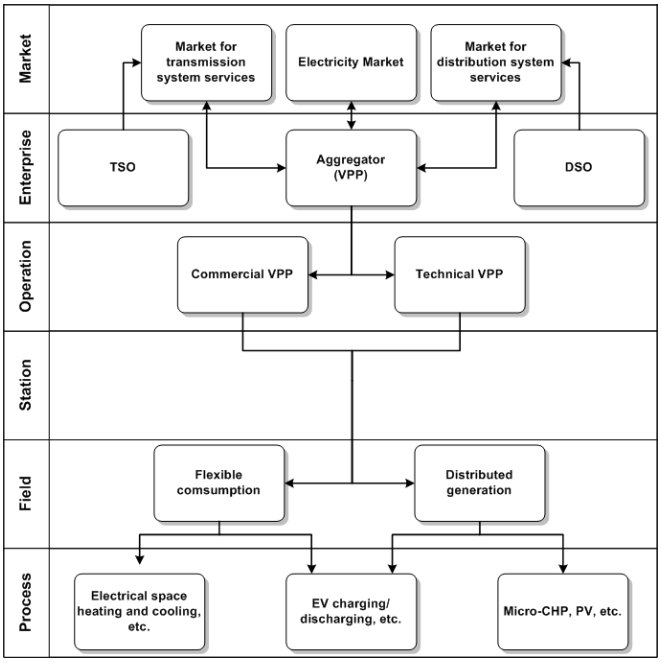

Figure 7.2: Envisioned smart grid framework.

power system services, and sellers of flexibility, i.e. aggregating companies or just aggregators. On the operational level, the aggregators can be split into two categories: the technical VPP (TVPP) and commercial VPP (CVPP), which defines the capabilities of the aggregator and hence the types of services they can deliver. Further down, in the field zone, the VPP can be further separated into mediators of either flexible consumption or generation (CBRPs or GBRPs).

CVPPs are characterised by an economical optimisation of the power consumed by its portfolio of DERs and in this way CVPPs are increasing the revenue of the DER owners. The optimisation of the aggregated flexibility is either with respect to the cost of electricity in the market or alternatively the flexibility is sold as ancillary services to the TSO, however, CVPPs are only addressing the overall power balance in the power system. Hence, the capabilities of CVPPs are

related to frequency control issues: either for long term balancing or short-term as ancillary services. Like most currently running commercial aggregators, Power Hub falls within this category. However, DR services are not of interest to the TSO alone; DSOs can also utilise demand response services for a more efficient operation of their distribution grid. In [41], a series of flexibility services that are applicable to DSOs have been identified. These services include a limitation of power consumed by an activated aggregator during peak load hours. In this way control of flexible demand in the low voltage grid can be used to reduce the annual peak power consumption on a feeder and hence serve as a tool to reduce – or alternatively postpone – investments in grid reinforcements. Likewise, more advanced services have been identified, for example provision of voltage support by control of both active and reactive power. Due to the more technical nature of such services, compared to those delivered by CVPPs, aggregators delivering such services have been named technical VPPs [20]. This means that, as opposed to CVPPs, which does not need know any specific grid location of its DERs, TVPPs do need to maintain a thorough knowledge about the topology of the transmission and distribution grid, and especially where its DERs are located. Though there exists a large number of implementation of CVPPs that are running commercially, research within TVVPs is still an open research topic and still we lack to experience TVPPs running on commercial terms. As outlined in Section 3.1, there exists a substantial potential for savings in grid reinforcements if a smart grid is implemented in Denmark. This, however, indeed requires the capabilities of TVVPs, whereas CVPPs can actually increase congestion problems if the cost of electricity declines rapidly within a short period, or even becomes negative. Here, the problem is simply that CVPPs neglects grid constraints, whereas TVPPs do not. This does not mean that the one is superior to the other: in many ways the TVPP and CVPP complement each other in the services they can provide.

7.3.2 Development of demand response markets

Demand response has many applications in the power system, both for frequency control for maintaining the balance in the power system and for congestion management in the distribution grid. This means that demand response services can possibly generate value for both TSOs and DSOs, and therefore VPPs should be able to provide services to both. As with the current market setup for buying and selling electricity, a market approach is expected to ensure a transparent and seamless transaction of demand responses services as well. As shown in Figure 7.2, two different markets are envisioned addressing respectively the TSO and DSOs. The market for the TSO is envisioned to include the ancillary services that is requested by the TSO today; however, compared to today, where ancillary services are often exchanged more or less manually using bilateral contracts, ancillary services can be exchanged through an open market, which ensures a flexible and transparent process for exchange of services. Similarly, as presented in [63], a market is envisioned for exchange of services to the DSO. Therefore, a market infrastructure for transaction of demand response services is needed. Future work should investigate how such markets can be implemented, if demand response services have any value for the system operators at all and if it is economical feasible to implement and maintain. Related to this, further work should also investigate whether DSO services provides a real economical alternative to grid reinforcement at all.

7.3.3 Standardisation and validation of services

Finally, as a prerequisite to the market approach just described and to be able exchange power system services seamlessly, these services have to be formalised and standardised. In the iPower project, a series of services that could be of interest to DSOs have already been identified [41]. These services include curtailment of power consumption during peak load hours and voltage support. As part of the standardisation, methods for validation of delivered services should also be developed. Related to this is what is commonly known as the *baseline* problem,

where the buyer and seller of a services have to agree on an expected consumption profile, which will serve as a baseline for validation.

Finally, another import topic is cyber security which should receive more attention. With aggregators, which are communicating with a large number of DERs, upon which the stability and security of the power system relies, the vulnerability of the whole power system increases. Therefore, cyber security technologies that are sufficient light to handle communication with numerous of DERs, but still secure enough to secure each individual unit being controlled, have to be developed.

7.4 Potential Barriers

Several potential barriers against flexible demand from private consumers have been identified during this project. This section presents three potential barriers for an efficient integration of DR from DERs connected in the low voltage grid: varying tariffs, standardised interfaces and energy efficiency.

7.4.1 Standardised interfaces for control of appliances

For a seamless integration of flexible demand appliances at residential level, the provision of demand response from household appliances has to be fully automated: either directly controlled by an outside aggregator or potentially through a building management system – or house aggregator. Presently, appliances that allow their power consumption to be shifted, e.g. heat pumps and washing machines, are usually manually controlled by the end-user, typically using a time-delay that has to be set manually prior start-up. Other appliances can be controlled remotely, however still manually, using mobile applications. Hence, for a building management system to be able to control several in-house appliances it has to be able to handle multiple – often proprietary – communication protocols or the end-user has to confine his selection of appliances to one manufacturer only. This situation is by no means optimal, neither from an aggregation point of view,

due to the loss of flexibility that is associated with the amount of appliances that can be controlled, nor from the end-users point of view due the limitation of appliances that he can choose among. Therefore, DR from residential sources should – ideally – be fully automated using standardised communication, either using a direct approach as in this project or by an indirect approach using incentive signals, e.g. price signals, provided by the aggregator. A solution to these issues could be to certify new appliances to be able to provide DR, similar to how TVs were certified as being HD-ready in the mid-2000s, with the emerging of High Definition (HD) technology. In a similar way appliances could be certified as being Smart Grid-ready, thus guaranteeing that a given appliance complies with the standards for demand response.

7.4.2 Varying tariffs

If DR from residential households should ever gain acceptance in the private sector there should be an incentive for the end-users of electricity to provide this flexibility. Currently, taxation on electricity in Denmark is used to influence the consumption pattern of end-users. However, due to the static composition of taxes and dues on electricity, this approach exclusively addresses an overall reduction of power consumption. For most consumers this approach works well, hence an economical incentive is expected to be a likely driver of flexible demand as well. With the current tariff system on electricity only approximately 15% of the electricity bill comes from the actual cost of electricity, whereas the remaining 85% is comprised of taxes, public obligations and distribution fees. These tariffs are fixed, which means that potential savings of shifting consumption from one period to another will only influence the 15% of the electricity bill. This will most likely not incentivise end-users to invest in the equipment that is required to be able to control their appliances.

This calls for a new tariff system where the tariffs are dynamically varying with the cost of electricity such that the overall variation in the price is preserved after the tariffs have been added. Alternatively, a multiple tariff system could be developed using different tariffs dur-

ing day as, for example, in the UK Economy 10 system. However, such a system would most likely not be flexible enough to reflect the daily variation that will be present in the output of a power generation side based entirely on renewable energy sources.

7.4.3 Energy Efficiency

Though not immediately intuitive, also energy efficiency poses a barrier against flexible demand from residential households. As refrigerators and freezers, as well as washing appliances, become more energy efficient, the potential for DR from such resources will diminish. The future duty cycle in these appliances will likely be more or less the same as now and hence the flexibility; however, their need for electricity will be significantly smaller and thus the magnitude of flexibility. This does not mean that energy efficiency should be opposed, but we should be aware of the potential for flexibility will likely decrease over time. It would therefore be unwise to base a flexible demand side on such resources alone in the long term. A potential candidate that can undertake the role as a residential resource for DR on the longer timescale are EVs. With the introduction of EVs, a significant share of the energy consumption for transportation, i.e. from oil, will be supplied by electricity instead. With a large amount of distributed batteries in the power system that have to be charged daily, these can be utilised for DR when the EVs are connected to the power system. Moreover, technologies like vehicle to grid (V2G) will allow car batteries to be discharged into the distribution grid, thus providing local generation support during peak load hours. Similarly, the EV batteries can be charged during periods with less demand for electricity, e.g. during night time.

As a potential risk posed by the integration of EVs, the charging of numerous EVs in a distribution grid can lead to a significant increase in the amount of electricity that has to be distributed to the end-users on a daily basis. Consequently, this can result in an increased peak demand and ultimately in black-outs if no coordination is enforced among them.

7.5 Recommendations

The aggregation framework presented in this thesis relies on a centralised estimation of the capacity of each of the DERs in the aggregator portfolio. The estimation is based on the Power Hub energy model, as presented in Section 4.7, which is a simple first order difference model of an often quite complex process. Moreover, measurements of external disturbances can not be measured on-site and communicated to Power Hub, as with PowerFlexHouse, but are estimated or even assumed constant. This gives a rather crude approximation of the available capacity. Even though the sum of errors, due to approximations, should even out for a large portfolio, the DERs themselves will often have a higher insight in the flexible processes that they are running, as well as the disturbances that are affecting the process. It is therefore natural that it is the DERs themselves that estimates the available capacity, which could also take into account unplanned changes in operation compared to what was reported the day before. As discussed in Paper C, the locally estimated capacity could be communicated to the aggregator using two parameters: one for the maximum power consumption over a suitable time horizon and likewise another for the minimum. This predefined time horizon should be defined to address the application of interest; for example, 15 minutes for frequency control applications up to a few hours for selling and buying electricity in the power market. This type of control could be implemented by extending the existing Power Hub interface with an additional analogue channel, which could be used to communicate one of the two parameters to Power Hub and then the current capacity reading could communicate the other. In this way, liability is also shifted away from the aggregator towards the DERs as long as the given power setpoint is within the bounds given by the DER. Furthermore, the interface could be extended with an additional input, specifying the preferred power consumption – or generation – by the DER, which would be the ideal power consumption seen from the DER.

Chapter 8

Conclusion and Perspectives

In this thesis, a method for integration of demand response from entities connected in the low voltage network has been presented and demonstrated. Demand response from resistive heating in an office building has been utilised using direct control from the commercial power plant Power Hub, which is currently running on fully commercial terms in Denmark and England. In this chapter, a conclusion is given on the work presented in this thesis and some perspectives on future scientific work and business opportunities are outlined.

8.1 Conclusion

Initially, this thesis has provided a profound analysis of typical available appliances in households that can be utilised for demand response applications. The analysis shows that electric space heating – when available – provides the highest potential for demand response especially when considering the expected increase in heat pumps in Denmark towards 2035. Next, comes refrigerators and freezers, and finally water heaters which have a high potential for down regulation in the summertime.

Several models have been formulated and validated for the heat dynamics of PowerFlexHouse. The models have been used in several diverse applications including simulation, forecast of heat loads and real time control. A simple linear model has shown good results in implementations of model predictive control on a short time-scale, but has shown to be inadequate to describe long time dynamics, i.e. on a daily time-scale, thus a non-linear model was formulated instead. The non-linear model shows significant better results, both on the shorter- and longer time-scale, however, at the cost of being more complex and not as easy to integrate into existing linear model predictive control frameworks and dispatch problems. Moreover, cf. Figure 7.1, it has been shown how such models can be used to estimate the duration of up- and down regulation of aggregated loads.

Furthermore, a generic dispatch problem has been formulated, which is used – with some modifications – to allocate power to a series of entities on both aggregator level and building management system level.

A remote terminal unit has been installed in PowerFlexHouse, which provides a communication interface between Power Hub and the building management system in PowerFlexHouse. Furthermore, a local heat load controller has been implemented in the building management system, which delivers the optimal control of the ten resistive heaters installed in PowerFlexHouse, cf. the dispatch problem formulated in Section 4.6. Using control from Power Hub to facilitate a series of field experiments it has been demonstrated how electric space heating in households can be utilised for demand response applications in the low voltage network. The provided demand response was observed to react within seconds when a setpoint change was given, thus making resistive heating a potential source for fast responding regulating power, i.e. as primary or secondary reserve capacity. Even though focus has explicitly been placed on electric space heating from resistive heaters, there is nothing that suggests that the found results can not easily be extended to include electric space cooling and water heating as well, which means that there is a substantial potential for demand response services from thermal applications in detached

buildings. This includes both services for frequency control as requested by the TSO, i.e. for maintaining the balance of the power system, as well as services that could be utilised by DSOs, e.g. for curtailment of power consumption during peak load hours and voltage support in the distribution grid.

Two-way communication has been implemented to provide feedback of available capacity to the aggregator. In this way, the aggregator maintains knowledge about the utilisation of its DERs, and hence the power consumed by the aggregator can be controlled with a very high reliability and accuracy. Local control at DER level ensures that constraints on the indoor temperature are kept at all times during operation and that the power consumption complies with the given power setpoint as long as the indoor temperature is within the comfort range that is specified by the house residents.

Through simulations it has been demonstrated that at least 20% of the power consumption for space heating can be shifted within a 12 hour time frame if a $\pm 0.6\,^{\circ}\mathrm{C}$ temperature band can be utilised. Alternatively, heating can be entirely postponed for up to two hours, but at a cost of significant higher power consumption following the period of decoupling, i.e. the kickback effect as presented in Section 3.7.

An overall conclusion of this thesis is that resistive heat loads of detached households can indeed be utilised for dynamic demand response applications in the low voltage grid, offering a fast, reliable and accurate response to setpoint changes, and hence is able to replace conventional power plants when aggregated into a virtual power plant framework.

8.2 Perspectives for Future Scientific Work

With the emerging utilisation of demand response in the low voltage grid there are many paths that remains to be explored in detail. In this project emphasis has primarily been placed on demonstration and thus naturally many limitations exist on the presented method.

Especially four areas require further scientific attention: firstly, better algorithms for optimisation of a portfolio of DERs are needed, which are both scalable and computational fast such that control in near real time can be achieved. Also, as has been shown in this thesis, the dynamics of some DERs will be non-linear and thus the dispatch problem will have both a non-linear cost function and constraints. Therefore, methods for formulating and solving the dispatch problem with non-linear entities have to be developed as well. Secondly, scientific work within standardisation of communication between aggregator and the BMS, as well as between the BMS and flexible appliances, will have to be developed. This is considered a prerequisite for an efficient integration of the demand side in the control of the power system, which will help facilitate the transformation of the present power system into the envisioned smart grid. Thirdly, secure communication between aggregators and DERs are needed for this transformation as well. With the utilisation of more distributed resources, upon the stability of the whole power system relies, the need for fast and secure communication is essential. Fourthly, research within market infrastructures for flexible services should receive more attention, such that flexible services can be transacted seamlessly and transparently. Related to this is also standardisation of power system services.

8.3 Perspectives for Future Implementations and Business Opportunities

With a total phase-out of coal and oil in the Danish energy supply in the near future, the demand for electricity is expected to increase significantly as oil burners are replaced with heat pumps and petrol driven vehicles are replaced by EVs. On the other side, an increased share of the electricity will come from renewable sources, e.g. wind and solar, which implies that the power generation will become more intermittent and less controllable. To address these issues, we need a more flexible consumption side in the power system that will adjust its demand to the current output of the generation side. Initially, DR from industrial processes should be integrated into the power market.

Here, there will be an economical incentive which will decrease the costs of operation for the DER owners. Eventually, as cost of embedded controllers and communication declines, demand response from small entities will also become economically feasible. This, however, will not drive the integration alone: as long as there is no demand for demand response services there is no incentive to develop such. Currently, the capacity of the Danish transmission and distribution system is so large that there is no urgent need for flexible services in the low voltage network. Furthermore, with the current tariff scheme on electric energy, where only 15% of the final electricity bill comes from the actual cost of electricity, the amount of savings will simply be too small to justify the investments required in the infrastructure needed to utilise demand response from small entities. Therefore, a new tariff scheme has to be developed, where tariffs will be varying with the cost of electricity.

Over the resent years, several companies have had a huge success in developing business cases, where excess capacity is being utilised. Two well-known examples are Airbnb, mediating available housing capacity, and Uber, mediating transportation capacity. Basically, despite the problem with DR is more technical than the two given examples, the basic problem is the same: utilise excess capacity in the power system. This implies that there could exists a potential business case for utilisation of flexible demand in the low voltage grid in the near future, which would increase the efficiency of the whole power system, thus providing savings not only to end-users but to the society as a whole.

APPENDIX A

Calculation of Convection Heat Transfer Coefficient

This appendix derives an equation for how to calculate the convective heat transfer coefficient and heat transfer resistance between a rectangular space heater and the surrounding air.
Assuming that the resistance heaters in PowerFlexHouse can be approximated with a vertical plate with rectangular dimension $W \times L$ and average surface temperature T_s, the resistance to transfer heat between the heater and the surrounding is given by

$$R_{ih} = \frac{1}{Ah} = \frac{1}{WLh} \tag{A.1}$$

where A is the area of the heater and h is the convective heat transfer coefficient which is given by

$$h = \frac{k}{L}Nu = \frac{k}{L}\left[0.68 + \frac{0.67Ra^{1/4}}{\left(1 + (0.492/Pr)^{9/16}\right)^{4/9}}\right] \tag{A.2}$$

where k is the thermal conductivity of air, Nu is the Nusselt number, which for a vertical mounted rectangular plate is given by the term in square brackets ([49]), Pr is the Prandtl number and Ra is the

Rayleigh number which is given by

$$Ra = \frac{g\beta\left(T_s - T_\infty\right)L^3}{\nu^2}Pr \tag{A.3}$$

where g is the gravitational acceleration, T_∞ is the temperature of the surrounding air sufficiently far from the heater, $\beta = 1/T_f$ [1/K], where $T_f = \left(T_s - T_\infty\right)/2$ is called the film temperature, and ν is the kinematic viscosity of air. Values for thermal conductivity, kinematic viscosity and Prandtl number for air at varying film temperatures are presented in Table A.1.

Film temperature T_f, [°C]	**Thermal conductivity** k, [W/(m K)]	**Kinematic viscosity** v, [m^2/s]	**Prandtl number** Pr
30	0.02588	1.608×10^{-5}	0.7282
35	0.02625	1.655×10^{-5}	0.7268
40	0.02662	1.702×10^{-5}	0.7255
45	0.02699	1.750×10^{-5}	0.7241
50	0.02735	1.798×10^{-5}	0.7228
60	0.02808	1.896×10^{-5}	0.7202

Table A.1: Physical properties of air, source: [49].

From Equation (A.1) to (A.3) the heat transfer resistance can be found by initially determining the Rayleigh number, then the heat transfer coefficient and finally the heat transfer resistance.

PAPER A

A Heat Dynamic Model for Intelligent Heating of Buildings

Part of proceedings of the *International Conference on Applied Energy* (ICAE 2012), Suzhou, China, 2012. Revised and accepted for publication in *International Journal of Green Energy*, Special Issue of ICAE2012.

International Journal of Green Energy (2015) **12**, 240–247

ISSN: 1543-5075 print / 1543-5083 online
DOI: 10.1080/15435075.2014.891516

Taylor & Francis
Taylor & Francis Group

A Heat Dynamic Model for Intelligent Heating of Buildings

ANDERS THAVLOV and HENRIK W. BINDNER
DTU Electrical Engineering, Technical University of Denmark, Roskilde, Denmark

This article presents a heat dynamic model for prediction of the indoor temperature in an office building. The model has been used in several flexible load applications, where the indoor temperature is allowed to vary around a given reference to provide power system services by shifting the heating of the building in time. This way the thermal mass of the building can be used to absorb energy from renewable energy source when available and postpone heating in periods with lack of renewable energy generation. The model is used in a model predictive controller to ensure the residential comfort over a given prediction horizon.

Keywords: Heat dynamic modeling, Demand side management, Flexible load, Smart grid, Power system services

Introduction

A part of the solution to the growing global interest in reducing CO_2 emissions is an increased integration of renewable energy into our power systems. However, coping with an increasing multitude of small, highly fluctuating, non-controllable, and often distributed energy sources puts a high demand on the future power system. As an example the newly elected government in Denmark has set the goal that the power consumption in the national grid, covered by wind energy, should be increased to 50% by year 2020, from an already world high of 22% in 2010 (Danish Energy Agency 2010). Integration of that high amount of intermittent generation, without flexible consumption, would lead to great power fluctuations in the power system with only little means of control. Such a situation is depicted in Figure 1 where the projected power consumption and wind power production is plotted, if such a scenario was implemented in Denmark in year 2025.

The figure shows that the power production from wind turbines exceeds the consumptions several times during the second quarter of 2025. To ensure the stability of the power system, some of the wind turbines would have to be shut down, but this is both undesirable from a socio-economic point of view and expensive for wind turbine owners. Therefore, if such an ambitious goal is to be reached, we have to rethink how electric energy is distributed, utilized, and especially the role of consumers has to be reconsidered.

If excess power generation could somehow be stored temporarily, it would greatly benefit to the stability of the power system, without wasting energy. There are many different technologies offering energy storage, but these are usually expensive and associated with energy losses. Another option is to store the energy locally on the consumer side, whenever there is such a capacity. The thermal mass of buildings offers such a capacity and can therefore be used as a unidirectional storage for electrical power, wherever electrical space heating is used. In practice, this can be done by increasing electrical space heating in periods with excess power production and postpone consumption in periods with low production. Such a contribution might seem modest, but many buildings aggregated intelligently in the distribution grid can have a huge impact on power balancing, within the hourly timescale. Varying space heating with power generation of course affects the indoor temperature in a building. If comfort should not be compromised for the residents of the building, the indoor temperature should not be allowed to vary more than a few degrees Celsius. But for well-insulated buildings with a high thermal mass, even letting the indoor temperature vary within a single degree, means that heating can be precipitated or postponed up to an hour, which would benefit the power system.

To ensure the comfort of the residents of the house, models for prediction of indoor temperature, based on heating decisions, are needed. This article presents a heat dynamic model for prediction of the indoor temperature and future energy needs for electrical heating in an office building. The model has successfully been used in several applications for providing power system services in the small distributed power system, SYSLAB.

Several studies have been carried out in modeling the heat dynamics of buildings, e.g., Madsen and Holst (1995) and Andersen, Madsen, and Hansen (2000), but these have been conducted either for small buildings with few rooms or for test cells. The research in this article uses principal component analysis to estimate one representing parameter for the temperature of an office building, with eight rooms. Also pseudo-random sequences have been used to design a heat input from 10 electrical space heaters to ensure optimal conditions for parameter estimation. The model is derived and estimated for a light office building placed at the DTU Risø campus in Denmark. For heat dynamic models of other types of buildings, see Bacher and

Address correspondence to Anders Thavlov, DTU Electrical Engineering, Technical University of Denmark, Frederiksborgvej 399, Building 776, Roskilde 4000, Denmark. E-mail: atha@elektro.dtu.dk
Color versions of one or more of the figures in the article can be found online at www.tandfonline.com/ljge.

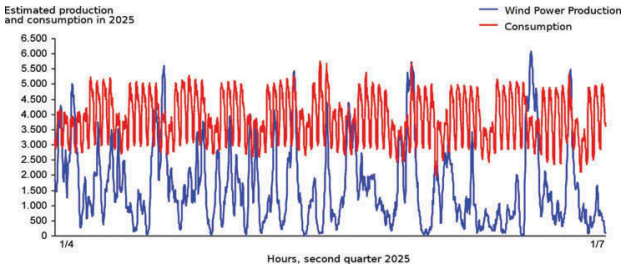

Fig. 1. Projected power consumption and wind power generation in 2025 (Energinet.dk, 2011).

Madsen (2011). For a more detailed description of the model, see Thavlov (2008). Also several studies have been conducted in implementation of flexible demand, e.g., see Aswani et al. (2012) where a simple autoregressive model is used to control the cooling output from an air conditioner in a computer lab at UC Berkeley. Duić, Lerer, and Carvalho (2003) give an example of how a hydrogen storage can be used to store excess wind and solar production in an island system. The stored hydrogen can then be used at a later time, e.g., for providing peak shaving services.

Materials and Methods

Initially, this section describes the distributed power system SYSLAB, which the intelligent office building FlexHouse is a part of. The thermal model has been derived specifically for FlexHouse, which has also formed the basis for collecting data for parameter estimation. The following section describes the general theory behind heat transfer and how models of the mechanisms behind it can be used as sub-models in an overall model of heat exchange in an office building. Next, a description of how the heat input was designed for optimal parameter estimation is given. This section also describes how the collected temperature data was processed to reduce dimensionality from eight measurements to one parameter representing an aggregated temperature in the building. Finally, a technique for parameter estimation is briefly described, along with the software CTSM that can be used to find parameter estimates.

SYSLAB and FlexHouse

The DTU Risø campus is housing an experimental research facility for distributed power systems called SYSLAB. SYSLAB is a small power system with a high share of generation from renewable energy sources. The power system consists of a number of small distributed power generating and consuming units that can be coupled together in any given configuration. Also part of the system can be decoupled from the local distribution grid, thus allowing parts of the system to be run in island mode. Among the components of interest are:

Two wind turbines, 11 kW and 10 kW [Generation]
Photovoltaics, 7 kW [Generation]
Diesel generator, 48 kW [Generation]
Vanadium battery, 15 kW/120 kWh [Storage/Generation/Consumption]
Plug-in hybrid vehicle, 9 kWh [Consumption/Storage]
Electric vehicle, 16 kWh [Consumption/Storage]
FlexHouse, 20 kW [Consumption/Storage]

Most of the power-generating units in SYSLAB are renewable and SYSLAB is therefore an ideal laboratory for research in power systems with a high penetration of renewable energy. Each unit in SYSLAB is controlled locally by a small computer on which custom build control software can be implemented and tested. This gives a very flexible setup with emphasis on control of the distributed energy resources.

On the consumption side there is an intelligent office building, called FlexHouse, with a peak consumption of 20 kW. The building has been built from light materials and consists of seven small office rooms, a main hall with a kitchenette and a toilet. The layout of the building can be seen in Figure 2.

From the layout, it can be seen that the house has a big window facade in the southward direction, why solar radiation has a big impact on the heat dynamics of the building.

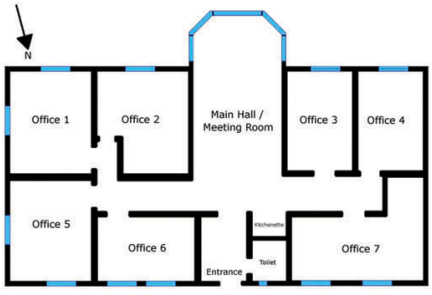

Fig. 2. FlexHouse layout.

FlexHouse has been equipped with wireless sensors and actuators to enable the building to be easily monitored and controlled. Each of the eight rooms has been equipped with a temperature sensor, mounted centrally on the wall and a motion sensor for monitoring of presence in the room. All windows and doors have been equipped with sensors, such that the state of these can be monitored as well.

The main power consumption of the house comes from 10 electrical space heaters, with a total consumption of 10 kW. Also a water heater, a refrigerator, and heat pumps have been installed in the building. Each of the units is controlled individually by an actuator that communicates wirelessly with a house controller.

A software platform has been developed for control of the building. It gathers sensor input, logs the building state in a database, and sends commands to the actuators. The platform makes implementation of custom control algorithms simple, allowing different control concepts to be tested easily.

The software platform is also gathering local weather data from a weather mast placed outside FlexHouse. The weather data can be used to estimate future needs for electric heating.

Thermal Model Formulation

The approach to develop the heat dynamic model for FlexHouse is to use a gray-box modeling technique, thus using prior physical knowledge about heat dynamics of buildings to establish the model structure together with collected data and statistics to estimate the model parameters.

Modeling is typically an iterative process that involves model formulation, parameter estimation, and model validation. Due to the complexity of the heat flow in FlexHouse, several model structures were proposed and investigated before a final model was accepted. It is only the model that has shown the best performance that will be derived in this article. For further information about the iterative process of formulation heat dynamic models of building, see Bacher and Madsen (2011).

Heat dynamic models are usually composed of sub models for the mechanisms behind heat transfer. The most general of these are

Conduction:	Heat transfer through a medium
Convection:	Heat transfer between two different media
Ventilation:	Heat transfer due to mass transfer, e.g., heated air through an open window
Radiation:	Heat transfer between objects that are in optical contact, e.g., solar radiation

Heat transfer between two media by conduction or convection is proportional to the temperature difference between the two media involved. In the following also heat exchange by ventilation is assumed to be linear with the temperature difference between the indoor and outdoor air. This approximation holds for low wind speed, however, it is well know that for high wind speed, the natural ventilation of buildings becomes nonlinear with both wind speed and direction. To keep the model in a linear framework, the linear approximation is accepted to be good enough. The heat transfer from conduction, convection, and ventilation can therefore be modeled using thermal resistance,

$$\dot{Q} = \frac{dQ}{dt} = \frac{1}{R}(T_1 - T_2) \tag{1}$$

where T_1 and T_2 are the temperatures of each media involved and R is the resistance to transfer thermal energy.

Another important aspect of heat dynamics is the heat capacity that describes a material's ability to accumulate heat. The temperature development in a medium is given by the differential equation

$$\dot{Q} = C(T)\frac{dT}{dt} \approx C\frac{dT}{dt} \tag{2}$$

As seen in the equation the heat capacity is dependent on temperature, however, the temperature interval in which the house is operated is very small, thus the heat capacity can be assumed constant.

The heat dynamics of FlexHouse is modeled as one large room with some interior walls and a house envelope. The air temperature inside the room, house envelope, and interior walls and floors is assumed to be homogenously distributed. Thereby the model can be formulated as a lumped model with three temperature states; the temperature of the indoor air (T_i), the temperature in the house envelope (T_{om}), and in the interior walls and floors (T_{im}). It should be noted that T_{im} described the long time constant of the interior of the building, hence also the temperature of furniture, computers, desktops, etc.

The modeled heat flow in a one room model is depicted in Figure 3. It can be seen that the interior medium exchanges heat with the indoor air by convection, (1). Likewise does the indoor air exchange heat with the inside of the house envelope (2) and directly to the outside by ventilation, (3). Moreover, the outside of the house envelope exchanges heat with the ambient environment, (4). Energy is feed into the building from the controllable space heaters (5) and by solar radiation through the windows, (6). The solar radiation is partly absorbed when it passes through the indoor air before hitting the interior walls. It is assumed that the fraction of solar radiation absorbed by the air is given by (1 - p), thus only the fraction p reaches the interior walls. Heat conduction between interior walls and the house envelope is neglected due to the small surface being shared between these two media.

Due to similarities between Equations (1) and (2) and those of electrical resistance and capacitance, the heat dynamics of a building is usually modeled as an electrical network, consisting of resistors and capacitors, with temperature equivalent to voltage and heat flow equivalent to flow of electrical charge, i.e. current. The equivalent electrical diagram to the heat flow in Figure 3 can be seen in Figure 4.

It should be noted that T_{om} and T_{im} are not directly observable in FlexHouse, but they can be estimated, e.g., using a Kalman filter.

From Figure 4, the three coupled differential equation describing the temperature states can be derived as

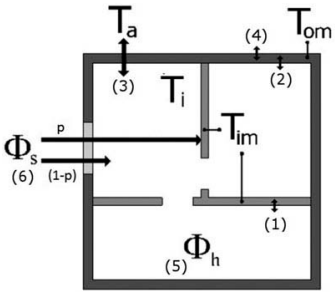

Fig. 3. Exchange of heat in a building.

$$
\begin{aligned}
C_i \frac{dT_i}{dt} &= \frac{1}{R_c}(T_a - T_i) + \frac{1}{R_i}(T_{im} - T_i) + \frac{1}{R_{im}}(T_{om} - T_i) \\
&\quad + A(1-p)\Phi_s + \Phi_h \\
C_{im} \frac{dT_{im}}{dt} &= \frac{1}{R_i}(T_i - T_{im}) + Ap\Phi_s \\
C_{om} \frac{dT_{om}}{dt} &= \frac{1}{R_{im}}(T_i - T_{om}) + \frac{1}{R_{am}}(T_a - T_{om})
\end{aligned} \tag{3}
$$

where C_i, C_{im}, and C_{om} are the heat capacities of the indoor air, interior walls, and house envelope, respectively. A is the effective window area and p is the fraction of solar radiation not being absorbed by the indoor air before hitting an interior wall.

Equation (3) can be reformulated on matrix form

$$
\frac{dT}{dt} = AT + BU \tag{4}
$$

where $T = [T_i, T_{im}, T_{om}]^T$ is a state vector containing the temperature states and $U = [T_a, \Phi_s, \Phi_h]^T$ is the exogenous inputs to the system; ambient temperature, solar radiation, and heater input. The 3×3 matrices, A and B define how the current state and exogenous input affects future states, respectively.

Equation (4) describes a purely deterministic system. To account for deviations from this ideal world, a stochastic process is usually added to the differential equation, which leads to the stochastic differential equation given by

$$
dT = ATdt + BUdt + d\omega(t) \tag{5}
$$

where $\omega(t)$ is a stochastic process that in the following is assumed to be a process with independent increments, i.e., a Wiener process, with incremental covariance R_1.

For predictions at time t, Equation (5) can be integrated over a given prediction horizon, τ. The solution can analytically be found to be

$$
T(t+\tau) = T(t)\, e^{A\tau} + \int_t^{t+\tau} e^{A(t+\tau-s)} BU(s)\, ds + \int_t^{t+\tau} e^{A(t+\tau-s)} d\omega(s) \tag{6}
$$

Assuming that the exogenous input, U, is constant over the prediction horizon, Equation (6) can be reduced to the linear stochastic state space model.

$$
T(t+\tau) = \Phi(\tau)\, T(t) + \Gamma(\tau)\, U(\tau) + v(t,\tau) \tag{7}
$$

where

$$
\begin{aligned}
\Phi(\tau) &= e^{A\tau} \\
\Gamma(\tau) &= \int_0^{\tau} e^{As} B ds \\
v(t,\tau) &= \int_t^{t+\tau} e^{A(t+\tau-s)} d\omega(s)
\end{aligned} \tag{8}
$$

Assuming that $\omega(t)$ is a Wiener process, $v(t,\tau)$ becomes normal-distributed white noise with zero mean and covariance,

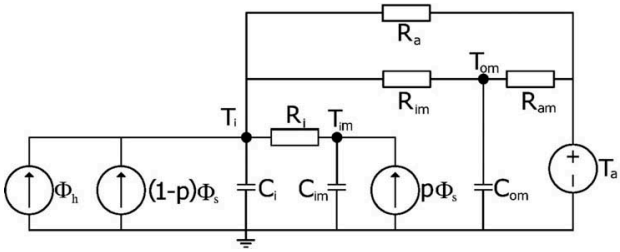

Fig. 4. Equivalent RC-diagram.

$$R_1(\tau) = \begin{bmatrix} R_{11} & 0 & 0 \\ 0 & R_{22} & 0 \\ 0 & 0 & R_{33} \end{bmatrix}$$

A white-noise process is a random process, which in the frequency domain contains all frequencies with an equal amount of power. This means that spectral density is constant. Further a white-noise process has zero mean and shows no correlation in time, i.e., it has zero autocorrelation for lags different from 0.

Only one of the three states in T is observable, therefore an observation equation is introduced,

$$T_r(t) = CT(t) + e(t) \tag{9}$$

where $e(t)$ is the measurement error of the temperature. The measurement error is assumed to be normal-distributed white noise with zero mean and variance R_2. In this case, only indoor air temperature is measured, i.e., the first state in T, thus $C = [1, 0, 0]^T$.

Data Processing

Four time series of the room temperatures and ambient parameters were collected in FlexHouse during four experiments in February and March 2008. The data in the time series were collected with a sampling time of 5 min. The heaters in FlexHouse were controlled in a binary synchronous pattern, i.e., all 10 heaters on or off, in any given time step. To ensure optimal conditions for parameter estimation, the binary control signals were generated as pseudo random binary sequences, which is a deterministic signal with white-noise properties. This was done to ensure independence from all other exogenous input, e.g., solar radiation. Also the signal can be generated such that the system is excited in the right area of the time domain where the time constants are expected to be. To meet the assumption about the heat being homogenously distributed in the building, all interior doors were open during the measurements, to allow the heat from the heaters to dissipate freely between rooms. Further it was considered whether fans should have been used to distribute the temperature more homogenously in the building. However, the collected temperature data from the individual rooms has shown a standard deviation below 1°C, from the mean temperature. Thus, indicating that the temperature is close to being homogenously distributed in the building.

Since the indoor temperature is modeled as a single state, the dimension of the temperature measurements has to be reduced from eight to one. An obvious approach would be simply to use the average temperature, but since the rooms are not equal in size, the measurements should not be weighted equally. Therefore, principal component analysis has been used to decrease the dimension of measurements to a single temperature representing parameter. It was found that the first principal component accounts for more than 90% of the variance in data, why the first principal component gives a sufficiently good estimate of an indoor temperature to be used as the temperature representing parameter. A plot of the average temperature development, the first principal component, and the heat input can be seen in Figure 5. The plot clearly shows how the heat input excites the indoor temperature. Also the effect of solar radiation can be seen in the plot. It is especially clear around measurement number 500, where the indoor temperature raises despite that all the heaters are off.

Parameter Estimation

The parameters in Equation (3) have been estimated using CTSM; a parameter estimation tool developed at the Department of Informatics and Mathematical Modelling at the Technical University of Denmark (DTU). CTSM can be used to find maximum likelihood estimates that are given by

$$\hat{\theta} = \arg\max_{\theta} \{L(T(N); \theta)\}$$

where θ is a vector containing the unknown model parameters in Equation (3), $T(N)$ is a vector with all the observations up to and including N and L is the joint probability function. Given the model structure and observed date, a routine in CTSM maximizes the joint probability function, i.e., determines the most likely parameter set, using a Kalman filter, and returns the estimates including the standard deviation of the estimates.

CTSM is a great tool for the estimation of model parameters in stochastic linear state space models. The system and measurement equations are easily implemented in CTSM, along with the assumption about the Wiener process and the normal-distributed measurement error.

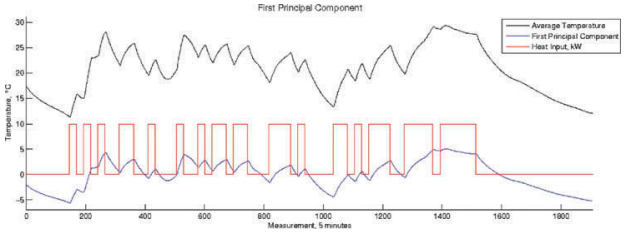

Fig. 5. Average temperature, first principal component and electrical heater input for the first experiment.

Results

This section initially states the maximum likelihood estimates and then the performance of the model is presented. Finally, a description of the model validation is given.

Based on the four time series collected in FlexHouse model, parameters have been successfully estimated using CTSM. The parameters were first estimated, allowing the fraction of the solar radiation absorbed by the interior walls, p, to be free. The estimate was found to be 0.995, i.e., 99.5%, which imply that none of the incoming solar radiation is absorbed by the indoor air, but is absorbed entirely by the interior walls and floors. The parameters were re-estimated assuming that none of the solar radiation is absorbed by the indoor air, i.e., $p = 1$. The final parameter estimates can be seen in Table 1.

The estimates shows that the heat capacity of the house envelope is quite large compared to the other heat capacities, which is what was expected, since the interior walls are made from lightweight materials. It is also noted that the heat capacity of the interior wall is very small compared to that of the indoor air. This is not what would be expected since the interior walls should be able of store more heat than the indoor air. The very low heat capacity can partly be explained by the estimate of the variance of the temperature in the interior walls, $\hat{R}_{22,1}$, which is quite large, indicating that there is a very large uncertainty on the temperature in the interior walls. Additional collected data could be used to reduce this uncertainty.

Unfortunately, there is no building data available, for FlexHouse, to compare with the found estimates. However, the total window area can be measured and compared to the estimate. Assuming that the effective area is approximately 60% of the physical area, which has been measured to be 30 m^2, the estimate is very close to the expected.

From the estimates in Table 1 and by use of Equation (7) with $\tau = 5$ min, a discrete model has been derived for 5 min predictions. The 1 h temperature predictions seen in Figure 6 were found by recursively calculating the 5 min prediction, 12 times.

Table 1. Maximum likelihood estimates for p = 1

Maximum likelihood estimates with $p = 1$		
Parameter	ML estimate	Standard error of estimate
$\hat{R}_i$	46.848°C/kW	0.134
$\hat{C}_i$	8.120 kWh/°C	0.294
$\hat{R}_{im}$	1.809°C/kW	0.147
$\hat{R}_a$	8.021°C/kW	0.501
$\hat{C}_{im}$	0.006 kWh/°C	0.001
$\hat{C}_{om}$	292.950 kWh/°C	7.675
$\hat{R}_{am}$	0.085°C/kW	0.029
$\hat{A}$	20.212 m^2	1.491
$\hat{p}$	1.000	n/a
$\log\left(\hat{R}_{11,1}\right)$	-2.754°C^2	0.299
$\log\left(\hat{R}_{22,1}\right)$	6.368°C^2	0.059
$\log\left(\hat{R}_{33,1}\right)$	-0.943°C^2	0.312
$\log\left(\hat{R}_2\right)$	-7.066°C^2	0.076

When the predictions were made the input to the model, i.e., $U = [T_a, \Phi_s, \Phi_h]^T$, was assumed constant within the following hour. The top plot shows the predicted indoor temperature (blue) and the measured indoor temperature (red). The bottom plot shows the 1 h prediction residuals, i.e., the difference between the predicted and actual temperature. The residuals shows that the indoor temperature can be predicted within 1°C over an hour, which is acceptable when considering the natural variations of the weather, which is assumed to be constant within the following hour, when the predictions are made.

The model has been validated using the 5 min prediction residuals. If these resemble white noise, the model can be assumed to be correct. The autocorrelation function for the residuals in

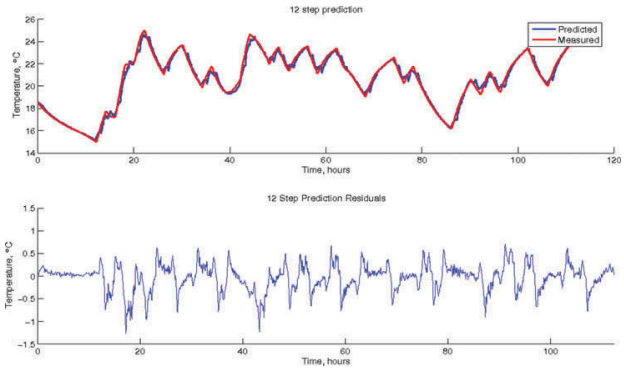

Fig. 6. One hour temperature predictions and residuals.

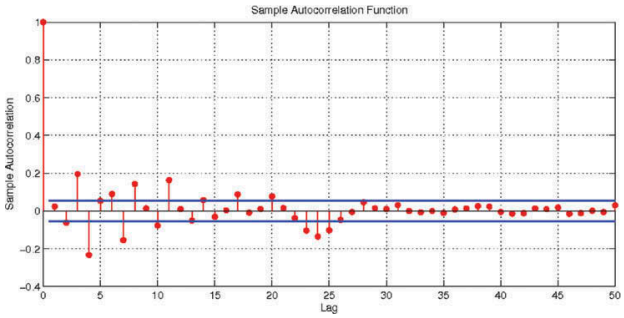

Fig. 7. Autocorrelation function for 5 minute prediction residuals.

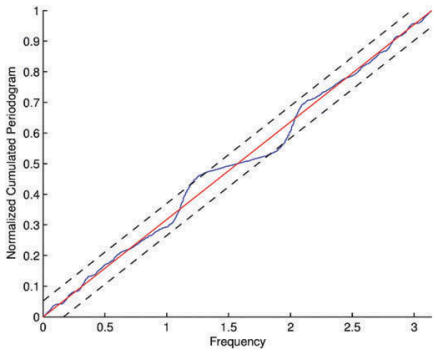

Fig. 8. Cumulated periodogram for 5-minute prediction residuals.

Figure 7 shows some autocorrelation outside the 95% confidence interval. This indicates that the residuals are not fully described by white noise. However, the autocorrelations are in general small and drops quite fast, why the model can be used as a good approximation.

Another test has been used to validate the model in the frequency domain. If the residuals were white noise, the spectrum of these should be equally distributed over all frequencies. This can be shown by a cumulated periodogram that should form a straight line, if all frequencies are equally represented. Figure 8 depicts the cumulated periodogram for the residuals, which almost stays within the 95% confidence interval. This shows that almost all frequencies are equally represented, thus the residuals show white-noise properties in the frequency domain.

Discussion

This section describes some of the applications of the heat dynamic model.

Applications

The heat dynamic model has been used in several applications for letting FlexHouse act as a flexible load, thus providing system services within SYSLAB. These applications have demonstrated that the power consumption in FlexHouse can be used as a unidirectional storage for wind power. By allowing the indoor temperature of the building to vary between 19 and 23°C, the thermal mass of the building can absorb variations in wind power production, thus providing balancing control in the power system. The flexible control has been demonstrated for both indirect control, i.e., using price signals, and direct control in a virtual power plant (VPP) setup. In the VPP setup, FlexHouse was integrated into a virtual power plant, run by the Danish electricity company DONG Energy. The house controller receives a power set point from the VPP controller, which the house controller uses to modify its power consumption, if not violating constraints for user comfort. The given set point is based on an hourly consumption forecast for the house generated by the heat dynamic model. The forecast is generated every day at 10 a.m. for the following 38 h, i.e., until midnight the following day. This allows the flexibility of the building to be bid into the day-ahead market, which closes at 12:00. The 14 h overlap cannot be used for bids in the day-ahead market, but it can be compared with the previous forecast to update possible changes in demand. These changes can then be used as a tool for balancing control. A local weather forecast, with predicted solar radiation and outdoor temperature, is used as model input. Given the forecast the virtual power plant optimizes the power consumption over a given day, asking the house deviate from the forecast if necessary.

The model has also been implemented in a model predictive controller for indirect control of power consumption. The controller downloads a price signal for the following 12 h, which is then used to optimize the heating of FlexHouse, such that cost of heating is minimized. Figure 9 shows the optimized power consumption such that heating during peak load hours is avoided. The figure clearly illustrates how the controller avoids heating the building during periods of high prices, postponing the heating to periods with low prices.

For more information about indirect control using price signals and model predictive control, see Zong et al. (2011).

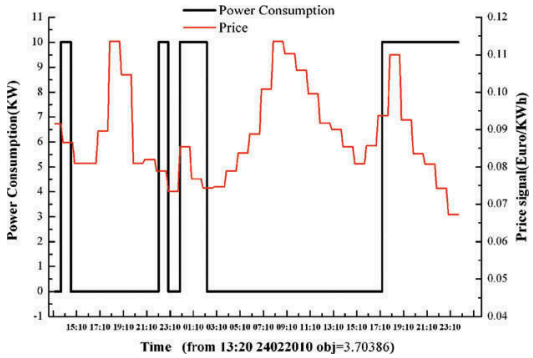

Fig. 9. Indirect control of power consumption using price signals and model predictive control.

Conclusions

This article demonstrates that a heat dynamic model can be used in applications for intelligent control of electrical heating. By controlling the electrical space heating in an office building intelligently, power consumption can often be increased or postponed within the hourly timescale, thus allowing the building to provide ancillary services in a power system. This has been demonstrated using two control schemes, i.e., direct and indirect. The demonstrations have shown that thermal mass of buildings can offer the flexibility to temporarily store excess power production from renewable sources.

The model has shown good results in predicting indoor temperatures and future power consumption needs, up to 38 h. Despite the good performance of the model, much can be done to improve the performance of model. Due to high amount of natural ventilation in FlexHouse especially the nonlinear effects from wind conditions should be integrated in the model, due to its influence on the indoor temperature.

Unfortunately, FlexHouse is a very light building that does not allow a lot of thermal energy to be stored in the building. Brick buildings with thick concrete floors offer larger thermal capacities and would therefore be preferred as flexible loads when using thermal storage. However, for demonstration and proof of concept, the applications have shown good results and demonstrated that FlexHouse can be used as a flexible load in SYSLAB.

Nomenclature

Abbreviation

CTSM	Continuous time stochastic modeling
VPP	Virtual power plant

Symbols

$\dot{Q}$	Heat transfer [kW]
T_i	Indoor air temperature in the building [°C]
T_{im}	Temperature in interior walls of the building [°C]
T_{om}	Temperature in the house envelope [°C]
T_a	Outdoor temperature [°C]
Φ_s	Solar radiation [kW/m^2]
Φ_h	Heat input from electric space heaters [kW]
R_a	Thermal resistance between indoor air and ambient environment [°C/kW]
R_i	Thermal resistance between interior walls and indoor air [°C/kW]
R_{im}	Thermal resistance between indoor air and house envelope [°C/kW]
R_{am}	Thermal resistance between house envelope and ambient environment [°C/kW]
C_i	Heat capacity of indoor air [kWh/°C]
C_{im}	Heat capacity of interior walls [kWh/°C]
C_{om}	Heat capacity of house envelope [kWh/°C]
P	Fraction of solar radiation absorbed by interior walls

References

Andersen, K.K., H. Madsen, and L. Hansen. 2000. Modelling the heat dynamic of a building using stochastic differential equations. *Energy and Buildings* 31:13–24.

Aswani, A., N. Master, J. Taneja, D. Culler, and C. Tomlin. 2012. Reducing transient and steady state electricity consumption in HVAC using learning-based model-predictive control. *Proceedings of the IEEE*. 100:240–253.

Bacher, P. and H. Madsen. 2011. Identifying suitable models for the heat dynamics of buildings. *Energy and Buildings* 43:1511–22.

Danish Energy Agency. 2010. *Energy statistics 2010*. Available at: http://www.ens.dk/sites/ens.dk/files/dokumenter/publikationer/downloads/energy_in_denmark_2010_2.pdf.

Duić, N., M. Lerer, and M.G. Carvalho. 2003. Increasing the supply of renewable energy sources in island energy systems. *International Journal of Sustainable Energy* 23:177–86.

Madsen, H. and J. Holst. 1995. Estimation of continuous-time models for the heat dynamics of a building. *Energy and Buildings* 22:67–79.

Thavlov, A. 2008. Dynamic optimization of power consumption. Master's thesis. DTU IMM, Technical University of Denmark.

Zong, Y., D. Kullmann, A. Thavlov, O. Gehrke, and H. Bindner. 2011. Model predictive control strategy for a load management research facility in the distributed power system with high wind penetration - Towards a Danish power system with 50% wind penetration. *Asia-Pacific Power and Energy Engineering Conference 2011 (APPEEC 2011),* Wuhan, China.

PAPER B

A Stochastic Model for an Office Building with Air Infiltration

---

This paper has been accepted for publication in the *International Journal of Sustainable Energy Planning and Management*.

International Journal of Sustainable Energy Planning and Management Vol. 07 2015 59-70

International Journal of
Sustainable Energy Planning and Management

A Non-linear Stochastic Model for an Office Building with Air Infiltration

Anders Thavlov[a] and Henrik Madsen[b]

[a] *Department of Electrical Engineering, Technical University of Denmark, Frederiksborgvej 399, Building 776, 4000 Roskilde, Denmark.*
[b] *Department of Applied Mathematics and Computer Science, Technical University of Denmark, Richard Pedersens Plads, Building 303B, 2800 Kgs. Lyngby, Denmark.*

ABSTRACT

This paper presents a non-linear heat dynamic model for a multi-room office building with air infiltration. Several linear and non-linear models, with and without air infiltration, are investigated and compared. The models are formulated using stochastic differential equations and the model parameters are estimated using a maximum likelihood technique. Based on the maximum likelihood value, the different models are statistically compared to each other using Wilk's likelihood ratio test. The model showing the best performance is finally verified in both the time domain and the frequency domain using the auto-correlation function and cumulated periodogram. The proposed model which includes air-infiltration shows a significant improvement compared to previously proposed linear models. The model has subsequently been used in applications for provision of power system services, e.g. by providing heat load reduction during peak load hours, control of indoor air temperature and for generating forecasts of power consumption from space heating.

Keywords:

Non-linear modelling,
heat dynamic modelling,
stochastic differential equations,
power systems,
air infiltration
URL:
dx.doi.org/10.5278/ijsepm.2015.7.5

1. Introduction

In large-scale power systems with a high penetration of wind power, the intermittent output of the generation side often has a negative impact on the power balance and hence the stability of the power system. Therefore, to counterbalance this intermittency, methods of making the consumption side more flexible are currently being perused. One approach is to use the thermal mass in cold storages to absorb excess power generation from renewable energy sources by temporarily lowering the temperature setpoint. However, the thermal mass of both residential and office buildings can also offer this type of uni-directional energy storage wherever electrical heating is utilised. By allowing the indoor temperature in a typical Danish detached household to vary by one degree around a given reference, a storage capacity of around 10 kWh can be achieved. Such capacity may seem quite modest, but with aggregation of several households a quite large capacity can be utilised. To be able to utilise the potential flexibility from detached buildings, estimates on future power consumption for heating in buildings and future available capacity are required, and hence adequate heat dynamic models of buildings are needed. This paper presents a non-linear model for prediction of the indoor air temperature in an intelligent office building, based on electric heating and weather input.

Adequate models for the heat dynamics of buildings also have applications in other fields. Among these are real-time control of indoor temperature given a varying cost of electricity, e.g. using price signals. Here, heat dynamic models of buildings can be utilised to

*Corresponding author e-mail:

guarantee that the indoor comfort of the residents of the building is not compromised in economic optimisation of electricity consumption. Furthermore, another application is estimation of specific building characteristics like the UA-value of walls and windows and heat capacities. These estimates can be used to form a strategy for how a building can be renovated with respect to energy savings.

The model proposed in this paper is for a specific building called PowerFlexHouse located at the DTU Risø Campus in Denmark. However, the model and estimation technique can be applied to similar types of buildings. So far, the model has been used in several smart grid applications, where flexible demand from PowerFlexHouse is provided within a small power system, see for examples [1] and [2]. Another application of the heat dynamic model is prediction of power consumption from electrical heating, given a weather forecast and an indoor temperature reference.

Following the pioneering work by [3] and [4] on the use of data for modelling the heat dynamics of buildings, several studies have been carried out using linear stochastic differential equations, see for example [5] and [6]. Likewise, several linear models have been proposed for the heat dynamics of PowerFlexHouse, see [7], [8] and [9]. However, none of these studies have included the non-linear effects that the wind has on the convection from the house envelope and on the natural ventilation of the building. Thus, this paper focusses on modelling the heat loss due to natural ventilation as being non-linearly dependent on the wind speed. Likewise, the convection from the house envelope is studied to see if the convection from the surface is non-linear.

To these authors knowledge, no previous work has been carried out in using non-linear stochastic differential equations for modelling the air infiltration in buildings. However, it should be noted that a similar approach has been used to estimate the non-linear heat exchange from photovoltaic modules in [10] and [11].

The outline of this paper is as follows; Section 2 gives an introduction to non-linear stochastic differential equations and parameter estimation. This section also describes PowerFlexHouse, which has formed the basis for data gathering and the building for which the parameter estimation is carried out. Next, a generic model is derived using prior physical knowledge about heat transfer. Section 3 presents the results from the parameter estimation and the model is verified using residual analysis of the model's one step predictions. Finally, in Section 4 the results are discussed together with possible model extensions and applications.

2. Methodology

In this section, an outline is given on how a grey-box approach can be used to formulate a non-linear model for the heat dynamics of an office building. The specific building of interest is an intelligent office building, called PowerFlexHouse, which is located on the DTU Risø campus in Roskilde, Denmark. The method uses non-linear stochastic differential equations to model the dynamics of an observable indoor temperature state variable as well as the non-observable temperature state variables of the electrical space heaters and building envelope. The model is formulated as a lumped model, thus assuming a homogeneously distributed temperature in each of the modelled media. By using a grey-box approach, prior physical knowledge is first used to formulate a set of differential equations. Then statistics on the collected data are used to estimate model parameters, thus combining white-box and black-box modelling. An advantage of this approach is that the physical parameters, i.e. heat capacity and UA-values, are directly given after parameter estimation. This means that the results can be directly compared with results found for similar buildings as well as different types of buildings.

2.1. Model type and parameter estimation

Given a time series of N temperature observations,

$$\mathcal{T}_N = [\boldsymbol{T}_N, \boldsymbol{T}_{N-1}, \boldsymbol{T}_{N-2}, ..., \boldsymbol{T}_0] \tag{1}$$

a mathematical model of the heat dynamics of PowerFlexHouse should be formulated such that the model describes the dynamics as represented by the time series (1). The heat dynamic model will be formulated using non-linear stochastic differential equations. The reason for using stochastic differential equations is to compensate for minor influences not encompassed by the model or unrecognised input, e.g. precipitation or noisy input to the system. Thus, a stochastic process, which accounts for the variations not fully described by a deterministic model, is added to a deterministic model yielding the following set of stochastic differential equations,

$$d\boldsymbol{T}_t = \boldsymbol{f}(\boldsymbol{T}_t, \boldsymbol{u}_t, t, \boldsymbol{\theta}), dt + \boldsymbol{\sigma}(\boldsymbol{u}_t, t, \boldsymbol{\theta}) d\boldsymbol{\omega}_t \tag{2}$$

Anders Thavlov and Henrik Madsen

where $\boldsymbol{f}(\cdot)$ is a non-linear function called the drift term, $\boldsymbol{T}_t$ is a vector containing the modelled temperature states of the building at time t, $\boldsymbol{u}_t$ is a vector containing input to the system and θ is a vector containing the unknown parameters. In the following, the parameters in θ are assumed to be time-invariant and ω_t is assumed to be a standard noise process with independent Gaussian distributed increments, more specifically a Wiener process. $\sigma(\boldsymbol{u}_t, t, \theta)$ is the diffusion term of the process. For an elaborated introduction to stochastic differential equations we refer to [12].

Since only some of the states in (1) are observable, and the sampling is conducted in discrete time, a measurement equation is introduced

$$\boldsymbol{T}_{m,k} = \boldsymbol{h}(\boldsymbol{T}_t, \boldsymbol{u}_t, t, \boldsymbol{\theta}) + \boldsymbol{e}_k \tag{3}$$

where $\boldsymbol{T}_{m,k}$ is the k'th measured output, $\boldsymbol{h}(\cdot)$ is a non-linear function linking the modelled states in (2) with the measured output and $\boldsymbol{e}_k$ is the measurement error. In the following it is assumed that the indoor air temperature state is directly measured, thus $\boldsymbol{h}(\cdot)$ is a linear function picking out the measured temperature states. Hence, (3) simplifies to

$$\boldsymbol{T}_{m,k} = \mathbf{C}\boldsymbol{T}_t + \boldsymbol{e}_k \tag{4}$$

were **C** is a matrix picking out the measured temperature states.

The maximum likelihood estimator has been used as an estimator for θ, which provides the most likely parameter set, $\hat{\theta}$, describing the process observed in $\boldsymbol{T}_{m,k}$ in (3), see [13]. That is, we find parameter estimates such that the likelihood function or the joint probability distribution function is maximised. For a given time series (1) the joint likelihood function is given by

$$\begin{aligned} L(\mathcal{T}_N;\boldsymbol{\theta}) &= p(\mathcal{T}_N \mid \boldsymbol{\theta}) \\ &= p(\boldsymbol{T}_N \mid \mathcal{T}_{N-1}, \boldsymbol{\theta}) p(\mathcal{T}_{N-1} \mid \boldsymbol{\theta}) \\ &= \left(\prod_{k=1}^{N} p(\boldsymbol{T}_k \mid \mathcal{T}_{k-1}, \boldsymbol{\theta}) \right) p(\boldsymbol{T}_0 \mid \boldsymbol{\theta}) \end{aligned} \tag{5}$$

where the rule $P(A \cap B) = P(A|B)\,P(B)$ has been applied N-times to form the joint likelihood function as the product of conditional densities. On the assumption that both ω_t in (2) and $\boldsymbol{e}_k$ in (3) are normally distributed and mutually independent, the conditional density function for a linear model is also normally distributed and thus fully characterised by its mean and variance. In the non-linear case it will be assumed that the conditional densities in (5) are approximately Gaussian and this assumption can be validated. Introducing the innovation or one step prediction error,

$$\boldsymbol{\epsilon}_k = \boldsymbol{T}_k - \hat{\boldsymbol{T}}_{k|k-1} \tag{6}$$

where $\hat{\boldsymbol{T}}_{k|k-1}$ is the estimated mean given by

$$\hat{\boldsymbol{T}}_{k|k-1} = \mathrm{E}\{\boldsymbol{T}_k \mid \mathcal{T}_{k-1}, \boldsymbol{\theta}\} \tag{7}$$

and with the covariance

$$\hat{\boldsymbol{R}}_{k|k-1} = \mathrm{V}\{\boldsymbol{T}_k \mid \mathcal{T}_{k-1}, \boldsymbol{\theta}\} \tag{8}$$

the likelihood function in (5) can be formulated as

$$L(\mathcal{T}_N;\boldsymbol{\theta}) = \left(\prod_{k=1}^{N} \frac{\exp\left(-\frac{1}{2}\boldsymbol{\epsilon}_k^T \hat{\boldsymbol{R}}_{k|k-1}^{-1} \boldsymbol{\epsilon}_k\right)}{\sqrt{(2\pi)^n \det\left(\hat{\boldsymbol{R}}_{k|k-1}\right)}} \right) p(\boldsymbol{T}_0 \mid \boldsymbol{\theta}) \tag{9}$$

where $n = \dim(\boldsymbol{T}_m)$. The innovation and covariance in (6) and (8), respectively, can be calculated using an Extended Kalman filter, see e.g. [14] or [15].

2.2. Continuous time stochastic modelling

A procedure for optimisation of (9) with respect to θ has been implemented in the software tool CTSM - *Continuous Time Stochastic Modelling*. CTSM is a computer program for continuous time stochastic modelling, which uses a quasi-Newton method to find the maximum likelihood estimate, $\hat{\theta}$. The software is distributed freely and can be downloaded from the CTSM webpage, [16]. For further information about parameter estimation using CTSM, see [16] and [17].

2.3. Model Validation

It follows from (5) that, for an adequate model, the conditional densities are independent and consequently the one step ahead residuals can be used for model validation. The independence of the residuals can be tested both in the time domain using the auto-correlation function and in the frequency domain using the cumulated periodogram, see [18]. Residual analysis on the proposed models is conducted in Section 3.

2.4. PowerFlexHouse and SYSLAB

PowerFlexHouse is an office building located at the DTU Risø Campus near Roskilde in Denmark. The building has been equipped with various types of sensors and actuators, which allows it to be controlled as a flexible load in the small power system of SYSLAB. SYSLAB is a laboratory and an experimental platform for research in smart-grids and a part of PowerLabDK[1]. Depending on the state of the power system, PowerFlexHouse can postpone or accelerate its energy needs, thus offering power system balance services within SYSLAB.

PowerFlexHouse comprises eight rooms, including a large meeting room in the centre of the building. Each room is individually monitored and controlled and is equipped with a number of different types of sensors and actuators, including

- Temperature sensors
- Motion sensors
- Window- and door sensors
- Actuators for electrical heaters
- Actuators for lighting
- Actuators for opening windows and doors

The sensors and actuators allow the building to be monitored and controlled seamlessly from a house controller. Also, the actuators for the windows, doors and lighting can be used for emulations of residents being present. A picture of PowerFlexHouse and its layout can be seen in Figure 1 (a) and Figure 1 (b), respectively.

In addition to the indoor sensor input, the house controller receives data from a weather mast next to PowerFlexHouse. The weather mast collects data on outdoor temperature, horizontal solar irradiance, as well as wind speed and direction. The collected data is stored in a database together with the indoor sensor states.

A house controller has been developed to handle all communication with sensors and actuators. The controller also implements a high level heat controller for the whole building. Additionally, the house controller is responsible for data acquisition and for storing the house state, i.e. all sensor states, in a database at a sampling rate of 10 seconds. The house controller enables different control strategies to be easily implemented and tested, and currently a number of control strategies have been implemented; from a simple thermostatic controller to a high level model predictive controller that optimises heating over the following 24 hours with respect to a given price signal for the cost of electricity.

The 120 m^2 building is a pavilion-type building, standing freely on concrete slabs, leaving a gap between the ground and the base of the building of approximately 40 cm. The gap has been enclosed with planks. The house is placed such that the south-facing facade, which has a large window area, is turned 17° to the west from direct south. This means that the indoor temperature is highly dependant on the solar irradiance, especially around noon. The width of the outer walls is 170 mm and consists of 100 mm insulation, sandwiched between a plywood facade and interior plasterboards. The inner walls are 70 mm thick and mounted with plasterboards on both sides, sandwiching 50 mm of insulation in-between. The heating for the building comes from ten electrical space heaters, ranging from 750 W to 1,250 W, with a total installed heating power of 9,750 W. For the data generated in this paper, a number of heaters were selected to generate a given total output. The selected heaters were controlled synchronously using a PRBS controller implementing a pre-defined Pseudo-Random Binary Sequence (PRBS). Using PRBS-signals

(a)

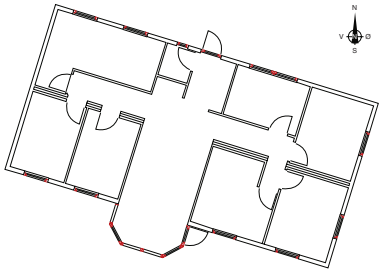

(b)

Figure 1: PowerFlexHouse south facing facade (a) and building layout (b).

[1] http://www.powerlab.dk/

as input to the system ensures optimal conditions for system identification. For a further description about PRBS signals, see [19].

2.5. PowerFlexHouse Model

The heat dynamic model for PowerFlexHouse presented in this paper has three temperature states for the building. These states reflect the temperature of the interior thermal mass, T_i, the average temperature of the ten space heaters, T_h, and the temperature of the building envelope, T_e. Prior physical knowledge is used to formulate a mathematical model of the thermal flow between these three states and the ambient environment. Sub-models for conduction, convection and ventilation are used to compile a total model.

The heaters are hanging freely in the indoor air, thus exchanging heat with the interior media only. The heat transfer is caused by convection from the heater surface. From this the differential equation describing the temperature of the heaters, can be formulated as

$$dT_h = \left(\frac{T_i - T_h}{R_{ih} \cdot C_h} + \frac{\Phi_h}{C_h} \right) dt + \sigma_h \cdot d\omega_1 \tag{10}$$

where C_h is the thermal heat capacity of the heaters, Φ_h is the electrical input and R_{ih} is the convective resistance to transfer heat between the interior thermal mass and the heater.

Likewise, the differential equation describing the temperature of the house envelope is given by,

$$dT_e = \left(\frac{T_a - T_e}{R_{ea} \cdot C_e} + \frac{T_i - T_e}{R_{ie} \cdot C_e} + \frac{A_e \cdot \Phi_s}{C_e} \right) dt + \sigma_e \cdot d\omega_2 \tag{11}$$

where C_e is the thermal heat capacity of the building envelope, R_{ea} and R_{ie} are the thermal resistances related to the combined conductive and convective heat transfer from the envelope to the ambient environment and interior, respectively, T_a is the ambient temperature and A_e is the effective area of the house envelope that is absorbing solar irradiance Φ_s, which is measured on the horizontal plane.

Finally the differential equation for the interior mass is,

$$dT_i = \left(\frac{T_h - T_i}{R_{ih} \cdot C_i} + \frac{T_e - T_i}{R_{ie} \cdot C_i} + \frac{T_a - T_i}{R_{ia} \cdot C_i} + \frac{A_w \cdot \Phi_s}{C_i} \right) dt + \sigma_i \cdot d\omega_3 \tag{12}$$

where C_i is the thermal heat capacity of interior mass, i.e. air, inner walls, furniture, etc. R_{ia} is the resistance to transfer heat directly to the ambient environment, primarily due to natural ventilation of the building, and $A_w \cdot \Phi_s$ is the solar irradiance through the windows, where A_w is the effective size of the windows and Φ_s is the horizontal solar irradiance.

Due to the wind influence on the outside of the building envelope, both the convection from the building envelope and natural ventilation changes from free to forced, hence the resistance to transfer heat can not be assumed to be linear as formulated in (11) and (12), but should instead be a non-linear function of the wind speed. Therefore, in the following the resistances are assumed to take the form,

$$\begin{aligned} R_{ia}\left(W_{spd}\right) &= \frac{1}{k_1 \cdot W_{spd}^{k_2}} \\ R_{ea}\left(W_{spd}\right) &= \frac{1}{k_3 \cdot W_{spd}^{k_4}} \end{aligned} \tag{13}$$

where W_{spd} is the wind speed and $k_x \geq 0$ are unknown parameters to be estimated. For k_2, $k_4 = 0$, we find the linear relation as formulated in (11) and (12). For k_2, $k_4 \neq 0$, both equations in (13) assume the heat transfer to be purely convective and hence conductive heat transfer is neglected. This assumption only holds if the thermal mass of the building envelope is located in the outer surface of the envelope and not inside the walls; however, the approximation is used to investigate whether convective heat transfer is predominant over conduction. Alternatively, a constant term could be added to (13), which would account for the conductive heat transfer.

In Figure 2 the total formulated model, as described by (10) to (12), can be seen as an equivalent RC-network, where electric resistors equal resistance to transfer heat, electric capacitance equals heat capacity, flow of electricity equals flow of heat and voltage differences equal temperature differences. The non-linear resistors have been marked with arrows, indicating varying resistance, i.e. varying with wind speed.

Based on physical knowledge, it can be argued that heat is transferred through the building envelope, but whether the natural ventilation is significant and should be included in the model is a bit more unclear. Therefore different combinations of linear, non-linear and no ventilation, i.e. $R_{ia} = \infty$, have been studied. These results are presented in Section 3.

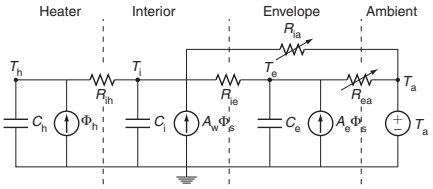

Figure 2: RC-circuit equivalent diagram for the PowerFlexHouse model

Assuming that the indoor measured temperature is a direct representative for the interior state temperature, the model takes the form,

$$
\begin{aligned}
dT_i &= \left(\frac{T_h - T_i}{R_{ih}\cdot C_i} + \frac{T_e - T_i}{R_{ie}\cdot C_i} + \frac{T_a - T_i}{R_{ia}(W_{spd})\cdot C_i} + \frac{A_w\cdot\Phi_s}{C_i}\right) dt + \sigma_1\cdot d\omega_1 \\
dT_h &= \left(\frac{T_i - T_h}{R_{ih}\cdot C_h} + \frac{\Phi_h}{C_h}\right) dt + \sigma_2\cdot d\omega_2 \\
dT_e &= \left(\frac{T_a - T_e}{R_{ea}(W_{spd})\cdot C_e} + \frac{T_i - T_e}{R_{ie}\cdot C_e} + \frac{A_e\cdot\Phi_s}{C_e}\right) dt + \sigma_3\cdot d\omega_3 \\
T_{m,k} &= T_i(k) + e_k
\end{aligned}
\tag{14}
$$

where $R_{ia}(W_{spd})$ and $R_{ea}(W_{spd})$ can take the form as either linear or non-linear as defined in (13). Also, $R_{ia}(W_{spd}) \to \infty$ for $W_{spd} \to 0$, implying no heat transfer due to natural ventilation.

2.6. Data

Four experiments were conducted in PowerFlexHouse in the period from February to March 2008. The purpose of the experiments was to collect data for model parameter estimations. The only input to the system in (14) that can be directly manipulated is the heat input from the electrical space heaters. The heaters were controlled synchronously, i.e. all heaters were on or off in the same time instance, using a binary signal generated as a Pseudo Random Binary Sequence. A different PRBS signal was generated for each experiment and each signal was designed such that the heat input from the electrical space heaters would excite the temperature states in the time domain around where time constants were expected to be found. The number of heaters being controlled was chosen such that the temperature in any room would not exceed 30 ^{0}C at any time during the experiment. This was done to prevent the house controller from being overridden by the internal space heater thermostat which only allows room temperatures up to 30 ^{0}C, after which the heater switches off. The time series of the observed interior temperature $T_{m,k}$, ambient temperature T_a, heat input Φ_h and solar irradiance Φ_s are plotted in Figure 3.

The dynamics of the interior temperature state can be seen to vary with the external input. Especially the PRBS-controlled heat input can be seen in the variation of the interior temperature. Also, the effects from the daily variation in ambient temperature and solar irradiance can be clearly seen in the figures.

Wind data was also collected during the four experiments. The wind speed and direction are depicted in Figure 4, where the wind measurements are plotted.

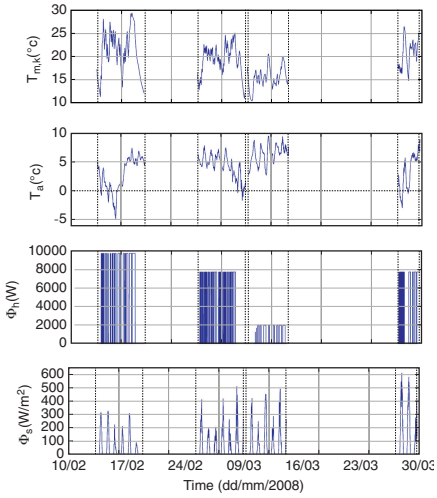

Figure 3: Input to the dynamic system formulated in (2) for parameter estimation.

Anders Thavlov and Henrik Madsen

Each dot in the figure represents the direction from which the wind is blowing. The plot shows that the wind in the period of the experiments came mainly from the west, with measured wind speeds of up to 25 m/s. To remove high order frequency variations, the wind speed and direction have been filtered with a low-pass filter.

The model of the interior temperature, i.e. (12), only takes one indoor temperature, i.e. T_i. As a representative temperature, the average indoor air temperature of the eight rooms has been used. Instead of weighing the temperatures equally, other weights could have been applied to weight larger rooms higher. For example, this could have been done using principal component analysis; however, no significant improvement in log-likelihood has been observed using different weights.

3. Results

This section presents the model parameter estimates for four different non-linear models and compares the results with previously proposed linear models from [8] and [7]. The maximum of the log-likelihood for the non-linear models is compared to the log-likelihood found for similar linear models Also, the best performing model is verified in both the time domain and frequency domain.

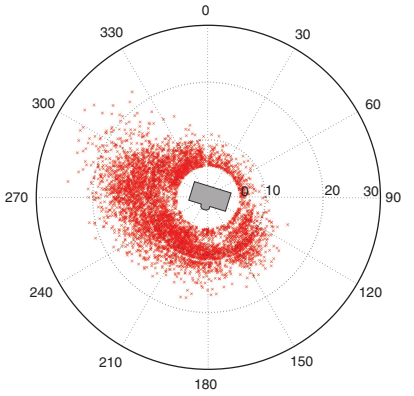

Figure 4: Wind rose data collected during the experiments sampled at intervals of 5 minutes. The wind direction relative to the house can be deducted from the outline of PowerFlexHouse in the middle of the plot.

3.1. Parameter Estimates

Six different combinations of non-linear and linear heat transfer, with and without air infiltration, were examined and model parameters estimated for each model. The parameter estimates, together with their respective standard deviations, are presented in Table 1. In the table, the models have been named Model A to F, where Model A is the linear reference model as presented in [7], Model B is a linear reference model with natural ventilation presented in [8] and Model C to F are non-linear variations of Model A and B.

The table shows that the parameter estimates are much alike for the six models, except R_{ia} for Model B and E. As seen from the table, the two estimates are both associated with a relative high standard deviation, signifying that they could potentially be the same. Likewise, the relative standard deviations on R_{ih} and C_h are quite high, thus implying that the modelling uncertainty on T_h is high and that the model therefore can not be used to estimate the temperature of the space heaters. However, together these two estimates simply imply a fast transfer of heat from the heater to the indoor air, i.e. a fast discharge of the capacitor.

The highest log-likelihood is achieved by Model C and F, were the natural ventilation is non-linear and the convection from the envelope is modelled as linear and non-linear, respectively.

Since the linear models are sub-models of the non-linear models, a statistical test can be used to verify whether the increase in log-likelihood is significant or not. For this, Wilk's likelihood ratio test can be used, see [20]. The test is given by,

$$\lambda = -2(\mathrm{LL}_0 - \mathrm{LL}_1) \tag{15}$$

where LL_0 and LL_1 is the log-likelihood for the sub-model and sufficient model, respectively. As the number of observations increases, λ converges to a χ^2-distribution with k-degrees of freedom, where k is the difference in number of model parameters for the two models. From this, the p-values in Table 1 have been found. The log-likelihood values show that all the non-linear models are significantly better than the linear models, and that Model C and F have the lowest p-values, when compared to Model A.

For Model C and F, the model estimates for k_1 and k_2 are almost the same. Plotting the resistance to natural ventilation R_{ia} using (13) reveals that the resistance is

Table 1: Model parameter estimates and their respective standard deviation noted in brackets.

Name	**Model A**	**Model B**	**Model C**	**Model D**	**Model E**	**Model F**
R_{ia}	∞	Linear	Non-linear	∞	Linear	Non-linear
R_{ea}	Linear	Linear	Linear	Non-linear	Non-linear	Non-linear
Coefficient			**Estimates**			
A_e, [m^2]	23.15	22.64	20.93	21.37	21.02	21.09
	(3.91)	(3.60)	(3.00)	(2.86)	(2.90)	(3.01)
A_w, [m^2]	9.66	9.55	9.52	9.23	9.15	9.48
	(0.70)	(0.80)	(0.67)	(0.61)	(0.68)	(0.70)
C_e, [kWh/°C]	8.12	7.81	6.64	7.14	6.93	6.69
	(1.03)	(1.18)	(0.79)	(0.74)	(0.81)	(0.79)
C_h, [kWh/°C]	0.000367	0.000367	0.000370	0.000372	0.000372	0.000371
	(0.000526)	(0.000569)	(0.000359)	(0.000534)	(0.001780)	(0.000574)
C_i, [kWh/°C]	2.48	2.48	2.46	2.45	2.45	2.46
	(0.06)	(0.06)	(0.06)	(0.06)	(0.06)	(0.06)
R_{ea}, [°C/kW]	2.24	2.48	2.91	–	–	–
	(0.16)	(0.67)	(0.33)	(–)	(–)	(–)
R_{ie}, [°C/kW]	0.83	0.85	0.87	0.81	0.82	0.87
	(0.04)	(0.06)	(0.05)	(0.04)	(0.05)	(0.05)
R_{ia}, [°C/kW]	–	40.33	–	–	51.35	–
	(–)	(100.99)	(–)	(–)	(63.03)	(–)
R_{ih}, [°C/kW]	898.27	898.35	898.42	898.15	898.37	897.45
	(1287.80)	(1389.20)	(875.97)	(1287.90)	(4289.10)	(1384.20)
$k_1(R_{ia})$	–	–	0.0141	–	–	0.0152
	(–)	(–)	(0.0113)	(–)	(–)	(0.0110)
$k_2(R_{ia})$	–	–	0.9032	–	–	0.9366
	(–)	(–)	(0.2880)	(–)	(–)	(0.3168)
$k_3(R_{ea})$	–	–	–	0.3353	0.3053	0.3343
	(–)	(–)	(–)	(0.0314)	(0.0488)	(0.0385)
$k_4(R_{ea})$	–	–	–	0.1857	0.1954	0.0391
	(–)	(–)	(–)	(0.0486)	(0.0575)	(0.0632)
Log-likelihood	9242.27	9242.32	9256.94	9247.23	9247.23	9257.09
Parameters	15	16	17	16	17	18
***p*-value**	**Model A**	**Model B**	**Model C**	**Model D**	**Model E**	**Model F**
Model A	–	0.751	4.25×10^{-7}	1.68×10^{-3}	6.96×10^{-3}	1.64×10^{-6}
Model B	–	–	6.39×10^{-8}	–	1.71×10^{-3}	3.85×10^{-7}
Model C	–	–	–	–	–	0.585

very dependent on the wind speed as seen in Figure 5, where also the obtained constant estimate from Model B is plotted. Likewise, a plot of the non-linear R_{ea} from Model F, together with the constant estimate from Model B are presented.

The plot shows that R_{ia} is much more dependent on the wind speed than R_{ea}, and that the non-linear estimates are close to their respectively constant estimates, as obtained in Model B, for wind speeds around 2–3 m/s, which is quite close to the average measured wind speed. Furthermore, R_{ia} increases rapidly when the wind speed goes towards zero. Hence, it can be concluded that for wind speeds below 5 m/s, the heat loss due to ventilation is quite small compared to conduction through the envelope. For wind speeds around 20 m/s, the resistance is approximately of the same size as the heat loss through the envelope, and as the wind speed increases the resistance drops and the air infiltration becomes the dominant factor in the heat loss of the building. This is consistent with the theory for natural ventilation. Furthermore, from the plot is seen that R_{ea} is nearly constant relative to R_{ia} which implies that the heat transfer through the envelope is approximately linear and hence behaves like conductive heat transfer. This further strengthens the argument for Model C being the most adequate model.

Anders Thavlov and Henrik Madsen

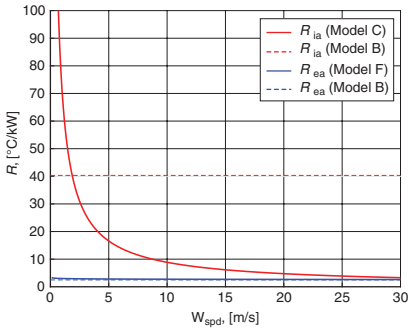

Figure 5: Comparison between the convective resistance through the building envelope, R_{ia}, and from the outside surface, R_{ea}, versus wind speed, W_{spd}.

3.2. Model Validation

The formulation of the model in Section 2 assumed that ω_t is independent for non-overlapping time intervals and that $\boldsymbol{e}_k$ is white noise. Hence, the residuals for the one step prediction in (6) should resemble white noise. Using tests in both the time domain and frequency domain, all the non-linear models have been validated. In Figure 6, the auto-correlation function is plotted for the one step predictions for Model C. The auto-correlation function shows some correlation at lags 1 and 4, which fall outside the 95% confidence interval; however, they are still quite small, hence indicating that the residuals do resemble a white noise process.

Also the spectrum for Model C is seen to be approximately equally distributed over all frequencies, which is also apparent from the cumulated periodogram, where the cumulated periodogram is seen to fall within the 95% confidence interval, except around 0.4, where the confidence interval is broken. The exact cause of this has not been identified, but could be caused by the time delay from the propagation of heat in the temperature sensor; hence, the temperature sensor should be modelled separately using an additional temperature state. The three plots in Figure 6 imply that the model can certainly be improved, but also that the residuals to a large extent do resemble a white noise process and that Model C thus gives an adequate description of the heat dynamics of PowerFlexHouse.

4. Discussion

The study presented in this paper has shown that non-linear stochastic differential equations can be used to describe the non-linear effects caused by forced ventilation or infiltration in a thermally light building. A parameter estimation technique for a non-linear state space model has been demonstrated for a specific building, based on data collected in the office building and from a weather mast on-site.

From the *p*-values in Table 1, it can be seen that the non-linear models are significantly better than any previous linear models of the heat dynamics of PowerFlexHouse as suggested in [7] and [8]. Also from the log-likelihood estimates it can be seen that Model C and F achieve the highest log-likelihood. However, with an equally high log-likelihood and with one additional parameter in Model F, it can be concluded that Model C, with 16 parameters, is sufficient to describe the heat dynamics of PowerFlexHouse. Also, the correlation matrix of the estimates for Model F has off-diagonal values close to one, which implies that the model is over-parameterized. This further supports that Model C is the best performing model. Additionally it is seen that with an increasing number of parameters in the model, the log-likelihood is seen to stagnate, which further confirms that the model becomes over-parameterized and that 16 parameters are sufficient to describe the heat dynamics.

Unfortunately, no building data is available for PowerFlex-House that could confirm whether the parameter estimates are correct. However, the estimates can be compared to expected building data given by building regulations from the time of construction, to see whether they comply with the requirements. For example, the required *u*-values at time of construction were $u_{window} = 2.90$ W/(°Cm^2) and $u_{wall} = 0.40$ W/(°Cm^2) for windows and walls respectively. By approximating the surface of PowerFlexHouse with a rectangular box with dimension 15 m × 8 m × 3 m, the total surface of the building is A = 378 m^2 of which approximately 27 m^2 are windows. From this, the weighted *u*-value of the whole building can be calculated as:

$$u = \frac{(378-27)\text{m}^2 \cdot 0.40\text{W}/\left(^\circ\text{C m}^2\right) + 27\text{m}^2 \cdot 2.90\text{W}/\left(^\circ\text{C m}^2\right)}{378\text{m}^2}$$
$$= 0.58\text{W}/\left(^\circ\text{C m}^2\right)$$

Furthermore, by assuming a wind speed of 3 m/s giving R_{ia} = 23.6°C/kW and a steady state in the heat

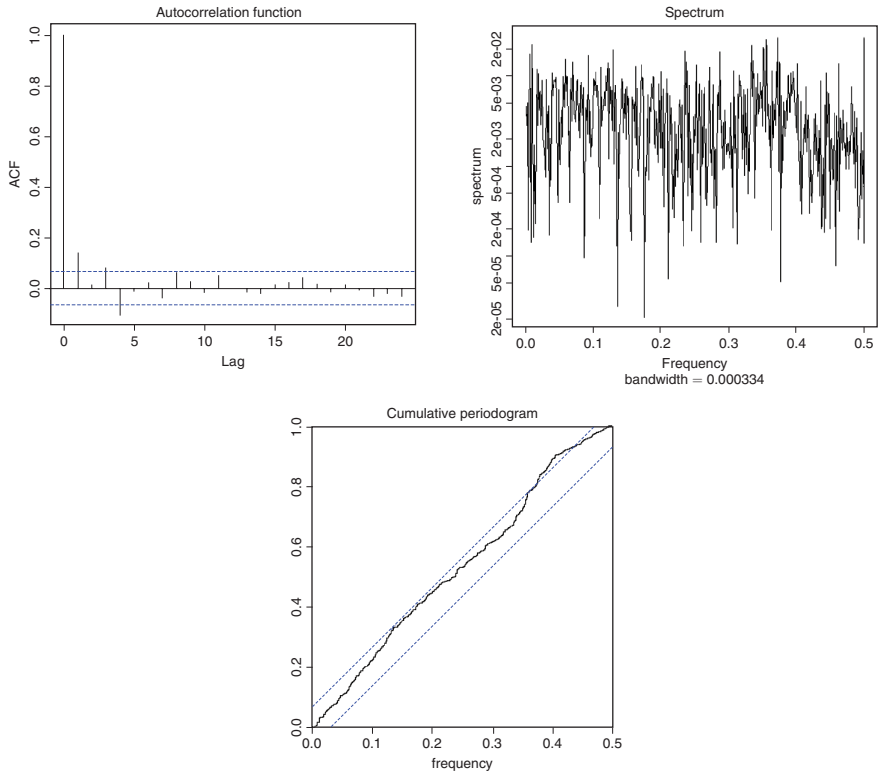

Figure 6: Auto-correlation, spectrum and cumulated periodogram for the one step prediction for Model C.

transfer from the building, the total thermal resistance from the building can be calculated as,

$$R = \frac{1}{1/R_{ia} + 1/(R_{ie} + R_{ea})} = \frac{1}{1/23.6 + 1/(2.91 + 0.87)} = 3.26\,^{\circ}\mathrm{C/kW}$$

which is equivalent to a u-value around 0.8W/(°Cm^2) $\left(u = \frac{1}{R \cdot A}\right)$. Considering the wear of the building envelope, including draughty air registers, the estimated value is not far from what was required by the building regulations at the time of construction. Moreover, the total heat capacity of the building is estimated to around 9 kWh/°C, which is equivalent to 75 Wh/(°C m$^{2)}$. This value falls in the range of what is characterised as thermally light buildings, which is expected considering the light construction materials that the building is composed of. Finally, the window area of PowerFlexHouse is approximately 27 m^2. Assuming that the effective window area is approximately 60% of the real window area, as were used in [5], the estimates of A_w are also close to what would be expected.

Anders Thavlov and Henrik Madsen

4.1. Model Extensions

During this study it was also investigated whether the model could be improved by projecting the wind vector onto the orthogonal of each surface of the building. This, however, would require an additional six parameters in the model, which makes the model highly over-parameterized and reasonable parameter estimation impossible. As an alternative approach the model parameters were estimated four times using the projected wind speed as the basis for parameter estimation, instead of the general wind speed. This revealed that a slightly higher log-likelihood could be achieved when using the wind speed projected on the south-ward direction, indicating a higher sensitivity to south-ward wind compared to the other directions. It can be argued that the result is reasonable, since PowerFlexHouse is sheltered from the north and east by other buildings and to the west by trees and bushes. However, another argument against the model extension could be that the model estimates come from a data-set where the wind has mainly been blowing from the west. The decision whether the first or second argument holds is left for another study.

4.2. Applications

As stated in Section 1, the model is used in a heat controller to ensure indoor comfort and to predict power consumption. However, the model technique presented in this paper can be applied in many other areas; for example for estimating specific building parameters which are directly given by the estimation technique, or for estimation of a given building's annual energy need for heating. Furthermore, the model can also be used to estimate heat loss due to air infiltration though the envelope. Assuming steady state in the envelope, i.e. no net flow into the envelope, and a temperature difference at 10°C over the envelope, the heat loss distribution between the infiltration loss and loss through the envelope can be calculated. This is presented in Table 2, where the heat loss due to natural ventilation increases rapidly for wind speeds over 10 m/s and for a wind speed above 25 m/s, 50% of the total heat loss is due to ventilation.

Table 2: Percent-wise heat loss due to natural ventilation and through building envelope.

Wind speed, [m/s]	10	20	30
R_{ia}, [°C/kW]	8.86	4.74	3.29
$R_{envelope}$, [°C/kW]	3.78	3.78	3.78
Ventilation heat loss, [%]	29.90	44.37	53.50
Envelope heat loss, [%]	70.10	55.63	46.50

The results presented in Table 2 show that natural ventilation should be minimised, e.g. by closing air vents or registers when the wind speed increases above 10–15 m/s. At present, the air registers in PowerFlexHouse are manually controlled, but installing actuators to close the registers when the wind speed reaches a given threshold would greatly reduce heat loss due to air infiltration. However, this type of control would change the dynamics of the heat transfer through the house envelope and another functional description of R_{ia} should most likely be used. An investigation of the heat transfer as a function of the state of the air registers is left as a subsequent study.

Acknowledgement

The work was partly funded by DSF (Det Strategiske Forskn-ingsråd) through the ENSYMORA (DSF No. 10-093904) project, which is hereby acknowledged.

References

[1] Y. Zong, D. Kullmann, A. Thavlov, O. Gehrke, H. W. Bindner, Application of model predictive control for active load management in a distributed power system with high wind penetration, Transactions on Smart Grid, IEEE 3 (2012) 1055–1062.

[2] A. Thavlov, H. Bindner, Utilization of flexible demand in a virtual power plant set-up, IEEE Transactions on Smart Grid 6 (2) (2015) 640–647. doi:10.1109/TSG.2014.2363498.

[3] R. Sonderegger, Diagnostic tests to determine the thermal response of a house, ASHRAE Transactions 91.

[4] A. Rabl, Parameter estimation in buildings; methods for dynamic analysis of measured energy use, Journal of Solar Energy Engineering 110 (1988) 52–66.

[5] H. Madsen, J. Holst, Estimation of continuous-time models for the heat dynamics of a building, Energy and Buildings 22 (1995) 67–79.

[6] K. K. Andersen, H. Madsen, L. H. Hansen, Modelling the heat dynamics of a building using stochastic differential equations, Energy and Buildings 31 (2000) 13-24.

[7] P. Bacher, H. Madsen, Identifying suitable models for the heat dynamics of buildings, Energy and Buildings 43 (2011) 1511–1522.

[8] A. Thavlov, Dynamic optimization of power consumption, Master's thesis, DTU IMM, Technical University of Denmark (2008).

[9] A. Thavlov, H. W. Bindner, A heat dynamic model for intelligent heating of buildings, International Journal of Green Energy 12 (3) (2015) 240–247. doi:10.1080/15435075.2014.891516.

[10] M. Jiménez, H. Madsen, J. Bloem, B. Dammann, Estimation of non-linear continuous time models for the heat exchange dynamics of building integrated photovoltaic modules, Energy and Buildings 40 (2008) 157–167.

[11] N. Friling, Stochastic modelling of building integrated photovoltaic modules, Master's thesis, Informatics and Mathematical Modelling, Technical University of Denmark, DTU, Richard Petersens Plads, Building 321, DK-2800 Kgs. Lyngby (2006).

[12] B. Øksendal, Stochastic Differential Equations, 4th Edition, Springer, Berlin, 1995.

[13] N. R. Kristensen, H. Madsen, S. B. Jørgensen, Parameter estimation in stochastic grey-box models, Automatica 40 (2) (2004) 225–237. doi:10.1016/j.automatica.2003.10.001.

[14] A. H. Jazwinski, Stochastic Processes and Filtering Theory, Academic Press, New York, 1970.

[15] P. S. Maybeck, Stochastic Models, Estimation and Control; Vol 1,2,3, Academic Press, New York, 1982.

[16] Continuous Time Stochastic Modelling webpage, *http://www.ctsm.info.*

[17] N. R. Kristensen, H. Madsen, CTSM 2.3 - Mathematics Guide. URL *http://www2.imm.dtu.dk/ctsm/MathGuide.pdf*

[18] H. Madsen, Time Series Analysis, Chapman & Hall, 2008.

[19] K. R. Godfrey, Correlation methods, Automatica 16 (1980) 527-534.

[20] H. Madsen, P. Thyregod, An Introduction to General and Generalized Linear Models, Chapman & Hall, 2011.

PAPER C

An Aggregation Model for Households Connected in the Low-voltage Grid using a VPP Interface

---

Presented at the *4th European Innovative Smart Grid Technologies Conference* (IEEE ISGT Europe 2013), Copenhagen, Denmark, 2013.

An Aggregation Model for Households Connected in the Low-voltage Grid using a VPP Interface

Anders Thavlov and Henrik W. Bindner
Department of Electrical Engineering
Technical University of Denmark
Frederiksborgvej 399, Bldg. 776, 4000 Roskilde, Denmark

***Abstract*—To secure the stability in power systems with a high penetration from renewable energy sources, the demand side has to become more flexible than today. If the flexibility from the numerous units connected in the low-voltage grid is to be utilised, aggregation methods have to be developed. This paper presents an aggregation model using an interface defined by an operating virtual power plant. Simulations of the aggregator show that a large share of the power consumption, due to heating of households, can be postponed or accelerated in time to the benefit of the stability of the power system. Additionally the simulations show that peak demand due to heating can be significantly decreased.**

I. BACKGROUND

A global concern about CO_2 emissions is driving a shift from fossil based power generation towards more renewable power generation. In the last decade alone, the share of global electricity production generated by renewable sources, not including hydroelectric sources, has more than doubled and this development is expected to continue. As the penetration from renewable energy sources increases in national power systems, the output of the generation side becomes increasingly more intermittent and unpredictable, with less capability to control, thus threatening the stability of the power system. Additionally, subsidy schemes in many countries encourage small consumers to install photovoltaics, which change the role of the consumer to, in short time intervals, become producers as well, i.e. prosumers. This introduction of distributed power generation in the low-voltage grid may cause the power flow - from time-to-time - to be in the opposite direction to what the system was originally designed for, further threatening the stability of the distribution grid. Likewise, is the introduction of electrical vehicles expected to generate a substantial increase in peak demand during the late afternoon and in the evening, which may cause congestion problems in the distribution grid. In the future power system these potential problems call for better coordination between the numerous units connected in the low-voltage grid, and the role of consumers has to be reconsidered as a more active part of the power system, where demand becomes more flexible than today. Typical units in the low-voltage grid comprise of residential buildings which can offer flexible demand by use of the thermal mass in cold storages and in the building envelope itself. In this way the thermal mass of buildings can be used as unidirectional energy storage, and thus a buffer for intermittent renewable energy. In practice, this can be done by allowing the indoor temperature to vary within a given temperature band, which can be specified by the residents of the building; the wider temperature band, the bigger flexibility.

Not only is the activation of demand response in the power system fundamental, but if the capacity of the numerous small units connected in the low-voltage grid is to be utilised, also the coordination between them is of high importance. One approach for coordination among units is to use *virtual power plants* (VPPs, [1]) to group units either geographically or by similarity, and control them as a single aggregated unit. For this we need aggregators, which reduce the complexity of the problem seen from the top level controller, and distributes the computational load in optimising the dispatch problem. The problem with aggregation is how the flexibility of numerous of different types of units under the aggregator is aggregated and exposed upwards in the aggregation hierarchy. This requires a generalised model of units connected to the aggregator, such that the description of a units flexibility is adequate but without loss of generality.

This paper presents an aggregation model for small units connected in the low-voltage grid using an existing interface from a virtual power plant operating in Denmark. The interface relies on a direct control approach, giving the VPP operator direct control over the aggregator or the connected unit, which sends a feedback signals about its current state back to the controller. A similar approach of direct control is seen in The Cell Controller Pilot Project, [7], run by the Danish TSO, where local wind turbines and combined heating and power plants are aggregated to form a VPP. Another approach is to create an incentive for end users to change their consumption during the day using a price signal. Simulations of indirect control can be seen in [2] and [3], and in [4] the thermal storage of an office building has been used for flexible demand using a price signal. For a large-scale demonstration project using price signals, see [5] or [6].

In this paper a model of an aggregator for direct control of heat consumption in households is proposed. It should be emphasised that only electrical heating, i.e. from electrical space heaters or heat pumps, is consider as a source of flexible power consumption in this paper, despite other sources could be included, e.g. refrigerators, water heaters and washing machines.

This paper is organised as follows; Section II initially introduces the VPP from the Power Hub project and specifies the interface that forms the basis for communication between connected units and Power Hub. Then the aggregator is introduced and a model for aggregation is proposed. In the following section, simulations of the aggregator flexibility are presented. Finally, in the last section, the performance of the simulated aggregator is discussed.

II. Methodology

The aggregation model presented in this paper implements an interface defined by an operational VPP, running in Denmark. The interface defines what data to be communicated to and from the controlled unit, as well as commands that can be send to the unit, e.g. start and stop commands. This section initially gives a short description of the running VPP, called Power Hub, and then a generalised model of connected units is introduced. This model is adopted to describe the heat load in a household. Lastly, the aggregator is introduced, which optimises the consumed power by its connected units using a set point received from Power Hub, or a higher level aggregator.

In the following only control of electrical heating is considered as a source for residential demand response, it is not considered how other types of consumption interfere with the heating and thus simply seen as non-controllable loads. To ease comprehension, the aggregator can be seen as having influence only on the fuse block, to which the electrical heating is coupled. This simplification serves to demonstrate that power consumption, due to heating, can be postponed or accelerated in time, thus delivering system services in the low-voltage grid.

A. Power Hub

Power Hub (PH) is an implementation of a VPP developed by the Danish energy company DONG Energy as part of the Twenties project, supported by the European Union. One of the main purposes for the development of PH has been to create a tool that can coordinate demands response from large industrial companies and use it to balance power in power systems with a high penetration of renewable energy. A large scale demonstration of the VPP capabilities of Power Hub was carried out in November 2012 at the Faroe Islands, where a 10% power failure of the national power supply, was simulated and three large scale companies were coordinated to reduce their consumption, such that a total black out of the islands was be prevented. Currently, PH is being trialled on commercial terms in Denmark and has several loads and generation units under its control; this includes hydro power plants, a combined heating and power plant and a water company, delivering drinking water to 35.000 customers. So far only large and medium sized industrial companies, i.e. with an average consumption larger than 100kW, have been connected to Power Hub. There is, however, also a large potential in the integration of small power consuming units, like residential households, which can contribute substantially to demand response due to their numerosity. By allowing the indoor temperature in residential buildings to vary one degree around a given reference, several kilo-watts of power consumption can be accelerated or postponed, thus providing power system services in the low voltage network.

In operation Power Hub manages a portfolio of power generating or consuming units, in the following named *local units* (LUs). PH optimises the power consumption and generation of the units as a dispatch problem, with respect to the present electricity price, thus maximising the profit for owners of generating unit and minimising the cost of operation for owners of consuming units. This way PH provides an interface to the power market to units, which are otherwise too small to participate and not able to provide the required services individually. Also it allows large electricity consuming companies, to 'sell' their flexibility in the power market, thus getting a discount on the cost of electricity.

For easy integration of new units a standard interface for communication between Power Hub and LUs has been developed. The interface relies on unit control to be run locally using a set point provided by Power Hub. The interface comprises following data being exchanged by PH and the LU's

Current generation/consumption (O)
The instantaneously generated or consumed power by the unit in kW.

Set point for generation/consumption (I)
The power set point in kW, of the requested consumption or generation provided by Power Hub.

Current capacity (O)
The current capacity of the LU.

Running (O)
States whether the LU is on-line and available to PH.

Error (O)
States whether the unit has any problems in its operation.

Power Hub enabled (O)
States whether the unit allows remote control by PH and thus acknowledges the given set point.

where (O) marks data sent from the local unit to Power Hub and (I) marks data sent from Power Hub to the local unit. The capacity is an abstract measure of the current level of the energy reservoir of the unit being controlled. In implementation, the capacity is LU dependant and should reflect the current state of the LU energy reservoir; that could be the level of diesel fuel in a tank for a diesel genset or the volume of water that has to be pumped from one reservoir to another in a water treatment plant. In addition to the continuous data communicated between Power Hub and the LUs, Power Hub maintains a set of static data for each LU, this comprises maximum and minimum power generation or consumption, and maximum and minimum level of capacity.

B. Model of local units

Power Hub uses a generalised model of its LUs to describe the development of the capacity state. The LU models are used to formulate and solve a dispatch problem, from which optimum the development of the set points communicated to each unit is found. As seen in Fig. 1, the level of energy stored in an reservoir, which defines the capacity, depends on a non-controllable energy flow into and out of the energy reservoir and a controllable inflow and outflow through a process that converts electrical energy into 'capacity'.

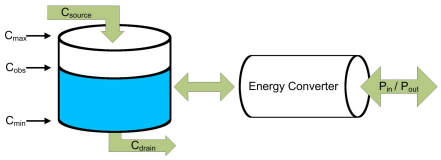

Fig. 1. Energy flow in and out of a energy reservoir of a local unit.

In the following the generalised model is adopted and used to formulate a model for the heat consumption of a household. When formulating the model it is natural to use the indoor temperature as a measure of the available capacity, where the medium of storage is the thermal mass of the building. Using the difference from a minimum acceptable indoor temperature as a measure of capacity, the capacity is given by, $C_i = T_i - T_{min}$, where T_i is the indoor temperature at time i. This gives a lower constraint on the capacity, $C_{min} = 0$ and the maximum is then given by the maximum acceptable indoor temperature. Thus, if $T_{min} = 20°C$ and $T_{max} = 22°C$ then then $C_{max} = 2$. Two of the major influences on the indoor temperature in buildings are the outdoor temperature and solar irradiance, recognised as the non-controllable input in Fig. 1. Assuming, a linear heat transfer through the building envelope to the outside with the outside temperature and a linear heat transfer into the building, due to solar irradiance, the model of the household capacity can be formulated in discrete time as,

$$\begin{aligned} C_{i+1} &= C_i + \tau\left(a \cdot T_{a,i} + b \cdot \phi_{s,i} + c \cdot P_{in,i}\right) \quad \Leftrightarrow \\ \frac{\Delta C_i}{\tau} &= a \cdot T_{a,i} + b \cdot \phi_{s,i} + c \cdot P_{in,i} \end{aligned} \tag{1}$$

where C_i is the capacity level at time i, $T_{a,i}$ is the outdoor temperature, $\phi_{s,i}$ is the solar irradiance and $P_{in,i}$ is the heat input. a, b and c are unknown parameters that can be estimated given a time series of C. Δ is the one step forward difference operator. Rewriting Equation 1 on vector form gives,

$$\begin{aligned} \frac{1}{\tau}\left[\Delta C_1, \Delta C_2, \ldots, \Delta C_n\right]^T &= \left[\boldsymbol{u_1}, \boldsymbol{u_2}, \ldots, \boldsymbol{u_n}\right]^T \boldsymbol{\theta} \\ \boldsymbol{C} &= \boldsymbol{U\theta} \end{aligned} \tag{2}$$

where $\boldsymbol{u_i} = [T_{a,i}, \phi_{s,i} P_{in,i}]^T$ and $\boldsymbol{\theta} = [a, b, c]^T$. In the work presented in this paper the parameters in the regression model were estimated using unweighted least square method. The parameters were estimated for each LU based on a 24 hours time series sampled with 5 minutes interval. The least square estimates are given by,

$$\hat{\boldsymbol{\theta}} = \left(\boldsymbol{U}^T\boldsymbol{U}\right)^{-1}\boldsymbol{U}^T\boldsymbol{C} \tag{3}$$

Using this method the aggregator can use the data collected during the first 24 hours of operation of a newly connected LU, to acquire estimates of the model parameters. From Equation 1 and with the estimates of parameters in $\boldsymbol{\theta}$ the predicted capacity at time $i+n$, can be found as

$$C_{i+n} = C_i + \tau \cdot n\left(a \cdot T_{a,i} + b \cdot \phi_{s,i} + c \cdot P_{in,i}\right) \tag{4}$$

C. Aggregator control

In the following it is assumed that the aggregator has access to the same static data as PH and that the aggregator has access to weather data and forecasts. With these assumptions a minimisation problem can be formulated, which is solved by the aggregator at each time step, i

$$\begin{aligned} &\min \left| \sum_{j=1}^{n}\left(s_{i,j}\right) - S_i \right| + \sum_{j=1}^{n} s_j \mathrm{W}\left(C_{i+1,j}\right) \\ &\text{s.t.} \quad P_{min,j} \leq s_{i,j} \leq P_{max_j} \end{aligned} \tag{5}$$

where n is the number of connected households, $s_{i,j}$ is the set point sent to household j at time i, S_i is the set point received by the aggregator through the interface and $\mathrm{W}\left(C_{i+1,j}\right)$ is a weight function of the capacity in the following time step. The first term minimises the absolute difference between the sum of set points sent to the LU's and the set point received by the aggregator. The second term penalises deviation of the capacity outside the given constraints, i.e. C_{min} and C_{max}. The weight function should be constructed such that $\mathrm{W}\left(C_{i+1,j}\right) > 1$ for $C_{i+1,j} > C_{max,j}$ forcing the last term to exceed the first, when the capacity is above $C_{min,j}$, thus forcing the set point down. Likewise, should $\mathrm{W}\left(C_{i+1,j}\right) < -1$ for $C_{i+1,j} < C_{min,j}$, forcing the set point up. As weight function a linear function from $(C_{min}, -1)$ to $(C_{max}, 1)$ is proposed, i.e.

$$\begin{aligned} \mathrm{W}\left(C_{i+1}\right) &= \frac{2\left(C_{i+1} - C_{min}\right)}{C_{max} - C_{min}} - 1 \Leftrightarrow \\ &= \frac{2C_i + 2\tau \cdot n\left(a \cdot T_{a,i} + b \cdot \phi_{s,i} + c \cdot P_{in,i}\right)}{C_{max} - C_{min}} - 1 \end{aligned} \tag{6}$$

which is a linear function of P_{in}, i.e.

$$\begin{aligned} \mathrm{W}\left(C_{i+1}\right) &= \tilde{a}P_{in,i} + \tilde{b}, \text{ where } \tilde{a} = \frac{2\tau \cdot n \cdot c}{C_{max} - C_{min}} \\ \text{and} \quad \tilde{b} &= \frac{2C_i + 2\tau \cdot n\left(a \cdot T_{a,i} + b \cdot \phi_{s,i}\right)}{C_{max} - C_{min}} - 1 \end{aligned} \tag{7}$$

Other weight functions could be defined, but a linear function ensures that Equation 5 can be formulated as quadratic programming problem. Equation 5 can be split into two sub-problems, for $\sum_{j=1}^{n} s_{i,j} \geq S_i$ we get

$$\underset{s_i}{\operatorname{argmin}} \sum_{j=1}^{n} s_{i,j} - S_i + \sum_{j=1}^{n} s_{i,j} \mathrm{W}\left(C_{i+1,j}\right) = \sum_{j=1}^{n} s_{i,j} \left(\mathrm{W}\left(C_{i+1,j}\right) + 1\right)$$

$$\text{s.t.} \quad P_{min,j} \leq s_{i,j} \leq P_{max,j} \tag{8}$$

$$\sum_{j=1}^{n} s_{i,j} \geq S_i$$

Assuming that each LU can dispatch the electrical power requested by the set point as long as the constraints of the capacity are not violated, we have $s_{i,j} = P_{in,i,j}$. Inserting Equation 7 into Equation 8 gives

$$\underset{s_i}{\operatorname{argmin}} = \sum_{j=1}^{n} s_{i,j} \left(\tilde{a}_j P_{in,i,j} + \tilde{b}_j + 1\right) = \sum_{j=1}^{n} s_{i,j} \left(\tilde{a}_j s_{i,j} + \left(\tilde{b}_j + 1\right)\right)$$

$$= \left(\tilde{\boldsymbol{b}} + \mathbf{1}\right)^T \boldsymbol{s}_i + \boldsymbol{s}_i^T \tilde{\boldsymbol{a}}^T \boldsymbol{I}_j \boldsymbol{s}_i$$

$$\text{s.t.} \quad P_{min,j} \leq s_{i,j} \leq P_{max,j} \tag{9}$$

$$\sum_{j=1}^{n} s_{i,j} \geq S_i$$

where $\tilde{\boldsymbol{a}}$ and $\tilde{\boldsymbol{b}}$ are vectors containing all $\tilde{a}_j$ and $\tilde{b}_j$, $\tilde{\boldsymbol{s}}_i$ is a vector containing all the set points at time i and $\boldsymbol{I}_j$ is the $j \times j$ identity matrix. Likewise can a quadratic programming problem be formulated for $\sum_{j=1}^{n} s_{i,j} < S_i$.

D. Aggregate capacity estimation

Given a forecast of the outdoor temperature and solar irradiance, the maximum and minimum power that can be dispatched by a household can be found from Equation 4. When estimating the maximum power consumption, the highest outdoor temperature and solar irradiance within the time horizon is used, thus providing conservative estimates. Likewise, is the minimum consumption found using minimum outdoor temperature and solar irradiance. The aggregate minimum and maximum power consumption can then be found as the sum of all minima and maxima, which can then be forwarded upward in the aggregation hierarchy, though the interface as available capacity. This way PH knows the maximum or minimum power that can be dispatched by the aggregator. The aggregated estimate is only valid for the given time horizon, n. It is therefore important that the aggregator and Power Hub agrees on the length of the horizon for maximum and minimum dispatch. Unfortunately, only one channel is available for communication of capacity. Therefore, the aggregator and PH has to agree on what is being communicated.

III. Results

The aggregator was simulated using MATLAB with 100 households connected. Two models of households were used in the simulations; one model with one time constant, to simulate an old thermally light building with electrical space heaters, and another model with two time constants to simulate a modern house heated with a water based heat pump through underfloor heating. The models were scaled to simulate an average Danish residential house, with an acceptable temperature band between 20°C and 22°C. 50 of each model type were simulated connected to the aggregator. As input to the simulations weather data for ten days in January 2012 were used. A plot of the weather data can be seen in Fig. 2.

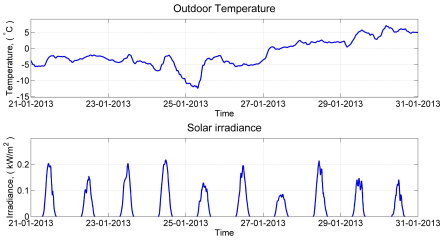

Fig. 2. Outdoor temperature (top) and solar irradiance (bottom).

Fig. 3 shows aggregated power consumption without control from the aggregator. In the simulation each household consumes the energy required to maintain a temperature reference at 21°C. The simulation is seen to correlate well with the weather input, having a peak at 500kW in consumption at midnight between the 24'th and 25'th, where the outdoor temperature is at its lowest. The plot also shows little or no need for heating around noon, where the solar irradiance provides sufficient energy to maintain temperature reference.

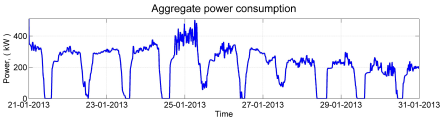

Fig. 3. Aggregate control without power set point.

Fig. 4 shows the aggregated power consumption with a aggregator set point generated by a sine wave, which is distributed to the house holds. The plot shows that the aggregated consumption can almost be controlled to follow the generated set point, and that the consumption can be moved from night to day, if desirable. Furthermore, the peak demand is reduced from 500kW without control, to below 400kW, corresponding to more than 20%.

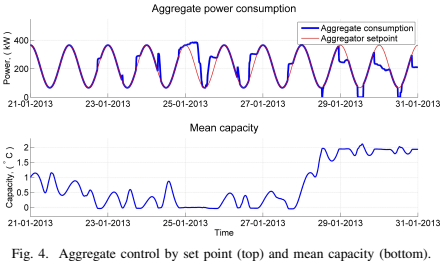

Fig. 4. Aggregate control by set point (top) and mean capacity (bottom).

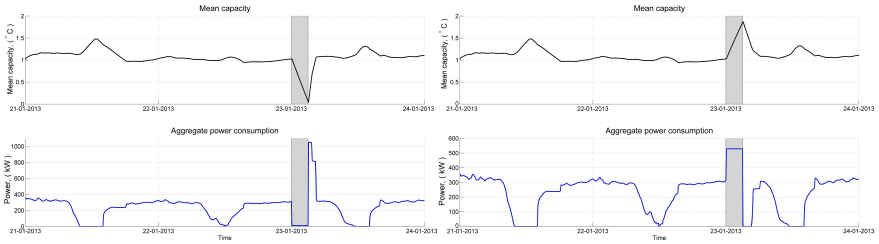

Fig. 5. Three hours maximum down (left) and up (right) regulation.

Fig. 5 shows three hours maximum down and up regulation, respectively. The aggregator runs without set point for the first two days and then the maximum down and up regulation is estimated and requested. In both cases the capacity constraints are not violated within the three hours horizon.

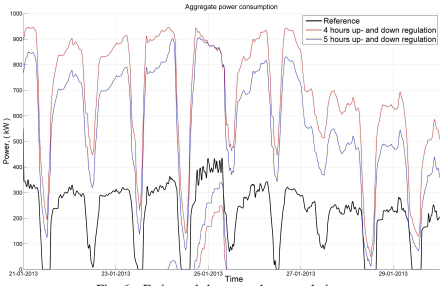

Fig. 6. Estimated down- and up regulation.

In Fig. 6 is the four and five hours maximum up- and down regulation plotted. The aggregated flexibility is seen to vary during the day, with limited opportunity to do up regulation around noon where the solar irradiance is providing energy to the building, and down regulation during the night between the 24'th and 25'th, where the outdoor temperature reaches a minimum. The plot also shows that in general the up regulation is higher than down regulation.

IV. Discussion

This paper has presented an aggregation model for aggregation of heat consumption in small households. Simulations of the aggregator show that consumption for heating of household can be moved in time and that peak demand can be significantly lowered; at least 20%, which is approximately the same as achieved in [6]. Additionally, simulations of short-term power system services, show that a large share of power consumption from heating, can be utilised as balancing power in the low-voltage grid. An even higher flexibility can be achieved, by allowing the temperature constraints to vary during the day, i.e. by allowing the temperature band to be increased, when households are empty.

One problem arise using the Power Hub interface for communication; only one channel exist for communication of down and up regulation. Therefore, Power Hub and the aggregator has to agree on which one of them should be used. This problem can be solved by extending the existing interface with an additional communication channel.

Using heat consumption as balancing power is only an option during the cold months of the year, making the flexibility of the aggregator very limited during warm periods. This, however, correlates well with a renewable energy source like wind power, that peaks during winter time. To increase flexibility during warm periods indoor cooling could be included in the aggregation model.

References

[1] S. You, "Developing Virtual Power Plant for Optimized Distributed Energy Resources Operation and Integration", Ph.d. Thesis, 2010

[2] S. Koch, D. Meier, M. Zima, M. Wiederkehr and G. Andersson, An active coordination approach for thermal household appliances Local communication and calculation tasks in the household, IEEE PowerTech 2009, Bucharest

[3] A. Barbato, A. Capone, G. Carello, M. Delfanti, M. Merlo and A. Zaminga, House energy demand optimization in single and multi-user scenarios, IEEE International Conference on Smart Grid Communications, SmartGridComm 2011, Brussels

[4] Y. Zong, D. Kullmann, A. Thavlov, O. Gehrke, H. Bindner, Model Predictive Control Strategy for a Load Management Research Facility in the Distributed Power System with High Wind Penetration -Towards a Danish Power System with 50% Wind Penetration, Asia-Pacific Power and Energy Engineering Conference 2011 (APPEEC 2011), Wuhan

[5] Y. Ding, P. Nyeng, J. Ostergaard, M. D. Trong, S. Pineda, K. Koen, G.B. Huitema, O.S. Grande, "Ecogrid EU - a large scale smart grids demonstration of real time market-based integration of numerous small DER and DR", IEEE PES Innovative Smart Grid Technologies Europe 2012 (ISGT Europe), Berlin

[6] D. J. Hammerstrom et al, "Pacific Northwest GridWise™ Testbed Demonstration Projects", Technical report, 2007

[7] Energinet.dk, Cell Controller Pilot Project, http://www.energinet.dk/SiteCollectionDocuments/Engelske%20dokumenter/Forskning/Cell%20Controller%20pilot.pdf, [Accessed Aug. 15, 2013]

[8] DONG Energy, Power Hub, http://www.dongenergy.com/en/innovation/developing/pages/power_hub.aspx, [Accessed Aug. 15, 2013]

PAPER D

Utilization of Flexible Demand in a Virtual Power Plant Set-Up

This paper has been accepted for publication in the *IEEE Transactions on Smart Grid*.

640 IEEE TRANSACTIONS ON SMART GRID, VOL. 6, NO. 2, MARCH 2015

Utilization of Flexible Demand in a Virtual Power Plant Set-Up

Anders Thavlov, *Student Member, IEEE,* and Henrik W. Bindner, *Member, IEEE*

***Abstract*—High penetration levels from renewable energy sources in large-scale power systems demand a high degree of flexibility in the transmission and distribution system. This paper presents a method for utilization of flexible demand in the low-voltage distribution system using the thermal mass of a building to defer power consumption from electric space heating. The power consumption for heating is controlled by an operational virtual power plant, which is sending a set point for requested power consumption to the building management system. An optimization problem is formulated such that the discrete dispatch of power from ten electric space heaters is following the power set point given constraints on the indoor comfort that is defined by the users of the building. The controlling method has been implemented in an intelligent office building and used for demonstration of flexible demand in the low voltage network.**

***Index Terms*—Demand response (DR), demand-side management, flexible load, heat dynamics, smart grid, virtual power plant (VPP).**

I. Introduction

FLEXIBLE demand for power is expected to play a key role in the future power system—or smart grid—and is by many seen as a prerequisite for integration of large amounts of renewable energy. The benefits of implementation of flexible power consumption are many; these include the possibility of shifting power consumption from peak load hours to periods with less demand, consequently reducing the need for spinning reserves. Furthermore, by a better coordination of the units connected in the low-voltage network congestion problems can be avoided, and hence flexible demand can help to reduce investments in the distribution grid.

Until recently, power consumers have been regarded as passive players in the power system and only the generation side has been involved in the process of controlling the system balance. Now, large industrial companies are being integrated as active players in the power system through the power market, trying to reduce cost of operation by running industrial processes during periods with inexpensive power. The variety of flexible processes is large and varies from pumping a fixed volume of water during a day to cold storages which have to maintain a maximum temperature. There is, however, also a large potential in the integration of the numerous small entities connected in the low voltage grid. Two main approaches for control of demand-side resources (DSR) are currently being pursued; the first one is utilizing indirect control, where an incentive signal, possibly a price signal, is broadcast to a large number of DSRs to incentivize changes in power consumption. The second one is direct control, where a centralized controller—or coordinator—is directly controlling a number of distributed energy resources (DERs) by sending a reference set point for requested power consumption or generation to each of them. Moreover, there exist other approaches for control, for example autonomous and transactional control as defined in [1]. Whereas indirect control relies on a stochastic demand response (DR) from DSRs, direct control can deliver a requested DR with a high certainty relative to indirect control. This, however, comes at a higher investment cost, due to the need of establishing a dedicated communication link, possibly bidirectional, between the central controller and the DSR. When direct control is used to aggregate a number of units, the aggregator is typically called a virtual power plant (VPP). The reference to power plants refers to the high certainty of up- and down-regulation of the aggregator, due to the usage of direct control.

Several projects are investigating the benefits of integration of residential households as active players in the power system. In the Pacific Northwest GridWise Demonstration project, a 20% reduction in peak load was obtained by control of appliances in residential and commercial buildings using a broadcast electricity price signal [2]. A similar approach is used in the ongoing EcoGrid EU project, where flexible demand from 2000 residential customers, on the Danish island Bornholm, is used to balance power in a power system with 50% power generation from renewable energy sources [3]. In the cell controller pilot project, a direct control approach is used to coordinate the response from DER, e.g., CHP plants and wind turbines, to deliver power system services in the distribution system [4].

Research within DR has gained a lot of attention within the last decade; consequently, there exists many studies in building management systems (BMS) providing optimal control of commercial and residential appliances with respect different criteria. As outlined earlier, these can generally be separated into indirect and direct control; especially indirect control using economic model predictive control (EMPC) with respect to price signals has received a lot of attention. In [5],

Manuscript received September 20, 2013; revised January 8, 2014, April 26, 2014, and August 5, 2014; accepted October 9, 2014. Date of publication October 31, 2014; date of current version February 16, 2015. This work was supported in part by DONG Energy and in part by the Danish Academy of Wind Energy. Paper no. TSG-00742-2013.

The authors are with the Department of Electrical Engineering, Technical University of Denmark, Rosiklide 4000, Denmark (e-mail: atha@elektro.dtu.dk).

Color versions of one or more of the figures in this paper are available online at http://ieeexplore.ieee.org.

Digital Object Identifier 10.1109/TSG.2014.2363498

an autoregressive model with exogenous input (ARX) is used together with EMPC to determine an optimal space cooling schedule with respect to a given rate plan. Likewise, in [6] a nonconvex EMPC method is proposed to minimize cost of refrigeration in a nonlinear commercial refrigeration system using hourly spot prices from the Nordic power market. In [7], EMPC is used to optimize space heating from a heat pump, with respect to both cost of electricity as well as the load level of the distribution grid. Similarly, in [8] predictive control is used to comply with a contractual peak power constraint, which is typically imposed on private customer in France and Italy. Direct control has received less attention despite that DR using direct control has been implemented by several energy companies; for example by Southern California Edison, the primary electric company in California, which is enrolling their private customers in DR programs, by offering a discount on electricity if they allow the utility to switch off their central air conditioning (A/C) unit during peak load hours. This paper presents a novel approach for delivering DR from an intelligent office building, using a VPP set-up. Due to the server/client relationship between the VPP and the controlled DSR, EMPC is implicitly carried out by the VPP. Hence, EMPC is not an option on the client side; instead, a dispatch problem is formulated, which optimizes the discrete power consumption from a number of resistance heaters—or Ohmic heaters—with respect to a set point for power consumption provided by the VPP.

This paper is organized as follows; initially, in Section II, a description of the VPP, Power Hub [9], and the interface to the VPP is given. Next, a model for heat load predictions is derived, and an optimization problem for the control of electric space heating in a building is formulated. In Section III, results from a series of experiments using an intelligent office building as a flexible load, are presented. Finally, in Section IV, the results are discussed and the conclusion is given.

II. Methodology

In this section, we present the VPP set-up and the theory for implementation of flexible heat consumption in an intelligent building that is heated by electric resistive heaters.

A. Power Hub

Power Hub is an implementation of a VPP that is currently being tested under market conditions in the Nordic power market. Power Hub has been developed by the Danish energy company DONG Energy as part of the Twenties project [10], which is supported by the European Commission. The main objective of the Twenties project is to investigate how large amounts of wind energy can be integrated into large-scale power systems. The main purpose of Power Hub is to increase the flexibility in the power system by allowing small power consuming and generating units to participate actively in the power market, thus contributing as a balance to the intermittent generation from the renewable energy sources.

By aggregation of small units, i.e., units with rated power generation or consumption of less than 1 MW, Power Hub is able to coordinate the response of numerous of units thus increasing the total effect of DR. Additionally, Power Hub lets small generation and consumption units, that are otherwise too small, to participate in the power market. A large-scale demonstration of Power Hub was carried out on the Faroe Islands in November 2012, where load shedding from three industrial companies were actuated to prevent a total island blackout due to a simulated 10% power loss in the total national supply.

In operation, Power Hub manages a portfolio of consumption and generation units, which in the following are named local units (LUs). During the day, Power Hub minimizes the cost of operation for consuming LUs, by shifting power consumption to periods with less expensive power. Likewise, the output of power generating LUs are increased—or activated—when the price is relatively high, thus increasing the income for the LU owner. Each unit is controlled locally given a set point for a requested consumption or generation, which is provided centrally from Power Hub. To ease integration of new units a standardized interface has been developed, which is available on the site of the LU through a remote terminal unit (RTU).

To plan the day of operation, a daily load or generation forecast is generated for each LU by their respective owner. These forecasts have to be received by Power Hub no later than 10 A.M. the day before operation, such that potential flexibility can be bid into the day-ahead market in the Nordic power market, Elspot. Bids into the day-ahead market have to be received by Elspot before gate-closure at noon, the day before operation. Flexibility that is not bid into the day-ahead market, or did not receiving any contract therein, can be saved for primary reserve, which can be activated on request from the transmission system operator. During the day of operation Power Hub can request changes to the power generation or consumption of an LU if imbalances in the power system emerge or if regulation power is needed. This is achieved by sending an updated power set point of the requested generation or consumption to an LU through the RTU. Within some predefined constraints, defined by the LU owners themselves, an LU is expected to comply with changes in power set point.

In the following, the heat consumption of an office building is being modeled and controlled by Power Hub; other parts of power consumption, which are mainly inflexible, are not considered in this paper since they cannot be postponed or accelerated. The controller can be seen as having influence on the fuse block which contains the electric heating only.

B. Power Hub Interface

On the LU—or client—side, the interface is represented physically by an RTU, which is communicating with Power Hub over a GPRS connection. The connection is facilitated by the IEC 60870-5-104 transmission protocol and encrypted using a virtual private network (VPN) connection. The interface is presented in Table I. In the table, input is relative to the house controller, i.e., input means input to the BMS. Of special interest are the first three signals: the first one sends a reading of the current power generation or consumption of the LU to Power Hub, the second method provides a requested

TABLE I
POWER HUB INTERFACE

Current generation/consumption	Analogue output for the current consumption
Set point for generation/consumption	Analogue input for the requested consumption
Current capacity	Analogue output for the current capacity
Power Hub enabled	Digital output for LU owners to turn on/off Power Hub control
LU running	Digital output reading LU running state
LU error	Digital output for reading potential LU error state
LU start	Digital input for starting LU
LU stop	Digital input for stopping LU

power set point to the LU, which is the optimal power consumption or generation with respect to the power market. The third method sends an abstract measure of the capacity of the unit back to Power Hub, which is LU specific and depends on the process that the LU is running. Examples of capacity can be the level of fuel in diesel genset, level of water in a reservoir for hydro power or deviation from a reference temperature in a cold storage. Using the measure of capacity Power Hub maintains knowledge of the state of its LUs and how much consumption or generation that can be postponed or accelerated. Constraints on capacity and power consumption—or generation—are defined by LU owners together with Power Hub administrators prior initialization of the LU, and are maintained as static data in Power Hub. Additionally to the methods stated above, there is a digital input in the RTU reading the pulse output from an electricity meter mounted on the site of the LU. This input is for Power Hub to verify consumption or generation.

C. FlexHouse

FlexHouse is an intelligent office building located at the DTU Risø Campus near Roskilde, Denmark. The building is a part of SYSLAB, a research facility for control in distributed power systems, where it is utilized as a flexible load. It is fitted with a wide range of sensors and actuators, which allow the building to be monitored and controlled from a custom-made BMS. The area of FlexHouse is approximately 120 m^2, distributed over seven offices and a large meeting room, together with a small kitchenette and a toilet. The building is free-standing, mounted on concrete slaps, thus leaving a gap between the ground and the underside of the building. The building envelope is made from plywood on the outside and plasterboards on the inside, sandwiching a layer of insulation. Consequently, FlexHouse is a thermally light building, relative to an average Danish building. Likewise, the level of insulation is quite low compared to an average Danish building. Space heating in FlexHouse comes from ten electrical space heaters that are distributed equally inside the building. The rated power of the heaters ranges from 0.975 to 1.250 kW, with a total rated peak power of 9.75 kW. Moreover, there are five heat pumps providing heating during winter and cooling during summer. These have not been utilized in the research presented in this paper.

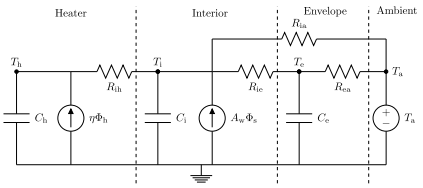

Fig. 1. RC-diagram for prediction model.

D. Heat Dynamic Model for Prediction of the Heat Load

Daily, for each LU, Power Hub expects to receive a load or generation forecast for the following day of operation. In this section, we derive a heat dynamic model for prediction of the heat load of FlexHouse. No later than 10 A.M. Power Hub must receive the forecast of the expected heat consumption in FlexHouse for the following day. Hence, the heat load should be predicted from 14 to 38 h in advance. Naturally, predictions of the heat load up to 38 h in advance has a high uncertainty attached, especially considering the uncertainty coming from the weather forecast. However, the heat load of a small house connected in the low voltage grid should—ideally—be seen as part of an aggregate system, where the uncertainty of an aggregate forecast decreases as the number of heat loads increases. An exception to this is, naturally, when a weather forecast is wrong the aggregate forecast is also likely to be wrong. This, however, is one of the main reasons why Power Hub has been developed; to handle imbalances during the day. Another example is when a weather front is delayed with respect to a forecast, potentially delaying the power generation from a wind farm. This can be handled by Power Hub, by postponing the heating of households until the weather front has arrived and power generation has reached a predicted level.

A linear time-invariant model of the heat dynamics of FlexHouse has been developed for predictions of the indoor temperature and heat load. This model is currently being used in various applications using FlexHouse as a source for provision of DR, e.g., in EMPC of the heat load using an actual time varying price signal from the Nordic power market [11]. By approximating the temperature to be homogeneous distributed in the indoor air, including the interior mass, the space heaters, and the building envelope, respectively, the model can be formulated as a lumped model. The RC-diagram presented in Fig. 1 illustrates how the heat dynamics of the building are modeled. At the top is noted the three temperature states, i.e., the heaters, interior, and envelope states, each represented by a capacitor in the diagram, together with the ambient environment to the far right. The heaters are seen to receive a heat input Φ_h, which is multiplied by the efficiency factor, η. The heaters are seen to exchange heat with the interior state only, which exchanges heat with the ambient environment directly and through the building envelope. Moreover, the interior state receives heat input from solar irradiance, Φ_s, coming through the windows with an effective area A_W. Finally, the envelope is exchanging heat with both the interior state and the ambient environment. To account for disturbances not encompassed

TABLE II
MAXIMUM LIKELIHOOD ESTIMATES OF MODEL PARAMETERS IN (1)

Parameter	Estimate
A_w	14.52 m^2
C_e	4.17 kWh/°C
C_h	0.00227 kWh/°C
C_i	2.54 kWh/°C
R_{ea}	3.61 °C/kW
R_{ie}	0.84 °C/kW
R_{ih}	139.22 °C/kW
R_{ia}	36.99 °C/kW
η	$\equiv 1$

by the model, e.g., unrecognized or noisy measurement of input, the energy balance equations are formulated as three coupled stochastic differential equations (SDE). From Fig. 1, the energy balance equation can be derived

$$\begin{aligned} dT_i &= \left(\frac{T_h - T_i}{R_{ih}C_i} + \frac{T_e - T_i}{R_{ie}C_i} + \frac{T_a - T_i}{R_{ia}C_i} + \frac{A_w\Phi_s}{C_i}\right)dt + \sigma_1 d\omega_1 \\ dT_h &= \left(\frac{T_i - T_h}{R_{ih}\cdot C_h} + \frac{\Phi_h}{C_h}\right)dt + \sigma_2 \cdot d\omega_2 \\ dT_e &= \left(\frac{T_a - T_e}{R_{ea}\cdot C_e} + \frac{T_i - T_e}{R_{ie}\cdot C_e}\right)dt + \sigma_3 \cdot d\omega_3 \end{aligned} \tag{1}$$

where T_i, T_h, and T_e are the temperature states for the indoor air, heaters, and building envelope, respectively. R_{ih} is the thermal resistance—also known as the UA-value—between the heaters and indoor air, R_{ie} is the thermal resistance between the indoor air and the house envelope, R_{ea} is the thermal resistance between the envelope and the outdoor environment, and R_{ia} is the heat transfer from the indoor air directly to the outdoor environment. C_i, C_h, and C_e are the heat capacities of the interior mass, heater mass, and envelope mass, respectively. The exogenous disturbances to the equations from the ambient environment are the outdoor temperature T_a and the solar irradiance, Φ_s. Φ_h is the controllable electric input of the space heaters. The disturbances not encompassed by the model are described by a diffusion process, added to each of the equations, which is driven by the stochastic process $d\omega$ with variance σ^2. Equation 1 can be written in the state space form

$$d\boldsymbol{T} = \mathbf{A}\,\boldsymbol{T}dt + \mathbf{B}\,\boldsymbol{U}dt + \boldsymbol{\sigma}\,d\boldsymbol{\omega} \tag{2}$$

where $\boldsymbol{T} = [T_i, T_h, T_e]^T$ is the state vector, $\boldsymbol{U} = [T_a, \Phi_s, \Phi_h]^T$ is the input vector. $\mathbf{A} \in \mathbb{R}^{3\times3}$ and $\mathbf{B} \in \mathbb{R}^{3\times3}$ are the state and input matrix, respectively. $\boldsymbol{\sigma} \in \mathbb{R}^{3\times3}$ is a diagonal matrix containing the variances of the diffusion process $d\boldsymbol{\omega} \in \mathbb{R}^{3\times1}$. Assuming $\boldsymbol{\omega}$ is described by a standard Wiener process the parameters in (2) can be estimated using a maximum likelihood estimation method as described in [12]. Based on a five days time series of the input $\boldsymbol{U}$, sampled at a 5-min interval, the maximum likelihood estimates presented in Table II have been found. In the table, the efficiency of the resistance heaters are assumed to be equal to one which is reasonable for resistance heaters; however, if another heating method were used, e.g., using a heat pump, the efficiency could be significant higher.

By integration of (2), using the parameter estimates presented in Table II, a discrete model with 5 min steps has been derived. This model can be used for discrete prediction of the heat load of FlexHouse given an indoor temperature reference and a forecast of solar irradiance and outdoor temperature. For a more detailed description of the heat dynamic model of FlexHouse, readers are referred to [13] and for maximum likelihood estimates in linear state space models in general [12] and [14].

E. Optimization of Power Consumption

The power consumed by a number of electric space heaters in the building should be controlled as close to the given set point as possible but without compromising the indoor comfort of the residents of the building. Thus, the controller should take into consideration the trade-off between flexibility and comfort, allowing the users of the building to specify the level of comfort. Assuming n individual electric space heaters, each with rated power P_j, an optimization problem can be formulated as

$$\min \left| \sum_{j=1}^{n} \left(x_j P_j\right) - S \right| + \sum_{j=1}^{n} x_j P_j \, w\left(T_j\right) \tag{3}$$

where the decision variable $x_j \in \{0, 1\}$ is the off/on state of heater j, P_j is the rated power of heater j, S is the power set point received from Power Hub and n is the total number of heaters in the building. The weight function, $w(\cdot)$, of the temperature in the room with heater j, is used to implement a soft constraint on the discomfort felt by the resident, by gradually penalizing temperature deviations from the reference, where $T_{\min}$ and $T_{\max}$ are the minimum and maximum tolerable indoor temperature, respectively. The weight function should penalize heaters being on when the indoor temperature reaches $T_{\max}$. Likewise, should the weight function penalize heaters being off when the indoor temperature reaches $T_{\min}$. In the implementation of flexible demand in FlexHouse, the following weight function has been used:

$$w\left(T_j\right) = \left(\frac{2\left(T_j - T_{\text{ref}}\right)}{\Delta T}\right)^m \tag{4}$$

where m is an odd number to create an odd function around the indoor reference temperature, T_{ref}. $\Delta T = T_{\max} - T_{\min}$ is the width of the comfort band—or temperature band—in which the temperature is allowed to vary. T_{ref} and ΔT can be specified by the residents, whereas m is a BMS specific parameter defining the steepness of the weight function on the boundaries. In Fig. 2, some examples of weight functions are presented for a varying m.

From the figure it is seen that $w(T_j) < -1$ for $T_j < T_{\text{ref}} - \Delta T/2$, making the last term in (3) to dominate, thus forcing heaters to be turned on. Likewise, $w(T_j) > 1$ for $T_j > T_{\text{ref}} + \Delta T/2$ is forcing heaters to be turned off. Due to the time delay in the heat transfer from heaters to the indoor air, the boundaries specified by ΔT, should not be seen as "hard"

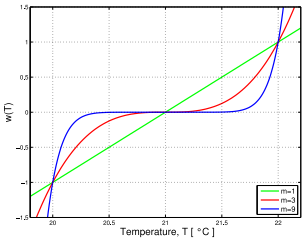

Fig. 2. Weight function with $T_{\text{ref}} = 21$, $\Delta T = 2$, and $m = 1, 3, 9$.

boundaries, but a boundary where the heaters are forced to be switched on or off.

The optimization problem formulated in (3) can be split in two, for $\sum_{j=1}^{n}(x_j P_j) \geq S$ and $\sum_{j=1}^{n}(x_j P_j) < S$, and formulated as two constrained optimization problems. For $\sum_{j=1}^{n}(x_j P_j) \geq S$, we find

$$\begin{aligned} &\min \sum_{j=1}^{n}(x_j P_j) - S + \sum_{j=1}^{n} x_j P_j\, w(T_j) \\ &\quad = \min \sum_{j=1}^{n}(w(T_j) + 1)\, x_j P_j \\ &\quad \text{s.t.} \sum_{i=1}^{n} x_j P_j \geq S. \end{aligned} \tag{5}$$

Likewise, a constrained optimization problem can be formulated for $\sum_{j=1}^{n}(x_j P_j) < S$

$$\begin{aligned} &\min \sum_{j=1}^{n}(w(T_j) - 1)\, x_j P_j \\ &\text{s.t.} \sum_{i=1}^{n} x_j P_j < S. \end{aligned} \tag{6}$$

These two constrained optimization problems, (5) and (6), can be solved using mixed integer linear programming individually, where the solution with the lowest cost function gives the global solution to (3).

F. Implementation

For demonstration of flexible demand using FlexHouse, an optimization process for the problem derived in Section II-E was implemented in the BMS, which is controlling the power input to the ten space heaters. Using a bus coupler, the output from the RTU is converted to Modbus over Ethernet, which is read by the BMS. In the optimization process $m \equiv 9$ were used to enforce relative sharp boundaries on the weight function. To ensure a fast response on changes in power set point the optimization problem, derived in (5) and (6), was solved every time changes in set point was detected. Using the GNU Linear Programming Kit, the problem was solved in sub-seconds; consequently, delivering a DR within a few second from when the updated set point was received. In periods with no changes in set point, the problem was solved every fifth minute. Finally, a fallback controller was implemented in case of lost communication with Power Hub or other errors, e.g., set point out of range. This controller emulates a thermostatic controller with the same reference temperature, T_{ref}, as the set point controller and 0.5 °C hysteresis.

III. Results

Several experiments were conducted during the period from January to April 2013 using FlexHouse as a flexible load. The results from three of these experiments are presented in this section. The indoor temperature reference for all experiments were set to $T_{\text{ref}} = 21$ °C, with $\Delta T = 4$ °C for the first experiment and $\Delta T = 8$ for the second and third experiment. The comfort band used for control should be consider an approximation to the actual indoor comfort and should merely serve to illustrate the possibilities in demand response in the low voltage grid rather than providing optimal thermal comfort as in large-scale HVAC systems. Daily, a heat load forecast was generated from the discretized state space model presented in Section II-D using 5 min steps.

A. Flexible Consumption Experiment

The first experiment was conducted to demonstrate that the heat load can be shifted from day to night, where a surplus of electricity is often available and thus less expensive. Daily, a consumption plan was transferred to Power Hub (see Section II-A). The set point given by Power Hub was the reported forecast, at the given time, with a sinusoid added. The amplitude of the sinusoid was set to 1 kW and the period to one day, with minima at noon and maxima at midnight. By superimposing the sinusoid on the forecast, 1 kW of heat load was shifted from midday to midnight. The outcome of the experiment can be seen in Fig. 3, where the heat consumption is seen to follow the set point (top) while the indoor temperature is within the temperature band (bottom). The average heat load during the experiment was close to 6 kW and hence the 1 kW load shifted from midday to midnight corresponds approximately to 17% of the average heat load. The first day the indoor temperature is seen to drop to the boundary of the comfort band and that the power consumption is increasing relative to the set point when the boundary is reached. The drop was caused by an inaccurate forecast of the outdoor temperature, where a 2 °C lower temperature was observed compared to the forecast; thus, consequently estimating the heat load too low for the given day. From the top plot is noted a daily abrupt drop in set point at noon and likewise the power consumption. The drop in set point was caused by a necessary restart in the FlexHouse BMS, an error that was solved for the following experiments. This drop caused the indoor temperature to decline outside the comfort band, but the controller brought the temperature back up, when the controller was restarted. Furthermore, there was an error in the timestamps in the reported load forecast made for January 27th which resulted in that the set point was not updated after midnight (gray area). The controller is seen to handle the nonupdated set point and is able to

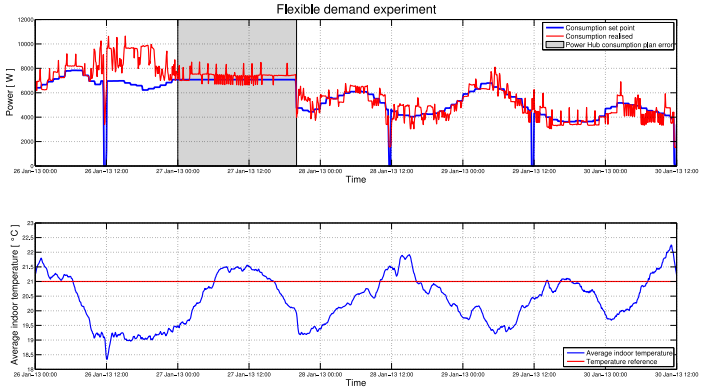

Fig. 3. Flexible load experiment. Top: power set point and actual consumption. Bottom: indoor air temperature.

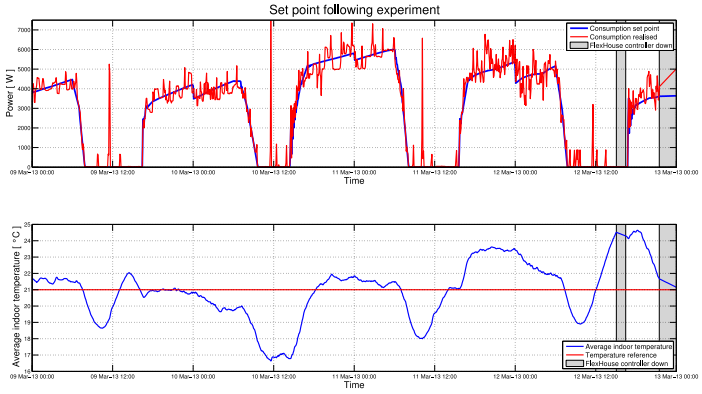

Fig. 4. Set point following consumption. Top: power set point and actual consumption. Bottom: indoor air temperature.

maintain the indoor reference temperature within the comfort band. The error was realized during the 27th and corrected in the evening. The following three days are seen to proceed without reaching the comfort limits and the controller is actually able to dispatch the requested consumption through the heaters.

B. Set Point Following Experiment

Subsequently, with the gathered experience from the initial experiments, a new experiment was conducted to see how well the heat load forecast performed by investigating how wide the temperature band had to be to dispatch the predicted power. Thus, the comfort temperature band was widened to 8 °C and the set point returned by Power Hub was simply given by the load forecast. The outcome of the experiment is presented in Fig. 4, where the actual power consumption is seen to follow the set point quite close considering the discretized power consumption of the ten space heaters, which can only be controlled with a resolution of 0.250 kW. Ideally, if the forecast model described in Section II-D was perfect, the indoor temperature would stay at 21 °C during the experiment. However, the indoor temperature is seen to vary significantly around the reference temperature, with a maximum of ± 4 °C. Especially, around noon, the temperature is seen to decrease periodically and in the afternoon it increases again. The spikes during midday are caused by a restart of the controlling software, where the fallback thermostatic controller takes over. During the restart of the BMS, which takes a few minutes, the thermostatic controller turns on all the heaters in the rooms where the temperature is below T_{ref} (see Section II-F).

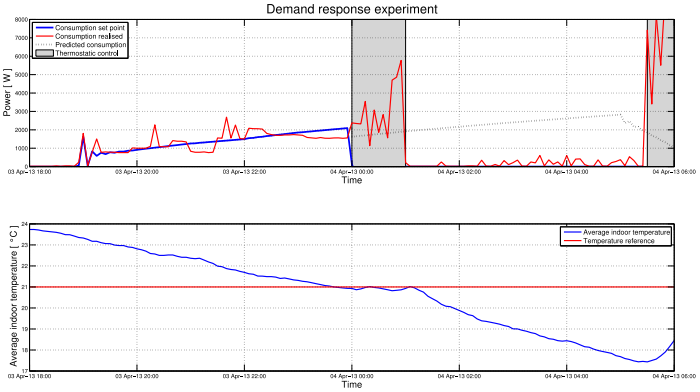

Fig. 5. Demand-response experiment. Top: power set point predicted and actual consumption. Bottom: indoor air temperature.

C. Demand-Response Experiment

Fig. 5 shows the outcome of the last experiment, where the impact on the indoor temperature was investigated as a consequence of postponing the heating on request from Power Hub. At the initial day of the experiment, the set point was given by the load forecast as in the previous experiment. At midnight, a negative set point was given, thus activating the fallback thermostatic controller (gray area), which brought the indoor temperature into a known state, i.e., 21 °C in all rooms. At 1 A.M. the set point was set to zero, thus requesting all heating in the building to be switched off. After a few seconds, the building switched off all heating and within the first hour the indoor temperature is seen to decline approximately 1 °C after four hours the indoor temperature was declined 3.5 °C. At 5:30 A.M., thermostatic control was reestablished, thus bringing the indoor temperature back to the temperature reference. It is noted that the power consumption is significant higher, relative to the predicted consumption, after heating has been reestablished.

IV. Conclusion

In this paper, a method for providing flexible demand in the low-voltage grid using a direct control scheme has been presented. The method utilizes the infrastructure provided by an operational VPP, by implementing a specified interface. In this way, the BMS of an intelligent office building is able to communicate with the VPP and receive a set point for the requested power usage. It has been demonstrated that the building is able to track a given set point over time, by acceleration and postponement of its power consumption for electric space heating, and in this way adapt to the needs of the power system. Furthermore, with the first experiment it has been demonstrated, that by allowing the indoor temperature to vary within ±2 °C, approximately 17% of the heat load can be shifted from midday to midnight; a similar result was obtained in [2], where an indirect approach was used to control household appliances.

From the outcome of the 2nd experiment, it is concluded that better models for the prediction of heat loads are needed if the flexibility is to be traded in the day-ahead market. Predictions of the heat load up to 38 h in advance is simply subject to high uncertainties and likewise is the input data, i.e., weather. However, as stated in Section II-D, the heat load should be seen as an aggregate system, where the uncertainty of the aggregate forecast decreases as the number of LUs increase. Alternatively, due to the small time constants of FlexHouse, the flexible demand could more suitably be traded as balancing power in the intraday market, which has a much shorter trading horizon.

Finally, the last experiment demonstrates that the heat load of a thermally light building can be postponed up to an hour, without having significant impact on the indoor comfort. Considering an aggregate system, under control of a VPP, this means that the heat load of an aggregator can be reduced by 50% during peak load hours, assuming a 2 h peak load period. Likewise, in power systems where frequent brownouts or blackouts are experienced, an ability to postpone power consumption for heating—or cooling—could be an important tool to maintain the stability of the power system. Another important thing to notice from this experiment is how fast heating can be reestablished; if no coordinating control is enforced on the reestablishing of heating, congestion problems might arise in the distribution grid. Also, this experiment shows that postponement of heating comes at a price, meaning that lost heating has to be provided later in time.

The results presented in this paper should be seen in the light of that the heat capacity of FlexHouse is quite small; approximately 3–4 kWh/°C, Bacher and Madsen [12] compared to approximately 15 kWh/°C for a regular Danish house of similar size, but constructed from bricks and concrete. Also,

the level of insulation of Danish houses is substantial higher than in FlexHouse, which means that the need for heating is less per area. The average annual power consumption of electrically heated households is around 100 kWh/m^2 and the average size of single-family houses is around 140 m^2. This means that the annual heat consumption in a single-family household is approximately 14 000 kWh/y. When distributed over the seven months heating season in Denmark, this gives an average heat consumption of around 2–3 kW, which is equivalent to what is used for heating FlexHouse. With higher thermal mass and insulation, the time constants of average households are expected to be significantly larger compared to FlexHouse and with the same amount of heating needed, better results with respect to the amount of energy that can be stored in the building structure and variations in indoor temperature, are expected to be found.

In this paper, the parameter used to describe indoor comfort is exclusively given by the indoor temperature. However, indoor comfort is a complex measure and is therefore not given by the temperature alone; generally, indoor comfort comprises parameters for CO_2 level, humidity, and thermal radiation from interior walls. Further work should therefore strive to include more optimal comfort indicators like for example predicted mean vote (PMV) and predicted percentage dissatisfied (PPD). Using such indicators, parameters like CO_2 level and humidity could be controlled using actuators on windows for control of natural ventilation of the building. Moreover, the discrete state space model, used for prediction of the heat load, should be improved, such that a better forecast of the heat load can be achieved. Instead of formulating the heat dynamic model using SDE existing ISO models, e.g., ISO 13 790 [15], could be used to formulate a more adequate model. Finally, future work should include control of the A/C from the five heat pumps in FlexHouse, taking into consideration the coefficient of performance, η, of the heat pumps.

REFERENCES

[1] A. M. Kosek, G. T. Costanzo, H. W. Bindner, and O. Gehrke, "An overview of demand side management control schemes for buildings in smart grids," in *Proc. IEEE Int. Conf. Smart Energy Grid Eng. (SEGE)*, 2013, pp. 1–9.

[2] D. J. Hammerstrom *et al.*, "Pacific Northwest GridWise testbed demonstration projects—Part I, Olympic Peninsula project," U.S. Dept. Energy, Pacific Northwest Nat. Lab., Richland, WA, USA, Tech. Rep. PNNL-17167, 2007.

[3] J. Jorgensen, S. Sorensen, K. Behnke, and P. Eriksen, "EcoGrid EU—A prototype for European Smart Grids," in *Proc. IEEE Power Energy Soc. Gen. Meeting*, San Diego, CA, USA, 2011, pp. 1–7.

[4] Energinet.dk "Cell controller pilot project," Energinet.dk, Tech. Rep. 8577/12, 2011.

[5] J. Ma, S. Qin, B. Li, and T. Salsbury, "Economic model predictive control for building energy systems," in *Proc. IEEE PES Innov. Smart Grid Technol. (ISGT)*, Hilton Anaheim, CA, USA, 2011, pp. 1–6.

[6] T. Hovgaard, L. Larsen, J. Jørgensen, and S. Boyd, "Nonconvex model predictive control for commercial refrigeration," *Int. J. Control*, vol. 86, no. 8, pp. 1349–1366, 2013.

[7] F. Oldewurtel, A. Ulbig, A. Parisio, G. Andersson, and M. Morari, "Reducing peak electricity demand in building climate control using real-time pricing and model predictive control," in *Proc. 49th IEEE Conf. Decis. Control (CDC)*, Atlanta, GA, USA, 2010, pp. 1927–1932.

[8] A. Barbato *et al.*, "House energy demand optimization in single and multi-user scenarios," in *Proc. IEEE Int. Conf. Smart Grid Commun. (SmartGridComm)*, Brussels, Belgium, 2011, pp. 345–350.

[9] DONG Energy. (2013, Aug. 15). *Power Hub*. [Online]. Available: http://www.dongenergy.com/en/innovation/developing/pages/power_hub.aspx

[10] TWENTIES, (2013, Jul. 17). *Twenties, Transmission System Operation With Large Penetration of Wind and Other Renewable Electricity Sources in Networks By Means of Innovative Tools and Integrated Energy Solutions* [Online]. Available: http://www.twenties-project.eu

[11] Y. Zong, D. Kullmann, A. Thavlov, O. Gehrke, and H. W. Bindner, "Application of model predictive control for active load management in a distributed power system with high wind penetration," *IEEE Trans. Smart Grid*, vol. 3, no. 2, pp. 1055–1062, Jun. 2012.

[12] P. Bacher and H. Madsen, "Identifying suitable models for the heat dynamics of buildings," *Energy Buildings*, vol. 43, no. 7, pp. 1511–1522, Jul. 2011.

[13] A. Thavlov, "Dynamic optimization of power consumption," Master's dissertation, DTU IMM, Tech. Univ. Denmark, Lyngby, Denmark, 2008.

[14] K. K. Andersen, H. Madsen, and L. H. Hansen, "Modelling the heat dynamics of a building using stochastic differential equations," *Energy Buildings*, vol. 31, no. 1, pp. 13–24, Jan. 2000.

[15] ISO 13790, "Energy performance of buildings—Calculation of energy use for space heating and cooling," 2008.

Anders Thavlov (S'12) was born in Copenhagen, Denmark, in 1979. He received the master's degree from the Department of Informatics and Mathematical Modeling, Technical University of Denmark, Kongens Lyngby, Denmark, in 2008, where he is currently pursuing the Ph.D. degree in the Energy System Operation and Management Group from the Department of Electrical Engineering.

His current research interests include stochastic modeling, demand-side management, and power system modeling.

Henrik W. Bindner (M'10) was born in Copenhagen, Denmark, in 1964. He received the M.Sc. degree in electrical engineering from the Technical University of Denmark (DTU), Kongens Lyngby, Denmark, in 1988.

Since 1990, he has been with DTU, where he is currently leading a research group concerned with operation and control of active distribution grids, control of distributed energy resource, and associated information and communications technology (ICT) infrastructures. His current research interests include the fields of integration of renewable energy into the power system, control systems, and ICT infrastructure for management of DERs to enable them to be active participants in the control of the power system.

PAPER E

Application of Model Predictive Control for Active Load Management in a Distributed Power System With High Wind Penetration

---

Minor contribution: Presented in *IEEE Transactions on Smart Grid*, vol. 3, nr. 2.

IEEE TRANSACTIONS ON SMART GRID, VOL. 3, NO. 2, JUNE 2012 1055

Application of Model Predictive Control for Active Load Management in a Distributed Power System With High Wind Penetration

Yi Zong, Daniel Kullmann, Anders Thavlov, Oliver Gehrke, and Henrik W. Bindner

***Abstract*—This paper introduces an experimental platform (SYSLAB) for the research on advanced control and power system communication in distributed power systems and one of its components-an intelligent office building (PowerFlexHouse), which is used to investigate the technical potential for active load management. It also presents in detail how to implement a thermal model predictive controller (MPC) for the heaters' power consumption prediction in the PowerFlexHouse. It demonstrates that this MPC strategy can realize load shifting, and using good predictions in MPC-based control, a better matching of demand and supply can be achieved. With this demand side control study, it is expected that MPC strategy for active load management can dramatically raise energy efficiency and improve grid reliability, when there is a high penetration of intermittent energy resources in the power system.**

***Index Terms*—Active load management, distributed power system, flexible consumption, model predictive control, wind power penetration.**

NOMENCLATURE

CHP	Combined heat and power.
$C_{(k)}$	Dynamic price signal at sample time k.
CTSM	Continuous time stochastic modelling.
DERs	Distributed energy resources.
DGs	Distributed generators.
DR	Demand response.
H_p	Prediction horizon.
MPC	Model predictive control.
RMI	Remote method invocation.
$P_{heat-max}$	Maximum permitted electrical power consumption of heating units.
T_a	Ambient (outdoor) temperature.
T_i	Indoor air temperature.
T_{i-max}	Set-point of the maximum indoor air temperature.
T_{i-min}	Set-point of the minimum indoor air temperature.
T_{im}	Temperature of the heat accumulating layer in the inner walls and floor.
T_i^k	Predictive indoor temperatures at each sample time k over the prediction horizon H_p.
$T_i^{(k/k)}$	Actual indoor temperature at sample time k.
$T_i^{(k/k-1)}$	Previous (at last sample time $k-1$) predictive indoor temperature (at next sample time k).
$T_i^{(k+H_P/k)}$	Predictive indoor temperature at the end of the predictive horizon.
T_{om}	Temperature of the heat accumulating layer in the building envelope.
T_{ref}	Reference indoor temperature.
Φ_s	Solar irradiation.
Φ_h	Energy input from the electrical heaters.
$\boldsymbol{u}_{(k)}$	Optimized heat input sequence at sample time k.

Manuscript received December 03, 2010; revised June 20, 2011; accepted November 12, 2011. Date of publication February 10, 2012; date of current version May 21, 2012. This work was supported by Interreg IV A program, project "Wind in Oresund" with Lund University, Technical University of Denmark-department IMM & CET, DTU and Risø DTU. Paper no. TSG-00391-2010.

The authors are with the Intelligent Energy Systems, Risø DTU, National Laboratory for Sustainable Energy, 4000 Roskilde, Denmark (e-mail: yizo@risoe.dtu.dk; daku@risoe.dtu.dk; atha@risoe.dtu.dk; olge@risoe.dtu.dk; hwbi@risoe.dtu.dk).

Digital Object Identifier 10.1109/TSG.2011.2177282

I. INTRODUCTION

THE REDUCTION of CO_2 emissions and the introduction of generation based on renewable sources become important topics at present. Wind power will cover 50% of the Danish electricity consumption in 2025 according to Energinet.dk [1], and the Danish government has set a long term target of achieving a Danish energy supply based on 100% renewable energy from combinations of wind, biomass, wave and solar power in 2050 [2]. The electric power system of Denmark exhibits some unique characteristics. Since 1980s, the Danish power system has been evolving from a centralized to a very much distributed system, due to increased penetration of wind turbines and distributed generators (DGs), such as combined heat and power (CHP). Most of these DGs are connected to the network at the distribution level. However, as most of the renewable sources (wind and solar) of electricity are intermittent, their contribution to the grid is limited, unless the grid is flexible enough to absorb the variations from these sources.

To integrate such a high share of intermittent resources into the energy system, especially the electricity supply, it places

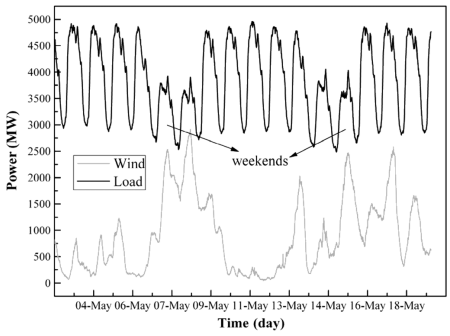

Fig. 1. Load and wind power variations (data source: Energinet.dk).

strong demands on flexibility elsewhere in the system. Fig. 1 shows power consumption and wind power generation in Denmark over a period of 16 days. It is shown that the load has a daily and weekly pattern with some stochastic variations and the wind power varies stochastically as well, but having no correlation with the load. Both the lack of correlation and the stochastic nature of the wind power put very strong requirements for flexibility on the rest of the system [3]. Traditionally, there has been a separation between the production and consumption of electricity: Consumption has been regarded a passive part of the system with respect to control, and therefore any generation mismatch caused by variations in renewable energy production has had to be compensated by other generating units. Furthermore, the introduction of new, energy-efficient technologies such as electrical cars can result in even more fluctuating electricity consumption. Lowering and shifting the peak loads is desirable to prolong the usage of the available grid capacity. In recent years, it has been realized that there is a large potential for additional flexibility in the control of power systems by enabling the active participation of the consumption side in the balancing of power supply and demand. Therefore, there is a great need to investigate how flexible consumption should be implemented, seen from the perspective of power system control as well as from that of a consumer. Any such system should be integrated with the rest of the power grid's control system—probably by means of an aggregation mechanism and a market for system services.

The introduction of distributed energy resources (DERs) together with the introduction of more information and communication technology in the electricity system provides interesting and novel automated demand response (DR) opportunities at the domestic user level. Household thereby becomes more active end-users of electricity. The two-way communication capability in the smart grid allows widespread deployment of "demand response" technologies and programs thereby allowing the load to adjust to supply variations. In order to gain acceptance, the user's needs should be met without much noticeable compromise on perceived comfort. Ideally, the user would stay in control while providing flexibility to the grid. A wide body of literature states that how to activate the potential of ancillary services from DERs and DR, thereby exploiting their ability to contribute to power system operation [4]–[11], but most of their work was based on the simulation study.

MPC refers to a class of control algorithms that compute a sequence of manipulated variable adjustments over a future time horizon by utilizing a process model to optimize forecasts of process behavior based on a linear or quadratic open-loop performance objective, subjected to equality or inequality constraints [12]. Today many MPC algorithms have been developed to guarantee some fundamental properties, such as the stability of the resulting closed-loop system or its robustness with respect to a wide class of external disturbances and/or model uncertainties. Therefore, MPC is now recognized as a very powerful approach with well established theoretical foundations and proven capability to handle a large number of industrial control problems [13], [14]. MPC for building climate control has been investigated in several papers before [15]–[17], mainly with the purpose of increasing the energy efficiency. The potential of MPC in power management was investigated in [18], but the ambient temperature was assumed to be constant in its simulation scenarios.

The objective of our research is to implement a control methodology, which uses residential optimization potential to support the introduction of a large penetration level of renewable energy (especially wind) and optimize usage of the current distributed power grid capacity. In this work we give a more detailed description of model predictive control (MPC) strategy applied on an experimental facility (SYSLAB) to investigate technical potential of active load management. Compared to the aforementioned literature, the novel contributions of this work are: 1) implementation of a low-complexity MPC scheme which is used to realize the load shifting for the heaters' power consumption in PowerFlexHouse; 2) integration of weather forecast information and dynamic power price in the MPC-based control strategy; and 3) field test the MPC strategy on a real power grid with high penetration of wind power.

The remaining of this paper is organized as follows: in Section II we briefly introduce Risø's new test facility (SYSLAB) for intelligent, active and distributed power systems and one of its components—PowerFlexHouse. How to implement a thermal model predictive controller for the power consumption prediction in PowerFlexHouse is provided in Section III, including the description on a heat dynamic model for temperature prediction. Then, some results and analysis of running the MPC controller on SYSLAB test platform are shown in Section IV. Finally, conclusion is drawn in Section V, followed by the discussion on future research.

II. Experimental Facility-Syslab Description

Risø DTU has established a flexible platform for research in advanced control systems and concepts, power system communication and component technologies for distributed power systems-SYSLAB. It is built around a small power grid with renewable (wind, solar) and conventional (diesel) power generation, battery storage, and various types of consumers [19]. Currently components on the SYSLAB platform are listed as following (see Fig. 2):

- Gaia wind turbine (11 kW);
- Bonus wind turbine (55 kW);
- Diesel generator set (48 kW/60kVA);
- Solar panel (7 kW);

Fig. 2. Components in SYSLAB.

- Vanadium battery (15 kW/120kWh);
- Capacitor bank (46 kVAr);
- Back-to-back converter (30 kW/45kVA);
- Dump load (75kW);
- Office building-PowerFlexHouse (20 kW);
- Plug-in hybrid car (9 kWh).

The SYSLAB facility is spread across multiple locations at Risø DTU and its backbone is formed by a 400 V grid with several busbars and substations (see Fig. 3). A central crossbar switch with tap-changing transformers enables meshed operation and power flow control. All components on the grid—generators, loads, storage systems, switchgear—are automated and remote-controllable. Each component is supervised locally by a dedicated controller node. The node design combines an industrial PC, data storage, measurement and I/O interfaces, backup power, and an Ethernet switch inside a compact, portable container. All nodes are interconnected via redundant high speed Ethernet, in a flexible setup permitting on-line changes of topology and the simulation of communication faults. The whole system can be run centrally from any point on the network, or serve as a platform for fully decentralized control [20]. All SYSLAB controller nodes run the SYSLAB software stack, which is a modular framework for developing distributed control systems for power systems. It is written in the Java (TM) programming language. Each physical SYSLAB component is controlled by a software module designing on one of the SYSLAB nodes. Distributed controllers can control these components by using one of the supported types of communication. The one most used is the Java RMI (Remote Method Invocation) system.

One of the components on the SYSLAB grid is a small, intelligent office building, PowerFlexHouse. It contains seven offices, a meeting room, and a kitchen. Each room is equipped with a motion detector, temperature sensors, light switches, window and door contacts, and actuators. A meteorology mast outside of the building supplies local environmental measurements of ambient temperature, wind speed, wind direction, and solar irradiation. The electrical load of the building consists of heating, lighting, air-conditioning, a hot-water supply, and various household appliances, such as a refrigerator and a coffee machine. The combined peak load of the building is close to 20 kW. All individual loads in the building are remote-controllable

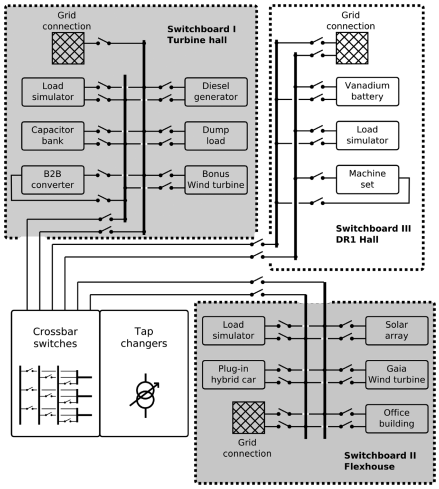

Fig. 3. Layout of SYSLAB.

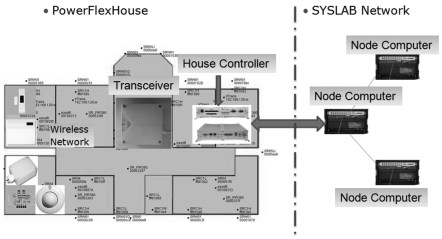

Fig. 4. Communication between PowerFlexHouse and SYSLAB.

from a central building controller. The controller software runs on a Linux-based PC. It is written in Java (TM) and is based on the SYSLAB software stack. The controller software consists of several modules working together. The hardware module collects data from the sensors and sends commands to the actuators. It does this via serial port (communication with the meteorology mast), modbus (switchboard instruments), and wireless transceivers (Enocean and infrared). The database module collects all sensor measurements and all commands sent to the actuators for further analysis. Another module collects data from external sources: the Nord Pool power price, the local weather forecast data, and some state information from the Danish power system. Finally, the controller module supports the development of any kind of controller algorithm for the PowerFlexHouse. The controller is able to communicate with the SYSLAB grid through its own node computer (See Fig. 4). Information can also flow in the other direction, for example providing the power system controller with the expected near-future behavior of the building loads.

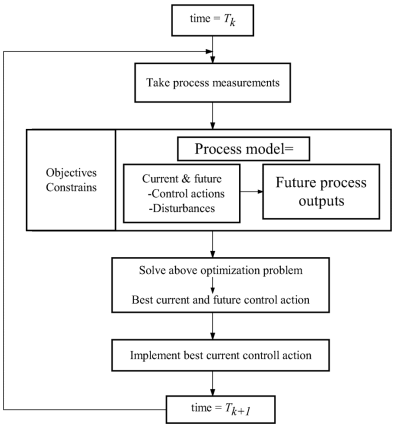

Fig. 5. Model predictive control scheme.

III. MPC Controller For Load Shifting In PowerFlexHouse Heating Strategy

One of the main energy consumption in northern Europe is the electrical heating in the long winter. Heaters are designated as one of the most obvious areas of flexible consumption or demand response. Due to the prediction horizon, an MPC controller can take benefit of knowledge over the future, such as predictive energy demand and it was selected to realize the load shifting for heating in PowerFlexHouse. The objective of this project is to minimize the daily operational cost of heating and provide ancillary services for the power system. Fig. 5 presents the model predictive control scheme.

The main principle of MPC is to transform the control problem into an optimization one and solve this optimization problem over a prediction horizon at each sample time, subjected to system dynamics, an objective function (linear or quadratic), and constraints on states, actions and inputs. At each control step the optimization obtains a sequence of actions optimizing expected system behavior over the prediction horizon. Only the first step of the sequence of control actions is executed by the controller on the system until the next sample time, after which the procedure is repeated with new process measurements [21]. The following subsections describe in detail the prediction model, objective function and control law, which are three important components for MPC algorithm.

A. Thermal Predictive Model For PowerFlexHouse

The indoor temperature model of PowerFlexHouse is given as a stochastic discrete-time linear state-space model, which was directly obtained from [22]. The heat flow in PowerFlexHouse is modeled by a gray-box approach, using physical knowledge about heat transfer together with statistical methods to estimate model parameters. To reduce the complexity, the model of heat dynamics of the PowerFlexHouse is formulated as one large room exchanging heat with an ambient environment. That is to say, we regard the 8 rooms in PowerFlexHouse building as one large room. Heat transfer due to conduction, convection

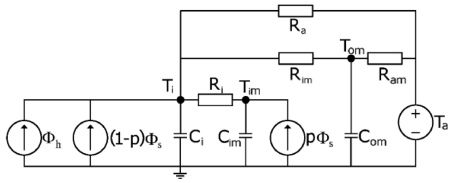

Fig. 6. Equivalent RC-circuit for the heat dynamic model.

and ventilation is assumed linear with the temperature difference on each side of the medium. When assuming these properties, the heat model can be formulated as an equivalent electric circuit with resistors and capacitors (an RC-circuit), where potential differences are equal to temperature differences and flow of charge equals heat flow. In such a circuit, the resistors can be regarded as resistance to transfer heat and the capacitors as heat storage. The equivalent RC-circuit for the heat dynamic model is shown in Fig. 6. In Fig. 6 the parameter p means a percentage of the solar irradiation, which is absorbed by the inner walls and the rest is absorbed by the indoor air. Based on four time series collected in PowerFlexHouse in the first quarter of 2008, the parameters in Fig. 6 were estimated using maximum likelihood estimation. The estimator was continuous time stochastic modelling (CTSM), which is an estimation tool developed at IMM DTU [23].

The control object is the indoor air temperature T_i. The state-space equations were expressed in (1) and (2):

$$T(\mathrm{t}+1) = \Phi T(\mathrm{t}) + \Gamma U(\mathrm{t}) \tag{1}$$

$$\mathrm{Output}: \mathrm{y}(t) = CT(\mathrm{t}) = [\,1 \quad 0 \quad 0\,] \begin{bmatrix} T_i(t) \\ T_{im}(t) \\ T_{om}(t) \end{bmatrix}. \tag{2}$$

Φ is the system matrix [3 × 3]. Γ is the control matrix [3 × 3]. $T = [T_i, T_{im}, T_{om}]$ is the state vector and $U = [T_a, \Phi_s, \Phi_h]$ is the input vector to the system. Here, $T_i(t)$ is the indoor air temperature; $T_{im}(t)$, and $T_{om}(t)$, which are the temperature of the heat accumulating layer in the inner walls and floor, and the temperature of the heat accumulating layer in the building envelope. T_a is the ambient (outdoor) temperature; Φ_s is the solar irradiation; and Φ_h is the energy input from the electrical heaters. Among them, $T_{im}(t)$ and $T_{om}(t)$ cannot be measured and state estimator-Kalman filter can be used to estimate these two states.

B. MPC Objective Function

The goal of the MPC control strategy for the electrical space heaters in PowerFlexHouse is to minimize the total cost of the energy used in heating over a prediction horizon (H_p). At the same time, it should keep the indoor air temperature close to the given reference temperature T_{ref}. The objective function can be formulated as

$$J = \min \left[\sum_{k=0}^{H_p-1} C_{(k)} \times u_{(k)} + \sum_{k=0}^{H_p-1} w \times \left| T_i^k - T_{\mathrm{ref}} \right| \right] \tag{3}$$

Subject to: $u_{(k)} \in int[0, 1, 2, 3, 4, 5, 6, 7, 8, 9, 10]$ in kW, which means the heat input that the MPC controller determines by using a mixed integer optimization approach. There are totally

10 heaters in the PowerFlexHouse. Each of them has a power of 1 kW. Therefore the maximum permitted electrical power consumption of heating units is $P_{\mathrm{heat-max}} = 10 \times 1\ \mathrm{kW} = 10\ \mathrm{kW}$. The weight coefficient w in (3) is used to tune performance of the MPC controller. In (3), $C_{(k)}$ is the dynamic power price signal obtained from the Nord Pool spot market [24]. The Nordic electricity market is well-known for its efficient market function. The central market is the Nord Pool spot market, which is owned by the four Nordic Transmission System Operators (Statnett SF, Svenska Kraftnätt, Fingrid, and Energinet.dk) and where a daily competitive auction establishes a price for each hour of the next day. The trading horizon is 12–36 h ahead and is done for the next day's 24-h period. That is to say, the minimum prediction horizon is at least 12 h and the actual maximal prediction horizon can reach 36 h. In the Nordic system, during the night, there is a large production by wind turbine. It can be expected that sometime the price variation reflects the level of wind power penetration.

C. MPC Control Strategy

For the purpose of flexible consumption, there is a temperature set-point margin for the consumer to choose via a user interface. For example, when the wind energy production is low, the heaters will work at the lower temperature limit, otherwise, they will be set up to the upper limit. Only when the indoor air temperature is in the range of $[T_{\mathrm{i-min}} T_{\mathrm{i-max}}]$, the MPC control algorithm is executed. In addition, the local forecast data of the ambient (outdoor) temperature T_a and the solar irradiation Φ_s are updated twice a day for the next 48 h, which are provided by the meteorology group in Wind Energy Division at Risø DTU. The maximum relative error between the actual weather measurement and the weather forecast data is $\pm 5\%$ on test. Therefore, we concluded that the local weather forecast data are available to be integrated into the MPC-based control strategy.

First, the controller output is initialized by the vector of dimension $1 \times H_p$, $\boldsymbol{u}_0 = [u_0, \ldots, u_{Hp-1}]$, containing the input variables of the plant which are optimized. However, the initialization of the algorithm assumes that the heating units are switched off, $\boldsymbol{u}_0 = [0, \ldots, 0]$. By this way, the search direction is always positive and the optimization speed can be accelerated. Second, the difference between the predictive indoor air temperature at the end of the predictive horizon and the desired T_{ref} is evaluated at each control step. If this difference is small enough to be acceptable: $|T_i^{(k+H_P/k)} - T_{\mathrm{ref}}| \leq \varepsilon$, an optimal solution is achieved and only the first element of the controller output sequence (u_0) is used to control the process. At the next sample $(k+1)$, the whole procedure is repeated. Otherwise, the first element of the controller output sequence with the maximum or minimum power consumption of the heating units is used to control the process ($u_0 = P_{\mathrm{heat-max}}$ or $u_0 = 0$). Finally, to overcome the model's error, here we use the process's real-time output and model's (previous) predictive output to structure one model output feedback correction (see Fig. 7). [25].

The detailed MPC control law is described as follows:

Step 1: Initialization step. $\boldsymbol{u}_0 = [u_0, \ldots, u_{Hp-1}]$, where H_p is the prediction horizon, $\boldsymbol{u}_0 = 0$.

Step 2: At current time k, measure the current indoor air temperature $T_i^{(k/k)}$ and compare it with the previous predictive value $T_i^{(k/k-1)}$ to obtain the predictive error $e = T_i^{(k/k)} - T_i^{(k/k-1)}$.

Step 3: Calculate the optimal control sequence that minimizes the objective function.

$$\left\{\boldsymbol{u}_{(k)} = [u_0, \ldots, u_{Hp-1}]\right\} = \arg J = \min\left[\sum_{k=0}^{H_p-1} C_{(k)} \times u_{(k)} + \sum_{k=0}^{H_p-1} w \times \left|T_i^k - T_{\mathrm{ref}}\right|\right].$$

Use the model to predict the indoor air temperature at each sample time k over the prediction horizon H_p.

$$T_i^k = \left[T_i^{(k+1/k)}, \ldots T_i^{(k+i/k)} \ldots, T_i^{(k+H_p/k)}\right],\ 1 \leq i \leq H_p$$

and correct the predictive value to $T_i^k + e$.

If $|T_i^{(k+Hp/k)} - T_{\mathrm{ref}}| \leq \epsilon$ and $\forall T_i^{(k+i/k)}, T_{i-\min} \leq T_i^{(k+i/k)} \leq T_{i-\max}$, where $1 \leq i \leq H_p$ and ϵ is a small number.
Go to step 4.
else
if $\forall T_i^{(k+i/k)}, T_i^{(k+i/k)} \geq T_{i-\max}$, where $1 \leq i \leq H_p$

$$u_o = 0$$

else

$$u_0 = P_{heat-max} = 10$$

end if
end if

Step 4: Apply u_0 to heating units.
Next sample, update $k := k+1$, and repeat from step 2 to step 4.

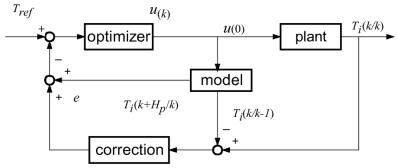

Fig. 7. Block diagram of PowerFlexHouse's MPC.

When we test this MPC controller on the SYSLAB platform, it employs a control step of 10 min. It means that every 10 min, the controller determines which control action to take at the current time. First of all, the MPC controller obtains a measurement of the current state of the house, including the disturbances like the state of doors and windows, and the grid information, such as dynamic power price signal, available power and frequency signal from the test platform SYSLAB. To find the best predicted performance over the prediction horizon, the mixed-integer linear programming problem is solved by GLPK's (GNU Linear Programming Kit) solver with Java native interface [26]. Then it integrates the weather forecast data (ambient temperature and solar irradiation, etc.) with the prediction model for the house indoor temperature, and verifies the predictive values. At

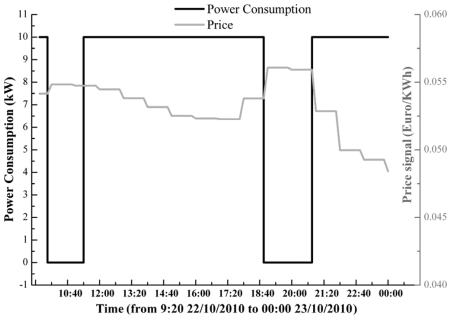

Fig. 8. Optimized predictive power consumption in the next 15 h.

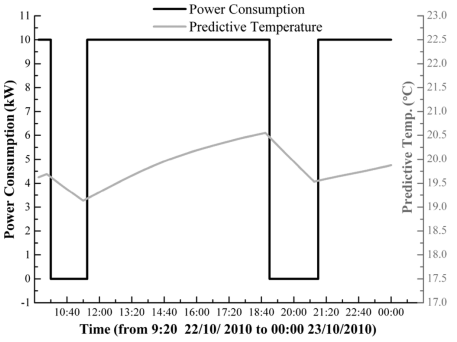

Fig. 9. Predictive indoor air temperature in the next 15 h.

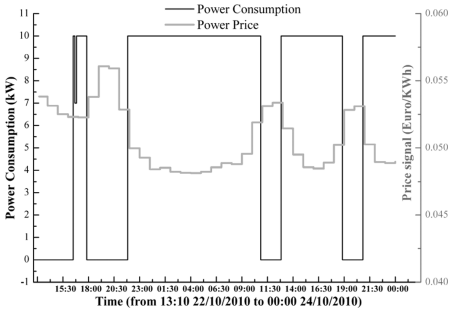

Fig. 10. Optimized predictive power consumption in the next 35 h.

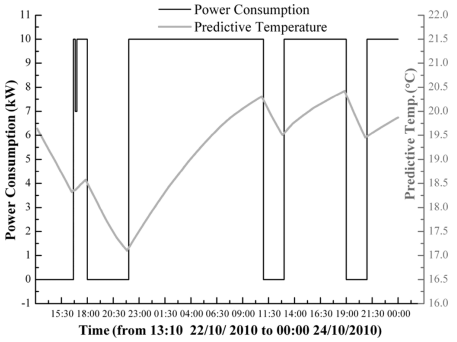

Fig. 11. Predictive indoor air temperature in the next 35 h.

last, only the first step in the found best sequence of actions is executed.

IV. Results

We obtained some results from the field test on October 22-24, 2010. At 9:20 the MPC control algorithm was running on the SYSLAB platform and it provided the optimized profile of the predictive power consumption in the next approximately 15 h for the PowerFlexHouse's heaters, as shown in Fig. 8. Fig. 9 demonstrates the predictive indoor air temperature in the next 15 h according to the optimized switch schedule (the same as in Fig. 8). At 13:10, the MPC produced the results shown in Fig. 10. It presents the optimized profile of the predictive power consumption in the next almost 35 h for the PowerFlexHouse's heaters. At this moment, the prediction horizon could reach 35 h, because the Nord Pool spot market at 13:00 (on the same day) provided next day's 24 h price information for the users. The predictive indoor air temperature in the next 35 h is shown in Fig. 11, according to the optimized switch schedule (the same as in Fig. 10) for heaters in PowerFlexHouse. It can be observed in Fig. 11 that during a few hours the predictive temperature dropped to 17 ^{circ}C. Comparing Fig. 9 with Fig. 11, it can be found that the shorter the prediction horizon the better the predictive control effect. We could tune MPC performance by penalizing this temperature deviation with different weight coefficient values w in (3). Otherwise, users will have some discomfort if they would like to accept a reduced energy bill and allow this deviation on the room temperature. Compared with one thermostat controller, it was observed that the MPC-based controller almost worked within the low price period and it was able to shift the load and reduce the total cost of operating electrical heaters to meet certain indoor temperature requirements.

The hours when the maximum and minimum spot prices occur in 2010 (data source: Nord Pool) are presented in Fig. 12 and Fig. 13 respectively. There is certain predictability in the occurrence of peak load periods during the day, and this predictability is reflected in the hourly spot price. In Fig. 12, the peak load periods and high spot prices occur mainly in the same hours of the day (morning 8:00-11:00 and afternoon 17:00–20:00), because in the morning the main loads are from the industries and offices; and in the afternoon from 17:00-20:00 it is rush time to cook and amuse at home in Denmark. Fig. 13 illustrates the low spot prices take place in the deep of night, due to industries and domestic users shut down most of their consumption at night while the wind turbines are still producing roughly amount of energy. Fig. 8 and Fig. 10 illustrate that MPC control strategy can achieve energy savings by shifting load from on-peak to off-peak period. According to [27], it is concluded that the spot price, generally decreases when the wind power penetration in the power system increases, that is

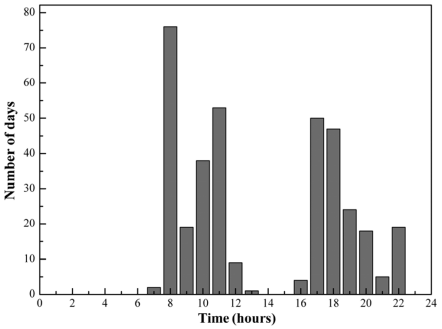

Fig. 12. Histogram of the occurrence of maximum spot prices in 2010 from Nord Pool.

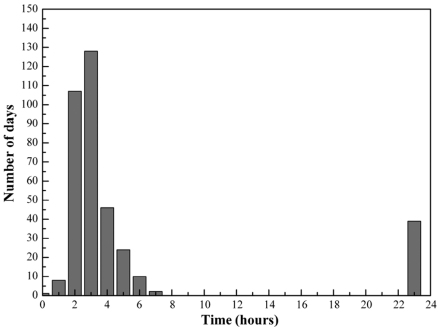

Fig. 13. Histogram of the occurrence of minimum spot prices in 2010 from Nord Pool.

to say, the Nordic Electricity spot prices reflect the amount of wind power in the system. At the same time, it shows that MPC control strategy can be investigated on active load management in this intelligent house, which is used to stabilize fluctuations in the power grid with a high penetration of wind power and other renewable energy.

V. Conclusion And Future Research

Flexible consumption must be established in order to enable more use of renewable energy in power system. The predictive behavior of power consumption for Power FlexHouse's heaters shows that the MPC strategy is feasible for active load management of intelligent houses in a distributed power system with high wind penetration. Using dynamic power prices and integrating the weather forecast data, it demonstrates that the MPC control strategy is able to shift the electrical load to periods with low prices. Residential customers can avoid high electricity price charge at peak time, and the power grid can benefit from load control. It also shows that the local (within the house) MPC controller can result in a generic solution supporting different technologies and houses with different optimization potential, which can provide services for the global controllers (aggregators) in a scope of a group of houses, e.g., a neighborhood (micro grid) or a global scope (virtual power plant). The load in a power grid is widely seen as one of the keys to achieving additional operational flexibility to ensure the stability of the grid as penetration levels rise. However, in comparison with the actual power system presented within the SYSLAB, it shows that the efficient use of load management demands a tight integration with the control system of the power grid.

Future work should be focused on the different optimization methods, analyzing the effect of the predictive horizon length on the performance in the MPC controller, and the robustness of this MPC controller against uncertainty in measurements and prediction. Furthermore, a multiagent MPC should be taken into account to find an acceptable near-optimal solution for the whole distributed power system.

Acknowledgment

The authors would like to express their appreciation to Andrea N. Hahmann, Senior Scientist, from Wind Energy Division, Risø DTU National Laboratory for Sustainable Energy, for her work on providing us with the local weather forecast data.

References

[1] Ministry of Transport and Energy, Energistrategi 2025 2007.
[2] K. Richardson, D. Dahl-Jensen, J. Elmeskov, C. Hagem, J. Henningsen, J. A. Korstgård, N. B. Kristensen, P. E. Morthorst, J. E. Olesen, and M. Wier, "Green energy—The road to a Danish energy system without fossil fuels," Danish Commission on Climate Change Policy 2010 [Online]. Available: http://greengrowthleaders.org/green-energy-the-road-to-a-danish-energy-system-without-fossil-fuels/
[3] Y. Zong, D. Kullmann, A. Thavlov, O. Gehrke, and H. W. Bindner, "Model predictive control strategy for a load management research facility in the distributed power system with high wind penetration-towards a danish power system with 50% wind penetration," in *Proc. 2011 Asia-Pacific Power Energy Eng. Conf.*, p. 106494.
[4] R. R. Negenborn, M. Houwing, B. D. Schutter, and H. Hellendoorn, "Active prediction model accuracy in the control of residential energy resources," presented at the IEEE Int. Conf. Control Appl., San Antonio, TX, Sep 3–5, 2008.
[5] M. A. A. Pedrasa, T. D. Spooner, and I. F. MacGill, "Coordinated scheduling of residential distributed energy resources to optimize smart home energy services," *IEEE Trans. Smart Grid*, vol. 1, no. 2, pp. 109–119, Sep. 2010.
[6] P. Nyeng, K. O. Helgesen Pedersen, and J. Østergaard, "Ancillary services from distributed energy resources-perspectives for the Danish power system," presented at the Int. Youth Conf. Energitics, Budapest, Hungary, May 31–Jun. 2 2007.
[7] A. Molderink, V. Bakker, M. G. C. Bosman, J. L. Hurink, and G. J. M. Smit, "Management and control of domestic smart grid technology," *IEEE Trans. Smart Grid*, vol. 1, no. 2, pp. 109–119, Sep. 2010.
[8] J. Medina, N. Muller, and I. Roytelman, "Demand response and distribution grid operations: Opportunities and challenges," *IEEE Trans. Smart Grid*, vol. 1, no. 2, pp. 193–198, Sep. 2010.
[9] T. J. Lui, W. Stirling, and H. O. Marcy, "Get smart," *IEEE Power Energy Mag.*, vol. 8, no. 3, pp. 66–78, May/Jun. 2010.
[10] X. Guan, Z. Xu, and Q. Jia, "Energy-efficient buildings facilitated by microgrid," *IEEE Trans. Smart Grid*, vol. 1, no. 3, pp. 243–252, Dec. 2010.
[11] H. Saele and O. S. Grande, "Demand response from household customers: Experiences from a pilot study in Norway," *IEEE Trans. Smart Grid*, vol. 2, no. 1, pp. 90–97, 2011.
[12] R. Soeterboek, *Predictive Control—A Unified Approach.* Upper Saddle River, NJ: Prentice-Hall, 1992, ch. 1.
[13] R. Scattolini, "Architectures for distributed and hierarchical model predictive control-A review," *J. Process Control*, no. 19, pp. 723–731, 2009.
[14] D. Q. Mayne, J. B. Rawlings, C. V. Rao, and P. O. M. Scokaert, "Constrained model predictive control: Stability and optimality," *Automatica*, vol. 36, pp. 789–814, 2000.
[15] F. Oldewurtel, A. Ulbig, A. Parisio, G. Andersson, and M. Morari, "Reducing peak electricity demand in building climate control using real-time pricing and model predictive control," in *Proc. 2010 IEEE Conf. Decision Control (CDC)*, pp. 1927–1932.

[16] Y. Ma, F. Borrelli, B. Hencey, B. Hencey, B. Coffey, and P. Haves, "Model predictive control for the operation of building cooling systems," *IEEE Trans. Control Syst. Technol.*, pp. 1–8, Mar. 2011 [Online]. Available: http://ieeexplore.ieee.org
[17] F. Oldewurtel, A. Parisio, C. N. Jones, M. Morari, D. Gyalistras, M. Gwerder, V. Stauch, B. Lehmann, and K. Wirth, "Energy efficient building climate control using stochastic model predictive control and weather predictions," in *Proc. 2010 Amer. Control Conf.*, pp. 5100–5105.
[18] T. G. Hovgaard, K. Edlund, and J. B. Jørgensen, "The potential of economic MPC for power management," in *Proc. 2010 IEEE Conf. Decision Control (CDC)*, pp. 7533–7538.
[19] [Online]. Available: http://www.risoe.dtu.dk/research/sustainable_energy/wind_energy/projects/syslab.aspx
[20] B. Pedersen and H. Bindslev, "Risø DTU annual report 2009," Risø DTU, Denmark, Rep. Risø-R-1723 (EN), Jun. 2010.
[21] Y. Zong, D. Kullmann, A. Thavlov, O. Gehrke, and H. W. Bindner, "Active load management in an intelligent building using model predictive control strategy," presented at the IEEE PES PowerTech2011 Conf., Trondheim, Norway, Jun. 19–23, 2011.
[22] A. Thavlov, "Dynamic optimization of power consumption," M.S. thesis, Tech. Univ. Denmark, Kongens Lyngby, Denmark, 2008, Ch. 7.
[23] "Continuous time stochastic modelling" [Online]. Available: http://www2.imm.dtu.dk/~ctsm/
[24] "The Nord Pool Spot Market" [Online]. Available: http://www.nordpoolspot.com/reports/systemprice
[25] Y. Zong, D. Kullmann, A. Thavlov, O. Gehrke, and H. W. Bindner, "Active load management in an intelligent building using model predictive control strategy," in *Proc. PowerTech 2011 Conf.*, p. 1700589.
[26] GNU Linear Programming Kit [Online]. Available: http://glpk-java.sourceforge.net/
[27] W. Hu, Z. Chen, and B. Bak-Jensen, "The relationship between electricity price and wind power generation in Danish electricity markets," in *Proc. 2010 Asia-Pacific Power Energy Eng. Conf.*, p. 5448739.

Yi Zong was born in Wuhan, Hubei province, China, on August 21, 1971. She graduated in Control Engineering and Control Theory from Wuhan University of Science and Technology. She received the Ph.D. degree in system engineering and automation, from the University Complutense, Madrid, Spain, in 2006.

Her employment experience includes the Wuhan Institute of Technology. Since 2006 she was employed as a postdoc in the Wind Energy Division, Risø DTU National Laboratory for Sustainable Energy, Roskilde, Denmark. She is currently a Scientist at Intelligent Energy Systems, Risø DTU. Her special fields of interest include advanced and intelligent control for demand side units in households and industry supporting flexible power consumption.

Daniel Kullmann was born in Frankfurt/Main, Germany, on August 15, 1973. He graduated in computer science from Darmstadt University of Technology, Darmstadt, Germany, in 2002. He is currently working toward the Ph.D. degree at Risø National Laboratory, Roskilde, Denmark.

He worked for several years in the IT industry. His fields of interest are distributed control and communication in power systems.

Anders Thavlov was born in Copenhagen, Denmark, on June 3, 1979. He graduated from Department of Informatics and Mathematical Modeling at Technical University of Denmark in 2008. He is currently working toward the Ph.D. degree at the Intelligent Energy Systems at Risø DTU National Laboratory for Sustainable Energy, Roskilde, Denmark.

His main research interests are energy systems modeling and control.

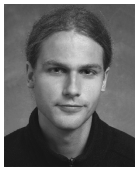

Oliver Gehrke was born in Frankfurt am Main, Germany, on March 15, 1975. He graduated in electrical power engineering from the Darmstadt University of Technology, Darmstadt, Germany. He received the Ph.D. degree from Risø National Laboratory, Roskilde, Denmark.

He is currently a Scientist at Risø DTU. His special fields of interest include the embedded and distributed control of power systems with a high penetration of renewable energy sources.

Henrik Bindner was born in Copenhagen, Denmark, on June 30, 1964. He received the M.S. degree in electrical engineering from the Technical University of Denmark in 1988.

Since 1990 he has been with Risø DTU National Laboratory for Sustainable Energy, Roskilde, Denmark, in the Wind Energy Division, currently as a Senior Scientist. He has mainly been working on integration of wind energy into power system. The work has included analysis, design, and control of small island systems as well as technologies and techniques for integration of wind in large systems. Currently, he is researching how distributed energy resources can be applied to increase penetration of wind energy.

PAPER F

Active Load Management in an Intelligent Building using Model Predictive Control Strategy

---

Minor contribution: Presented in *IEEE Transactions on Smart Grid*, vol. 3, nr. 2.

Paper accepted for presentation at the 2011 IEEE Trondheim PowerTech

Active Load Management in an Intelligent Building Using Model Predictive Control Strategy

Yi Zong, Daniel Kullmann, Anders Thavlov, Oliver Gehrke, Henrik W. Bindner

***Abstract*--This paper introduces PowerFlexHouse, a research facility for exploring the technical potential of active load management in a distributed power system (SYSLAB) with a high penetration of renewable energy and presents in detail on how to implement a thermal model predictive controller for load shifting in PowerFlexHouse heaters' power consumption scheme. With this demand side control study, it is expected that this method of demand response can dramatically raise energy efficiencies and improve grid reliability, when there is a high penetration of intermittent energy resources in the power system.**

***Index Terms*--Active load management; distributed power system; flexible consumption; model predictive control; wind power penetration**

I. Introduction

Wind power will cover 50% of the Danish electricity consumption in 2025 according to Energinet.dk [1], and the Danish government has expressed a long term target of achieving a Danish energy supply based on 100% renewable energy from combinations of wind, biomass, wave and solar power in 2050 [2]. However, as most of the renewable sources of electricity are intermittent, their contribution to the grid is limited, unless the grid is flexible enough to absorb the variations from these sources.

To integrate such a high share of intermittent resources into the energy system, especially the electricity supply, it places strong demands on flexibility elsewhere in the system. Traditionally, there has been a separation between the production and consumption of electricity: Consumption has been regarded a passive part of the system with respect to control, and therefore any generation mismatch caused by variations in renewable energy production has had to be compensated by other generating units. In recent years, it has been realized that there is a large potential for additional flexibility in the control of power systems by enabling the active participation of the consumption side in the balancing of power supply and demand. Nowadays the production of electricity system follows the load. In the intelligent energy system (Smart Grid) the production controls the consumption. For example, when the wind blows or the sun shines, consumption will automatically be adjusted, and consumption and consumers will go from being passive participants to be active players in the electricity system.

The introduction of Distributed Energy Resources (DERs) together with the introduction of more information and communication technology in the electricity system provides interesting and novel automated Demand Response (DR) opportunities at the domestic user level. Household thereby become more active end-users of electricity. The two-way communication capability in the smart grid allows widespread deployment of "demand response" technologies and programs thereby allowing the load to adjust to supply variations. A widely body of literature states that how to activate the potential of ancillary services from DERs, thereby exploiting their ability to contribute to power system operation [3]-[8].

Developing the smart grid and linking it to smart appliances and other products having DR capabilities will reliably and predictably reduce appliance electricity consumption in real time [8]. This will create the opportunity for significant increases in energy efficiency and conservation and meaningful reductions in greenhouse-gas emissions. Therefore, there is a great need to investigate how flexible consumption should be implemented, seen from the perspective of power system control as well as from that of a consumer. Any such system will have to be integrated with the rest of the power grid's control system – probably by means of a market for system services and an aggregation mechanism. In order to gain acceptance, the user's needs would need to be met without much noticeable compromise on perceived comfort. Ideally, the user would stay in control while providing flexibility to the grid. The goal of our research is to implement a control methodology to use residential optimization potential to support the introduction of a large penetration level of renewable energy (especially wind) and optimize usage of the current distributed power grid capacity. In this work we give a more detailed description of Model

This work was supported by Interreg IV A program, project "Wind in Oresund" with Lund University, Technical University of Denmark - department IMM & CET (DTU) and Risø.

Yi Zong is with the Intelligent Energy Systems, Risø DTU, National Laboratory for Sustainable Energy, 4000, Roskilde, Denmark, (phone: +45-4677-5045; e-mail: yizo@risoe.dtu.dk).

Daniel Kullmann is with the Intelligent Energy Systems, Risø DTU, National Laboratory for Sustainable Energy, 4000, Roskilde, Denmark (e-mail: daku@risoe.dtu.dk).

Anders Thavlov is with the Intelligent Energy Systems, Risø DTU, National Laboratory for Sustainable Energy, 4000, Roskilde, Denmark. (e-mail: atha@risoe.dtu.dk).

Oliver Gehrke is with the Intelligent Energy Systems, Risø DTU, National Laboratory for Sustainable Energy, 4000, Roskilde, Denmark. (e-mail: olge@risoe.dtu.dk).

Henrik W. Bindner is with the Intelligent Energy Systems, Risø DTU, National Laboratory for Sustainable Energy, 4000, Roskilde, Denmark. (e-mail: hwbi@risoe.dtu.dk).

978-1-4244-8417-1/11/$26.00 ©2011

Predictive Control (MPC) strategy applied on an experimental facility (SYSLAB) to exploit technical potential of active load management.

MPC refers to a class of control algorithms that compute a sequence of manipulated variable adjustments by utilizing a process model to optimize forecasts of process behavior based on a linear or quadratic open-loop performance objective, subject to equality or inequality constraints over a future time horizon [9]. Here MPC-based control strategy is used to implement a controller for load shifting in an intelligent office building-PowerFlexHouse heaters' power consumption scheme.

This paper is organized as follows. In Section II we shortly introduce Risø's new experimental facility (SYSLAB) for distributed power systems and one of its components-PowerFlexHouse. How to implement a thermal model predictive controller for the power consumption prediction in PowerFlexHouse is provided in Section III, followed by some results and analysis of running the MPC controller on SYSLAB platform are shown in Section IV. Finally, Section V offers the conclusion and the future research.

II. Experimental Facility-SYSLAB Description

Risø DTU has established a flexible platform for research in advanced control systems and concepts, power system communication and component technologies for distributed power systems-SYSLAB. It is built around a small power grid with renewable (wind, solar) and conventional (diesel) power generation, battery storage, and various types of consumers [10]. Currently components on the SYSLAB platform are listed as following (See Fig. 1):

- Gaia wind turbine (11 kW)
- Bonus wind turbine (55 kW)
- Diesel generator set (48 kW/60kVA)
- Solar panel (7 kW)
- Vanadium battery (15 kW/120kWh)
- Capacitor bank (46 kVAr)
- Back-to-back converter (30 kW/45kVA)
- Dump load (75kW)
- Office building-PowerFlexHouse (20 kW)
- Plug-in hybrid car (9 kWh)

Fig. 1. Components in SYSLAB

The SYSLAB facility is spread across multiple locations at Risø DTU and its backbone is formed by a 400V grid with several busbars and substations (See Fig. 2). A central crossbar switch with tap-changing transformers enables meshed operation and power flow control. All components on the grid – generators, loads, storage systems, switchgear – are automates and remote-controllable. Each component is supervised locally by a dedicated controller node. The node design combines an industrial PC, data storage, measurement and I/O interfaces, backup power and an Ethernet switch inside a compact, portable container. All nodes are interconnected via redundant high speed Ethernet, in a flexible setup permitting on-line changes of topology and the simulation of communication faults. The whole system can be run centrally from any point on the network, or serve as a platform for fully decentralized control [11].

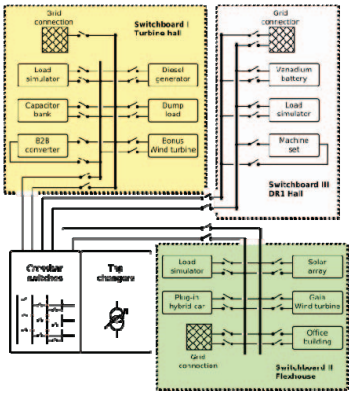

Fig. 2. Layout of SYSLAB

One of the components on the SYSLAB grid is a small, intelligent office building, PowerFlexHouse. It contains seven offices, a meeting room and a kitchen. Each room is equipped with a motion detector, temperature sensors, light switches, window and door contacts and actuators. A meteorology mast outside of the building supplies local environmental measurements of ambient temperature, wind speed, wind direction, and solar irradiation. The electrical load of the building consists of heating, lighting, air-conditioning, a hot-water supply and various household appliances, such as a refrigerator and a coffee machine. The combined peak load of the building is close to 20kW. All individual loads in the building are remote-controllable from a central building controller. This controller is able to communicate with the SYSLAB grid through its own node computer (See Fig. 3). The controller can access different services to obtain power system information, e.g. dynamic power price, available power and grid frequency signal. Information can also flow in the other direction, for example providing the power system

controller with the expected near-future behavior of the building loads.

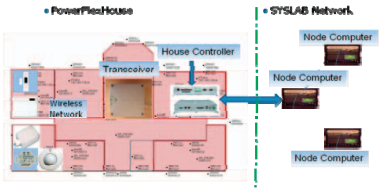

Fig. 3. Communication between PowerFlexHouse and SYSLAB

III. MPC CONTROLLER FOR LOAD SHIFTING IN POWERFLEXHOUSE HEATING STRATEGY

One of the main electricity consumptions in the northern Europe is the heating in the long winter. Heaters are designated as one of the most obvious areas of demand response. The objective of MPC controller is to minimize the daily operational cost of heating use and provide ancillary services for power system. Fig. 4 presents the model predictive control scheme. It is to solve an optimization problem over a prediction horizon at each control step subjected to system dynamics, an objective function (linear or quadratic), and constrains on states, actions and inputs. At each control step the optimization can obtain a sequence of actions optimizing expected system behavior over the prediction horizon. Only the first step of the sequence of control actions is implemented by controller on the system until the next control step, after which the procedure is repeated with new process measurements.

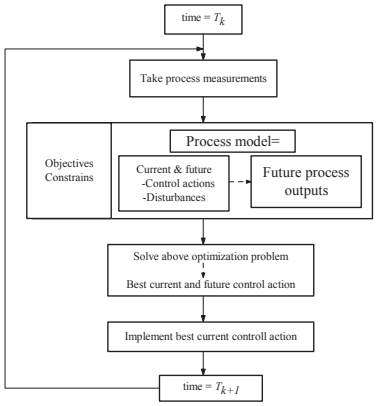

Fig. 4. Model predictive control scheme

A. Thermal Predictive Model for PowerFlexHouse

The indoor temperature model of PowerFlexHouse is given as a stochastic discrete-time linear state-space model, which was directly obtained from [12]. To reduce the complexity, the model of heat dynamics of PowerFlexHouse is formulated as one large room exchanging heat with an ambient environment. That is to say, we regard 8 rooms in PowerFlexHouse building as a large room. The control object is the one representing indoor temperature T_{in}. The states space equations were expressed in (1) and (2):

$$T(t+1)= \Phi T(t) + \Gamma U(t) \quad (1)$$

$$\text{Output: } y(t) = C\,T(t) = [1\ 0\ 0]\begin{bmatrix} T_{in}(t) \\ T_{im}(t) \\ T_{om}(t) \end{bmatrix} \quad (2)$$

Φ is the system matrix. Γ is the control matrix. $T = [T_{in}, T_{im}, T_{om}]$ is the state vector and $U = [T_a, \Phi_s, \Phi_h]$ is the input vector to the system. Here, $T_{in}(t)$ is the indoor air temperature; $T_{im}(t)$, and $T_{om}(t)$, which are the temperature of the heat accumulating layer in the inner walls and floor, and the temperature of the heat accumulating layer in the building envelope. T_a is the ambient (outdoor) temperature; Φ_s is the solar irradiation; and Φ_h is the energy input from the electrical heaters.

B. MPC Control Strategy

The MPC control strategy for the electrical space heaters in PowerFlexHouse should be found so that the total cost of the energy used in heating is minimized over a time horizon (*Hp*). At the same time, it should keep the indoor air temperature around the given reference temperature T_{ref}. The objective function can be formulated as:

$$J = \min\left[\sum_{k=0}^{H_p-1} C(k)\times u(k) + \sum_{k=0}^{H_p-1} w\times\left|T_{in}^{k} - T_{ref}\right|\right] \quad (3)$$

Subject to: $u(k) \in$ *int* [0, 1, 2, 3, 4, 5, 6, 7, 8, 9, 10], which means the heat input that the MPC controller determines by mixed integer optimization approach. There are totally 10 heaters in the PowerFlexHouse. Each of them has the power of 1kW. Therefore the maximum permitted electrical power consumption of heater units is $P_{heat\text{-}max}$=10×1kW=10kW. In (3), *C(k)* is the dynamic power price signal obtained from the Nord Pool spot market [13]. The Nordic electricity market is well-known for its efficient market function. The central market is the Nord Pool spot market where a daily competitive auction establishes a price for each hour of the next day. The trading horizon is 12-36 hours ahead and is done for the next day's 24 hours period. That is to say, there is an actual maximal prediction horizon of 36 hours. In the Nordic system at night-hours, there is a large production by wind turbine. It can be expected that sometime the price variation reflects the level of wind power penetration. The weight coefficient *w* in (3) is used to tune performance of the MPC controller.

For the purpose of the flexible consumption, there is a temperature set-point margin for the consumer to choose via a user interface. For example, when the wind energy production is small, the heaters working at the lower temperature limit,

otherwise, they will be set up to the upper limit. Only when the indoor temperature is in the range of $[T_{in\_min}\ T_{in\_max}]$, the MPC control algorithm is executed. In addition, the forecast data of the ambient (outdoor) temperature T_a and the solar irradiation Φ_s are updated twice a day (10:00 in the morning and 22:00 in the evening) for the next 48 hours, which are provided by the Wind Energy Division, Risø DTU.

Firstly, the controller output is initialized by the vector of dimension $1 \times Hp$, $\boldsymbol{u_0} = [u_0, \ldots, u_{Hp-1}]$, containing the input variables of the plant which are optimized. However, the initialization of the algorithm assumes that the heating units are switched off, $\boldsymbol{u_0} = [0, \ldots, 0]$. This way, the search direction is always positive. Secondly, the difference between the predicted indoor temperature at the end of the predictive period and the desired T_{ref} is evaluated at each control step. If this difference is small enough to be acceptable: $\left|T_{in}^{k+H_p} - T_{ref}\right| \le \varepsilon$, an optimal solution is achieved and only the first element of the controller output sequence (u_0) is used to control the process. At the next sample (hence, at $k+1$), the whole procedure is repeated. Otherwise, the first element of the controller output sequence with the maximum or minimum power consumption of the heating units is used to control the process ($u_0=P_{heat-max}$ or $u_0=0$). Finally, to overcome the model's error, here we use the process's real-time output and model's (previous) predictive output to structure one model output feedback correction (See Fig. 5.).

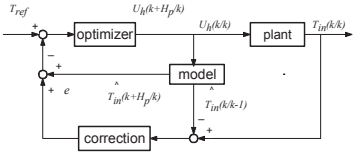

Fig. 5. Block diagram of PowerFlexHouse's MPC

The detailed MPC control law is described as following:

Step 1: Initialization step. $\boldsymbol{u_0} = [u_0, \ldots, u_{Hp-1}]$, where Hp is the prediction horizon, $\boldsymbol{u_0} = 0$.

Step 2: At current time k, measure $T_{in}(k/k)$ and compare it with the previous predictive value $\hat{T}_{in}^{(k/k-1)}$ to obtain the predictive error $e = T_{in}^{(k/k)} - \hat{T}_{in}^{(k/k-1)}$.

Step 3: Calculate the optimal control sequence that minimizes the objective function.

$$\{\boldsymbol{u}(k) = [u_0, \ldots, u_{Hp-1}]\} = \arg J = \min\left[\sum_{k=0}^{H_p-1} C(k) \times u(k) + \sum_{k=0}^{H_p-1} w \times \left|\widehat{T_{in}^{k}} - T_{ref}\right|\right]$$

Use the model to predict $\widehat{T_{in}} = \left[\hat{T}_{in}^{k+1}, \ldots, \hat{T}_{in}^{k+Hp}\right]$ and correct the predictive error by $\widehat{T_{in}} + e$.

If $\left|\hat{T}_{in}^{k+Hp} - T_{ref}\right| \le \varepsilon$ and $\forall \hat{T}_{in}^{k+i}, T_{in\_\min} \le \hat{T}_{in}^{k+i} \le T_{in\_\max}$, where $0 \le i \le H_p$ and ε is a small number.

Go to step 4.

else if $\left|\hat{T}_{in}^{k+Hp} - T_{ref}\right| > \varepsilon$

if $\forall \hat{T}_{in}^{k+i}, \hat{T}_{in}^{k+i} \ge T_{in\_\max}$, where $0 \le i \le H_p$

$u_0 = 0$

else if $\forall \hat{T}_{in}^{k+i}, \hat{T}_{in}^{k+i} \le T_{in\_\min}$, where $0 \le i \le H_p$

$u_0 = P_{heat-max}$

end if

end if

Step 4: Apply u_0 to heating units.

Next sample (hence, at $k+1$), $k=k+1$, and repeat from step 2 to step 4.

IV. Results

The MPC controller employs a control period of 10 minutes, while we test it on the SYSLAB platform. It is meaning that every 10 minutes the controller determines which control action to take at the current time. First of all, the MPC controller obtains a measurement of the current state of the house, including the disturbances like the state of doors and windows; the grid information e.g. dynamic power price signal, available power and frequency signal. To find the best predicted performance over the prediction horizon, the mixed-integer linear programming problem is solved by GLPK's (GNU Linear Programming Kit) Java native interface. Then it integrates the weather forecast data (ambient temperature, solar irradiation, wind speed and wind direction, etc.) with the prediction model for the house indoor temperature, and verifies the predictive error. At last, only the first step in the found best sequence of actions is implemented.

At 9:20 on October 22, 2010, the MPC control algorithm was running on the SYSLAB platform and it provided the optimized profile of the predictive power consumption in the next approximant 15 hours for the PowerFlexHouse's heaters, as shown in Fig. 6. Fig. 7 demonstrates the predictive indoor temperature in the next 15 hours according to the optimized switch schedule (the same as in Fig. 6). When the current time was 13:10 on October 22, 2010, the MPC produced the results shown in Fig. 8. It presents the optimized profile of the predictive power consumption in the next almost 35 hours for the PowerFlexHouse's heaters. At this moment, the prediction horizon could reach 35 hours, because the Nord Pool spot market at 13:00, on October 22, 2010, provided next day's 24 hours' price information for the users. The predictive indoor temperature in the next 35 hours was shown in Fig. 9, according to the optimized switch schedule (the same as in Fig. 8) for heaters in PowerFlexHouse. It was observed in Fig. 9 that during a few hours the predictive temperature dropped to 17ºC. Comparing Fig. 7 with Fig. 9, it can be found that the shorter the prediction horizon the better the predictive control effect. We probably could tune MPC performance by penalizing this temperature deviation with different weight

coefficient value. Otherwise, users will have some discomfort if they would like to accept a reduced energy bill and allow this deviation on the room temperature.

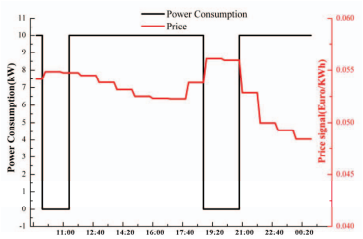

Fig. 6. Optimized predictive power consumption in the next 15 hours

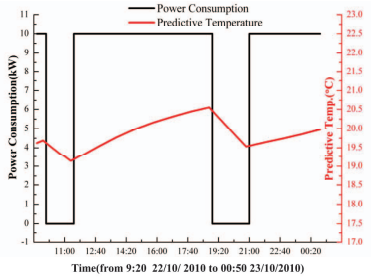

Fig. 7. Predictive indoor temperature in the next 15 hours

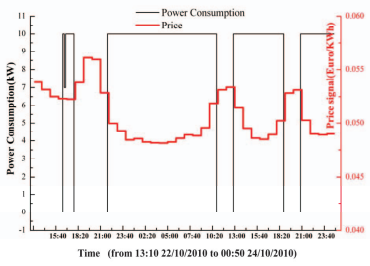

Fig. 8. Optimized predictive power consumption in the next 35 hours

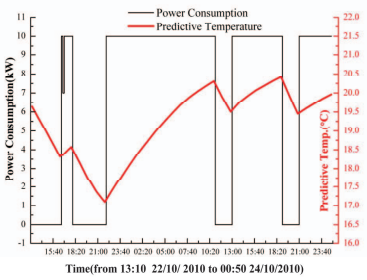

Fig. 9. Predictive indoor temperature in the next 35 hours

V. Conclusion and Future Research

The predictive behavior of power consumption for Power FlexHouse's heaters shows that the MPC strategy is feasible for active load management of intelligent houses in a distributed power system with high wind penetration. Residential customers can avoid high electricity price charge at peak time, and the power grid can benefit from load control. It also shows that the local (within the house) MPC controller can result in a generic solution supporting different technologies and houses with different optimization potential, which can provide services for the global controllers (aggregators) in a scope of a group of houses, e.g., a neighborhood (micro grid) or a global scope (virtual power plant). The load in a power grid is widely seen as one of the keys to achieving additional operational flexibility to ensure the stability of the grid as penetration levels rise. However, in comparison with the actual power system presented within the SYSLAB, it shows that the efficient use of load management demands a tight integration with the control system of the power grid.

On one side, the future research will focus on analyzing the effect of the predictive horizon length on the performance in MPC controller. On the other side, a multi-agent MPC should be taken into account to find an acceptable near-optimal solution for the whole distributed power system.

VI. Acknowledgment

The authors would like to express their appreciation to Andrea N. Hahmann, Senior Scientist, from Wind Energy Division, Risø DTU National Laboratory for Sustainable Energy, for her work on providing us the weather forecast data.

VII. References

[1] Ministry of Transport and Energy, "Energistrategi 2025", 2007.

[2] H. Lund, B.V. Mathiesen, "Energy system analysis of 100% renewable energy systems—The case of Denmark year 2030 and 2050, " *Energy,* vol. 34, issue.5, pp. 524-531, 2009

[3] Rudy R. Negenborn, Michiel Houwing, Bart De Schutter, Hans Hellendoorn, "Active prediction model accuracy in the control of residential energy resources," presented at the . IEEE International Conference on Control Applications, San Antonio, Texas, USA, Sep 3-5, 2008.

[4] Michael Angelo A. Pedrasa, Ted D. Spooner, Iain F. MacGill, " Coordinated scheduling of residential distributed energy resources to optimize smart home energy services, " *IEEE Trans. Smart Grid*, vol. 1, No.2, pp. 109-119, Sep. 2010.

[5] Preben Nyeng, Knud Ole Helgesen Pedersen, Jacob Østergaard, "Ancillary services from distributed energy resources-perspectives for the Danish power system," presented at the International Youth Conf. Energitics, Budapest, Hungary, May31-Jun.2, 2007.

[6] Albert Molderink, Vincent Bakker, Mauricw G.C. Bosman, Johann L. Hurink, Gerard J. M. Smit, "Management and control of domestic smart grid technology, " *IEEE Trans. Smart Grid*, vol. 1, No.2, pp. 109-119, Sep. 2010.

[7] Jose Medina, Nelson Muller, Ilya Roytelman, "Demand response and distribution grid operations: opportunities and challenges, " *IEEE Trans. Smart Grid*, vol. 1, No.2, pp. 193-198, Sep. 2010.

[8] T. Joseph Lui, Warwick Stirling, Henry O. Marcy, " Get smart, " *IEEE Power & energy magazine*, pp. 66-78, May/Jun. 2010.

[9] Ronald Soeterboek, *Predictive control-a Unified Approach*, chapter 1. Prentice Hall(UK) Limited,1992, Great Britain.

[10] http://www.risoe.dtu.dk/research/sustainable_energy/wind_energy/projects/syslab.aspx

[11] Birgit Pedersen, Henrik Bindslev "Risø DTU annual report 2009," Risø DTU, Denmark. Rep. Risø-R-1723 (EN), Jun. 2010

[12] Anders Thavlov, "Dynamic Optimization of Power Consumption", Chapter 7. Master thesis. Kongens Lynby 2008.

[13] The Nord Pool spot market [Online] available: http://www.nordpoolspot.com/reports/systemprice

VIII. BIOGRAPHIES

Yi Zong was born in Wuhan, Hubei province, China, on August 21, 1971. She graduated in Control Engineering and Control Theory from Wuhan University of Science and Technology. She got PhD degree on System Engineering and Automation in 2006, at the University Complutense of Madrid, Spain.

Her employment experience included the Wuhan Institute of Technology, China. Since 2006 she had been employed as Post.doc at the Wind Energy Division of Risø DTU National Laboratory for Sustainable Energy. She is currently a Scientist at Intelligent Energy Systems, Risø DTU. Her special fields of interest include advanced and intelligent control for demand side units in households and industry supporting flexible power consumption.

Daniel Kullmann was born in Frankfurt/Main, Germany, on August 15, 1973. He graduated in Computer Science from Darmstadt University of Technology in 2002.

After working for several years in the IT industry, he started in 2008 a PhD degree at Risø National Laboratory in Denmark. His fields of interest are distributed control and communication in power systems.

Anders Thavlov was born in Copenhagen, Denmark, on June 3, 1979. He graduated from Department of Informatics and Mathematical Modeling at Technical University of Denmark in 2008.

He is currently conducting his Ph.D. study at the Intelligent Energy Systems at Risø DTU National Laboratory for Sustainable Energy. His main research interests are energy systems modeling and control.

Oliver Gehrke was born in Frankfurt am Main, Germany, on March 15, 1975. He graduated in Electrical Power Engineering from Darmstadt University of Technology and got his PhD degree at Risø National Laboratory in Denmark. He is currently a Scientist at Risø DTU.

His special fields of interest include the embedded and distributed control of power systems with a high penetration of renewable energy sources.

Henrik Bindner was born on 30 June 1964 in Copenhagen, Denmark. He received his master in electrical engineering from the Technical University of Denmark in 1988. Since 1990 he has been with Risø DTU National Laboratory for Sustainable Energy in the Wind Energy Division, currently as a Senior Scientist.

He has mainly been working on integration of wind energy into power system. The work has included analysis, design and control of small island systems as well as technologies and techniques for integration of wind in large systems. Currently, he is researching how distributed energy resources can be applied to increase penetration of wind energy.

PAPER G

Model Predictive Controller for Active Demand Side Management with PV Self-consumption in an Intelligent Building

---

Minor contribution: Presented at the *3rd European Innovative Smart Grid Technologies Conference* (IEEE ISGT Europe 2012), Berlin, Germany, 2012.

2012 3rd IEEE PES Innovative Smart Grid Technologies Europe (ISGT Europe), Berlin

Model Predictive Controller for Active Demand Side Management with PV Self-consumption in an Intelligent Building

Yi Zong, *Member, IEEE*, Lucian Mihet-Popa, *Member, IEEE,* Daniel Kullmann, Anders Thavlov, Oliver Gehrke, *Member, IEEE,* and Henrik W. Bindner, *Member, IEEE*

***Abstract*—This paper presents a Model Predictive Controller (MPC) for electrical heaters' predictive power consumption including maximizing the use of local generation (e.g. solar power) in an intelligent building. The MPC is based on dynamic power price and weather forecast, considering users' comfort settings to meet an optimization objective such as minimum cost and minimum reference temperature error. It demonstrates that this MPC strategy can realize load shifting, and maximize the PV self-consumption in the residential sector. With this demand side control study, it is expected that MPC strategy for Active Demand Side Management (ADSM) can dramatically save energy and improve grid reliability, when there is a high penetration of Renewable Energy Sources (RESs) in the power system.**

***Index Terms*— Active demand side management; load shifting; model predictive control; solar/wind power penetration**

NOMENCLATURE

***Abbreviation*:**

ADSM	Active demand side management.
CPS	Conventional power supply.
DERs	Distributed energy resources.
DG	Distributed generation.
DSM	Demand side management.
DTU	Technical university of Denmark.
MPC	Model predictive control.
RESs	Renewable Energy Sources.
RMI	Remote method invocation.
RPS	Renewable power supply.

***Variables & Parameters*:**

FF	Fill factor.
G_a	Solar irradiation.
H_p	Prediction horizon.
I_o	Open-circuit currents.
I_{sc}	Short-circuit currents.
n_s	Number of cells in the panel connected in series.
n_{ps}	Number of panels in series.
n_{sp}	Number of strings in parallel.
$P_{C(k)}$	Dynamic power price signal of CPS at control step k.
$P_{heat-max}$	Maximum permitted electrical power consumption of heating units.
P_{max}	Maximum power point of a solar cell.
$P_{R(k)}$	Dynamic power price signal of RPS at control step k.
R_s	Cell series resistance.
T_a	Ambient (outdoor) temperature.
T_c	Cell temperature.
T_i	Indoor air temperature.
T_i^k	Predictive indoor temperatures at each control step k over the prediction horizon H_p.
T_{im}	Temperature of the heat accumulating layer in the inner walls and floor.
T_{om}	Temperature of the heat accumulating layer in the building envelope.
T_{ref}	Reference indoor air temperature.
V_{oc}	Open circuit voltage.
V_T	Junction thermal voltage.
W_s	Wind speed.
Φ_h	Energy input from the electrical heaters.
β_I	Correction coefficients for current.
χ	Correction coefficients for voltage.
$\boldsymbol{u}_{(k)}$	Optimized heat input sequence at control step k.
$\boldsymbol{u}_{s(k)}$	Predictive solar power at control step k.
ΔT	Absolute temperature.

This work was supported by Interreg IV A program, project "Wind in Oresund", and the EU project "Smooth PV" (No. 228449).

The authors are with the department of Electrical Engineering, Intelligent Energy Systems, Risø Campus, Technical University of Denmark, 4000 Roskilde, Denmark (e-mail: yizo@elektro.dtu.dk; lmih@elektro.dtu.dk; daku@elektro.dtu.dk; atha@elektro.dtu.dk; olga@elektro.dtu.dk; hwbi@elektro.dtu.dk).

I. INTRODUCTION

TO MEET the rapidly increasing demand of the energy consumption, and to achieve a significant reduction in CO_2 emissions, more Renewable Energy Sources (RESs), and other low-carbon energy sources will become major contributors to the future electricity system. The Danish government has adopted a long term goal that the Danish energy system (including transport) can be completely independent of fossil fuels by 2050 without using nuclear energy, based on 100% renewable energy from combinations of wind, biomass, solar power and wave [1], and wind power will cover 50% of the Danish electricity consumption in 2025 [2].

978-1-4673-2597-4/12/$31.00 ©2012 IEEE

Due to an increased contribution of fluctuating RESs to the energy system, there are many concerns about the flexibility, variability, non-controllability of these sources, and they have the impact on the ability to keep the balance between supply and demand. Currently, the main method to regulate the supply-demand imbalance is a set of supply-side generation reserves, known as ancillary services. The rising share of RESs decreases the controllability of the supply side. The rise in needed balancing power can be fulfilled by utilizing the flexibility potential in demand and Distributed Generation (DG). The introduction of Distributed Energy Resources (DERs) (e.g. household, industrial consumers and electric vehicles), together with the introduction of more information and communication technology in the electricity system provides interesting and novel automated Demand Side Management (DSM) opportunities at the end user level. The combination of DSM with an automatic control of the DERs demand can be called "Active Demand Side Management" (ADSM) [3, 4]. ADSM can modify the demand profile to reduce the losses in the grid, maximize consumption while RESs are available, decrease congestions, and save energy [5, 6].

MPC is a control algorithm that optimizes a sequence of manipulated variable adjustments over a prediction horizon by utilizing a process model to optimize forecasts of process behavior based on a linear or quadratic objective, which is subjected to equality or inequality constraints. In MPC, the optimization is performed repeatedly *on-line*. This is the meaning of receding horizon, and the intrinsic difference between MPC and the traditional optimal control. The limitation of this finite-horizon optimization is that, under ideal situations only the suboptimal solution for the global solution can be obtained. However, the receding horizon optimization can effectively incorporate the uncertainties incurred by model-plant mismatch, time-varying behavior and disturbances [7]. MPC is now recognized as a very powerful approach with well established theoretical foundations and proven capability to handle a large number of industrial control problems [8]. The building sector is one of the largest energy consumptions. Based on the vision of the future electricity system, building controls design becomes challenging since it is necessary to move beyond standard controls approaches and to integrate predictions of weather, occupancy, renewable energy availability, and dynamic power price signals. MPC naturally enters the picture as a control algorithm that can systematically incorporate all the aforementioned predictions to improve building thermal comfort, decrease peak load, and reduce energy costs [9]. MPC for building climate control was investigated in several papers, such as references [9]-[13], mainly with the purpose of increasing the energy efficiency. The potential of MPC in power management was investigated in [14]-[18], but the weather forecast information (e.g. the ambient temperature) was assumed to be constant in their simulation scenarios.

The goal of our research is to implement an MPC-based control strategy for ADSM, using DERs' predictive optimization potential to support the introduction of a large penetration level of renewable energy. In this paper, an MPC controller was implemented for load shifting in an intelligent office building's heating power consumption scheme, with a maximization of the PV self-consumption. The term "self-consumption" focuses on the usage of the own generated energy, while the energy provided by the grid remains an optional generator. The original contributions of this work are: 1) building an easy, fast to implement model for PV installed at an intelligent building (called PowerFlexHouse), and a stochastic discrete-time linear state-space model for this building; 2) implementing a low-complexity MPC-based control scheme which is used to realize the load shifting for the heaters' power consumption, including PV maximum self-consumption in PowerFlexHouse; 3) integrating weather forecast information and dynamic power price into the MPC-based control strategy; and 4) simulating and testing an MPC controller on a real power grid with high penetration of RESs.

The remainder of this paper is organized as follows: in Section II, we present a test platform for intelligent, active and distributed power systems at the Technical University of Denmark (DTU), Risø campus. How to implement a thermal MPC controller for the power consumption prediction in an intelligent building-PowerFlexHouse is provided in Section III, including a simple PV model for solar power prediction, a heat dynamic model for PowerFlexHouse's inside temperature prediction, formulated MPC objective functions and a basic MPC control law. Some field test results will be shown in Section IV. Finally, conclusion and future research are given in Section V.

II. Test Platform Description

SYSLAB is a laboratory for intelligent distributed power systems [19] in DTU Elektro, Risø campus. It is built around a small power grid with renewable (wind (11+10kW), solar (7kWp)) and conventional (diesel) power generation, battery storage, and various types of consumers (See Fig. 1). The whole system can be run centrally from any point on the network, or serve as a platform for fully decentralized control. All SYSLAB controller nodes run the SYSLAB software stack, which is a modular framework for developing distributed control systems for power systems. It is written in the Java (TM) programming language. Distributed controllers can control these components by using one of the supported types of communication, for example, the Java Remote Method Invocation (RMI).

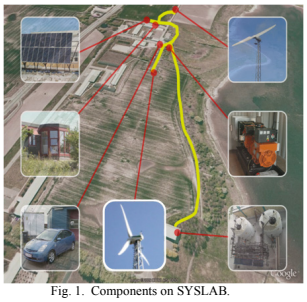

Fig. 1. Components on SYSLAB.

One of the components on the SYSLAB grid is a small, intelligent office building, PowerFlexHouse. It contains seven offices, a meeting room and a kitchen. Each room is equipped with a motion detector, temperature sensors, light switches, window and door contacts and actuators. A weather station outside of the building supplies local environmental measurements of ambient temperature, wind speed, wind direction, and solar irradiation. The electrical load of the building consists of heating, lighting, air-conditioning, a hot-water supply and various household appliances, such as a refrigerator and a coffee machine. The combined peak load of the building is close to 20kW. All individual loads in the building are remote-controllable from a central building controller. The controller software runs on a Linux-based PC. It is also written in Java (TM) and is based on the SYSLAB software stack. The controller can communicate with the SYSLAB grid through its own node computer (See Fig. 2). Information can also flow in the other direction, for example providing the power system supervisor controller with the expected near-future behavior of the building loads.

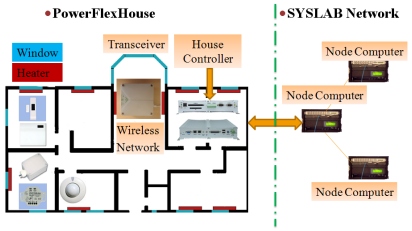

Fig. 2. Communication between PowerFlexHouse and SYSLAB.

III. MPC FOR ADSM IN AN INTELLIGENT BUILDING'S HEATING POWER CONSUMPTION

As described in Section II, the hybrid power supply system (SYSLAB) presented in this paper consists of two parts: a Conventional Power Supply (CPS), and a Renewable Power Supply (RPS). To use the power system efficiently, one of the good ways is to take the advantage of renewable power supply in a maximum degree. Therefore, home appliances primarily use RPS, and CPS is used when RPS is not enough to support the power required by the home appliances. We suppose that RPS has a low cost of power than CPS, considering its generation and CO_2 impact, etc. We denote the dynamic power prices of CPS and RPS by P_C and P_R, respectively. In this paper, to realize the load shifting, we use an MPC control strategy to minimize the daily operational cost of heating in PowerFlexHouse, at the same time to ensure the maximum self-consumption of solar power produced at PowerFlexHouse, and to guarantee users' comfort. There are three important components in MPC, such as the prediction model, the objective function, and the control law, which are present as follows.

A. PV Model

We use a single diode equivalent circuit for the PV model described by a simple exponential equation:

$$i = I_{sc} - I_o \cdot \left(e^{(v+i\cdot R_s)/n_s \cdot V_T} - 1\right) \qquad (1)$$

where I_{sc} and I_o are the short-circuit and open-circuit currents, R_s is the cell series resistance, n_s is the number of cells in the panel connected in series, and V_T represents the junction thermal voltage, which includes the diode quality factor, the Boltzmann's constant, the temperature at standard condition and the charge of the electron.

A solar cell can be characterized by the following fundamental parameters: the short circuit current I_{sc}, the open circuit voltage V_{oc}, the maximum power point P_{max} and the fill factor FF, which is the ratio of the maximum power that can be delivered to the load and the product of I_{sc} and V_{oc} ($FF = \frac{P_{\max}}{V_{oc} I_{sc}} = \frac{V_{\max} I_{\max}}{V_{oc} I_{sc}}$). The fill factor can be taken from the manufactures' data. Then it can be used to obtain P_{max} ($P_{\max} = FF \times V_{oc} I_{sc}$) under non-standard conditions.

Equations for I_{sc} and V_{oc} as a function of absolute temperature ΔT including temperature coefficients (β_I, χ: correction coefficients for current and voltage) that provide the rate of change with respect to temperature of the PV performance parameters, can be expressed as:

$$\begin{aligned} I_{sc} &= I_{sc25} \cdot (1 + \beta_I \cdot \Delta T) \\ V_{oc} &= V_{oc25} \cdot (1 + \chi \cdot \Delta T) \\ \Delta T &= T_c - T_a \end{aligned} \qquad (2)$$

To complete the model it is also necessary to take into account the variation of the parameters with respect to irradiance:

$$I_{sc} = I_{sc25} \cdot (G_a / 1000) \qquad (3)$$

Using a four-parameters model of a single diode equivalent circuit, the *v-i* characteristics for a solar panel string depending on irradiance and temperature has the following expressions:

$$v = n_{ps} \cdot V_{oc} + n_{ps} \cdot n_s \cdot V_T \cdot \ln\left(1 - i/(n_{sp} \cdot I_{sc25} \cdot G_a / 1000)\right) \qquad (4)$$

$$i = n_{sp} \cdot I_{sc} \cdot \left(1 - e^{(v - n_{ps} \cdot V_{oc} + R_s \cdot i)/(n_{ps} \cdot n_s \cdot v)}\right) \qquad (5)$$

where n_{ps} and n_{sp} represent the number of panels in series and the number of strings in parallel, respectively. The equations (4) and (5) can be used to calculate the voltage and current over a string of panels [20][21].

The temperature and irradiance play a central role in PV conversion process since it affects basic electrical parameters, such as the voltage and the current of the PV generator. If the PV panels are mounted in a region with high wind potential (as in our case), the wind speed must also be considered because it has a large influence [22].

The model was developed in MATLAB, using the equations presented above, and has the solar irradiation G_a and the cell temperature T_c as inputs on the panel, and it sweeps the voltage range of the PV panel in order to calculate the output current and power.

For the model input values, the measurements from the weather station had to be translated via additional function that were implemented, in order to reproduce the values on the

actual PV panel conditions. The three ambient measurements: ambient temperature, horizontal solar irradiation and wind speed are fed to an additional simulation module that calculates the cell temperature of the PV panel and the solar irradiation on it, as can be seen in Fig. 3.

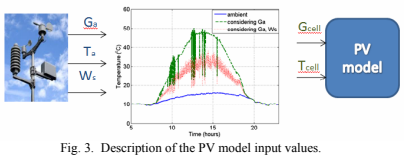

Fig. 3. Description of the PV model input values.

In Fig. 4 is shown a comparison between measured and simulated output power of the PV panel. Comparison with experimental data, acquired by SCADA system and processed by MATLAB, and with the characteristics of the PV panels [22], provided by manufacturers, has shown that this PV model implemented in MATLAB can be an accurate simulation tool to study and analyze the characteristics of individual units and for the prediction of energy production within MPC controller and active loads.

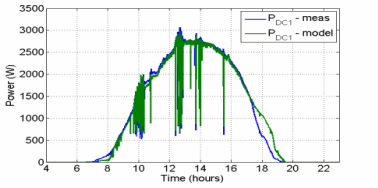

Fig. 4. Comparison between simulations (green) and measurements (blue) of the PV panel output power.

B. Simple Thermal Model for PowerFlexHouse

The indoor temperature model of PowerFlexHouse was given as a stochastic discrete-time linear state-space model, which was directly obtained from the reference [23]. To reduce the complexity, the model of heat dynamics of the PowerFlexHouse is formulated as one large room exchanging heat with an ambient environment. The heat flow in PowerFlexHouse is modelled by a grey-box approach, using physical knowledge about heat transfer together with statistical methods to estimate model parameters. The heat transfer due to conduction, convection and ventilation is assumed linear with the temperature difference on each side of the medium. The estimator was Continuous Time Stochastic Modelling (CTSM), which is an estimation tool developed at the department of Informatics and Mathematical Modeling DTU [24]. The model's states space equations are described by (6) and (7):

$$\boldsymbol{T}(t+1) = \Phi \boldsymbol{T}(t) + \Gamma \boldsymbol{U}(t) \qquad (6)$$

$$\text{Output: } \boldsymbol{y(t)} = \boldsymbol{C}\,\boldsymbol{T}(t) = [1\ 0\ 0] \begin{bmatrix} T_i(t) \\ T_{im}(t) \\ T_{om}(t) \end{bmatrix} \qquad (7)$$

where

$$\Phi = \begin{bmatrix} 9.93\times10^{-1} & 1.87\times10^{-4} & 5.64\times10^{-3} \\ 2.74\times10^{-1} & 7.25\times10^{-1} & 8.19\times10^{-4} \\ 1.56\times10^{-4} & 1.55\times10^{-8} & 9.96\times10^{-1} \end{bmatrix}$$

$$\Gamma = \begin{bmatrix} 1.28\times10^{-3} & 3.00\times10^{-2} & 1.02\times10^{-2} \\ 1.86\times10^{-4} & 2.61\times10^{2} & 1.48\times10^{-3} \\ 3.36\times10^{-3} & 1.61\times10^{-6} & 8.04\times10^{-7} \end{bmatrix}$$

$\boldsymbol{T} = [T_i, T_{im}, T_{om}]$ is the state vector and $\boldsymbol{U} = [T_a, G_a, \Phi_h]$ is the input vector to the system. Here, $T_i(t)$ is the indoor air temperature; $T_{im}(t)$ and $T_{om}(t)$, which are the temperature of heat accumulating layer in the building envelope and the temperature in the heat accumulating layer in the inner walls and floor, can not be measured. State estimator-Kalman filter can be used to estimate these two states; T_a is the ambient (outdoor) temperature; G_a is the solar irradiation; and Φ_h is the energy input from the electrical heaters. Using this model, the predicted indoor air temperature was compared with the measured values (See Fig. 5). It was shown that this simple discrete-time linear thermal model for PowerFlexHouse is good enough to be applied to MPC.

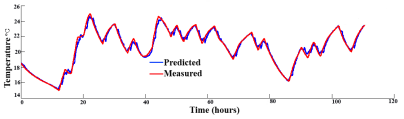

Fig. 5. Predictive (blue) & actual measured (red) indoor air temperature.

C. MPC Objective Function

In MPC the control objectives are translated into an optimization problem, which is formulated over a finite prediction horizon. The result of the optimization is a sequence of optimal control moves which drives the system states (or outputs) towards a given reference while respecting system constraints (such as upper and lower limits on the temperature) and minimizing a selected performance criterion (e.g. the reference temperature error, and minimum cost). The goal of the MPC control strategy for the electrical space heaters in PowerFlexHouse is to minimize the total cost of the energy used in heating over a prediction horizon (H_p), including the maximum usage of local PV generation. At the same time, it should keep the indoor air temperature close to the given reference temperature T_{ref}. In general, the objective function can be formulated as:

$$J = \alpha \sum_{k=0}^{H_p-1} P_{C(k)} \times u_{(k)} + (1-\alpha)[\sum_{k=0}^{H_p-1} P_{R(k)} \times u_{s(k)} + \sum_{k=0}^{H_p-1} P_{C(k)} \times (u_{(k)} - u_{s(k)})] + w \sum_{k=0}^{H_p-1} \left| T_i^k - T_{ref} \right| \quad (8)$$

and

$$\alpha = \begin{cases} 0; & when\ u_{s(k)} \geq min_{(rps)} \\ 1; & when\ u_{s(k)} < min_{(rps)} \end{cases}$$

Subject to: $u_{(k)} \in integer$ [0, 1, 2, 3, 4, 5, 6, 7, 8, 9, 10] in kW, which means the heat input that the MPC controller determines by using a mixed integer optimization approach. There are totally 10 heaters in the PowerFlexHouse. Each of them has a power of 1kW. Therefore the maximum permitted electrical power consumption of heating units is $P_{heat\text{-}max}$=10×1kW=10kW. The available solar power at control step k is expressed as $u_{s(k)}$. The minimum solar power supply $min_{(rps)}$=1kW. The above formulation provides a means of incorporating both the economic and user's comfort concerns. By assigning different weight coefficient w in (8) to user's comfort term, behaviour on trade-off between economic performance and user's comfort can be studied. In (8), $P_{C(k)}$ is the dynamic power price signal of CPS obtained from the Nord Pool spot market [25]. Its trading horizon is 12-36 hours ahead and it is done for the next day's 24 hours period. That is to say, the minimum prediction horizon is at least 12 hours and the actual maximal prediction horizon can reach 36 hours. To simply the problem, the dynamic power price signal of RPS, $P_{R(k)}$ are assumed to **[0]**. In case $u_{s(k)} \geq min_{(rps)}$, the objective function can be:

$$J = \sum_{k=0}^{H_p-1} P_{C(k)} \times (u_{(k)} - u_{s(k)}) + w \sum_{k=0}^{H_p-1} \left| T_i^k - T_{ref} \right| \quad (9);$$

in case $u_{s(k)} < min_{(rps)}$, the objective function can be expressed as :

$$J = \sum_{k=0}^{H_p-1} P_{C(k)} \times u_{(k)} + w \sum_{k=0}^{H_p-1} \left| T_i^k - T_{ref} \right| \quad (10)$$

To find the best predicted performance over the prediction horizon, the mixed-integer linear programming problem is solved by GLPK's (GNU Linear Programming Kit) solver with Java native interface [26].

D. MPC control law

The main principle of MPC is to transform the control problem into an optimization one and solve this optimization problem over a prediction horizon (e.g.12-36 hours) at each control step (e.g. 10 minutes). The MPC controller obtains a measurement of the current state of the house, including the disturbances like the state of doors and windows, and the grid information, such as dynamic power price signal, available RPS and CPS, and frequency signal from the test platform SYSLAB. It also integrates the weather forecast data (ambient temperature and solar irradiation, etc.) with the PV model for the predictive solar power, and with the prediction model for the house indoor temperature. All of them subjected to system dynamics, the objective function (linear or quadratic), constraints on states (e.g. user comfort could be transformed to a set of linear constraints.), and inputs. At each control step the optimization obtains a sequence of actions optimizing expected system behavior over the prediction horizon. But only the first step of the sequence of control actions is executed by the controller on the system until the next control step, after which the procedure is repeated with new process measurements. (See Fig. 6).

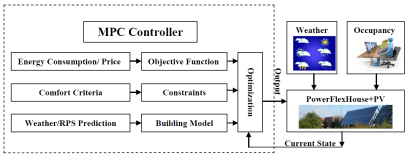

Fig. 6. Basic principle of MPC for building.

IV. RESULTS

We obtained some results from the field test on 18-20, February 2012. The local forecast data of the ambient temperature T_a and the solar irradiation G_a are provided by the meteorology group in DTU Wind Energy at Risø campus. Fig. 7 shows the predictive and the actual measured outside temperature; and in Fig. 8 the predictive and the actual solar irradiation is shown during the test period. The maximum relative error between the actual weather measurement and the weather forecast data is ±5% on test. Therefore, we concluded that the local weather forecast data are accurate in some degree to be integrated into the MPC-based control strategy. Using the PV model described in Section III A together with the local weather forecast data (Fig. 7(red) & Fig. 8(red)), we can obtain the predictive solar power for PowerFlexHouse PV from 8:00 18th to 0:00 20th, February 2012 (See Fig. 9). It was observed that the weather on 18th, February 2012 was bad and there was not solar power to be consumed by heaters. Only during the period of 9:00 to 16:00 on 19th, Feb 2012, there was available solar power supply. In this paper, PV electricity has been used as a local generator, and the concept of self-consumption is meaningful, only when the local PV generation is available.

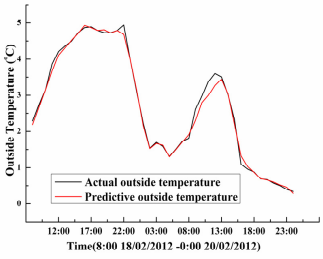

Fig. 7. Predictive (red) and actual measured (black) outside temperature.

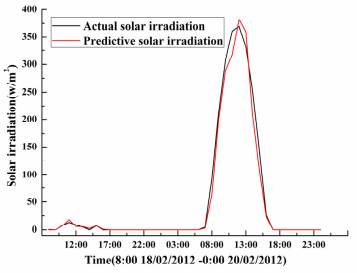

Fig. 8. Predictive (red) and actual measured (black) solar irradiation.

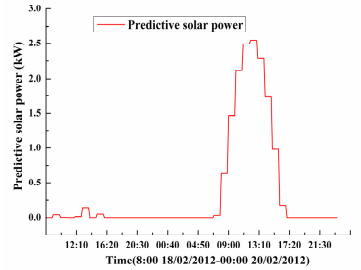

Fig. 9. Predictive solar power.

At 8:00 (18th, February 2012) the MPC control controller was running on the SYSLAB platform and it provided the optimized profile of the predictive power consumption in the next approximately 16 hours for the PowerFlexHouse's heaters, as shown in Fig. 10. Fig. 11 demonstrates the predictive indoor air temperature in the next 16 hours according to the optimized switch schedule (the same as in Fig. 10). At 13:00 (18th, February 2012), the MPC produced the results shown in Fig. 12. It presents the optimized profile of the predictive total power consumption in the next almost 35 hours for the PowerFlexHouse's heaters. At this moment, the prediction horizon could reach 35 hours, because the Nord Pool spot market at 13:00 (on the same day) provided next day's 24 hours' price information for the users. Since the solar power has a high priority to be used, the green area in Fig. 12 is the solar power consumption, which would be consumed by heaters from 9:00 to 16:00 on 19th, Feb 2012. The predictive indoor air temperature in the next 35 hours is shown in Fig. 13, according to the optimized switch schedule for heaters supplied with RPS and CPS, shown in Fig. 12. It was observed that the MPC-based controller almost worked within the low price period, including when there was solar power, and it was able to shift the load and reduce the total cost of operating electrical heaters to meet certain indoor temperature requirements. It is also shown that preheating during the night is a possible way to achieve energy savings.

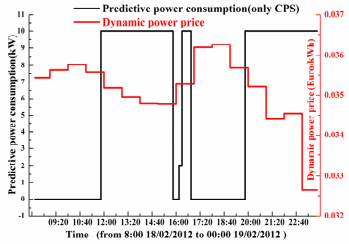

Fig. 10. Optimized heaters' power consumption (black) & dynamic power price (red) in the next 16 hours.

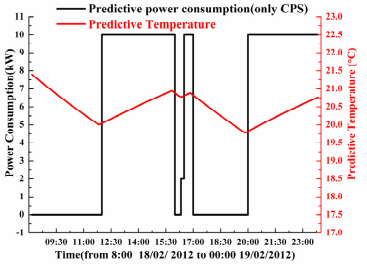

Fig. 11. Predictive indoor air temperature (red) according to the optimized heaters' power consumption (black) in the next 16 hours.

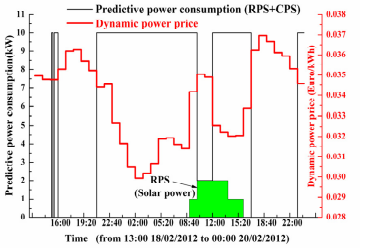

Fig. 12. Optimized heaters' power consumption (black) & dynamic power price (red) in the next 35 hours.

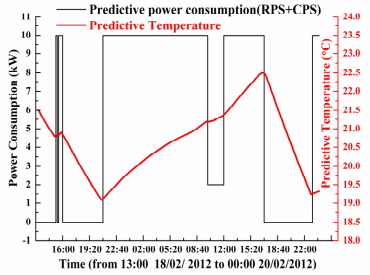

Fig. 13. Predictive indoor air temperature (red) according to the optimized heaters' power consumption (black) in the next 35 hours.

After analyzing the data of Nord Pool, it is concluded that there is certain predictability in the occurrence of peak load periods during the day in Denmark, and this predictability is reflected in the hourly spot price. The peak load periods and high spot prices occur mainly in the same hours of the day (morning 8:00-11:00 and afternoon 17:00-20:00) and the low spot prices take place in the deep of night [27]. In the Nordic system at night-hours, there is a large production by wind turbine. This is correlated with the dynamic power price, which is much lower during the period from 21:00 to 7:00. According to [28], it is concluded that the spot price, generally decreases when the wind power penetration in the power system increases, that is to say, the Nordic Electricity spot prices reflect the amount of wind power in the system. Fig. 10 and Fig. 12 illustrate that heaters are switched on most of the time at late night and MPC control strategy can achieve energy savings by shifting load from on-peak to off-peak period. At the same time, it shows that MPC control strategy can be investigated on ADSM in this intelligent building, which is used to stabilize fluctuations in the power grid with a high penetration of wind power or other renewable energy.

V. Conclusion and Future Research

To enable more use of renewable energy in the future power system, ADSM should be established to encourage consumers to improve energy efficiency, reduce energy cost, change the time of usage, or promote the use of different energy sources. In order to improve the operation of various energy resources, operation efficiency of building energy and loads should be coordinated and optimized. From the control systems view, these problems can be formulated as optimizing the cost, the use of the storage, the use of the wind/PV source, to match the production with the consumption in a predictive horizon.

The predictive behavior of power consumption for electrical heaters in PowerFlexHouse shows that MPC-based strategies are effective for active DSM in a distributed power system with high renewable energy penetration. Integrating dynamic power prices and the weather forecast data, it demonstrates that MPC control strategies are able to shift the electrical load to periods with low prices, and it can maximize the use of local PV generation. Simultaneously, the end users can avoid high electricity price charge at peak time, and the power grid can benefit from load control.

The predictive optimal problem, which is set up a residential sector, can be naturally modeled with discrete time steps, because balance settlement and markets work within discrete periods. Complex models cannot be readily used for control purposes, since the computation time for the optimal load scheduling should be short. Meanwhile, in real conditions, the efficiency of the predictive schedule depends on the accuracy of forecasts.

The future work will focus on the other different optimization methods for MPC controllers and the computation time for their optimal scheduling. Moreover, we need to analyze the effect of the predictive horizon length on the performance in the MPC strategies, and the robustness of these controllers against uncertainty in measurements and forecasts. At the same time, different home appliances, such as a hot-water supply, can be used for the purpose of the maximum PV self-consumption.

VI. Acknowledgment

The authors would like to express their appreciation to Andrea N. Hahmann, Senior Scientist, from DTU Wind Energy, Risø campus, Technical University of Denmark, for providing us with the local weather forecast data.

VII. References

[1] K. Richardson, D. Dahl-Jensen, J. Elmeskov, C. Hagem, J. Henningsen, J. A. Korstgård, N. B. Kristensen, P. E. Morthorst, J. E. Olesen, and M. Wier, "Green energy - the road to a Danish energy system without fossil fuels," Danish Commission on Climate Change Policy, 2010. [Online]. Available: http://greengrowthleaders.org/green-energy-the-road-to-a-danish-energy-system-without-fossil-fuels/

[2] Ministry of Transport and Energy, "Energistrategi 2025", 2007.

[3] M. Castillo-Cagigal, E. Caamaño-Martín, D. Masa-Bote, A. Gutiérrez, F.Monasterio-Huelin, and J. Jiménez-Leube, "PV selfconsumption optimization with storage and Active DSM for the residential sector", *Solar Energy*, vol. 85, issue 9, pp. 2338-2248, 2011.

[4] Y. Zong, D. Kullmann, A. Thavlov, O. Gehrke, and H.W. Bindner, "Active load management in an intelligent building using model predictive control strategy," in *Proc. 2011 PowerTech Conf.* pp. 1700589.

[5] G. Papagiannis, A. Dagoumas, N. Lettas, and P. Dokopoulos, "Economic and environmental impacts from the implementation of an intelligent demand side management system at the European level," *Energy Policy* , vol. 36, issue 1, pp. 163-180, 2008.

[6] G. Strbac, "Demand side management: benefits and challenges", *Energy Policy*, vol.36, issue 12, pp.4419-4426, 2008.

[7] D. Q. Mayne, J. B. Rawlings, C. V. Rao, and P. O. M. Scokaert, "Constrained model predictive control: stability and optimality," *Automatica* 36, pp.789-814, 2000.

[8] B. C. Ding, *Modern predictive control*, chapter 1. CRC Press ,2010, United States.

[9] Y. Ma, A. Kelman, and A. Daly, "Predictive control for energy efficient buildings with thermal storage," *IEEE control systems magazine*, pp. 44-64, Feb. 2012.

[10] J. Široký, F. Oldewurtel, J. Cigler, and S. Prívara, "Experimental analysis of model predictive control for an energy efficient building heating system," *Applied Energy*, vol. 88, issue9, pp. 3079-3087, Sep. 2011.

[11] Y. Ma, G. Anderson, and F. Borrelli, "A distributed predictive control approach to building temperature regulation," in *Proc. 2011 American Control Conf.* pp.2089-2094.

[12] F. Oldewurtel, A. Parisio, C. N. Jones, M. Morari, D. Gyalistras, M. Gwerder,V. Stauch, B. Lehmann, and K. Wirth, "Energy Efficient Building Climate Control using Stochastic Model Predictive Control and Weather Predictions", in *Proc. 2010 American Control Conf.*, pp.5100-5105

[13] Y. Ma, F. Borrelli, B. Hencey, B. Hencey, B. Coffey and P. Haves, "Model predictive control for the operation of building cooling systems", *IEEE Trans. Control Systems Technology*, pp. 1-8, Mar. 2011.

[14] F. Oldewurtel, A. Ulbig, A.Parisio, G.Andersson, and M. Morari "Reducing peak electricity demand in building climate control using real-time pricing and model predictive control," in *Proc. 2010 IEEE Conference on Decision & Control (CDC)*, pp. 1927-1932

[15] H. Hindi, D. Greene, and C. Laventall, "Coordinating regulation and demand response in electrical power grids using multirate model predictive control," in *Proc. 2011 IEEE PES* Innovative *Smart Grid Technologies Conf.* pp.1-8.

[16] T. G. Hovgaard, K. Edlund, and J. B. Jørgensen, "The potential of economic MPC for power management", in *Proc. 2010 IEEE Conference on Decision & Control (CDC)*, pp. 7533-7538

[17] L. Xie and M. D. Ilié, "Model predictive economic/environmental dispatch of power systems with intermittent resources," in *Proc. 2009 IEEE PES General Meeting,* pp.1-6.

[18] D. Zhu, and G. Hug-Glanzmann, "Real-time control of energy storage devices in future electric power systems," in *Proc. 2011 PowerTech Conf.* pp.1-7.

[19] http://www.powerlab.dk/English/facilities/SysLab.aspx

[20] D. Sera; R. Teodorescu and P. Rodriguez, "PV panel model based on datasheet values", in *Proc. 2007 IEEE International Symposium on Industrial Electronics*, pp. 2392-2396.

[21] D. Y. Goswani, *Principles of Solar Engineering*, (2nd ed.), Philadelphia: Taylor & Francis, 2000, p. 81-98.

[22] L. Mihet-Popa, C. Koch-Ciobotaru, F. Isleifsson and H. Bindner, "Development of Tools for Simulation Systems in a Distribution Network and Validated by Measurements", *The 13th IEEE OPTIM International Conference*, May 24-26, Brasov 2012, pp. 1022-1031.

[23] A. Thavlov, "Dynamic Optimization of Power Consumption", Chapter 7. Master thesis. Kongens Lynby 2008.

[24] Continuous Time Stochastic Modelling [Online] available: http://www2.imm.dtu.dk/~ctsm/

[25] The Nord Pool spot market [Online] available: http://www.nordpoolspot.com/reports/systemprice

[26] GNU Linear Programming Kit, [Online] available: http://glpk-java.sourceforge.net/

[27] Y. Zong, D. Kullmann, A. Thavlov, O. Gehrke and H. W. Bindner, "Application of Model Predictive Control for Active Load Management in a Distributed Power System with High Wind Penetration", *IEEE Transactions on Smart Grid*, vol. 3, issue 2, pp. 1055-1062, Jun. 2012.

[28] W. Hu, Z. Chen, B. Bak-Jensen, "The relationship between electricity price and wind power generation in Danish electricity markets", in *Proc. 2010 Asia-Pacific Power and Energy Engineering Conf.* pp. 5448739.

VIII. BIOGRAPHIES

Yi Zong (M'12) was born in Wuhan, Hubei province, China, on August 21, 1971. She graduated in Control Engineering and Control Theory from Wuhan University of Science and Technology. She got PhD degree on System Engineering and Automation in 2006, at the University Complutense of Madrid, Spain.

Her employment experience included the Wuhan Institute of Technology, China. Since 2006 she had been employed as Post.doc at the Wind Energy Division of Risø DTU. She is currently a Scientist at the department of Electrical Engineering, Intelligent Energy Systems, Risø Campus, Technical University of Denmark. Her special fields of interest include the integration of renewable energy sources in building energy management, optimization control for demand side units in households and industry supporting flexible power consumption.

Lucian Mihet-Popa (M'12) was born in Romania, in 1969. He received the B.S. degree, M.S. degree and Ph.D. degree from the POLITEHNICA University of Timisoara, Romania, in 1999, 2000 and 2003, respectively, all in electrical engineering.

He is currently working as a Scientist with the department of Electrical Engineering, Technical University of Denmark, since 1st March 2011. He is also an Associate Professor in the Department of Electrical Engineering at the POLITEHNICA University of Timisoara. His research interest includes control and modeling of DER components in micro grids, electrical machines and drives, detection and diagnosis of faults, especially for wind turbine applications.

Dr. Mihet-Popa received in 2005 the second prize paper award of the IEEE Industry Applications Society.

Daniel Kullmann was born in Frankfurt/Main, Germany, on August 15, 1973. He graduated in Computer Science from Darmstadt University of Technology in 2002. He is currently working toward the Ph.D. degree at department of Electrical Engineering, Technical University of Denmark.

He worked for several years in the IT industry. His fields of interest are distributed control and communication in power systems.

Anders Thavlov was born in Copenhagen, Denmark, on June 3, 1979. He graduated from Department of Informatics and Mathematical Modeling at Technical University of Denmark in 2008. He is currently conducting his Ph.D. study in the Intelligent Energy Systems group at department of Electrical Engineering, Technical University of Denmark.

His main research interests are power systems, modeling of demand, flexible power consumption and control.

Oliver Gehrke (M'12) was born in Frankfurt am Main, Germany, on March 15, 1975. He graduated in Electrical Power Engineering from Darmstadt University of Technology and got his PhD degree at Risø National Laboratory in Denmark.

He is currently a Scientist at the department of Electrical Engineering, Intelligent Energy Systems, Risø Campus, Technical University of Denmark. His special fields of interest include the embedded and distributed control of power systems with a high penetration of renewable energy sources.

Henrik Bindner (M'12) was born on 30 June 1964 in Copenhagen, Denmark. He received his master in electrical engineering from the Technical University of Denmark in 1988.

Since 1990 he has been with Risø DTU National Laboratory for Sustainable Energy in the Wind Energy Division, currently as a Senior Scientist at the department of Electrical Engineering, Intelligent Energy Systems, Risø Campus, Technical University of Denmark. He has mainly been working on integration of wind energy into power system. The work has included analysis, design and control of small island systems as well as technologies and techniques for integration of wind in large systems. Currently, he is researching how distributed energy resources can be applied to increase penetration of wind energy.

Bibliography

[1] Energinet.dk, "Wind turbines reached record level in 2014." http://energinet.dk/EN/El/Nyheder/Sider/Vindmoeller-slog-rekord-i-2014.aspx. Press release 20 January 2015.

[2] Danish Energy Agency, "Energy Statistics 2011." www.ens.dk. Accessed Aug. 15, 2013.

[3] Danish Energy Agency, "Energy Statistics 2012." www.ens.dk. Available in Danish only.

[4] Danish Energy Agency, "Energistatistik 2013." www.ens.dk. Available in Danish only.

[5] The Danish Government, "Our Future Energy," tech. rep., The Danish Government, 2011.

[6] Energinet.dk, "Cell Controller Pilot Project," tech. rep., Energinet.dk, 2011.

[7] Nord Pool Spot. http://www.nordpoolspot.com/.

[8] F. Schweppe, R. Tabors, J. Kirtley, H. Outhred, F. Pickel, and A. Cox, "Homeostatic Utility Control," *IEEE Transactions on Power Apparatus and Systems*, vol. PAS-99, no. 3, pp. 1151–1163, 1980.

[9] F. Schweppe, R. Tabors, and J. Kirtley, "Power/energy: Homeostatic control for electric power usage: A new scheme for putting the customer in the control loop would exploit microprocessors to deliver energy more efficiently," *IEEE Spectrum*, vol. 19, pp. 44–48, 1982.

[10] A. Barbato, A. Capone, M. Rodolfi, and D. Tagliaferri, "Forecasting the usage of household appliances through power meter sensors for demand management in the smart grid," in *IEEE International Conference on Smart Grid Communications (SmartGridComm)*, pp. 404–409, 2011.

[11] International Energy Agency, "Technology Roadmap: Energy-efficient Buildings: Heating and Cooling Equipment," tech. rep., International Energy Agency, 2011.

[12] Statistics Denmark, "Statistics Denmark." `http://www.dst.dk`. Accessed: 2013-08-01.

[13] "Danish Energy Agency." `http://www.ens.dk`. Accessed: 2013-08-01.

[14] The Danish Energy Association, "Power to the People - Energy Consumption in Denmark to be Carbon Neutral in 2050," tech. rep., The Danish Energy Association, 2009.

[15] Danish Ministry of Finance, "Aftale mellem regeringen og Enhedslisten om: Finansloven for 2013," 2012. Available in Danish only.

[16] International Energy Agency, "Nordic Energy Technology Perspectives," tech. rep., International Energy Agency and Nordic Energy Research, 2013.

[17] Energinet.dk, "Download of market data." `http://www.energinet.dk/EN/El/Engrosmarked/Udtraek-af-markedsdata/Sider/default.aspx`. Accessed: 2013-08-01.

[18] D. J. Hammerstrom et al., "Pacific Northwest GridWise™ Testbed Demonstration Projects - Part I. Olympic Peninsula Project," tech. rep., Pacific Northwest National Laboratory, 2007.

[19] J. Jorgensen, S. Sorensen, K. Behnke, and P. Eriksen, "EcoGrid EU - A prototype for European Smart Grids," in *Power and Energy Society General Meeting, 2011 IEEE*, 2011.

[20] FENIX, "Flexible Electricity Networks to Integrate the expected Energy Evolution," tech. rep., FENIX, 2009.

[21] Open Energi, "Open Energi webpage." `http://www.openenergi.com/`.

[22] P. Nyeng, J. Ostergaard, M. Togeby, and J. Hethey, "Design and implementation of frequency-responsive thermostat control," in *45th International Universities Power Engineering Conference (UPEC)*, 2010.

[23] P. B. Andersen, *Intelligent Electric Vehicle Integration - Domain Interfaces and Supporting Informatics*. PhD thesis, Department of Electrical Engineering, Technical University of Denmark, 2013.

[24] P. Kundur, *Power System Stability and Control*. McGraw-Hill Education (India) Pvt Limited, 1994.

[25] P. Nyeng, *System Integration of Distributed Energy Resources*. PhD thesis, Department of Electrical Engineering, Technical University of Denmark, 2010.

[26] Energinet.dk, "Regulation C1 – Terms of balance responsibility," 2011.

[27] Energinet.dk, "Ancillary services to be delivered in Denmark - Tender conditions," 2012.

[28] Energinet.dk, "Introduktion til systemydelser," February 2015.

[29] Eurostat, "Eurostat." `http://epp.eurostat.ec.europa.eu/portal/page/portal/eurostat/home/`. Accessed: 2013-08-01.

[30] Nord Pool Spot, "The power of transparency, Annual Report 2012," 2012.

[31] C. Bang, F. Fock, and M. Togeby, "The existing Nordic regulating power market - FlexPower WP1, Report 1," tech. rep., Ea Energianalyse, 2012.

[32] National Energy Technology Laboratory, "A Vision for the Smart Grid," tech. rep., U.S. Department of Energy, 2009.

[33] Energinet.dk and Danish Energy Association, "Smart Grid in Denmark," tech. rep., Energinet.dk and Danish Energy Association, 2010.

[34] Danish Ministry of Climate, Energy and Building, "Smart Grid Strategy - The intelligent energy system of the future," tech. rep., Danish Ministry of Climate, Energy and Building, 2013.

[35] Joint Research Centre, "Smart Grid projects in Europe: Lessons learned and current developments (2012 update)," tech. rep., European Commission, Joint Research Centre, Institute for Energy and Transport, 2013.

[36] A. M. Kosek, G. T. Costanzo, H. W. Bindner, and O. Gehrke, "An Overview of Demand Side Management Control Schemes for Buildings in Smart Grids," in *2013 IEEE International Conference on Smart Energy Grid Engineering (SEGE)*, 2013.

[37] European Commission, "Energy Labelling legislation of household appliances," tech. rep., European Commission, 2013.

[38] "INCAP – Inducing consumer adoption of automated reaction technology for dynamic power pricing tariffs." `http://www.cee.elektro.dtu.dk/research/projects/38_INCAP`.

[39] P. G. Wang, M. Scharling, K. P. Nielsen, K. B. Wittchen, and C. Kern-Hansen, "2001–2010 Danish Design Reference Year - Reference Climate Dataset for Technical Dimensioning in Building, Construction and other Sectors," tech. rep., Danish Meteorological Institute, 2013. Dateset: `http://www.dmi.dk/fileadmin/user_upload/Rapporter/TR/2013/TR13-19_DRY.zip`.

[40] H. Sæle, E. Rosenberg, and N. Feilberg, "State-of-the-art. Projects for estimating the electricity end-use demand," tech. rep., SINTEF Energy Research, 2010.

[41] Y. Ding, L. Hansen, P. Cajar, P. Brath, H. Bindner, C. Zhang, and N. Nordentoft, "Development of a DSO-market on flexibility services," tech. rep., iPower, 2013. iPower WP3.8 report, published on www.iPower-net.dk/publications, date:18-03-2013.

[42] DONG Energy, "The eFlex Project," tech. rep., DONG Energy, 2012.

[43] DONG Energy, "Power Hub webpage." `https://www.powerhub.dk/`.

[44] TWENTIES, "TWENTIES project Final report - short version," tech. rep., TWENTIES, 2013.

[45] Ea Energy Analyses, "Overview of European Union climate and energy policies," tech. rep., Ea Energy Analyses, 2012.

[46] DONG Energy, "Power Hub interoperability document," tech. rep., DONG Energy, 2012.

[47] B. Øksendal, *Stochastic Differential Equations*. Springer, 5ed ed., 2000.

[48] P. Bacher and H. Madsen, "Identifying suitable models for the heat dynamics of buildings," *Energy and Buildings*, vol. 43, 2011.

[49] Y. A. Cengel, *Heat & Mass Transfer: A Practical Approach*. Tata McGraw Hill Education, third edition ed., 2007.

[50] A. Thavlov, "Dynamic Optimization of Power Consumption," Master's thesis, DTU IMM, Technical University of Denmark, 2008.

[51] H. Madsen and J. Holst, "Modelling Non-Linear and Non-Stationary Time Series." Lecture notes, December 2006.

[52] CTSM, "CTSM." http://www.ctsm.info/. Accessed: 2013-10-01.

[53] H. Madsen, *Time Series Analysis*. Chapman & Hall, 2008.

[54] Danish Ministry of the Environment, "Varmeakkumulering i beton - Vurdering af betons termiske masse i relation til bygningsreglementet og energiberegninger." http://www2.mst.dk/common/Udgivramme/Frame.asp?http://www2.mst.dk/Udgiv/publikationer/2007/978-87-7052-443-8/html/default.htm, 2007. Accessed: 2013-09-23, Available in Danish only.

[55] The Danish Ministry of Economic and Business Affairs and Danish Enterprise and Construction Authority, "Bygningsreglement 1995 (BR 95)." http://w2l.dk/file/155699/BR10_ENGLISH.pdf, 1995. Available in Danish only.

[56] The Danish Ministry of Economic and Business Affairs and Danish Enterprise and Construction Authority, "Building Regulations." http://w2l.dk/file/155699/BR10_ENGLISH.pdf, December 2010. Accessed: 2013-12-01.

[57] H. Madsen and J. Holst, "Estimation of continuous-time models for the heat dynamics of a building," *Energy and Buildings*, vol. 22, pp. 67–79, 1995.

[58] Danish Technological Institute, "ifabrix." http://www.ifabrix.com/. Accessed: 2013-09-23, Available in Danish only.

[59] ROCKWOOL, "ROCKWOOL Energy Design." http://www.rockwool.dk/beregninger/energiberegning. Accessed: 2013-09-23, Available in Danish only.

[60] S. Boyd and L. Vandenberghe, *Convex Optimization*. Cambridge University Press, 2004.

[61] J. Rossiter, *Model-Based Predictive Control: A Practical Approach*. CRC Press, 2003.

[62] CEN-CENELEC-ETSI Smart Grid Coordination Group, "CEN-CENELEC-ETSI Smart Grid Coordination Group Smart Grid Reference Architecture," tech. rep., CENELEC, 2012.

[63] K. Heussen, D. Bondy, J. Hu, O. Gehrke, and L. Hansen, "A clearinghouse concept for distribution-level flexibility services," in *Innovative Smart Grid Technologies Europe (ISGT EUROPE), 2013 4th IEEE/PES*, pp. 1–5, Oct. 2013.